UNIVERSITY OF SOUTHAMPTON

FACULTY OF SOCIAL AND HUMAN SCIENCES

Academic Unit of Geography of Environment

Assessing the vulnerability of the rice-wheat production system in the north-west Indo-Gangetic Plains to climatic drivers

by

John Duncan

Thesis for the degree of Doctor of Philosophy

December 2013

UNIVERSITY OF SOUTHAMPTON

ABSTRACT

FACULTY OF SOCIAL AND HUMAN SCIENCES

Geography and Environment

Thesis for the degree of Doctor of Philosophy

ASSESSING THE VULNERABILITY OF THE RICE-WHEAT PRODUCTION SYSTEM IN THE NORTH-WEST INDO-GANGETIC PLAINS TO CLIMATIC DRIVERS

John Duncan

This thesis explores the spatial patterns in the vulnerability of the rice-wheat production systems of Punjab and Haryana to climate. Remote sensing monitoring is used to identify rice and wheat crop extents and to capture dynamics of the cropping system such as length of growing periods and cropland productivity. This remote sensing monitoring is integrated with analysis of climate datasets and other measures of the agricultural system to 1) identify the exposure of rice-wheat croplands to harmful climate drivers, 2) capture the sensitivity of the rice-wheat croplands to climate and to 3) inform targeted adaptations to improve climate resilience, ensure environmental sustainability and sufficient levels of production, the pillars of a climate-smart landscape.

Across all India, including Punjab and Haryana, there was a fragmented spatial pattern in the occurrence, and sign, in trends of monsoon precipitation. This highlights the need for locally sensitive water resources management. Over 5 million ha of rice-wheat croplands in Punjab and Haryana were exposed to unfavourable trends in facets of monsoon precipitation; this was mainly exposure to increasing recurrence of drought years and increasing inter-annual variability in monsoon precipitation. However, crop yield-climate regression models indicated that precipitation is not influencing variability in rice or wheat crop production but growing season temperatures are. Average minimum and maximum temperature during the thermo-sensitive periods of crop development have a greater negative impact on wheat crop yield than exceedance of critical temperatures. The negative impact of warming on wheat crop production increased with later start-of-season dates. Through an integrated use of remote sensing datasets the spatial patterns in the magnitude and varying nature of the vulnerability of crop production to climate were captured. This enabled identification of location-specific stresses, such as later sowing dates, and targeting locally optimum adaptations.

Contents

List of tables

List of figures

Declaration of Authorship

I, John Duncan

declare that the thesis entitled

Assessing the vulnerability of the rice-wheat production system in the north-west Indo-Gangetic Plains to climatic drivers

and the work presented in the thesis are both my own, and have been generated by me as the result of my own original research. I confirm that:

- this work was done wholly or mainly while in candidature for a research degree at this University;
- where any part of this thesis has previously been submitted for a degree or any other qualification at this University or any other institution, this has been clearly stated;
- where I have consulted the published work of others, this is always clearly attributed;
- where I have quoted from the work of others, the source is always given. With the exception of such quotations, this thesis is entirely my own work;
- I have acknowledged all main sources of help;
- where the thesis is based on work done by myself jointly with others, I have made clear exactly what was done by others and what I have contributed myself;
- parts of this work have been published as:

Duncan, J.M.A., Dash, J., & Atkinson, P.M. (2012) Analysing temporal trends in the Indian Summer Monsoon and its variability at a fine spatial resolution. *Climatic Change*, 117, (1-2), 119-131. doi:10.1007/s10584-012-0537-y

The work undertaken in chapter 3 has also led to three subsequent publications separate to my PhD research:

Duncan, J.M.A., & Biggs, E.M. (2012) Assessing the accuracy and applied use of satellite-derived precipitation estimates over Nepal. *Applied Geography*, 34, 626-638. doi:10.1016/j.apgeog.2012.04.001.

Biggs, E.M., Duncan, J.M.A., Atkinson, P.M., & Dash, J. (2013) Plenty of water, not enough strategy: How inadequate accessibility, poor governance and a volatile government can tip the balance against ensuring water security: the case of Nepal. *Environmental Science & Policy*. doi:10.1016/j.envsci.2013.07.004. (In Press).

Duncan, J.M.A., Biggs, E.M., Dash, J., & Atkinson, P.M. (2013) Spatio-temporal trends in precipitation and their implications for water resources management in climate-sensitive Nepal. *Applied Geography*, 43, 138-146. doi:10.1016/j.apgeog.2013.06.011.

Conference Presentations:

Duncan, J.M.A., Dash, J. & Atkinson. P.M. (2012) The use of phenology derived land use classifications to observe spatio-temporal trends in cropping season patterns across the Indo-Gangetic Plains between 1982-83 to 2005-06. Presented at 39th COSPAR Scientific Assembly, Mysore, India.

Signed: ……..

Date:…….

Acknowledgements

Firstly, I would like to thank Dr Jadu Dash and Professor Peter Atkinson for acting as supervisors for my PhD research. Their constant guidance, support and inspiration have been invaluable. I would also like to thank Dr Eloise Biggs; I am grateful for her advice and help throughout the duration of my PhD research.

Other mentions must go to Dr Gareth Roberts for help with processing MODIS data, and to Robin Wilson, Peter Dutey-Magni and Niall Quinn for assistance with handling and analysing datasets in R and Matlab. I must also thank my friends in the post-graduate community for their daily support over the past three years, especially Kim Davies and Niall Quinn.

I would also like to acknowledge the Academic Unit of Geography and Environment, University of Southampton for providing funding for this research.

Finally I would like to thank my family, my mum, dad and brother, for their constant support and backing in helping me achieve this goal. Similar thanks must also be extended to Ellie Tighe for her unrelenting encouragement.

Definitions and Abbreviations

AGDD – Accumulated Growing Degree Days

APHRODITE – Asian Precipitation – Highly-Resolved Observational Data Integration Towards Evaluation of Water Resources

BWLH – Wang and LinHo Method

CGIAR – Consultative Group on International Agricultural Research

CH_4 – Methane

CIMMYT – International Maize and Wheat Improvement Centre

CMAP – Centre for Merged Analysis of Precipitation

CMG – Climate Model Grid

CO_2 – Carbon Dioxide

CPM – Climatological Pentad Mean

CUM-$EVI_{(TSP)}$ – cumulative sum of EVI during the TSP

cumNDVI – cumulative sum of NDVI

EDD – Extreme Degree Days

EOS – End-of-Season

EVI – Enhanced Vegetation Index

FAO – Food and Agriculture Organisation of the United Nations

FEWSNET – Famine Early Warning System Network

GCM – Global Climate Model

GHG – Greenhouse Gas

GIMMS – Global Inventory Mapping and Modelling Studies

GLAM – Global Large Area Model

GLC2000 – Global Land Cover 2000

GRACE – Gravity Recovery and Climate Experiment

GSOD – Global Summary of the day

HYV- High Yielding Variety

IGP – Indo-Gangetic Plain

IMD – Indian Meteorological Department

IRRI – International Rice Research Institute

ISM – Indian Summer Monsoon

IWRM –Integrated Water Resources Management

LGS – Length of Growing Season

Log(CUM-$EVI_{(TSP)}$) – natural logarithm of CUM-$EVI_{(TSP)}$

LSP – Land Surface Phenology

LSWI – Land Surface Water Index

MTCI – Meris Terrestrial Chlorophyll Index

N_2O – Nitrous Oxide

NDSI - Normalised Difference Snow Index

NDVI – Normalised Difference Vegetation Index

NPP – Net Primary Productivity

O_3 – Ozone

QA – Quality Assurance

RCM – Regional Climate Model

SOS – Start-of-Season

SPA – Standardised Precipitation Anomaly

SRES – Special Report on Emissions Scenario

SSV – Spectral Similarity Value

TFP – Total Factor Productivity

TSP – Thermo-Sensitive Period

VI – Vegetation Index

VIF –Variance Inflation Factor

Y_p – Potential Yield

Chapter 1: Introduction

The productivity of cereal croplands is crucial to sustaining global food security; in 2011 the cereal crops of maize, rice and wheat were ranked second, third and fourth respectively in terms of global production of agricultural commodities and rice had the greatest global net production value (FAO 2013). Globally croplands cover 12% of the terrestrial land surface and together cropland and pasture are equivalent in terms of ecosystem coverage to forests and have already exhausted the best farmland (Foley et al. 2007; Foley et al. 2011; Fig. 1-1). The food security of large proportions of the global population relies upon 'focal' regions of intensive cropping (Fig. 1-1). For example, China's population of 1.37 billion (20% of the global population) is reliant on cereal croplands covering only 9.5% of the national and, less than 1% of the global, land surface (FAO 2013).

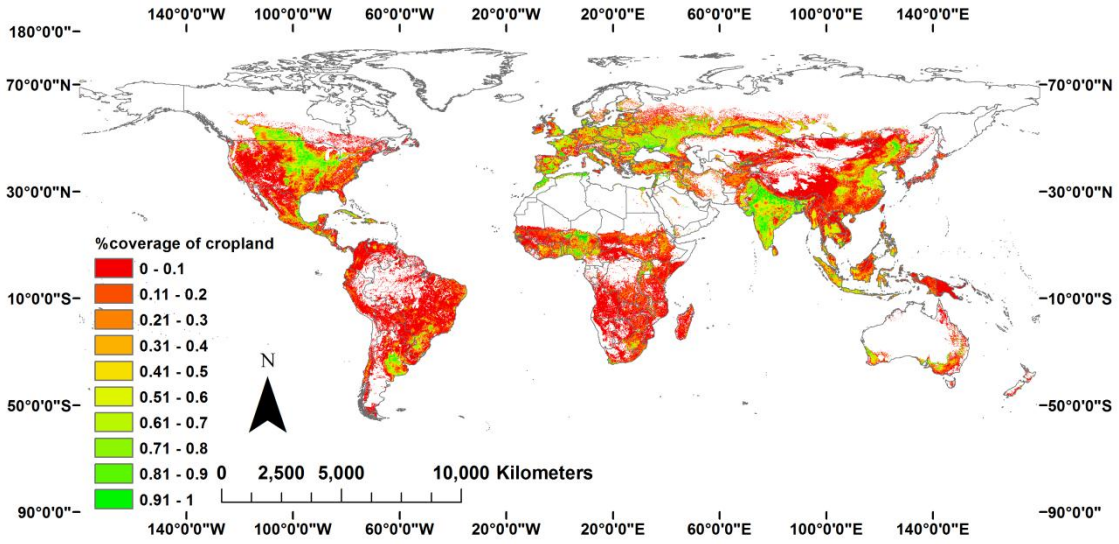

Figure 1-1 Map of global croplands, showing percentage coverage of cropland within a 5 minute grid cell in the year 2000 (Ramankutty et al. 2008).

Levels of production from cereal croplands are partly determined by climatic variables and are linked to the pulses of climatic variation (Krishna Kumar et al. 2004; Brown et al. 2010; Lobell et al. 2011a; Lobell et al. 2011b; Lobell et al. 2012). Changes in climate drivers or increases in climatic variation could limit levels of cereal crop production (Lobell et al. 2011b). Billions of people globally are vulnerable to productivity losses in

these ‘focal’ cereal production systems. This is evidenced by the recent food price crisis in 2008 where shortfalls in production and food price fluctuations had the greatest impacts on the poorest segments of society (Hajkowicz et al. 2012). It is therefore important that adaptations are implemented within cereal production systems to increase the resilience of crop production to projected climate changes and climatic variability (The Royal Society 2009; Teixeira et al. 2013).

However, cereal croplands are not just vulnerable to climate change and variability but also to a range of other stresses and pressures including growing populations increasing demands for food on limited or stagnating cultivated areas, increasing competition for land, water and energy resources from other sectors such as urbanisation or industry, changing diets with greater emphasis on meat products and environmental degradation and loss of land to salinization (The Royal Society 2009; Hanjra and Qureshi 2010 Foley et al. 2011; Foresight: The Final Project Report 2011; Gleeson et al. 2012; Table 1-1). Table 1-1 presents a summary of the key stresses affecting global cereal croplands. This situation has been articulated as the ‘perfect storm’ for food security by Beddington (2009). It is important to note that the magnitude of climate impacts on cereal crop production will vary between and within croplands due to underlying system factors such as soil type, access to irrigation and farmer management (Luers et al. 2003; Luers 2005).

Table 1-1 Global stresses on cereal crop production and cereal croplands.

Stress	Impact on cereal croplands
Population growth	Global population is projected to increase by two to three by billion by 2050 increasing crop demand by 100-110%. This is alongside feeding the 870 million currently food insecure through undernourishment.
Income and changing diets	With rising incomes a greater proportion of the global population will seek out meat based diets. This results in conversion of croplands to grazing lands and an increased water and environmental footprint. It takes 30kg of grain to produce one kg of beef.
Competition for resources (land and water)	Cereal crop production will increasingly have to compete with other sectors, such as urbanisation, biofuels, grazing land and industry for land and water inputs. This indicates the need to increase cereal productivity per unit land and per unit water.
Environmental degradation	Degradation of environmental resources and regulating ecosystem processes will limit cereal crop production. Often environmental degradation is the result of intensive agriculture over the past 50 years.
Stagnating yields	Whilst demand for food increases the rate of increase in crop yields has declined. Crop yields increased by 56% between 1965 and 1985, yet by only 20% between 1985 and 2005. Growth rates in the top four crops (maize, rice, wheat and soybean) are not sufficient to meet expected demand.
Climate change and variability	Warming trends have already limited cereal crop production. Projected warming, variable precipitation and increased frequency of extreme events will limit future cereal production and suitable croplands, especially in tropical and sub-tropical latitudes. Worryingly, between 1985 and 2005 there was a net redistribution of global croplands towards tropical latitudes.
The need for sustainability	There are pressures for cereal cropping to be more sustainable. Expansion of croplands at the expense of forests and biodiversity must be minimised, as must agricultures GHG emissions, inefficient use irrigation water and over-use of fertilisers.

Table sources: Tillman et al. (2002); Aggarwal et al. (2004); Foley et al. (2005); Millennium Ecosystem Assessment (2005); Easterling et al. (2007); Schmidhuber and Tubiello (2007); Thenkabail et al. (2010); Lobell et al. (2011b); Foley (2011); Foley et al. (2011); Tillman et al. (2011); Foresight: The Final Project Report (2011); Ray et al. (2013); Teixiera et al. (2013); Godfray and Garnett (2014).

It is emphasised both in the academic literature and in international policy that unless cereal croplands are moved onto a climate-resilient, environmentally sustainable trajectory whilst simultaneously increasing productivity the consequences for humanity will be negative and focused on the global poor (Morton 2007; Vermeulen et al. 2010; Godfray et al. 2010; World Bank 2011; Poppy et al. 2014). Cereal croplands

must be transformed such that agricultural practices ensure sufficient and stable production, in spite of uncertain future climate scenarios, for food security, and wider poverty alleviating and development goals. Changes to cereal cropping practices must aim to also preserve biodiversity, ecosystem service provision and ecological processes and, have a limited, or mitigating, impact as a driver of climate change. These goals are critical to the framework of 'climate-smart' agriculture; climate-smart agriculture approaches are advocated as the desired sustainable and climate-resilient development pathway by numerous international organisations (World Bank 2011; FAO 2011b). Beddington et al. (2012a) and Beddington et al. (2012b) discuss the need to find a 'safe operating space' for agricultural systems whereby they operate within environmental limits (conceptualised as 'planetary boundaries' by Rockstrom et al. (2009)), without contributing to climate change and whilst meeting the needs of a growing population. In this context, any assessment of the vulnerability of cereal crop production to climate change or climatic variation with the intention of informing climate-resilient adaptations must also consider the range of stresses placed on cereal production systems, and that agricultural practice must reduce their environmental and climatic footprints.

The situation in India is typical of this global issue. India's population, in excess of 1.2 billion people, with a decadal growth rate of 17.64% (DES 2011), is heavily dependent upon, the 'focal' areas of cereal cropping in Punjab and Haryana in the north-west Indo-Gangetic Plains (IGP) (Fig. 1-2). In 2011-2012, Punjab and Haryana comprised only 8.93% of the nationwide cropped area for foodgrains yet contributed significantly to national production with the largest state-wise foodgrain yields and proportional area under irrigation (Fig. 1-2) (DES 2011).

The dominant crops in Punjab and Haryana are *kharif* rice typically grown from June to October and *rabi* wheat grown from November to April. Rice and wheat crop yields, elevated using Green Revolution technologies in the 1960s and 1970s, are key to supporting 53 million local livelihoods as well as nationwide food security through state procurement for distribution to poor households (Aggarwal et al. 2004; Gupta and Seth 2007; DES 2011; Perveen et al. 2012). The rice-wheat cropping system is one of the worlds 'focal' cereal croplands and is typical of global croplands in being

affected by multiple stresses simultaneously including population pressure, limited room for expansion, environmental resource degradation, depleting water resources and climate change (Abrol 1999; Aggarwal et al. 2004; Ambast et al. 2006; DES 2011; Perveen et al. 2012; Mathison et al. 2013). However, the croplands are currently being managed in a way that degrades natural resources and are threatened by future changes in climate (Aggarwal et al. 2004; Ortiz et al. 2008; Teixeira et al. 2013; Mathison et al. 2013).

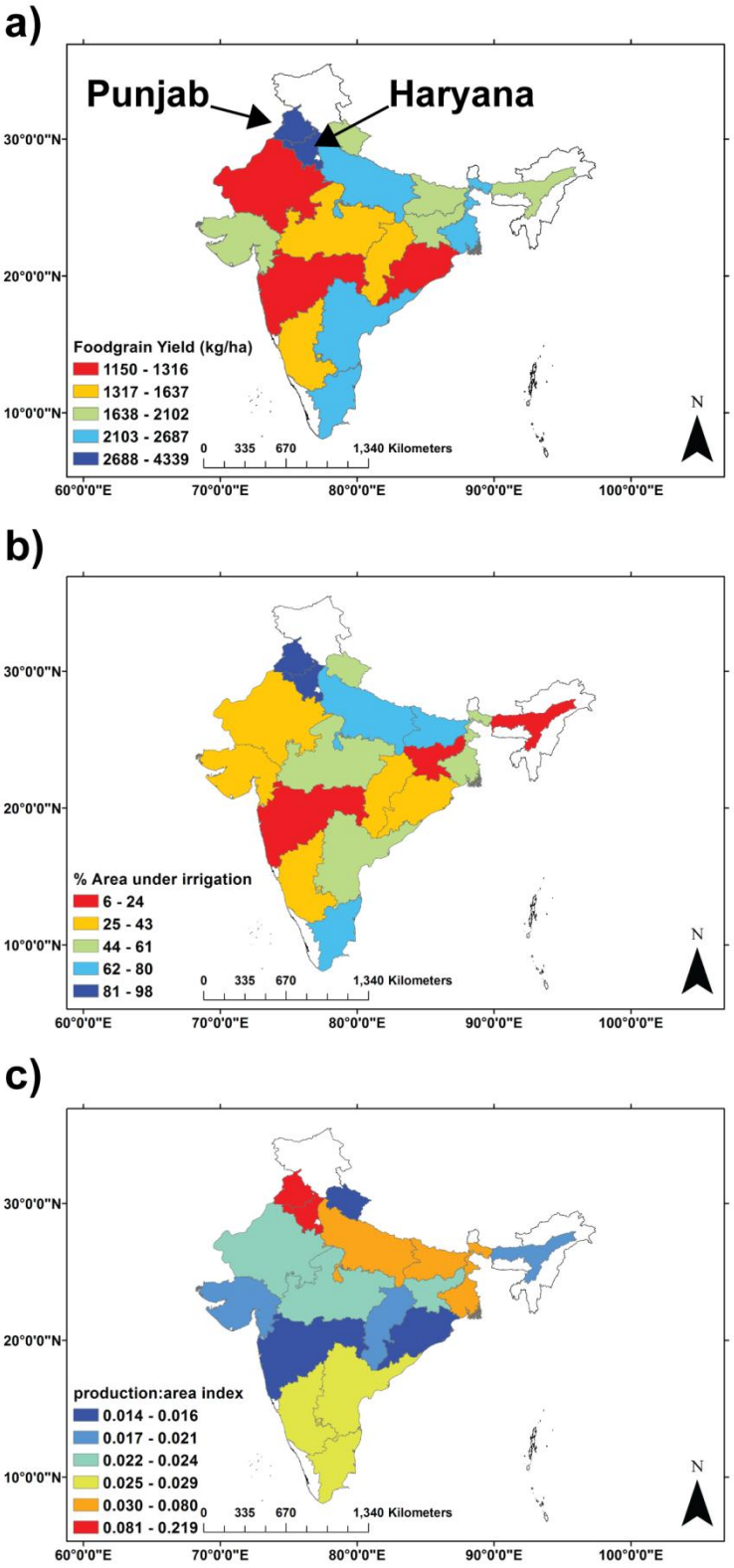

Figure 1-2 Illustration of Punjab and Haryana as the 'focal' foodgrain production centre in India; a) state-wise foodgrain yield (kg ha-1) (DES 2011), b) state-wise area under irrigation (expressed as a percentage of state area) (DES 2011) and, c) an index of percentage of state contribution to national foodgrain production normalised by state area (http://lus.dacnet.nic.in/). (The index was multiplied by one thousand to enhance figure clarity).

This thesis assesses **the vulnerability of the rice-wheat production system in the north-west IGP to climatic drivers**. An integrated remote sensing approach is used to 1) identify the spatial patterns of the exposure of rice-wheat croplands to harmful climate drivers including trends and climatic variation, 2) capture the sensitivity of rice-wheat crop production to variations in climate drivers and to 3) inform targeted adaptations sensitive to local stresses to enhance the climate-resilience of cropping, ensure environmental sustainability and sufficient levels of production.

The remainder of Chapter 1 will be broken into two sections. *Section 1.1* will provide a general discussion of the impacts of climatic changes and variability on cereal croplands with consideration to interactions with other multiple stresses which determine the vulnerability of crop production. *Section 1.2* is a review of the rice-wheat production systems of the north-west IGP, specifically Punjab and Haryana; it explores the key stresses affecting rice and wheat crop production here. Chapter 2 will discuss approaches to assess and measure vulnerability, outline the framework used to assess vulnerability in this thesis and culminates by posing key questions addressed through the thesis and answered in the concluding chapters. Chapters 3 to 6 represent four analysis chapters written in the style of research papers, each with unique aims, research questions and stand-alone conclusions but linked to the overarching theme of assessing the vulnerability of the rice-wheat production system of Punjab and Haryana to climate drivers. Chapter 7 provides a brief discussion of the current state of vulnerability of rice and wheat production in Punjab and Haryana to climate drivers and suggests some avenues for future research. Chapter 8 highlights the conclusions drawn from this thesis addressing key questions posed at the end of Chapter 2.

1.1 Climatic changes, variability and multiple stresses on cereal croplands

Intensification of agriculture, utilising Green Revolution advances of high yielding crop varieties (HYV) and altered agronomic practices (increased irrigation, access to fertilisers and increased cropping intensity) led to a dramatic increase in net production and productivity over the past 50 years (The Royal Society 2009; Ray and Foley; 2013). However, despite these gains, yield gaps still remain in many agricultural

systems and food insecurity is still prevalent globally, complicated by regional and sub-national variation; one billion people do not have enough to eat excluding those suffering from micronutrient deficiency and over-consumption and, thus, lack a basic human right (UN 1948; Godfray et al. 2010; Brussaard et al. 2010; Misselhorn et al. 2012; Godfray and Garnett 2014). It was often 'subsistence' and 'smallholder' farmers who did not receive the benefits from the Green Revolution due to numerous factors including weak governance and policy support, inability to make the transition to market-based agriculture, poor access to research and development and, limited integration into markets (Brussaard et al. 2010a; Hanjra and Qureshi 2010).

There are numerous interacting stresses placed on cereal cropping systems which inhibit their ability to provide complete food security. Of these stresses, climate change and climatic variability have a direct influence on crop productivity, yet also influences a wider range of food system activities which determine food security including access to, stability of and capacity to utilise food (FAO 1996; Vermeulen et al. 2012b; Wheeler and von Braun 2013). It is difficult to quantify and forecast the impacts of climate change on crop yields due to future uncertainties in: levels of adaptation and technological advances, community responses, projections of climate change relevant to crop growth using Global Climate Models (GCM) and, how the interaction of the various changing facets of the climate system will alter plant physiology (Annamalai et al. 2007; Tubiello et al. 2007; Lobell and Gourdji 2012; Gourdji et al. 2013a; Ramirez-Villegas et al. 2013). For example, GCM prediction and simulation of the Indian Summer Monsoon (ISM), the key driver of rice yield in South Asia, is poor, presenting a barrier to informed climate-resilient adaptation (Annamalai et al. 2007; Turner and Annamalai 2012).

Despite the theoretical benefits of increased carbon dioxide (CO_2) levels on crop physiological processes it is expected that cereal crop yields will decline with a warming climate (Easterling et al. 2007; Nelson 2010). The negative impact of warming on crop productivity is likely to be greater in the tropics than at higher latitudes (Easterling et al. 2007; Schmidhuber and Tubiello 2007; Vermeulen et al. 2012b). Elevated levels of atmospheric CO_2 may reduce cereal crop quality with lower protein concentrations in grains (Schmidhuber and Tubiello 2007; Vermeulen et al. 2012b).

Globally, observed climate trends between 1980 and 2008 resulted in a loss of 3.8% and 5.5% of maize and wheat yields, largely due to warming (Lobell et al. 2011b). Cereal crop yields are sensitive to both seasonal warming and extreme heat events during the reproductive development stage (Challinor et al. 2005; Jagadish et al. 2007; Welch et al. 2010; Lobell and Burke 2010; Lobell et al. 2011a; Teixeira et al. 2013). Significant portions of wheat, maize and rice croplands globally (83, 68 and 86% respectively) experienced warming trends during the growing season between 1980 and 2011 and 27, 32 and 15% of these croplands experienced increasing trends in reproductive days over critical temperatures (Gourdji et al. 2013b). GCMs project that these trends will increase up to 2050 indicating that yields across a greater proportion of the global croplands will be impacted by warming trends and extreme heat events (Teixeira et al. 2013; Gourdji et al. 2013b).The latest IPCC projections suggest global surface temperature will be 1.5˚C greater than baseline temperatures from 1850-1900 for all RCP scenarios except RCP 2.6; precipitation projections are more uncertain (IPCC, 2013). Downscaled GCM simulations suggest that by 2050 climatic changes will cause a 51% reduction in the area suitable for high-yield wheat cropping in the IGP with subsequent yield declines (Ortiz et al. 2008). The interaction between changes in precipitation, temperature and CO_2 will influence levels of available soil moisture, evapotranspiration and crop water use efficiency with subsequent yield impacts (Wassmann et al. 2009; Lobell and Gourdji 2012; Gourdji et al. 2013a).

Whilst being negatively impacted by climate change a large proportion of cereal cropping practices are also drivers of climate change emitting large quantities of greenhouse gases (GHG) and altering radiative forcing via land cover changes (Vermeulen et al. 2012b). Land use change in the tropics, specifically deforestation, contributes 12% of annual anthropogenic CO_2 emissions (DeFries and Rosenzweig 2010; Foley et al. 2011). After fossil fuel combustion, land use change is the largest global CO_2 emitter (Power 2010). Land use conversion from forest to croplands leads to loss of above-ground biomass, a carbon sink, alongside reductions in soil carbon; for example, residue burning of rice crops in India directly releases GHGs and also reduces organic matter which would be reincorporated into the soil (Pathak et al. 2006; Power 2010). Anaerobic decomposition of carbon substrates in flooded rice fields contributes

11% of global methane (CH_4) emissions (IPCC 1996; Power 2010). Increasing application of nitrogen fertilisers, an 800% increase in global applications in the last 50 years, increases the rate of nitrous oxide (N_2O) emissions from soils (IPCC 2006a; Foley et al. 2011). Whilst production contributes the largest share to agriculture's GHG emissions pre- and post- production activities in the food chain are also emitters; fertiliser production is energy intensive and, thus, generates GHG emissions (Saharawat et al. 2012; Vermeulen et al. 2012b).

Agriculture exerts a significant and often detrimental impact on the Earth's environment, climate and, biogeochemical cycles; in terms of ecosystem coverage agro-ecosystems are equivalent to forest cover, consume 70% of freshwater withdrawals and approximately 30% of global net primary productivity (NPP) is appropriated via humans (Foley et al. 2005; Foley et al. 2007; Global Water Partnership 2013) The increase in agricultural productivity due to intensive monocropping and use of Green Revolution technologies occurred with significant environmental costs (Foley et al. 2007; Brussaard et al. 2010). To realise the benefits of HYVs developed during the Green Revolution requires increased use of fertilisers, pesticides and irrigation water leading to unsustainable use, and pollution of, land and water resources (The Royal Society 2009). Agricultural and associated land use practices have degraded soil resources and reduced soil quality (e.g. loss of nutrients, salinity and, topsoil erosion) (Tilman et al. 2002; Aggarwal et al. 2004). Globally, 10 million ha of agricultural land is lost due to salinization per year (Hanjra and Qureshi 2010). Transformation from natural (e.g. forest) to agricultural lands increases runoff with subsequent loading of sediment and nutrients in water sources with negative impacts on aquatic ecosystems, both freshwater and marine (Vitousek et al. 1997). Climate change is a major driver of land degradation, which has secondary impacts on agricultural productivity via reducing soil and freshwater quality (Aggarwal et al. 2010). In the past 40 years there has been a significant increase in fertiliser use such that agriculture is now the largest source of nitrogen and phosphorus to water bodies; of nitrogen fertiliser applied to croplands only 30-50% is utilised by crops (Tilman et al. 2002; Foley et al. 2005). The resultant excessive nutrient loading of water bodies results in eutrophication, toxic algal blooms, disturbance of species composition and anoxic conditions depleting fish

stocks; it is also difficult to reverse these eutrophic conditions (Vitousek et al. 1997; Carpenter et al. 1998; Tilman et al. 2002; Carpenter 2005).

Aside from agricultural practices leading to the declining quality of many water sources, many cropping systems through excessive irrigation extract water beyond renewable limits. With projected increases in population and income changing demand, agriculture will need an extra 5600 km^3 of water per year; 800 km^3 is available from 'blue water' sources suggesting agricultural systems will need to find an extra 4800 km^3 per year (Hanjra and Qureshi 2010). It should be noted there are some uncertainties in estimating agricultural water use at a global scale; estimates range from 6685 km^3 per year to 7500 km^3 per year (Postel 1998; Siebert and Doll 2010; Thenkabail et al. 2010). This will compound existing issues of water scarcity, over-extraction and, degradation and depletion of water resources (Ambast et al. 2006; Comprehensive Assessment of Water Management in Agriculture 2007; Hanjra and Qureshi 2010; Gleeson et al. 2012). Often agriculture's negative environmental impacts such as deforestation, soil erosion and degradation and, declining water resource abundance and quality co-occur and are accentuated by positive feedbacks. Sub-optimal agricultural practices and governance have resulted in a loss of biodiversity and ecosystem service provision, thus, degrading the natural resource base upon which agriculture and a wider range of livelihood options are reliant (Millenium Ecosystem Assessment 2005; Scherr and McNeely 2008; Brussaard et al. 2010).

Projected growth in global population, to around 9 billion by 2050, will increase demand for food from cereal crop systems with limited room for sustainable expansion of cultivated areas (Godfray et al. 2010; Foley et al. 2011; Misselhorn et al. 2012). The Food and Agriculture Organisation of the United Nations (FAO) project a required increase in global cereal production of 800 million tonnes by 2030 (FAO 2006). There is uncertainty regarding the accuracy of population growth and food demand projections due to numerous factors such as disparities in regional growth rates, changing diets and income levels and, differing levels of female education (Foresight: Final Project Report 2011). Globally, changes in diet, with increased meat consumption, results in more cereal crops being fed to cattle (currently 33% of global

cereal grains) and reduced per capita availability for human consumption and increased demand on water resources (The Royal Society 2009; Hanjra and Qureshi 2010). The impact of this reduced availability of staple cereal grains disproportionately effects the world's poorest populations and will increase pressure on production in croplands devoted to human consumption (The Royal Society 2009).

Cereal croplands are vital in sustaining the livelihoods of many low-income and developing countries where rural populations and, 'smallholder' and 'subsistence' households spend the majority of their income on staple foods; Fig. 1-3 displays the global distribution of smallholder farming systems. Smallholder and subsistence farmers also generate a large proportion of their income and gain nutrition from local agricultural and cereal production systems (Morton 2007; Nelson 2010; Foresight: Final Project Report 2011; Hajkowicz et al. 2012). Therefore, the productivity and sustainability of production in these regions are crucial not only to achieve food security but also a wider range of poverty alleviation and development goals (Nelson 2010; Foresight: Final Project Report 2011; Vermeulen et al. 2012a). Stable and adequate production from cereal croplands, through increasingly globally inter-connected markets, provide food for growing urban populations and contribute to food stocks encouraging price stability (Hajkowicz et al. 2012). It is important to note that in both rural and urban locations a wider range of situation-specific factors (e.g. levels of accessibility to food, ability to utilise food) alongside levels of production interact to determine food security outcomes (Ericksen 2008a). In developing countries local cereal production will be of importance to rural populations due to increasing polarity in purchasing power and volatility of prices in global crop markets (Brown and Funk 2008). Despite the role of markets, local production is vital for food security in the developing world where within-country production contributes 83% of wheat consumption (Ortiz et al. 2008). It is likely climate change will accentuate the vulnerability of rural populations reliant on cereal croplands in developing countries through a range of direct and indirect influences (Morton 2007; Brown and Funk 2008).

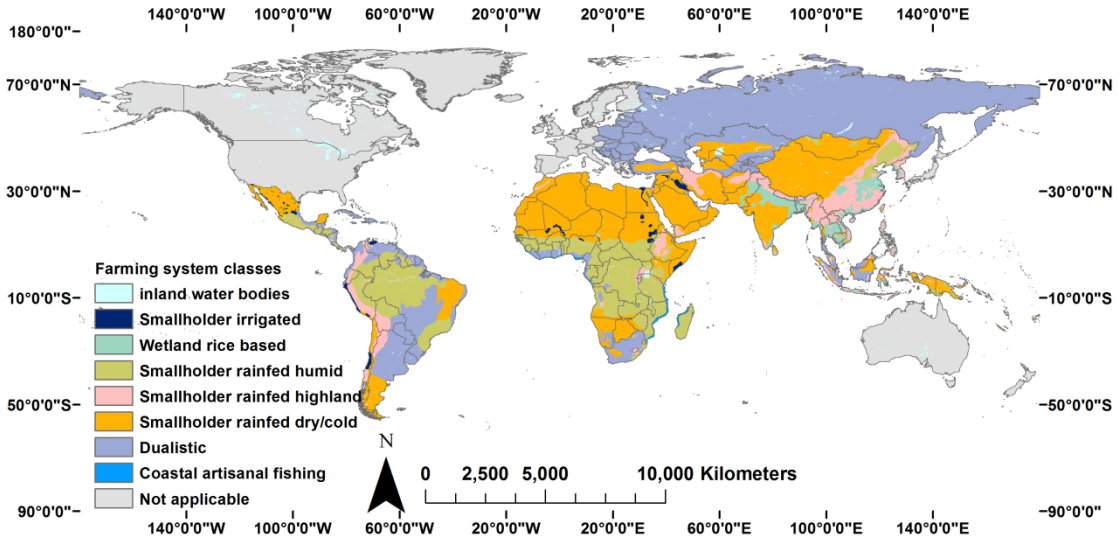

Figure 1-3 Global map of farming systems, including the distribution of smallholder farming systems. The data is displayed at a 5 minute resolution and is derived from the *Farming system classes in developing and transition countries, 2000* dataset from the FAO (http://www.fao.org/geonetwork/srv/en/main.home).

Climate change is expected to increase variability in weather (i.e. more droughts, extreme heat and rain events) which may reduce stability in crop production with subsequent impacts on crop prices (Schmidhuber and Tubiello 2007; Hajkowicz et al. 2012; Teixeira et al. 2013; Gourdji et al. 2013b). Droughts are often cited as a cause of the 2008 spike in global wheat prices and flooding in 1998 reduced rice production in Bangladesh with a knock-on increase in prices with the impacts exaggerated in poor households (Hajkowicz et al. 2012). If climate change reduces the productivity of cereal croplands it will lead to an increase in the price of crops and reduce the purchasing power of smallholder farmers for whom agriculture is their main source of income generation; thus, both factors contribute to a reduced capacity for smallholders to access food and mitigate shortfalls in production with food insecurity ensuing (Schmidhuber and Tubiello 2007). Increased climatic variability, and subsequent short-term reductions in crop yield and stability, and changes in mean climate with long-term declines in normal yields, are focused geographically in regions where there is the least environmental and socio-economic resilience and where communities have the lowest levels of adaptive capacity and least governance and policy support to cope (Morton 2007; Schmidhuber and Tubiello 2007; Brown and Funk 2008; Foresight: Final Project Report 2011; Hajkowicz et al. 2012).

The increased demand for cereal crops will be focused on already stressed land, water and energy resources, whilst also facing increased competition for resources from other sectors (e.g. industry, urban expansion, timber and transport) (Hanjra and Qureshi 2010; Harvey and Pilgrim 2011; Bogdanski 2012; Uphoff 2012; Misselhorn et al. 2012). The impacts of globalisation of the food, energy and governance sectors, integration into global food markets, investment in technology and research and development, cultural and gender differences and land tenure vary spatially and temporally between and within cereal systems and, thus, contribute to differing outcomes in terms of food security and productivity (Godfray et al. 2010; Foresight: Final Project Report 2011; Harvey and Pilgrim 2011; Uphoff 2012). This is not an exhaustive list of stresses and drivers determining cereal system outputs (see Table 1-1 for summary of stresses on cereal croplands). However, the key point is that there are complex interactions and feedbacks between varying drivers, internal and external, which control the ability of cereal systems to ensure food security.

Through contributions to both climate change and environmental degradation, agricultural practices in cereal croplands are generating harmful positive feedbacks (Godfray et al. 2010). These feedbacks limit the productivity and sustainability of croplands, reduce the provision of beneficial ecosystem services and, increase the exposure of a greater proportion of cropping systems and the human population to a wider range of dis-benefits including food insecurity (Millenium Ecosystem Assessment 2005; Scherr and McNeely 2008; Godfray et al. 2010; FAO 2011a). Climate change exerts a direct influence on the productivity of cereal crops largely through altering crop physiological and yield forming processes (Tubiello et al. 2007; Lobell and Gourdji 2012). It also interacts with and influences a wider range of drivers and stresses of cereal systems generating positive feedbacks with negative impacts crop production and therefore livelihoods whilst, eroding environmental resilience and societal adaptive capacity (Morton 2007; FAO 2011a; Vermeulen et al. 2012b; Wheeler and von Braun 2013). The anticipated negative impacts, on cereal production and food security, projected to occur without adaptation and readjustment of food-water-energy system interactions to account for pressures from population growth, globalisation and climate change has been eloquently described using the “perfect storm” metaphor

(Beddington 2009; Fig. 1-4). As climate change interacts with biophysical, demographic and socio-economic processes retaining a holistic, integrated approach to developing climate-resilient production within cereal systems which attempt to yield co-benefits increasing resilience to the multitude of cross-scale, cross-sectoral stresses and drivers which determine production and food security (Schmidhuber and Tubiello 2007; FAO 2011a). Adapting cereal croplands to avoid a "perfect storm" of widespread food insecurity and degradation of natural resource bases requires multidisciplinary scientific advances (Beddington 2009; Godfray et al. 2010; Misselhorn et al. 2012).

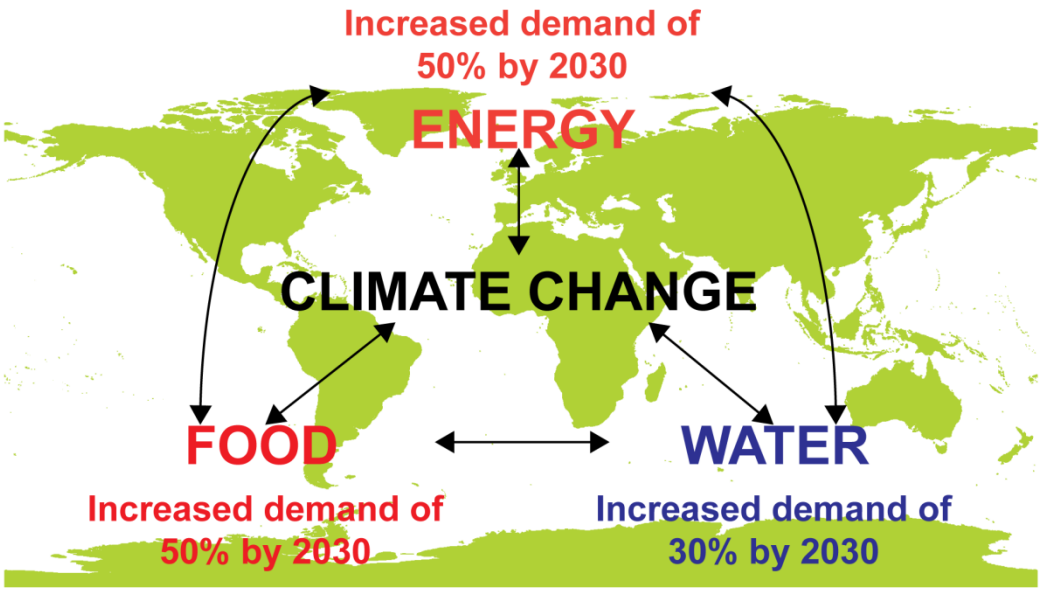

Figure 1-4 The "perfect storm" scenario which could occur by 2030 due to pressures within the food-energy-water nexus and interactions with climate change (Beddington 2009; Poppy et al. 2014).

In most situations, the expansion of croplands with consequent environmental degradation, deforestation, loss of biodiversity, increased GHG emissions, reduced ecosystem service provision and off-farm impacts polluting water resources is deemed unacceptable (Tillman et al. 2002; The Royal Society 2009; Brussaard et al. 2010; Foresight: Final Project Report 2011; Foley et al. 2011). Therefore, 'sustainable intensification', 'organic agriculture, 'integrated agro-ecological farming', 'genetic and crop breeding advances', 'conservation agriculture' or 'resource-conserving' approaches which aim to increase productivity without exceeding the renewable limits

of natural resources are seen as the solution to increase production in an environmentally sustainable manner (Lumpkin and Sayre 2009; The Royal Society 2009; Godfray et al. 2010; Bogdanski 2012; Uphoff 2012). Climate-smart agriculture intersects with these approaches when in a particular system or location they contribute to climate-resilience and realise adaptation and mitigation co-benefits (FAO 2011a; Scherr et al. 2012). While crop simulation modelling and experimental laboratory and field experiments have enhanced understanding of climate influences on crop physiological processes (Challinor et al. 2005; Jagadish et al. 2007; Rang et al. 2011b) there is a need to understand and monitor climate impacts on cereal crop productivity across real agricultural systems. Such an approach, sensitive to space and time varying climate-crop interactions, will more efficiently optimise climate-resilient adaptations across landscapes and agricultural systems and capture spatial trade-offs between increasing productivity and reducing agricultures environmental impact (DeFries and Rosenzweig 2010; FAO 2012; Scherr et al. 2012).

Table 1-2 Climate-smart adaptations for cereal croplands*.

	Sufficient and climate-resilient production	**Minimal impact on ecosystems and ecological processes**	**Reduced GHG emissions and climate change mitigation**
Close yield gaps	Increases production.	Prevents expansion of croplands reducing loss of tropical forests and biodiversity.	Reduced GHG emissions via land conversion.
Mulch and residue retention	Long-term yield benefits, increased resilience to extreme heat events, increased water use efficiency.	Preserves soil moisture, lowers soil and canopy temperature, reduced evaporation, increased infiltration, reduced run-off and soil and wind erosion, enhanced soil microbial activity.	Increased soil organic carbon assimilation, reduced GHG emissions via no residue burning.
Zero-tillage	Yield increases in some cropping systems, often long-term yield increases, reduced water inputs.	Improved water use efficiency, reduced run-off, reduced soil erosion, reduced exposure of soil organic carbon to air preventing its rapid oxidation, less variable soil temperatures.	Reduced GHG emissions via fewer tractor passes.
Alternate wetting and drying/System of Rice Intensification	Questionable rice yield benefits compared to puddled rice but reduced water and irrigation costs so more economic	Reduced irrigation water inputs, dry seeded so avoids formation of puddling pan,	Reduced CH_4 emissions via less anaerobic decomposition.
Laser bed levelling	May increase crop production via improving water use efficiency and reducing risk of water stress.	Reduces run-off and leaching from fields, increases infiltration, increases soil moisture content.	
Agroforestry	Yields can increase as mixture of trees within croplands can create more favourable and stable conditions for crop growth.	Trees protect soil from erosion, reduce run-off and increase infiltration. N-fixing trees can increase soil fertility. Trees can provide shade to crops and soil.	Leguminous trees reduce need for N fertilisers reducing N_2O emissions and also emissions from fertiliser manufacturing. Trees are a carbon sink.
Nutrient Management (Leaf colour chart,Urea Deep Placement)	Possible increase in yields, reduce impact of nutrient limitation. Reduces farmer's links to volatilities in fertiliser prices.	Reduced fertiliser use, reduced leaching of fertiliser, improved soil and water conditions (off-farm and on-farm).	Reduced N_2O emissions.

*** It should be noted that the climate-smart benefits derived from each of these adaptations is system specific and may not yield optimum results in every situation. Giller et al. (2009) provide a review of the limitations and trade-offs associated with implementing agricultural practices associated with climate-smart benefits in smallholder farming in Africa. For example, they comment that there is a trade-off between retaining residues on fields and removing residues for livestock feed. Also, there is need for policy and funding to incentivise uptake of climate-smart practices (Cooper et al. 2013).**

Table Sources: Gupta and Seth 2007; Erenstein and Laxmi 2008; Hobbs et al. 2008; Wassmann et al. 2009; World Bank 2011; Foley et al. 2011; FAO 2011b; Chauhan et al 2012; FAO 2013; Cooper et al. 2013.

1.2 The rice-wheat cropping systems in Punjab and Haryana, north-west Indo-Gangetic Plains

1.2.1 Prevailing environmental, climatic and agronomic conditions in Punjab and Haryana

This section elaborates on the discussion above; firstly the rice-wheat cropping systems of Punjab and Haryana are introduced before a detailed discussion of the multiple stresses placed on these croplands. The scale now shifts from a global and generic scale to the specific study region for this research. The north-west IGP, specifically the states of Punjab and Haryana, are a 'focal' cereal crop production region for India (Fig 1-2). Fig 1-2 shows the location of Punjab and Haryana relative to the rest of India. The cereal production system in Punjab and Haryana are commonly termed India's 'breadbasket' and provide ecosystem services (e.g. crop production) which support the livelihoods of the state's 53 million inhabitants (Saharawat et al. 2009; DES 2011; Chauhan et al. 2012). Cereal production in these states is also vital for national food security efforts; the Government of India purchases large quantities of foodgrains from Punjab and Haryana to supplement national buffer stocks and support the Targeted Distribution Service to poor households (Perveen et al. 2012). Punjab and Haryana supply about 50% of rice and 85% of wheat to Government stocks; the lower proportion of rice procurement is due to production of high quality Basmati rice in Haryana not purchased under government schemes (Singh 2000; Erenstein and Thorpe 2011; Chauhan et al. 2012). Government procurement of rice and wheat from Punjab and Haryana exceeds levels of procurement from the neighbouring state of Uttar Pradesh, despite Uttar Pradesh's significantly larger area under cultivation and greater levels of production (Fig 1-5); though yields are higher in Punjab and Haryana with a

greater percentage of croplands under irrigation (Fig. 1-2). It is clear that the livelihoods and food security of millions of people, nationwide, would be vulnerable to losses or variability in cereal production in Punjab and Haryana.

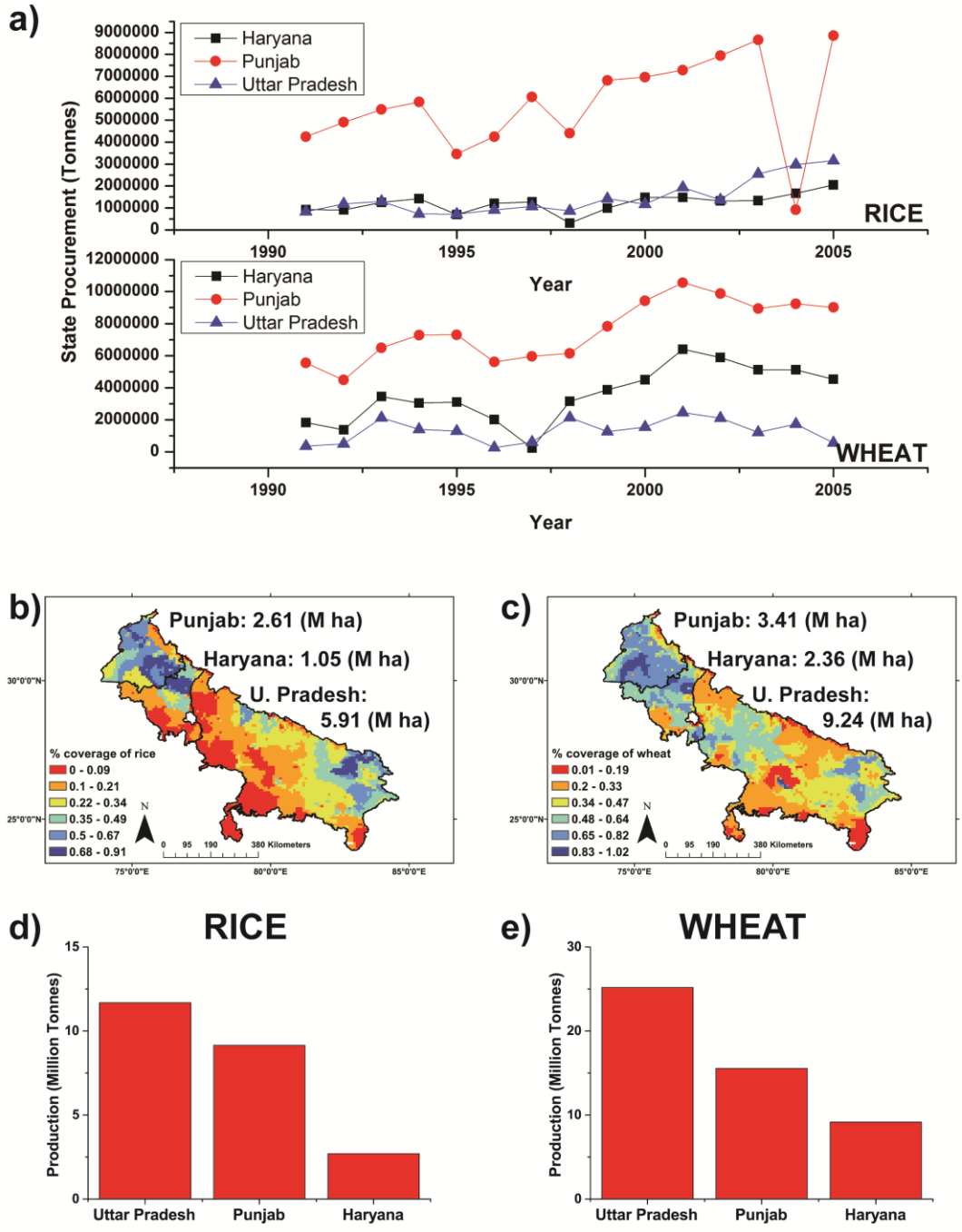

Figure 1-5 a) State-wise procurement of rice and wheat crops from Punjab, Haryana and Uttar Pradesh (DES, 2011), b) fraction a 5 minute grid cell covered by rice cropping (circa 2000) (Monfreda et al. 2008) and total area cropped, c) fraction of a 5 minute grid cell covered by wheat cropping (circa 2000) (Monfreda et al. 2008) and total area cropped, d) state-wise production of rice (Million Tonnes) in 2000 and e) state-wise production of wheat in 2000.

Typically the soils of Punjab and Haryana have a lower soil capability index score than the other reaches of the IGP (Erenstein et al. 2007). However the central plain regions have the highest soil capability index scores within the states of Punjab and Haryana (Erenstein et al. 2007). The majority of precipitation in Punjab and Haryana is received during the Indian Summer Monsoon (ISM) season, June to September (Tyagi et al. 2005). Normal ISM precipitation totals vary across Punjab and Haryana ranging from 156mm to 1091mm with large amounts of inter-annual variability (Fig. 1-6; Duncan et al. 2013). Punjab and Haryana also experience a higher frequency of drought years relative to the majority of other Indian states (Pai et al. 2011; Duncan et al. 2013). The regions of Punjab and Haryana which experienced the highest levels of inter-annual variability in precipitation, the lowest normal levels of ISM precipitation, the highest frequency of severe drought years and increasing trends in recurrence of drought years and inter-annual variability in ISM precipitation were located in the southern portions of the states in the arid regions (Pai et al. 2011; Duncan et al. 2013).

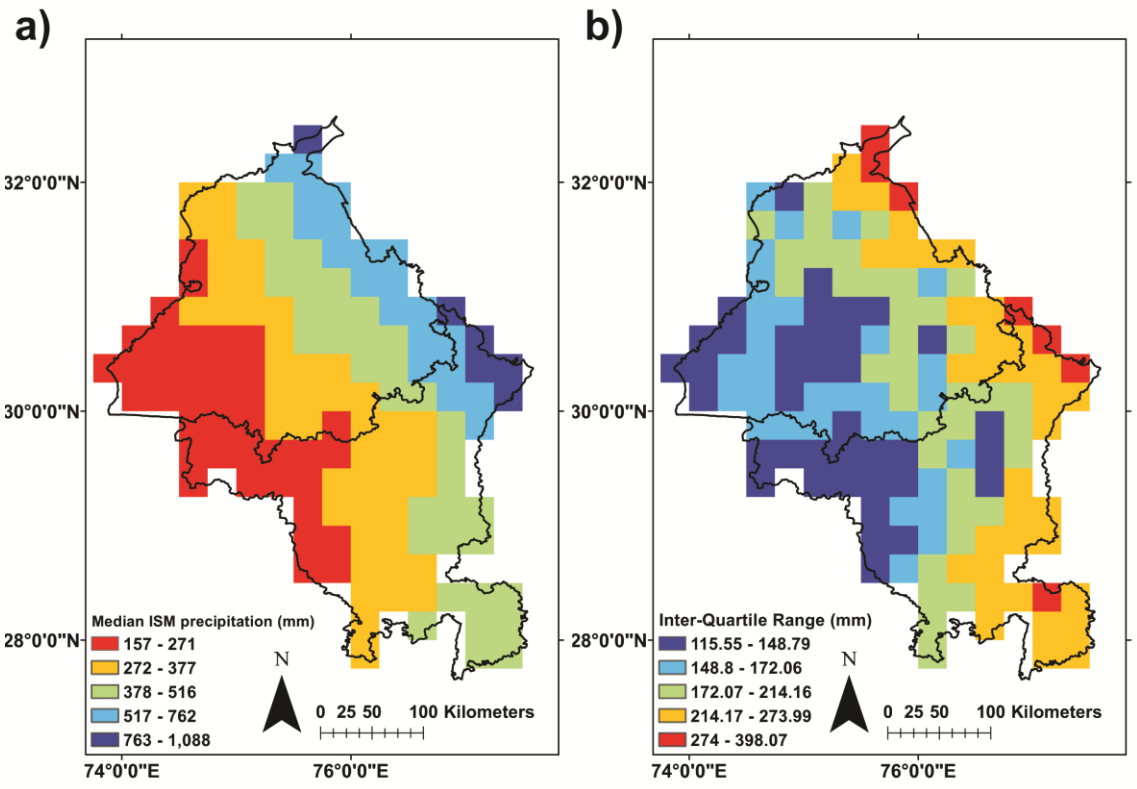

Figure 1-6 a) median Indian Summer Monsoon precipitation (June-September) from 1951-2007 and, b) inter-quartile range in Indian Summer Monsoon precipitation between 1951 and 2007. Both computed from the APHRODITE daily gridded precipitation dataset.

Punjab and Haryana were focal points for Green Revolution developments from the mid-1960's onwards as India sought to achieve self-sufficiency in food production (Singh 2000). Under the Green Revolution agricultural production in Punjab and Haryana was increased via both extensification and intensification of cereal croplands alongside shifts in cropping systems and technological advances (Singh 2000; Murgai et al. 2001). During the initial Green Revolution developments and in the subsequent decades a rice-wheat cropping system became dominant across both states (Singh 2000; Ambast et al. 2006; Perveen et al. 2012). Rice is grown in the monsoonal *kharif* season (June to October) and wheat is grown in the dry *rabi* season (November to April). The area under rice and wheat cropping in Punjab and Haryana has increased significantly since the mid-1960's (Ambast et al. 2006). Prior to the Green Revolution developments rice was not a dominant *kharif* crop in Punjab and crops such as barja (pearl millet), cotton and sorghum all had larger or equivalent proportions of cropped area (Singh 2000). As well as increasing area under cereal cropping, the productivity of rice and wheat crops increased under Green Revolution technologies. Rice and wheat yields in Haryana were 1.06 and 1.28 Tonnes ha^{-1} in 1965-1966 and were 2.7 and 5.03 Tonnes ha^{-1} in 2011-2012 respectively (Singh 2000; DES 2011).The technological and agronomic advances which facilitated increased production and productivity of croplands in Punjab and Haryana centred around high levels of fertiliser and irrigation inputs applied to HYVs (Murgai et al. 2001; Erenstein 2011; Chauhan et al. 2012).

Generally Punjab and Haryana have higher levels of physical, human, social and financial capital than other portions of the IGP (Erenstein et al. 2007). The average farm size, herd size, irrigation capacity, levels of farm mechanisation, rural female literacy, immunisation rate, share of villages with paved road access and, share of villages with credit and banking facilities are higher in Punjab and Haryana than other IGP states (Erenstein et al. 2007). This reflects the enhanced agricultural infrastructure developed under the Green Revolution; the benefits of Green Revolution technologies largely bypassed other portions of the IGP (e.g. Bihar and eastern Uttar Pradesh) (Aggarwal et al. 2004; RWC 2006). The dominant holdings are classified as semi-medium, medium and large which corresponds to average farm sizes of 2.87 ha, 6.09 ha and 17.95 ha respectively in Haryana and 2.64 ha, 5.74 ha and 14.75 ha in Punjab

(Agricultural Census 2012). This is a reflection that the majority of farms in Punjab and Haryana are market-orientated rather than subsistence, privately owned, with higher levels of seasonal in-migration of agricultural labourers and use of casual labour at specific times in the cropping calendar (Erenstein and Thorpe 2011). There is evidence that increased financial returns due to Green Revolution advances led to greater investment in schooling and, thus, boosted levels of education in Punjab (Murgai et al. 2001). Women in Punjab and Haryana play a limited role in crop production due to higher levels of mechanisation and use of hired labour (Erenstein and Thorpe 2011). There are also gender differences in wages with men receiving comparably higher wages than women in both Punjab and Haryana (Erenstein 2011). However, the increasing mechanisation of agriculture (e.g. tractors for ploughing and tillage, combine harvesters for harvesting) reduces demand for labour which compounds poverty issues in the poorest segments of the rural population (Erenstein and Thorpe 2011).

There is a lower proportion of the population below the poverty line in Punjab and Haryana (6.4 and 8.3% respectively) compared to the rest of the IGP region (27.7 – 39.3%) reflecting the importance of agricultural development (Erenstein et al. 2007; Erenstein and Thorpe 2011). The value of land in Punjab and Haryana is high especially in irrigated areas or areas where the high value basmati crop is grown (Erenstein 2011). Land access is a key asset in Punjab and Haryana, over half the households in the rice-wheat system have access to land with the remaining households often providing agricultural labour (Erenstein 2011). Livestock in Punjab and Haryana is predominantly Buffalo due to dietary preference for high-fat milk; crop residues from the wheat crop provide main livestock feed and livestock dung is the fuel source (Erenstein and Thorpe 2011). Livestock in Punjab and Haryana is stall-fed throughout the year with very little grazing land (Erenstein 2011). Despite large ruminant density in Punjab and Haryana being twice the national average, and over half the milk produced being sold in markets, compared to cereal cropping, livestock activities have a less significant role in supporting livelihoods (Erenstein and Thorpe 2011).

The development, and widespread adoption, of HYVs of rice and wheat supported by high levels of fertiliser and irrigation inputs led to increased crop yields. In the 1960's

semi-dwarf wheat cultivars developed at International Maize and Wheat Improvement Centre (CIMMYT) Mexico were introduced to Punjab and Haryana which had lower temperature requirements for germination and tillering (Chauhan et al. 2012). This enabled later sowing of the wheat crop subsequently lengthening the preceding *kharif* cropping season encouraging development of rice cropping. The first HYV rice variety was released in 1965 (Taichung Native 1), followed by releases of several improved varieties over the past 45 years which focus on improving grain size, quality and yield, shortening time to maturity and developing resistance to pests and disease (e.g. bacterial blight) (Rang et al. 2011a). In the early 1960's tall, low yielding basmati rice was grown over a limited extent in Punjab and Haryana; now HYV rice varieties are more dominant (Rang et al. 2011a). There is still significant cultivation of basmati rice in Haryana, which is India's leading state in exports of basmati rice (Erenstein 2011). The semi-dwarf HYVs are typically more sensitive to fertilisers and resistant to lodging due to their shorter stem length (Wassmann et al. 2009). The improved canopy architecture of semi-dwarf HYVs of rice crops lowers canopy temperature, facilitates transpiration cooling mechanisms enabling rice to be grown in warmer environments (Wassmann et al. 2009). This was an important development for growing rice in the semi-arid regions of Punjab and Haryana. Increases in fertiliser applications also contributed to the success of HYVs and increased crop yields since the Green Revolution. Fertiliser application in Haryana increased from three to 130 kg ha^{-1} between 1970 and 2000 (Singh 2000) and in Punjab fertiliser application increased from 33 to 155.9 kg ha^{-1} from 1966 to 1994 (Murgai et al. 2001).

There was a limited surface irrigation infrastructure developed during the 19th century in the IGP but the extensive irrigation development associated with the Green Revolution in the mid to late 20th century was predominantly centred on groundwater extraction (Erenstein 2009b). Currently irrigation in Punjab and Haryana is often a conjunctive use of electric and diesel powered tubewells for groundwater extraction and surface water extracted from canals (Tyagi et al. 2005; Erenstein 2009b). In Haryana there is a large proportion of electric tubewells as the State Electricity Board maintained a good electricity connection and electric power was subsidised (Tyagi et al. 2005; Erenstein 2009b). In 2009-2010 98.4% of foodgrains in Punjab were irrigated

and 89% of foodgrains in Haryana were irrigated (DES 2011). It was the access to irrigation in Punjab and Haryana which supported puddled rice cropping in the semi-arid environment with typically coarse and porous soils (Gajbhiye and Mandal 2000; Erenstein 2009b; Chauhan et al. 2012). The rice-wheat double cropping system, and in particular rice cropping, is focused in the central plain regions of Punjab and Haryana coinciding spatially with good and marginal groundwater quality, high density of tubewells, loamy alluvium soils, higher relative soil capability, and higher precipitation levels than the southern arid regions (Gajbhiye and Mandal 2000; Ambast et al. 2006; Erenstein et al. 2007; Duncan et al. 2013). Rice cropping is reliant on irrigation to maintain anaerobic, ponded conditions with an average of 34.5 irrigations per growing season in Haryana (Erenstein 2009b). This is 10 times more irrigations than is applied to the subsequent wheat crop; this is partly due to rice's higher water requirements and also poor water management. Puddled, transplanted rice has reduced water productivity compared to wheat crops; for example, Saharawat et al. (2010) noted water productivity[1] for rice of 2.41 kg ha^{-1} mm^{-1} whereas wheat had a water productivity of 15.31 kg ha^{-1} mm^{-1} on an experimental farm in Haryana in 2005.

In the southern portions of Punjab and Haryana, where there is sandy desert soils, lower precipitation levels and poor quality of groundwater, the *rabi* wheat crop is typically grown in rotation with cotton, maize and pearl millet (Ambast et al. 2006). In these regions the wheat crop is more resilient due to its salt tolerance and lower water requirements (Ambast et al. 2006). There is increasing reliance on groundwater sources to support the *rabi* wheat crop when water levels in surface canals are lower (Erenstein 2009b). The lack of reliability and equal distribution in flows of water in surface canals coinciding with approximately 70% of Punjab and Haryana having shallow groundwater of good or marginal quality led to the rapid uptake tubewells (Tyagi et al. 2005; Ambast et al. 2006). There is a 'warabandi', priority access, distribution scheme in operation which allocates flows of water in surface canals (Tyagi et al. 2005; Ambast et al. 2006). This system allocates water on a rotation principle of seven days of flow followed by 14 days of no-flow; this system often fails to deliver

[1] Water productivity refers to crop yield per unit volume of water applied.

water at key crop requirement stages and water quantities vary along the canals (Tyagi et al. 2005). That the annual evapotranspiration of rice-wheat double cropping system (>1400mm) exceeds annual precipitation totals highlights its dependency on reliable irrigation (Ambast et al. 2006; Erenstein 2009b).

A supportive policy and institutional environment contributed to the uptake of Green Revolution technologies and subsequent agricultural development and yield increases in Punjab and Haryana. Inputs to the rice-wheat system of credit, fertiliser, power and irrigation water were heavily subsidised by the Government of India (Murgai et al. 2001). Through Government procurement, and a minimum support price, a guaranteed market for rice and wheat crops was provided for farmers in Punjab and Haryana (Erenstein and Thorpe 2011; Perveen et al. 2012). This protected farmers growing rice and wheat crops from risks associated with price fluctuations in open markets (Erenstein and Thorpe 2011). In Haryana electricity costs for groundwater extraction were heavily subsidised whilst in Punjab power for agriculture was free from 1997 to 2002 and since 2005 (Erenstein 2009b; Perveen et al. 2012). The price of irrigation water is either free or heavily subsidised and the electric grid in Haryana is maintained at acceptable levels whilst in Punjab all rural villages were electrified in the 1980s (Murgai et al. 2001; Erenstein 2009b). This contributed to farmers investing in a low-diversity, irrigation dependent rice-wheat monoculture across much of Punjab and Haryana. There is also a focus of agricultural research institutes and universities in north-west India (e.g. Punjab Agricultural University which developed several HYV rice cultivars) (Murgai et al. 2001; Rang et al. 2011a). This ensured farmers in Punjab and Haryana were exposed to the latest technological and agronomic advances; recently this was reflected in the more rapid uptake in zero-tillage practices in Punjab and Haryana compared to other parts of the IGP (Erenstein and Laxmi 2008; Erenstein 2010a).

1.2.2 Multiple Stresses

Typical of agricultural landscapes globally, multiple interacting stresses and drivers impact the cropping systems of Punjab and Haryana (Table 1-3). It is the interaction and feedbacks between these drivers which determine levels of crop productivity,

vulnerability and resilience to climatic variability and change; this is illustrated by the conceptual diagram in Fig 2-3. However, recently several aspects of the rice-wheat production system are displaying negative trends suggesting the high levels of productivity and benefits delivered under current practices and system functioning are unsustainable (RWC 2006; Gupta and Seth 2007). Often these negative trends (e.g. stagnating or declining crop yields) are resultant from sub-optimal, intensive agricultural practices degrading the natural resource base undermining the yield of future cropping seasons (Aggarwal et al. 2004; Ambast et al. 2006; Erenstein and Thorpe 2011; Chauhan et al. 2012). For example, it has been noted that marginal and poor quality groundwater irrigation in Haryana has led to increased soil salinity in the lower reaches of irrigation canal systems lowering rice yields or forcing farmers to shift crop types (Tyagi et al. 2005). The following discussion will provide more detail on some of these negative trends and drivers which serve to undermine sustainable levels of crop production in the IGP. This will provide useful context for the subsequent research papers.

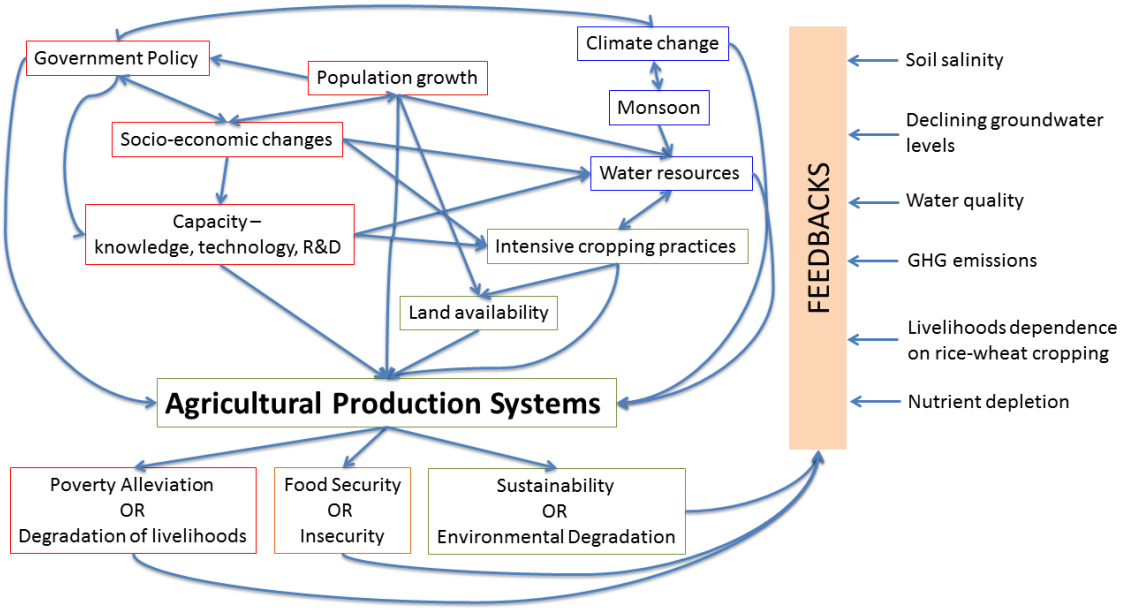

Figure 1-7 Conceptual diagram illustrating the systemic nature of rice-wheat cropping systems in Punjab and Haryana and associated interactions and feedbacks between drivers and outcomes. Red boxes correspond to socio-economic factors, green boxes to landscape, agronomic and environmental factors and blue boxes to climatic and water factors.

Table 1-3 Summary of key stresses affecting the rice-wheat production system in Punjab and Haryana

Stress	Impact
Population growth and demand for national welfare schemes	**The population in Punjab and Haryana is projected to increase, as is the population of India of which large portions are food insecure. This will place increased demand on the focal croplands on Punjab and Haryana.**
Stagnating productivity	**Whilst demand for rice and wheat production from Punjab and Haryana increases there has been a slow down, and in some locations, a decline in growth of crop yields.**
Limited room for expansion	**There is little room to expand croplands in Punjab and Haryana, either in terms of area or intensification. Worryingly some rice and wheat croplands are being lost due to environmental degradation.**
Soil degradation	**Intensive cropping and irrigation associated with Green Revolution developments has degraded the quality of soil, reducing soil physical properties, water holding capacity, nutrient and soil organic carbon status and increases salinity.**
Water availability	**There has been a dramatic decline in groundwater levels in Punjab and Haryana associated with irrigation withdrawals. This trend is not sustainable.**
Water quality	**Increased groundwater extraction from deeper reserves has increased salinity of water resources. Also, leaching of nutrients from fields has polluted water sources (often downstream).**
Climate change	**Climate change will have multiple impacts on rice-wheat cropping in Punjab and Haryana. Cereal crops are sensitive to extreme heat events during anthesis, and extreme heat days are projected to increase of northern India. Warming temperatures and more variable precipitation will place greater pressure on already stressed irrigation resources.**

Table sources: Aggarwal et al. (2004); Tyagi et al. (2005); Ambast et al. (2006); Hobbs et al. (2008); Rodell et al. (2009); Wassmann et al. (2009); DES (2011); Lobell et al. (2012); Perveen et al. (2012); Chauhan et al. (2012).

1.2.2.1 Stagnating crop yields and population growth

Despite gains in productivity during the Green Revolution, recently crop yields have stagnated and declined whilst population in Punjab and Haryana has continued to grow; this reflects a global situation as discussed in Table 1-1 (Aggarwal et al. 2004; Erenstein and Thorpe 2011). This situation places obvious pressure on the rice-wheat cropping systems to arrest declining productivity to keep up with demand (RWC 2006). Table 1-4 summarises some of the key factors limiting rice and wheat crop yields or contributing to stagnating productivity growth. In Punjab trends in rice yield have plateaued whereas in Haryana there has been a noted decline in rice yields, whilst yields of wheat have increased there has been a slowdown in productivity growth (Ambast et al. 2006). Similar trends have been observed in long-term field experiments where both rice and wheat yields showed widespread stagnation in yield trends, but declines in rice yield were more widespread than wheat (Ladha et al. 2003). The more pronounced yield declines in rice compared to wheat were partly attributed to greater

genetic gains made to wheat cultivars over the past 40 years, with little increase in the yield potential of rice cultivars since the release of IR8 in the 1960's (Ladha et al. 2003). The yield improvements in wheat cultivars generated a genetic gain of 1.6% per year due to a greater number of spikes per grain and grains per unit area (Ladha et al. 2003). Other causes for the slowdown in productivity and declining yields are degradation of the natural resource base (e.g. soil fertility), decrease in solar radiation and increases in minimum temperature (Pathak et al. 2003; Ladha et al. 2003; Aggarwal et al. 2004; Chauhan et al. 2012). There has also been a recent decrease in the total factor productivity (TFP), a ratio of inputs and outputs of a system which is a proxy measure of technological change, in rice-wheat systems in Punjab and Haryana (Murgai et al. 2001; Aggarwal et al. 2004). Of the cropping systems (rice-wheat, wheat-cotton, wheat-maize) in Punjab and Haryana, the rice-wheat system had the lowest total factor productivity growth due to intensive inputs required to deliver outputs (crop yield) (Murgai et al. 2001; Aggarwal et al. 2004).

Table 1-4 List of factors which explain stagnating or declining growth of rice and wheat crop yields in Punjab and Haryana*.

Cause	Explanation
Distance from irrigation canal	Observations suggest farmers closer to irrigation canals have higher crop yields.
Position within watercourse	Farmers towards the bottom of the irrigation watercourses receive more variable and lower quality irrigation water in canals. This results in lower rice and wheat crop yields.
Intensive tillage in a rice-wheat rotation (formation of puddling pan)	Intensive puddling of the rice crop leads to the formation of shallow puddling pan in the soil. Shallow rice roots cannot penetrate the pan and thus exhaust nutrients in upper soil layers.
Intensive tillage in tropical/sub-tropical climate	Intensive tillage in a tropical/sub-tropical environment constantly aerates the soil and accelerates the oxidation of already limited soil organic matter.
Water quality/quantity	Farmers irrigating with saline groundwater report lower crop yields. Also, reduced water availability means farmers mine deeper, more saline groundwater which has positive feedbacks on soil quality and water availability (more water required to flush out saline soils).
Nutrient depletion	There have been declines in the nutrient status of soils associated with intensive rice-wheat cropping (including micronutrient deficiency). Nutrient limitation has been attributed to yield declines and stagnation in on-farm yields.
Extreme heat events	Increased extreme heat events during the wheat crop growing season accelerate crop senescence.
Increased night-time temperatures	Trends of warming night-time temperatures linked to declining on-farm rice yields, warming temperatures increase photorespiration and accelerate phenological development.
Decreased solar radiation	Trends of decreased solar radiation linked to declining rice yields; solar radiation is key for photosynthesis.
Crop residue burning	Atmospheric particulates and brown clouds from crop residue burning can impact monsoon circulation. Models suggest atmospheric brown clouds limit rice crop production. Burning crop residue also removes nutrients from the soil: one tonne of wheat residue contains 4.8kg N, 0.7 kg P (phosphorus) and 9.8 kg K (potassium).
(Lack of) Genetic gains	There has been little increase in the yield potential of rice cultivars developed since the 1960s.

***It should be noted that these factors impact crop yields over varying spatial and temporal scales (i.e. some will be location specific such as distance to a canal, others will impact crop yields immediately such as an extreme heat event and some factors will take a longer period of time to influence crop**

yield such as the build up of a puddling pan depleting nutrients in the upper soil layers or long-term build up of salinity with poor quality irrigations).

Table sources: Pathak et al. (2003); Ladha et al. (2003) Aggarwal et al. (2004); Tyagi et al. (2005); Auffhammer et al. (2006); Lobell et al. (2010); Chauhan et al. (2012); Lobell et al. (2012).

1.2.2.2 Soil Quality

The conventional agricultural practices in Punjab and Haryana, associated with Green Revolution advances, have deteriorated the soil quality (Aggarwal et al. 2004; Erenstein et al. 2007). Rice and wheat crops are typically grown under different soil conditions; rice requires anaerobic soil conditions compared to wheat which favours aerobic soil (Erenstein 2009b; Erenstein 2010b; Chauhan et al. 2012). Conventional rice cropping requires continuous puddling with intensive tillage on ponded or submerged fields to reduce soil aggregate sizes, reduce macro-porosity between soil particles to achieve anaerobic conditions (Chauhan et al. 2012). This leads to increased soil compaction due to crystallisation of ferric oxides cementing soil particles and therefore the development of a hard pan, this increases the bulk density of the soil and reduces hydraulic conductivity below the surface ploughed layers (Ladha et al. 2003; Chauhan et al. 2012). The stagnating and declining rice yields may be partly caused by declines in soil quality over time associated with puddled rice cropping on unfavourable soils. Rice is a shallow rooting crop and is therefore sensitive to formation of surface pans and suffers from nutrient deficiency when nutrients are depleted in the top 30 cm of the soil (Ladha et al. 2003). Wheat cropping requires well drained, aerobic soils, thus, requiring intensive tillage after *kharif* rice cropping via several tractor led ploughing, harrowing and planking operations (Erenstein and Laxmi 2008). The hard pan developed under puddled rice cropping can harm root growth of the subsequent wheat crop (Chauhan et al. 2012). However, wheat is more resilient to deteriorating soil quality having greater salt tolerance, longer roots and a longer growing season enabling it to mine more nutrients (Ladha et al. 2003; Tyagi et al. 2005). This likely explains why yield declines in rice have been more pronounced than in the wheat crop (Ladha et al. 2003). The soil management operations required to shift soil from aerobic to anaerobic has noticeable implications for soil physical and biogeochemical

properties and is reported as one of the major contributors to observed stagnation in crop productivity (Ladha et al. 2003; Aggarwal et al. 2004; Chauhan et al. 2012).

Soils in Punjab and Haryana are becoming increasingly depleted of soil organic carbon and nutrients due to tillage and poor soil management and intensive cropping mining nutrients (Singh 2000; Aggarwal et al. 2004; Chauhan et al. 2012). Intensive rice-wheat cropping has led to declines in soil fertility in Punjab and Haryana. In Haryana the soil areas with low phosphorus levels increased from 3.3% in 1980 to 73% in 1995 (Singh 2000), though Ladha et al. (2003) suggest that adequate amounts of phosphorus fertiliser application can meet crop demands. Between 1967 and 1997 there have been noted declines in soil phosphorus across both Punjab and Haryana (Pathak 2010). The area of soils with high levels of potassium decreased from 91.1% in 1980 to 61.5% in 1995 (Singh 2000), soil potassium depletion was a contributing factor to noted yield declines in several long-term field experiments across the IGP (Ladha et al. 2003). Haryana has low levels of soil nitrogen, with Punjab having slightly higher levels (Singh 2000; Pathak 2010). The soils of the north-west IGP also have low organic matter and soil carbon content, which is further reduced due to intensive tillage operations (Ladha et al. 2003; Daughtry et al. 2006; Erenstein and Laxmi 2008). The loss of soil carbon and organic matter reduces soil cation exchange capacity, the number of active sites involved in nutrient transfer (Ladha et al. 2003). There is also a noted sulphur deficiency in the coarse textured, low organic matter soils of Punjab and Haryana (Chauhan et al. 2012) and evidence of micronutrient deficiency, especially declining zinc levels (Aggarwal et al. 2004). Farmers are having to apply greater amounts of fertiliser (N:P:K; nitrogen:phosphorus:potassium) for diminishing returns and account for losses in fertiliser via leaching, run off and soil erosion (Aggarwal et al. 2004; Chauhan et al. 2012). The nutrient usage of crops in the rice-wheat system in Punjab and Haryana is greater than in any other state in the IGP rice-wheat cropping system (Abrol 1999).

The development of an extensive irrigation infrastructure, especially irrigation with poor or marginal quality saline groundwater has led to increased soil salinity across Punjab and Haryana (Aggarwal et al. 2004; Tyagi et al. 2005; Ambast et al. 2006). Nearly two-thirds of Haryana is underlain by deep (>40m) brackish groundwater and

shallow groundwater is saline and of marginal quality (Tyagi et al. 2005). Deeper, saline, groundwater is increasingly being mined by lowering centrifugal pumps into pits, or using submersible pumps, to account for falling groundwater levels (Erenstein 2009b). This will lead to increased soil salinity problems. The porous soils of Punjab and Haryana require constant irrigation, especially to maintain puddled rice cropping conditions, which, thus, increases soil salinity (Ladha et al. 2003; Chauhan et al. 2012). Increasing temperatures associated with global warming will further compound soil salinity problems in Punjab and Haryana increasing crop evapotranspiration and, thus, capillary action drawing saline waters to the surface (Wassmann et al. 2009). The irregularity of surface canal water in Punjab and Haryana makes it difficult to leach salts away from the soil surface (Tyagi et al. 2005; Wassmann et al. 2009). This is particularly problematic for rice cropping as rice is more sensitive to saline soils than wheat; in some instances salinity forces farmers to growing *kharif* barja (pearl millet) in Haryana (Tyagi et al. 2005). A study of a rice-wheat cropping system with conjunctive use of groundwater and surface irrigation showed salinity to be the biggest factor reducing wheat and rice crop yield and that the quality of groundwater varies spatially (Tyagi et al. 2005).

1.2.2.3 Water Resources

Evidence from satellite observations from the NASA Gravity Recovery and Climate Experiment (GRACE) and simulations of soil-water variability showed that groundwater extraction is greater than recharge in Punjab and Haryana, with a mean decline in groundwater levels of 4 cm $year^{-1}$ between 2002 and 2008 (Rodell et al. 2009). There are local variations in this rate of decline, between 1982 and 1987 in central Punjab the average rate of decline was 18 cm $year^{-1}$ and this rose to 42 cm $year^{-1}$ between 1997 and 2002 (Perveen et al. 2012). This decline is attributed to extraction of groundwater for irrigation as there was no change in precipitation and other storage components of the hydrological cycle (soil moisture, glaciers, biomass, and surface water including rice paddies) (Rodell et al. 2009). Most of the water lost via groundwater extraction leaves the region via evapotranspiration or run-off (Rodell et al. 2009). This decline in groundwater is confirmed by other studies using satellite observations (Tiwari et al. 2009) and Central Groundwater Board monitoring in India

reported 80% of blocks (political subdivisions) in Punjab have over-exploited groundwater, and, state-wise groundwater availability for irrigation was deficient by 14.57 billion cubic metres (bcm) (Central Ground Water Board 2012). An assessment of groundwater footprints (the aquifer area required to sustain groundwater use and groundwater dependent ecosystem services) indicates that groundwater extraction in the Upper Ganges basin is the most unsustainable of all aquifers globally (Gleeson et al. 2012). The water table has fallen between 0m to >15m over the past 20 years through much of central and northern Punjab and Haryana, this corresponds to areas with the greatest density of tubewells and water intensive rice-wheat cropping (Ambast et al. 2006). In 2009 Punjab 33.97 billion cubic metres of groundwater are extracted for irrigation compared to only 0.69 billion cubic metres for industrial and domestic uses (Central Ground Water Board 2009).

Issues of declining groundwater quality also compound problems associated with groundwater declines. Much of the groundwater in north-west India is saline in nature with state-wise and local watershed gradients in levels of salinity (Tyagi et al. 2005). At the state level groundwater quality declines (increases in salinity) towards the southern portions of Punjab and Haryana (Abrol 1999; Ambast et al. 2006) whereas variations in irrigation water salinity have been documented within local watersheds and irrigation canal systems (Tyagi et al. 2005). The increasing extraction of shallow groundwater reserves has deteriorated groundwater quality due to increasing mining of deeper more saline groundwater (Abrol 1999; Tyagi et al. 2005). The intense use of fertilisers and pesticides in the rice-wheat cropping system has also caused declines in groundwater quality (Abrol 1999). It is likely that climate change (e.g. increasing temperatures increasing crop water demand), population growth and urbanisation will increase competition for already over-used groundwater resources (Rodell et al. 2009; Moors et al. 2011).

1.2.2.4 Government Policy

Government policy and incentives encouraged and facilitated the development of the rice-wheat cropping system and the subsequent productivity gains (Singh 2000; Erenstein 2009b; Perveen et al. 2012). However, such policy has created a policy

environment and agricultural system which degrades the natural resource base, compounds yield gaps, and contributes to undermining the long-term sustainability of agricultural production in the region (Aggarwal et al. 2004; Gupta and Seth 2007; Erenstein 2009b; Perveen et al. 2012). A combination of the Government providing a guaranteed market and minimum support price for the rice and wheat crops, subsidies and low prices for irrigation water and power for irrigation extraction have led to farmers investing their livelihoods in a rice-wheat monoculture (Murgai et al. 2001; Erenstein 2009b; Erenstein and Thorpe 2011; Perveen et al. 2012). The resident natural resource base (e.g. soil or water resources) cannot sustain the demands of the rice-wheat system, exemplified by increasing reliance on fertiliser applications and groundwater extractions (Aggarwal et al. 2004; Ambast et al. 2006; Rodell et al. 2009). These subsidies also encourage farmers to be wasteful in their use of irrigation water (Erenstein 2009b) There are also political issues which inhibit removal or readjustment of policy which supports rice-wheat cropping and encourages widespread groundwater extraction (Erenstein 2009b). For example, in Punjab farmers on small and medium sized holdings gain the most from subsidies for irrigation and also make up the majority of the electorate (Murgai et al. 2001).

1.2.2.5 Climate Change

Alongside stresses of water scarcity, degradation in the natural resource base, an existent unsustainable agronomic infrastructure, population growth and associated food demand the rice-wheat cropping systems will have to contend with and adapt to climate change over the coming decades (Aggarwal et al. 2004). Linear trend analysis applied to observational data showed statistically significant warming trends between 1971 and 2003 during winter and monsoon seasons, and annually, over north-west India (Kothawale and Rupa Kumar 2005). Ensemble runs of regional climate models (RCM) showed a uniform signal in warming trends over north India (Moors et al. 2011; Mathison et al. 2013). This modelling study suggested a rise in mean temperature of 2.5-3°C by 2050 under the Special Report on Emissions Scenarios (SRES) A1B scenario (Mathison et al. 2013). The projected warming temperatures will influence crop water use and irrigation requirements; Doll (2002) estimate irrigation water requirements in the Ganges basin will increase from 61.5 km^3 $year^{-1}$ to between 66.4 km^3 $year^{-1}$ and

74.6 km^3 $year^{-1}$ due to climate change. Another modelling study using the PRECIS RCM also reported warming trends over Punjab and Haryana for the time-slice 2070-2100 under the A2 and B2 SRES scenarios (Rupa Kumar et al. 2006). Given the range of models reporting a similar warming signal there is some certainty in forecasts of increasing temperature over Punjab and Haryana, however the magnitude of warming varies under different emissions scenarios (Rupa Kumar et al. 2006; Mathison et al. 2013).

GCMs suggest an increase in ISM precipitation associated with increased atmospheric moisture content over the Indian Ocean increasing vertically integrated moisture fluxes towards the Indian continent (Turner and Annamalai 2012). However, under A2 and B2 SRES scenarios simulated using the PRECIS RCM north-west India experienced declines in ISM precipitation between 2070-2100, though small increases were simulated in northern Punjab and Haryana (Rupa Kumar et al. 2006). Four models from the CMIP3 ensemble, which best simulate the monsoon cycle, also reported slight decreases in ISM precipitation in response to doubling atmospheric CO_2 in north-west India (Turner and Annamalai 2012). The best four CMIP5 models, judged in terms of ability to represent observed monsoon conditions, suggest slight increases in annual and ISM precipitation over north-west India, consistent with multi-model ensemble projections from CMIP3 models (Lee and Wang 2012). Generally in terms of representing the annual cycle and spatial pattern of ISM precipitation CMIP5 multi-model means have greater skill than CMIP3 multi-model means (Sperber et al. 2012). This is likely due to improved horizontal resolution in CMIP5 models facilitating better representation of orographic variability (Sperber et al. 2012). However, ensemble simulations of ISM precipitation, whether using RCMs or GCMs, show considerable uncertainty in future trends (Annamalai et al. 2007; Moors et al. 2011; Turner and Annamalai 2012; Mathison et al. 2013). RCM ensemble simulations of ISM precipitation over north India show little consistency in magnitude or sign of future precipitation totals, with fragmented spatial patterns in grid cells registering increasing trends relative to baseline levels (Moors et al. 2011; Mathison et al. 2013). Only six out of the 18 GCMs used in the IPCC AR4 produced a reliable simulation of monsoon conditions (Annamalai et al. 2007) and under the A1B SRES scenario the CMIP3 GCMs

display both increasing and decreasing trends and differences in inter-annual variability up to 2100 (Turner and Annamalai 2012). Inter-model spread in monsoon simulation is present in the more recent range of CMIP5 models too (Lee and Wang 2012). Given the uncertainty in projections of ISM precipitation, with ensemble model projection showing differences in sign and magnitude there is a need for flexibility in water resources management (Mathison et al. 2013).

1.2.2.6 Conventional versus conservation agricultural practices

Conventional agricultural practices in Punjab and Haryana, which became widespread with the adoption of Green Revolution technological advances, centre around a rice-wheat monoculture supported by intensive fertiliser and irrigation water inputs (Singh 2000; Gupta and Seth 2007; Chauhan et al. 2012; Perveen et al. 2012). Here conventional agricultural practices refer to agronomic practices involving tillage and intensive inputs following the distinctions between conventional and conservation agriculture of Hobbs et al. (2008). The *kharif* rice crop is transplanted onto paddy fields, maintained in a puddled state via irrigation applied to well drained soils with intensive tillage operations prior to sowing (Chauhan et al. 2012). Maintaining puddled, anaerobic paddy fields for rice cropping was a mechanism to prevent weed growth (Hobbs et al. 2008) In contrast to the rice crop, grown in anaerobic soil conditions, the *rabi* wheat crop is grown on aerobic soil after harvesting the rice crop. To achieve the turn-around between anaerobic soils for rice and aerobic soils for wheat requires several tillage operations for ploughing, harrowing, planking and seeding (Erenstein and Laxmi 2008). In a conventional rice-wheat system turn-around time between rice and wheat crops varies from 2 to 45 days with up to 12 tractor passes (Hobbs et al. 2008).The numerous tillage operations associated with conventional rice-wheat cropping practices, require several hours of tractor use and, thus, bear significant economic costs (e.g. petrol, machinery hire) and emit GHGs (Erenstein and Laxmi 2008). The long turn-around time between rice and wheat, delays wheat crop planting, and, thus, shortens the wheat growing season and exposes the wheat crop extreme heat events (Lobell et al. 2012).

Often rice crop residues are burnt in the north-west IGP, and wheat crop residues are either burnt or removed for livestock feed (Badarinath et al. 2006; Pathak et al. 2006; Erenstein and Thorpe 2011). This reflects the fact farmers do not value the use of rice crop residue as livestock feed due to low silica content and concerns about milk quality (Erenstein 2011). Combine harvester use is greatest in rice-wheat cropping systems, particularly for the rice crop to achieve a quick turn-around to allow timely planting of the succeeding wheat crop (Erenstein 2011). The increased use of combine harvesters in Punjab and Haryana increases the amount of crop residue left on fields (Badarinath et al. 2006; Erenstein 2009a). Combine harvesters are often followed by tractor passes with a straw reaper during wheat crop harvest, the combine harvester cuts the crop above ground level leaving remnant straw as stubble (Erenstein 2011). The straw reaper extracts remnant stubble and combine harvested straw as wheat crop residue has the greatest market value as livestock feed (Erenstein 2011). The burning, or removal of crop residues, results in loss of soil carbon and organic matter and, nutrients from the soil system which undermines soil fertility (Pathak et al. 2006). In basmati rice growing areas harvesting is often manual reflecting the taller basmati crops susceptibility to lodging and the fact it is a high value produce requiring careful handling of grains (Erenstein 2011).

Due to observed declining productivity and stagnating crop yields and degradation of the natural resource base associated with conventional agricultural practices there is a growing awareness of a need to adopt sustainable yet equally productive agricultural practices (RWC 2006; Gupta and Seth 2007; Erenstein 2011). Therefore, conservation agriculture practices are being advocated as a sustainable alternative to conventional rice-wheat cropping with aims of protecting natural resources and supporting livelihoods simultaneously (RWC 2006; Gupta and Seth 2007; Jat et al. 2009a; Erenstein 2011). Conservation agriculture approaches aim to achieve dual goals of improving farmers livelihoods and using environmental resources sustainably through integrated management of soil, water and biological systems as defined by the FAO (Hobbs et al. 2008)(http://www.fao.org/ag/ca/). However, there is not one clear definition of what constitutes conservation agriculture, in different agricultural settings a combination of agricultural practices and resource management approaches are

applicable. However, it is generally accepted that conservation agriculture approaches combine minimal soil disturbance (reduced or zero-tillage), permanent or semi-permanent soil cover and crop rotations (Hobbs et al. 2008; Lumpkin and Sayre 2009).

Maintaining permanent or semi-permanent cover of residues and mulch over soils improves water use efficiency reducing evaporation and soil erosion via wind or water and promotes infiltration over run-off (Hobbs et al. 2008). Therefore, crop residue cover on soils has potential to improve irrigation water productivity in cereal croplands (Lumpkin and Sayre 2009). Retaining crop residues, as opposed to removal for livestock feed or burning, prevents loss of nutrients, carbon and soil organic matter (Pathak et al. 2006; Hobbs et al. 2008). There are trade-offs between the value of crop residues for livestock feed (residue removal) and environmental and potential long term yield benefits of residue retention (Erenstein 2011). Soil cover promotes high levels of soil microbial biomass which is important for decomposing organic matter and releasing nutrients (Hobbs et al. 2008). Nutrient cycling and soil organic matter accumulation in soils is enhanced when mulch covers fields with legume cover crops promoting microbiological activity (Hobbs et al. 2008). This enhances levels of nitrogen fixation and, thus, reduces requirements for inorganic nitrogen fertilisers (The Royal Society 2009). Application of rice residue to wheat crop fields has little short-term yield impacts (1-3 years) but leads to longer term gains suggesting its importance in creating a sustainable, high yielding agricultural system (Chauhan et al. 2012).

Zero-tillage of the wheat crop has been the most widely adopted conservation agriculture practice in Punjab and Haryana (Erenstein and Laxmi 2008; Erenstein 2009a). The success of the uptake in zero-tillage wheat was due to farmer demand for the benefits including earlier sowing reducing labour requirements and therefore reduced risk of labour shortages, reduced impact of the weed *Phalaris Minor* and economic savings (Erenstein and Laxmi 2008; Erenstein 2009a). Inverted T-opener zero-tillage drills, common in Punjab and Haryana directly seed, and place fertilisers, into a narrow slot with no or minimal prior field preparation (Gupta and Seth 2007; Erenstein and Laxmi 2008). The seeds and fertilisers are planted at a depth of 7.5 to 10 cm and the T-opener zero-tillage drills cost around US $400 (Erenstein and Laxmi 2008). Adoption of zero-tillage is limited by farmer perceptions and awareness of the

benefits and availability of equipment, a large proportion of zero-tillage drills are hired (Hobbs et al. 2008; Erenstein and Laxmi 2008). Initial research on zero-tillage in India began in the 1970's, but it was in the 1990's when a favourable policy and research environment facilitated by the Rice-Wheat Consortium encouraged the development of zero-tillage incorporating farmer feedbacks and demonstrations (Erenstein and Laxmi 2008; Erenstein 2009a). This was in conjunction with farmers in Haryana requiring methods to enable more timely planting of the wheat crop after the longer maturing basmati rice crop (Erenstein and Laxmi 2008). There has since been a dramatic increase in the area under zero-tillage in Punjab and Haryana since 2000 (Gupta and Seth 2007; Erenstein and Laxmi 2008).

Zero-tillage, with reduced tractor passes and labour requirements delivers substantial economic savings to farmers (Erenstein and Laxmi 2008; Jat et al. 2009a). For the wheat crop, these economic benefits are boosted by improved yield returns with reduced input requirements (e.g. fertiliser, irrigation water) (Gupta and Seth 2007; Erenstein and Laxmi 2008; Saharawat et al. 2012). Zero-tillage wheat can be used with targeted crop rotations and herbicide use to reduce populations of the herbicide resistant weed *Phalaris Minor* (Gupta and Seth 2007). Through reducing soil movement zero-tillage practices provided a control mitigating *Phalaris Minor* outbreaks (Erenstein and Laxmi 2008). Studies have reported an increase in broadleaf weeds in zero-tilled wheat fields suggesting further research is required into integrated pest and weed management (Hobbs et al. 2008; Erenstein and Laxmi 2008). However, in general farmers perceive a reduced weed infestation due to zero-tillage, by as much as 43% less weeds in zero-tillage fields, often due to minimal soil disturbance promoting late emergence of weeds reducing competition with the crop (Gupta and Seth 2007; Erenstein and Laxmi 2008). Conventional tillage leads to declines in soil fertility, organic matter content and soil degradation (Hobbs et al. 2008). This is despite some benefits of nutrient release due to mineralisation and oxidation of soil organic matter after exposure to air; however in tropical environments this promotes rapid processing of organic matter which leads to depletion of soil carbon and soil fertility after continual intensive tillage (Hobbs et al. 2008). Experimental field studies showed improvement in soil physical properties under zero-tillage including stability in

soil aggregation and improved infiltration rates with penetration resistance/compaction reduced in soils between 10 and 25 cm (Jat et al. 2009a). Zero-tillage soils in rice-wheat systems have higher soil aggregates than contemporary conventional tilled and puddled soils; puddled soils also increase soil compaction, break capillary pores and form sub-surface hard pans impeding root growth (Jat et al. 2009a). It has been observed that each centimetre reduction in wheat crop root growth, due to soil compaction caused by puddling of the preceding rice crop, reduces yield by 0.4% (Jat et al. 2009a).

To maximise the long-term sustainability and yield gains of conservation agriculture there is a need to address trade-offs between residue retention and residue removal and combine residue management with zero-tillage in the IGP (Erenstein 2009a; Erenstein 2011). There is therefore a need to strengthen existing research into zero-tillage drills which can seed through crop residue (e.g. happy seeder) as the existing zero-tillage drills do not handle crop residue well (Erenstein 2009a; Erenstein 2011). Research is also being undertaken to develop straw spreaders attached to combine harvesters which evenly distribute straw over fields enhancing the performance of zero-tillage drills (Chauhan et al. 2012). One of the key concepts of conservation agriculture is integration of different management practices. Often crop residue retention and zero-tillage used in conjunction leads to the greatest gains in terms of enhanced carbon sequestration, soil organic matter content in upper soil layers, maintenance of soil physical properties (e.g. higher aggregate stability) and nutrient cycling (Hobbs et al. 2008). This is exemplified by the fact that conventional puddled rice undermines environmental and soil health gains generated from zero-tillage wheat (Erenstein 2011). This highlights the need for research and development to focus on demonstrating and delivering increased yields under zero-tillage rice (Hobbs et al. 2008). Research should focus on developing rice cultivars suitable for aerobic soil and direct seeding as well as investigating options for herbicide use and cover crops to control weeds (Hobbs et al. 2008).

The yield gains from zero-tillage wheat are evident, however the yield benefits from zero-tillage and other resource conserving agricultural practices applied to the rice crop are less clear (Wassmann et al. 2009; Jat et al. 2009a; Saharawat et al. 2010;

Chauhan et al. 2012). Yield losses were reported for rice grown under saturated soil culture, alternate wetting and drying and aerobic conditions compared to puddled rice, but water use efficiency improved under alternate cropping practices (Wassmann et al. 2009). Experimental field studies have shown that conventional tillage or transplanted rice with zero-tillage has a higher yield than direct seeded zero-tillage rice (Saharawat et al. 2010). The same experiments also highlighted that transplanted zero-tillage rice had equivalent yields but improved water savings compared to conventional tillage rice. Crop yields were lower in direct seeded rice with higher levels of spikelet sterility largely attributed to lower moisture content (Saharawat et al. 2010). Puddled rice crops suppress weed crop growth, thus, reducing competition for resources at the time of crop emergence; these benefits are not realised in direct seeded rice which require higher rates of herbicide application (Saharawat et al. 2010). However, given the poor water use efficiency, high water requirements and water losses via seepage and percolation in puddled rice cropping combined with, limited and diminishing water resources and negative impacts on soil conditions there is need for research to identify optimal synergies between numerous resource conserving practices applicable to rice crops. Direct seeded rice delivers water savings compared to conventional tillage, reduced labour requirements overcoming potential labour shortages in Punjab and Haryana and enables more timely sowing of the wheat crop (Chauhan et al. 2012). The reduced duration of direct seeded rice allows earlier planting of the wheat crop, raising wheat crop yields and, thus, contributing to enhanced system productivity despite lower rice crop yields (Saharawat et al. 2010). There is a need to breed rice cultivars for direct seeding which may generate comparable yields to conventional tilled puddled rice; also enhanced seeding rate for direct seeding can mitigate yield losses due to the increased exposure of seeds to pests, birds and rats (Saharawat et al. 2010; Chauhan et al. 2012). Further research on fertiliser applications could also raise yields in direct seeded rice, it is suggested that timing fertiliser applications closer to anthesis could enhance assimilation into grains and, thus, improve yields (Chauhan et al. 2012).

One of the key stresses to rice-wheat cropping in the IGP is water availability. Zero-tillage, especially when integrated with appropriate residue management can deliver significant irrigation water savings. Water savings and increased water productivity are

realised under both zero-tillage rice and wheat crops (Jat et al. 2009a; Saharawat et al. 2010). This can be through reduced turn-around time between rice and wheat crops enabling residual soil moisture from rice cropping to be used productively for wheat germination (Erenstein and Laxmi 2008). There is better infiltration in untilled soil due to improvements in soil structure under zero-tillage, this reduces issues of water logging and leads to 36% less water use compared to conventional tillage in wheat crops (Gupta and Seth 2007; Erenstein and Laxmi 2008; Lumpkin and Sayre 2009). Earlier sowing of the wheat crop also reduces the number of required end of season irrigations (Erenstein and Laxmi 2008).

There are other resource-conserving approaches shown to have sustainability and productivity benefits in rice-wheat cropping systems. Laser-bed levelling, when integrated with zero-tillage, reduces the amount of irrigation water applied without yield penalties also delivering improved soil physical properties and economic returns (Jat et al. 2009a). The International Rice Research Institute (IRRI) has developed leaf colour charts to enable farmers to identify the optimum time for nitrogen fertiliser application (Gupta and Seth 2007). Cropping on furrow-irrigated permanent raised beds is another conservation-agriculture practice which is increasingly being implemented in the IGP (Chauhan et al. 2012). The combination of zero-tillage and furrow-irrigation has been shown to deliver irrigation water savings (Lumpkin and Sayre 2009). Reduced and zero-tillage on raised beds potentially delivers several advantages including: improved soil structure and conditions as tractor activity is limited to spaces between beds, reduced waterlogging, improved fertiliser use efficiency as fertilisers are applied to raised-beds in the root zone, mechanical weed control through targeted herbicide application, reduced power for irrigation and reduced groundwater pollution (Chauhan et al. 2012). However, there is some evidence that yield levels are not improved on raised beds, that significant effort is required to develop and maintain the raised beds whilst in certain situations the extent of water savings has also been questioned (Chauhan et al. 2012). Cropping on raised beds does not show definitive yield benefits (Gupta and Seth 2007; Saharawat et al. 2012), suggesting research should focus on developing cultivars suited to raised bed

cropping and identifying optimum furrow width-bed height relationships (Gupta and Seth 2007; Chauhan et al. 2012).

Implementation of conservation agriculture practices in the rice-wheat cropping system of Punjab and Haryana will also contribute to mitigating agricultures GHG emissions. Reduced tillage and residue retention leads to enhanced levels of soil carbon and carbon sequestration, and residue retention as opposed to residue burning reduces emissions of GHGs and particulates (Gupta and Seth 2007; Lumpkin and Sayre 2009). Zero-tillage requires less tractor operations on fields and, thus, reduces fossil fuel use with subsequent reductions in GHG emissions (Gupta and Seth 2007; Erenstein and Laxmi 2008). Simulation studies show that CO_2 emissions from machinery use are reduced under zero-tillage, raised bed and direct seeded rice cropping as opposed to transplanted and conventional cropping practices (Saharawat et al. 2012). Transplanting rice on raised beds, after zero-tillage or direct seeding reduced CH_4 emissions compared to conventional puddled rice cropping (Saharawat et al. 2012). More efficient use of irrigation and temporary aeration of soils in rice cropping, for example alternate wetting and drying, reduces water requirements and also CH_4 emissions (Gupta and Seth 2007; Chauhan et al. 2012). However, there was little variation in N_2O emissions between conventional and conservation agriculture practices; this includes N_2O emissions from soils and also production of fertiliser exogenous to the farm (Saharawat et al. 2012). Several conservation agriculture practices offer adaptive options, and enhanced resilience, to harmful climate change. For example, better water use efficiency and reduced water requirements under zero-tillage and aerobic rice cropping can reduce vulnerability to uncertain future fluctuations in monsoon precipitation or evaporative demand (Lumpkin and Sayre 2009; Wassmann et al. 2009; Turner and Annamalai 2012). Inter-cropping promotes increased cropping diversity; an increase in diversity in agricultural landscapes increases resilience of the cropping system and incorporation of high-value commodities reduce stress on water resources (Aggarwal et al. 2004; Perveen et al. 2012; Abson et al. 2013; Mathison et al. 2013). Residue retention lowers soil and canopy temperature and, thus, can reduce the harmful effects of warming events on cereal crops (Jat et al. 2009b; Chauhan et al. 2012; Teixeira et al. 2013; Gourdji et al.

2013b). This illustrates potential climate resilience benefits gained from conservation agriculture approaches; the wheat crop in the IGP is particularly vulnerable warming trends (Lobell et al. 2012; Lobell et al. 2013).

The benefits of conservation and resource-conserving agricultural practices can address the environmental concerns associated with conventional practices, mitigate climate change and improve resilience to climate change in the rice-wheat systems of Punjab and Haryana. However, it is clear further research is needed to determine the optimum synergies and address trade-offs between various agricultural practices. It is also apparent that different agricultural practices will have different benefits depending upon the underlying environmental, climatic and socio-economic conditions in different locations. As stated at the beginning of this chapter the overarching aim for this thesis is to assess the vulnerability of the rice-wheat productions systems in Punjab and Haryana to climate drivers. It is therefore important this assessment of vulnerability is undertaken with an awareness that outcomes of cropping landscape management should aspire to deliver the multiple goals of climate resilience (low vulnerability) and maximum productivity without an excessive environmental or climatic footprint. The following chapter moves on to discuss approaches to assessing and measuring vulnerability before highlighting key research questions to be addressed through the thesis.

Chapter 2: Vulnerability

There are numerous definitions, conceptualisations and theories of vulnerability in the literature stemming from the diversity of contexts from which vulnerability can be assessed and measured (Adger 2006; Eakin and Luers 2006; Ericksen 2008b). However, vulnerability broadly relates to susceptibility to harm, damage or losses and in the context of climate change is defined as 'propensity of human and ecological systems to suffer harm and their ability to respond to stresses imposed as a result of climate change effects' (Adger et al. 2007, p. 720). It is well documented that the vulnerability of human entities (e.g. individuals, households, communities and associated livelihoods or food security) is determined largely by underlying social, economic, political and governance structures which influence access to resources and adaptive capacity (Adger 2006; Smit and Wandel 2006; Adger et al. 2007; Ericksen 2008b). This research focuses on the vulnerability of a biophysical entity, crop production, to climatic stressors; it does not examine human or societal vulnerability to a loss in crop production. Therefore, there is an emphasis through the research papers on understanding the relationship between crop yield and climatic drivers in a real world cropping system and not on social, economic and governance processes. However, analysis assessing the vulnerability of rice and wheat crop production throughout this thesis recognises the multitude of climatic drivers and the underlying system factors and human management practices which create differential sensitivities to climate stressors (Luers 2005) and long and short-term environmental impacts (Millenium Ecosystem Assessment 2005; Hobbs et al. 2008; Erenstein and Laxmi 2008).

Often vulnerability assessments use thresholds to distinguish a vulnerable state from a non-vulnerable state (Luers et al. 2003), or develop indices of vulnerability (O'Brien et al. 2004; Adger 2006). There are relative merits and limitations to these approaches; for example, the choice of variables, and weighting of variables, to construct indices is partly subjective (Luers et al. 2003; Luers 2005). The choice of a threshold to determine a vulnerable state is also limited by subjectivity and to a particular place at a given time. For example, the well-being threshold of 4 Tonnes ha^{-1} used by Luers et al. (2003) required for a farmer to 'break-even' in the Yaqui Valley, Mexico, in 2003 may

not provide enough income in the future given crop price fluctuations; it is not a time-space universal threshold (Luers 2005). Generalised measures of vulnerability do not account for its dynamic nature (Adger 2006; Eakin and Luers 2006). An index based approach to measuring vulnerability is limited by the purpose for which the index was constructed (e.g. proportional vulnerability, vulnerability gap, vulnerability severity) (Adger 2006). Vulnerability indices are useful to highlight an aspect of vulnerability of an entity or variable at a given time for a given purpose (e.g. inform policy targeting a given agricultural adaptation). Through their inherent simplification of a system, index based approaches do not always reveal the holistic and complex nature of vulnerability and its causation (Eakin and Luers 2006)[2].

Several studies have highlighted the overlap between vulnerability assessments and the literature on ecological resilience and the resilience of socio-ecological systems (Luers et al. 2003; Adger 2006; Gallopín 2006; Eakin and Luers 2006; Ericksen 2008b). Vulnerability can be conceptualised as the opposite of a resilient system where a resilient system can absorb or cope with a stress or perturbation without altering system functioning or the system can adapt (adaptive learning/capacity) or reorganise (self-organisation) following a stress or shock to maintain outputs (Walker et al. 2004; Folke 2006; Eakin and Luers 2006).

Utilising concepts common in assessing resilience in socio-ecological systems can offer several advantages when assessing the vulnerability of agricultural production systems to climate drivers and variability. Systems approaches are comfortable handling multiple drivers, processes and feedbacks (Ericksen 2008b); such a systemic focus is important as it enables a more holistic assessment of the vulnerability of a given variable to a given stressor or perturbation. In the context of assessing the vulnerability of agricultural production to climate drivers and variability, at the simplest level there is a cause-effect relationship between climate and crop yield. However, the size of the effect (i.e. shifts in crop yield) relative to the cause (climate

[2] In this thesis no attempt was made to generate an index or quantified measure of vulnerability. However, the four research papers (Chapters 3-6) produce a body of work enhancing understanding of vulnerability of the agricultural production systems of Punjab and Haryana to climatic drivers and variability, and its spatial manifestation. It is important to note the datasets generated here have the potential to be used in a multitude of indicator based studies; this point is briefly touched upon in Chapter 5 with an illustration of prioritising areas for targeting adaptations.

driver) varies in space and time due to underlying system interactions and feedbacks from past system activities. For example, it is recognised that agricultural production, and its current level of resilience to harmful climate change or variability, is in part determined by current levels of ecosystem services; these current levels of ecosystem services are determined by past activities within the ecosystem and longer-term trajectories of ecosystem drivers (Millenium Ecosystem Assessment 2005; Ericksen 2008b; Dearing et al. 2012; Hughes et al. 2013a). The vulnerability of wheat yield on all farms in the Yaqui Valley, Mexico, increases with increasing temperatures; however, the relative increase in vulnerability is greater on farms with poor management and less favourable soils (Luers 2005). This highlights the importance of understanding the system within which the variable being assessed for its level of vulnerability is situated.

A systemic approach, with a focus on processes and feedbacks as well as outcomes is useful in highlighting that vulnerability is not a static state (Eakin and Luers 2006), and that the system can accentuate or reduce the impacts of a perturbation or stressor and lead to differential levels of vulnerability (Turner et al. 2003). Assessments of resilience in complex and socio-ecological systems indicate that 'slow processes' undermine resilience, or increase vulnerability, without the outcome of vulnerability being apparent (Scheffer et al. 2001; Luers 2005; Hughes et al. 2013b; Hughes et al. 2013a). In the context of vulnerability Luers (2005) highlights the importance of monitoring processes which control, and cause gradual changes in, a systems sensitivity increasing the likelihood a system will yield a negative outcome when exposed to either a 'short-term' stochastic event (e.g. climatic extreme) or an accumulating stressor (e.g. gradual warming). In the resilience theory and complex systems literature an outcome of such vulnerability or loss of resilience would be a 'regime shift' (Scheffer et al. 2012; Hughes et al. 2013b), in the context of vulnerability in agricultural production systems it would be a loss in crop yield, possibly below a well-being threshold (Luers et al. 2003). Therefore, by understanding the processes and system interactions which accentuate vulnerability, it is possible to identify vulnerability in a system or at a given location before the negative impacts of low resilience or high vulnerability are realised.

The concept of resilience and, therefore, vulnerability being dynamic is inherent in resilience theory thinking of socio-ecological systems (Luers 2005; Eakin and Luers 2006), and is conceptualised via the adaptive cycle (Holling 2001). A systemic approach, recognising that vulnerability is dynamic, is important when assessing the vulnerability of agricultural production, and informing adaptations to reduce vulnerability, within the context of climate-smart agricultural production landscapes. The vulnerability, or resilience, of agricultural production levels at a given location and time-step is determined by historical and evolving human management decisions with subsequent impacts and interactions with biophysical processes and outcomes. This is of relevance to climate-smart adaptations (FAO 2011b) which in the context of this study would aim to reduce the current vulnerability of agricultural production to climatic drivers and variability without impeding the ecosystems ability to support required future production levels under uncertain future climate changes. This point is echoed by Turner et al. (2003) who comment that assessing vulnerability, and utilising resources to reduce vulnerability, without an awareness of the 'larger systemic context' could lead to unintended consequences or 'surprises'.

The vulnerability of a system is often characterised as a function of exposure, sensitivity and adaptive capacity/resilience. This framework has been used to assess climate change induced vulnerability to agriculture at varying spatial scales (e.g. farm level in Mexico (Luers et al. 2003) and district level in India (O'Brien et al. 2004)). Exposure to climate change refers to the degree of climate stress upon a given variable or system (O'Brien et al. 2004), Luers et al. (2003) and Luers (2005) define exposure in similar terms as the magnitude and frequency of a stressor force a system is exposed to. In reality exposure and sensitivity are interlinked, for example, the effect of the exposure and, thus, its magnitude relative to the variable or system in question, is dependent upon the sensitivity of the system or variable (Luers 2005; Smit and Wandel 2006).

Similar to the concept of resilience in a socio-ecological system sensitivity is often defined as the amount of stress or perturbation a system can absorb or cope with without experiencing long-term harm or change in state or structure (Luers 2005; Adger 2006; Gallopín 2006). In the context of the vulnerability of agricultural

production (crop yield), Luers et al. (2003) measure sensitivity as the derivative of crop yield relative to the stressor (e.g. climate driver). This essentially defines sensitivity as the rate of change in the system or variable of interest relative to the rate of change in, or degree of exposure to, the stressor (Luers et al. 2003; Gallopín 2006). It is the sensitivity that accounts for the differential response of two systems to the same exposure to a stressor or perturbation. As mentioned it is difficult to assess sensitivity without acknowledging the nature of the stressor or perturbation and the system's exposure to it (Luers 2005; Smit and Wandel 2006). For example, sensitivity to a short term perturbation or stochastic event (e.g. drought) is characterised by the system's ability to resist change (e.g. the amount of loss in crop yield) or to bounce back to normal conditions (e.g. the time taken for the system to deliver normal crop yields) (Luers 2005). Sensitivity to gradual change (e.g. global warming) is determined by the rate at which the systems resilience is eroded and movement towards a state of higher vulnerability, closer to thresholds of harm (e.g. the system cannot support break even yield levels) (Luers 2005). Often measures of vulnerability link exposure and sensitivity; Luers (2005) uses the coefficient of variation in crop yield as a metric of susceptibility to harm (loss in crop yield) which incorporates exposure and sensitivity, vulnerability is then quantified as a function of exposure and sensitivity (coefficient of variation) relative to the proximity of the state of the system (crop yield level) to a threshold of harm. Luers et al. (2003) apply a similar linked approach to measuring vulnerability but quantify sensitivity as the rate of change in crop yield to a change in the stressor (temperature); exposure is represented by the frequency distribution of the stressor. Therefore, vulnerability is quantified as the ratio of sensitivity to the state of the system relative to a threshold of harm multiplied by the stressor weighted by its probability of occurrence.

Adaptive capacity or resilience is often considered to be the third component of vulnerability (O'Brien et al. 2004; Gallopín 2006). Dependent upon the context of the assessment there are differences in how adaptive capacity is conceptualised (Gallopín 2006). In the context of adaptive capacity to climate change vulnerabilities it is defined as the 'ability or potential of a system to respond successfully to climate variability and change' and is a 'necessary condition for the design and implementation of effective

adaptation strategies so as to reduce the likelihood and magnitude of harmful outcomes resulting from climate change' (Adger et al. 200), p. 727). In resilience science and assessments of socio-ecological systems adaptive capacity is determined by the capability of actors, often human, to increase resilience to stressors and perturbations (Walker et al. 2004). Adaptive capacity in socio-ecological systems is also linked to adaptive self-organisation and the system's capacity for learning (Folke 2006). Human actions are often dominant in socio-ecological systems and, thus, adaptive capacity is inherently linked to human activity and is a social function (Walker et al. 2004). Adaptive capacity is determined by a range of context or place-specific interactions between social, cultural, economic, political and governance processes operating across multiple spatial and temporal scales (Smit and Wandel 2006; Adger et al. 2007; Ojha et al. 2013). Due to the complexity of processes determining adaptive capacity, and cross-scale linkages (e.g. national and international economic policy can cause differential levels of intra-community adaptive capacity), levels of adaptive capacity vary sub-nationally but also from community to community and even at individual or household levels (O'Brien et al. 2004; Smit and Wandel 2006). If adaptive capacity is included in vulnerability assessments it provides a measure of minimum potential vulnerability as opposed to current or existing vulnerability (Luers et al. 2003).

2.1 Thesis Structure

Following the above review of approaches to assess and measure vulnerability this thesis poses the following questions regarding an assessment of the vulnerability of the rice-wheat production system of Punjab and Haryana in the north-west IGP to climatic drivers:

1) What is the exposure the of rice-wheat crop production system to harmful climate drivers?

2) What is the sensitivity of rice-wheat crop production to variations in climate drivers?

3) Where are locations which can be targeted with adaptations, accounting for location-specific stresses and thereby enhance the resilience of crop production to climate changes and variation whilst minimising environmental impacts?

These three questions are explored through four, independent research papers each with a unique set of aims and standalone conclusions (Chapters 3 to 6). However, these four research papers are linked by the overarching theme of assessing the vulnerability of the rice-wheat production system to climatic drivers. The outline for each of these four papers is presented below including a brief description of how they provide information relevant to the three overarching research questions.

Chapter 3: Analysing temporal trends in the Indian Summer Monsoon and its variability at a fine spatial resolution. **(Research Paper 1)**

The ISM is a key driver of agricultural production across all-India (Mall et al. 2006); inter-annual shortfalls in ISM precipitation or long-term decreasing trends will have either negative impacts on crop production or increase pressure on already stressed water resources. It is important to know where locations are vulnerable to variability or harmful trends in ISM precipitation so water resources management and agricultural practices can be adapted accordingly (RQ 1, RQ 3). This chapter applied robust trend analysis to a gridded (0.25˚) climate dataset spanning the years 1951 to 2007 highlighting locations of increasing or decreasing trends in facets of ISM precipitation (RQ1). The facets of ISM precipitation to which trend analysis were applied included: total ISM precipitation, recurrence of drought years, inter-annual variation in ISM precipitation, onset date of ISM and inter-annual variation in ISM onset date. These facets of ISM precipitation were analysed because they are of relevance for agricultural production. The datasets generated here were subsequently integrated with satellite-derived measures of cropping over Punjab and Haryana to highlight locations in rice-wheat cropping landscapes which are exposed to unfavourable 'normal' ISM conditions or unfavourable trends in ISM precipitation (RQ 1, RQ 3). The analysis through this chapter was performed at a 'fine' spatial resolution (in terms of available gridded climatic datasets) so as to generate local detail and to be able to inform locally sensitive water resources management (RQ 3).

Chapter 4: Spatio-temporal dynamics in the phenology of croplands across the Indo-Gangetic Plains. **(Research Paper 2)**

Chapter 4 provides monitoring of the spatio-temporal dynamics of cropping intensity, length of growing season and cropland productivity over the entire IGP region from 1982-1983 to 2005-2006 using the pre-processed GIMMS NDVI dataset. It demonstrated how land surface phenology (LSP) parameters could be extracted per-pixel and per-agricultural season to document trends in cropping over a large region for a substantial time period. Utilising a long-term satellite data was important to capture long-term trajectories of the dynamics of the cropping system across its landscape. Through utilising a longer-term dataset it is possible to identify locations where crop production and length of growing seasons are variable suggesting vulnerability to climatic variation (RQ 1, RQ 2). This analysis enables assessment of landscape scale trade-offs between 'normal' levels of crop productivity and the risk (inter-annual variability in production) of cropping. Inter-annual variation in crop production is often taken as a measure of the vulnerability (specifically sensitivity and exposure) of crop production to climate (Luers 2005) (RQ 1, RQ 2). Analysing long-terms trends in the dynamics of the wider IGP crop production system (including Uttar Pradesh and Bihar) facilitates capturing locations where cropping could be expanded or intensified to take pressure off the exhausted croplands of Punjab and Haryana (RQ 3).

Chapter 5: Climate-smartening India's breadbasket. Locating vulnerability 'hotspots' to target with adaptive practices. **(Research Paper 3)**

LSP parameters from satellite observations from MODIS data were utilised to identify rice and wheat crop extent and provide yield estimates at a 500 m spatial resolution. These maps were integrated with spatially explicit ancillary datasets (e.g. climatic datasets developed in Chapter 3, groundwater levels, cropping diversity, sowing date, locations of crop residue burning) to provide landscape scale assessments of where crop productivity is vulnerable to prevailing climatic trends (identified in Chapter 3), water scarcity, sub-optimal agronomic practices or where cropping is contributing to climate change (via GHG emissions) or environmental degradation (RQ 1, RQ 2, RQ 3). This chapter takes a holistic view of the rice-wheat cropping system enabling

assessment of the vulnerability of the rice-wheat croplands to climate whilst retaining awareness of other pressures and stresses. It demonstrated how integration of spatial datasets can inform spatial targeting of adaptation and mitigation measures, capture synergies in adaptation and mitigate trade-offs between conflicting management goals; thus, contributing to moving the rice-wheat production system onto a trajectory towards a climate-smart landscape (RQ 3). It specifically highlights locations where adaptations could be targeted to address multiple stresses simultaneously.

Chapter 6: Satellite observations reveal the impact of climatic extremes and variability on cereal croplands. **(Research Paper 4)**

Satellite derived estimates of rice and wheat yield derived from MODIS data and daily, gridded temperature and precipitation datasets were used to train a crop yield-climate regression model. This crop yield-climate model explored whether temperature variables during key phenological development stages for crop yield formation are currently limiting production in the rice-wheat cropping system (RQ 1, RQ 2). The statistical framework uses fixed-effects terms in the models to account for spatial variation in time-invariant system variables (e.g. irrigation, farmer decisions) and omitted variable bias. The analysis reveals how sensitive rice and wheat crops are in Punjab and Haryana to warming during key crop development stages; it also captures how the sensitivity of crop yield varies with different sowing dates and thus can inform climate-resilient adaptations (RQ 2, RQ 3).

A common element to the analysis performed in the four papers which constitute this thesis is the use of spatial datasets. Remote sensing is used to monitor the extent of rice and wheat croplands and to capture some of the dynamics of the cropping system including length of growing seasons, cropping intensity and productivity. These remote sensing measures are integrated with analysis of climatic datasets and other agricultural statistics to enable landscape scale assessments of vulnerability. This approach facilitates capturing spatial patterns of the magnitude and varying nature of the vulnerability of crop production to climate drivers. This overcomes the limitations of assuming levels of vulnerability are delineated by distinct boundaries, and uniform within boundaries, which is an artefact of assessments made using data constrained to the political unit scale (O'Brien et al. 2004).

Monitoring cereal croplands at the landscape scale provides the opportunity to understand how real world cereal systems actually respond to climatic drivers and, thus, provides utilisable, situation-specific information for climate-resilient adaptation and mitigation. Bogdanski (2012) and Scherr et al. (2012) highlight the benefits of synthesising climate-smart approaches with integrated landscape approaches. Climate-smart approaches focus on resilience to climate change, adaptation and mitigation (FAO 2011b). Integrated landscape approaches recognise the multifaceted nature of drivers which determine landscape processes, that landscapes are required to provide socio-economic and environmental benefits to society and, that social, environmental and economic processes at work within a landscape are dynamic and, thus, require management sensitive to long-term uncertainties (Scherr et al. 2012). Here, the landscape scale refers to a wider spatial extent whilst retaining local detail. The ideal cropping practice to deliver climate-smart benefits will vary spatially and with underlying environmental and socio-economic conditions (DeFries and Rosenzweig 2010; FAO 2011a). Thus, monitoring cereal cropland-climate interactions across a landscape can highlight the best practice for a given locale. Assessing the vulnerability of cereal crops to climate across a landscape inherently acknowledges the complexity of actors and processes which determine vulnerability to climate change in real world situations (DeFries and Rosenzweig 2010).

Approaches to assess cereal cropland vulnerability should provide integrated monitoring of the landscape to inform on integrating climate-resilience into climate-smart cereal cropping practices to ensure short-term societal needs are met without hindering long-term provision of ecosystem services (Millenium Ecosystem Assessment 2005; Foley et al. 2005; Eakin and Luers 2006; FAO 2011b; Scherr et al. 2012; Dobermann and Nelson 2013). The immediacy of implementing such approaches is emphasised by the negative impacts of climate change on cereal production, which are already being realised (Lobell et al. 2011b) and projections suggesting interactions between climate change and current agricultural practices will result in a widespread loss of suitable land to support rice and wheat crops in the IGP (Ortiz et al. 2008; Ojha et al. 2013). An integrated spatial approach developed through this thesis is useful to highlight location-specific stresses, target locally optimum adaptations to reduce

vulnerability and to capture synergies and minimise trade-offs at a landscape scale addressing the multiple goals of a climate-smart landscape (Scherr et al. 2012; Dobermann and Nelson 2013).

Chapter 3: Analysing temporal trends in the Indian Summer Monsoon and its variability at a fine spatial resolution[34]

3.1 Introduction

The ISM occurs from June to September, is strongest during July and August, and contributes approximately 70% to the total annual precipitation in India (Ramesh Kumar and Prabhu Dessai 2004). ISM precipitation is a major driver of environmental and agricultural functioning in the sub-continent with subsequent impacts on individual livelihoods and economic activities. India's population is projected to rise to nearly 1.4 billion by 2026 (DES 2009). This population growth will increase water and food demand necessitating expansion and intensification of irrigated agricultural areas (Moors et al. 2011). Analysis of spatial heterogeneity and temporal trends in ISM precipitation can provide crucial information to planners charged with managing water resources sustainably.

Simulation of monsoon precipitation was not consistent across the range of GCMs used in the IPCC 4th Assessment Report (Annamalai et al. 2007; Christensen et al. 2007; Moors et al. 2011). Annamalai et al. (2007) found that only six out of 18 GCMs were able to provide an acceptable simulation of monsoon climatology; these six models

---

[3] Duncan, J.M.A., Dash, J., & Atkinson, P.M. (2012) Analysing temporal trends in the Indian Summer Monsoon and its variability at a fine spatial resolution. *Climatic Change*, 117, (1-2), 119-131. doi:10.1007/s10584-012-0537-y

The work undertaken in chapter 3 has also led to three subsequent publications separate to my PhD research:

Duncan, J.M.A., & Biggs, E.M. (2012) Assessing the accuracy and applied use of satellite-derived precipitation estimates over Nepal. *Applied Geography*, 34, 626-638. doi:10.1016/j.apgeog.2012.04.001.

Biggs, E.M., Duncan, J.M.A., Atkinson, P.M., & Dash, J. (2013) Plenty of water, not enough strategy: How inadequate accessibility, poor governance and a volatile government can tip the balance against ensuring water security: the case of Nepal. *Environmental Science & Policy*. doi:10.1016/j.envsci.2013.07.004. (In Press).

Duncan, J.M.A., Biggs, E.M., Dash, J., & Atkinson, P.M. (2013) Spatio-temporal trends in precipitation and their implications for water resources management in climate-sensitive Nepal. *Applied Geography*, 43, 138-146. doi:10.1016/j.apgeog.2013.06.011.

[4] Fine refers to 0.25˚ grid cells. This a 'fine' spatial resolution compared to many gridded climate products. It should not be regarded in comparison to fine resolution gridded remote sensing data.

failed to represent the regional variation in ISM precipitation across India and there was inter-model variation in the timing of peak precipitation. Krishnamurthy et al. (2009) commented that trends detected from observed data provide a useful reference point for assessing GCM simulations. In light of the uncertainty in GCM simulations of ISM precipitation, trend analysis from observational data provides a reliable source of information to water resource planners.

The amount and duration of ISM precipitation varies across India (Satyanarayana and Srinivas 2008; Ghosh et al. 2009). Recent studies have revealed spatial heterogeneity in the occurrence of significant increasing or decreasing trends in facets of ISM precipitation (Guhathakurta and Rajeevan 2008; Ghosh et al. 2009; Krishnamurthy et al. 2009; Ghosh et al. 2011). Ghosh et al. (2009) highlighted limitations in identifying temporal trends by aggregating precipitation over large areas receiving varied amounts of rainfall (e.g. Goswami et al. 2006). Aggregating precipitation data over a region which exhibits spatial variability in locally occurring temporal trends can lead to identification of false trends and loss of spatial detail. Given the spatial heterogeneity of ISM precipitation, trends in phenomena associated with ISM precipitation (e.g. extreme rain events, local onset of ISM and occurrence of drought conditions) should be analysed at the finest possible spatial resolution.

The spatial distribution of increasing or decreasing trends in extreme rain events across India has been well documented using a variety of statistical methods (Ghosh et al. 2009; Dash et al. 2009; Krishnamurthy et al. 2009; Ghosh et al. 2011). However, temporal trends in other facets of ISM precipitation, such as drought years or local onset date of ISM, which exert a control upon agriculture and livelihoods, have received little attention at a suitably fine spatial resolution. This research addresses this knowledge gap by performing trend analysis at the local scale for these variables from 1951-2007. When viewed in conjunction with the earlier mentioned studies on trends in extreme rain events contributes to an enhanced understanding of the manifestation of ISM precipitation, and its variability, at a fine spatial resolution across India. Providing such local detail is pertinent given Goal 5 of the Government of India's National Action Plan on Climate Change, National Water Mission to focus on basin

level integrated water resource management to cope with variability in precipitation (National Water Mission 2009). Specific outcomes from this research include:

1) Identifying 'normal' ISM conditions, inter-annual variation in ISM precipitation, frequency of drought years, 'normal' onset date of ISM and inter-annual variation in onset date of ISM at a 0.25˚ spatial resolution across India.
2) Developing a new method to define local onset of ISM from daily precipitation data.
3) Performing temporal trend analysis at the local scale across all India for three key variables: annual ISM precipitation, occurrence of severe drought years and local onset date of ISM.
4) Identifying locations where there are trends of increasing or decreasing inter-annual variation in ISM precipitation and local onset date of ISM.

3.2 Methods and Data

3.2.1 Precipitation Data

Asian Precipitation Highly-Resolved Observational Data Integration Towards Evaluation of the Water Resources (APHRODITE) daily 0.25°x0.25° gridded precipitation data were obtained for all India for the period 1951-2007 (http://www.chikyu.ac.jp). The APHRO_MA_V1003R1 data set was used in this study. The gridded precipitation data were interpolated from station gauge data obtained from Global Telecommunication System networks, precompiled datasets, records from national meteorological organizations and monthly climatologies using the methodology outlined in Yatagai et al. (2009) for the preceding APHRO_V0902 product, but with improved quality control. A dense network of gauges across India, which passed quality control, were utilised in the development of the APHRODITE product in every year (Yatagai et al. 2009) (see Appendix 1 for depiction of gauges used in the generation of the APHRODITE product and links for further information on product input datasets). The interpolation method incorporates weighting functions to account for topographic features improving representation of orographic precipitation and uses the WORLDCLIM dataset to correct for bias in areas with limited station gauge coverage (Yatagai et al. 2009).

For almost the entire extent of India, ISM precipitation from APHRODITE data and Indian Meteorological Department (IMD) gridded data are well correlated (correlation coefficient > 0.6) (Rajeevan and Bhate 2008). There is a smaller correlation between the two datasets in the northern Himalayan region and the far eastern states of Manipur and Mizoram because there are fewer rain gauges in these regions from which the gridded datasets were developed (Rajeevan and Bhate 2008). For most corresponding grids across India the difference between the two datasets is less than 3mm day^{-1} (Rajeevan and Bhate 2008). Several studies have used the IMD gridded dataset to analyse a variety of trends in ISM precipitation across India (e.g. Rajeevan et al. 2006; Rajeevan et al. 2008; Ghosh et al. 2009; Dash et al. 2009; Krishnamurthy et al. 2009). The strong match between APHRODITE and such a widely used and well validated product highlights the applicability of using APHRODITE to study trends in ISM precipitation. The IMD gridded dataset has a 1°x1° spatial resolution compared to the 0.25°x0.25° spatial resolution of the APHRODITE product; this suggests there is potential to capture greater spatial detail in occurrence of trends when using the APHRODITE data. This will be of obvious benefit to planners aiming to increase efficiency of water resource use at the local scale.

3.2.2 Trend Analysis

The non-parametric Mann-Kendall test (Mann 1945; Kendall 1975) was used to detect significant (p<0.05) increasing or decreasing temporal trends in examined facets of ISM precipitation. The Mann-Kendall test has been used widely to detect the presence of monotonic trends in climatological and hydrological time series (e.g. Partal and Kahya 2006; Modarres and de Paulo Rodrigues da Silva 2007; Bae et al. 2008; Krishnamurthy et al. 2009; Biggs and Atkinson 2010). The Mann-Kendall test is a rank-based test not sensitive to the data being skewed, containing extreme values, having a non-Gaussian distribution or containing non-linear trends (Partal and Kahya 2006; Biggs and Atkinson 2010). It is therefore a robust test for trend detection in the facets of ISM precipitation examined in this study.

The Mann-Kendall test statistic S was calculated by:

$$S = \sum_{k=1}^{n} \sum_{j=k+1}^{n-1} sgn(x_j - x_k)$$

(1)

$$sgn(x) = \begin{cases} +1 & x > 0 \\ 0 & x = 0 \\ -1 & x < 0 \end{cases}$$

(2)

where *n* is the length of the time series of data, x_i is the value of the data at time *i.* If the difference between $x_j - x_k$ is positive the sgn function assigns a value of one, a negative difference is assigned a value of negative one. If the Mann-Kendall test *S* is positive it indicates a positive or increasing trend, the opposite is true for a negative *S*. Kendall (1975) proved that values of *S* are normally distributed and that the mean *E* and variance *Var* of *S* are as follows:

$$E[S] = 0$$

(3)

$$Var[S] = \frac{n(n-2)(n2+5) - \sum_{i=1}^{p} t_i(i)(i-1)(2i+5)}{18}$$

(4)

where *n* is the length of the time-series, *p* is the number of tied values in *x* and *t* is the number of ties of extent *i*. The values of *Var* and *E* enable the calculation of a *Z-statistic* which follows the standard normal distribution used to determine the statistical significance of the observed trend (Douglas et al. 2000).

$$Z = \begin{cases} if\ S > 0 & \frac{S-1}{[Var]^{1/2}} \\ if\ \ S < 0 & \frac{S+1}{[Var]^{1/2}} \\ if\ S = 0 & 0 \end{cases}$$

(5)

The significance level for each trend was calculated by:

$$p = 2[1 - \Phi(|Z|)$$

(6)

where Φ is the standard normal distribution function (Douglas et al. 2000). If p is less than 0.05 then the observed trend is deemed to be significant at the 95% confidence level.

3.2.3 Field Significance Testing

Field or global significance addresses the question of whether the number of independent tests for significance reporting significant trends m could have occurred by chance (Livezey and Chen 1983). The probability of obtaining m significant (α_{local}) trends from N independent tests for significance can be estimated by the binomial distribution, where α_{local} is the local significance level (Livezey and Chen 1983; Wilks 2006). The field is the spatial extent over which local significance tests are performed (Wilks 2006). The value m_0 must be equalled by or exceeded by the number m to determine field significance at α_{global} (Livezey and Chen 1983; Wilks 2006). The value m_0 is the threshold number of significant tests which needs to be exceeded at α_{local} from N independent tests so that the probability of m observed number of significant tests realised is a chance occurrence equal to or less than 0.05 (Livezey and Chen 1983). The global null hypothesis states that the local null hypothesis of no significance is true for all local tests (Wilks 2006).

Positive spatial autocorrelation between data reduces the number of degrees of freedom at the field level; this results in the global null hypothesis being rejected too frequently if spatial autocorrelation is not accounted for (Livezey and Chen 1983; Wilks 2006). Following Livezey and Chen (1983) let n_0 be the minimum number of effective degrees of freedom which the field must contain for the realised number of significant tests α_{local} to be significant at α_{global}. If the data within the field are spatially autocorrelated then the field contains $n<N_{sig}$ degrees of freedom where N_{sig} is the

number of independent realisations of tests for significance (Livezey and Chen 1983). If n is greater than n_0 then the field is deemed statistically significant at α_{global}. Random resampling of the input data can be used to estimate thresholds for field significance in spatially autocorrelated fields (Wilks 2006). Livezey and Chen (1983) determined the threshold for field significance from the 5% tail of a histogram of percentage of grid cells reporting statistically significant correlations α_{local} with input data resampled randomly via Monte Carlo simulations. Random resampling of the time series of input data in a grid cell retains the spatial autocorrelation within the field without requiring knowledge of the spatial covariance structure (Wilks 1997).

3.2.4 Examined Facets of ISM Precipitation

3.2.4.1 Annual ISM precipitation

Annual ISM precipitation (sum of June-September precipitation) was calculated for every grid cell (0.25˚) for each year from 1951-2007. The median and inter-quartile range represent the central value and dispersion in the distribution of inter-annual ISM precipitation, respectively, over the specified time period. These measures were used as they are not distorted by extreme values. Locations experiencing significant (p<0.05) increasing or decreasing trends in annual ISM precipitation were identified using the Mann-Kendall test. To test if a location experienced increasing or decreasing trends in the variability of annual ISM precipitation, the coefficient of variation (equation 7) was calculated within a moving window passed through the time series of annual ISM precipitation. Three, five, seven and nine year moving windows were used to check if any observed trends in variation were artefacts of the size of moving window. The moving window included an equal number of years above and below a central value (e.g. a five year moving window for the year 1972 would include the range 1970-1974). For the time series of the coefficient of variation calculated within a moving window Mann-Kendall tests were applied to detect trends of increasing or decreasing variability over time.

$$C_v = \frac{\mu}{\sigma} \tag{7}$$

where μ is the mean annual ISM precipitation within the moving window and σ is the standard deviation.

3.2.4.2 Severe Drought Years

The standard IMD definition of a severe drought year, annual precipitation less than 50% of the long term normal (1951–2007 in this study), for a specified area was used (Shewale and Kumar 2005). The long term normal annual mean precipitation for 1951–2007 was obtained for each 0.25°x0.25° grid cell. If for a specific year the annual total precipitation was less than 50% of the long-term normal it was considered a severe drought year. In each grid cell a time series of the average number of severe drought years in a three, five, seven and nine year moving window from 1950 –2007 was calculated. Significant (p<0.05) increasing or decreasing trends in frequency of severe drought years in the time series were detected using the Mann-Kendall test.

3.2.4.3 Local onset date of ISM

There is no uniformly accepted definition of ISM onset (Fasullo and Webster 2003; Pai and Rajeevan 2007). Various studies, for example, Joseph et al. (2006); Pai and Rajeevan (2007) and, Wang et al. (2009), have criticised the IMD's subjective definition for the onset of monsoon over Kerala, a state in South West India, based on precipitation at selected weather stations, due to lack of a quantitative criterion and low long-term reliability. Moreover, defining onset of ISM based on conditions over Kerala is limited because local conditions may be misinterpreted as monsoon onset (bogus or false onset) (Fasullo and Webster 2003; Pai and Rajeevan 2007; Wang et al. 2009). Other methods defining onset date have used conditions of the westerly low level jet at 850 hPa (Joseph et al. 2006; Wang et al. 2009) or vertically integrated moisture transport (Fasullo and Webster 2003). Defining ISM onset using conditions over Kerala or circulation patterns can give an indication of whether the larger monsoon system formation is delayed relative to an average onset date of 1st June. However, such definitions do not identify the start date of the ISM at specific locations across all India accurately. A delayed or early onset at Kerala does not necessarily translate into a delayed or early onset of ISM in North India or represent variation across the country (Bansod et al. 1991; Fasullo and Webster 2003; Pai and Rajeevan

2007). Here, a methodology was developed which defined local onset date of ISM across India using daily precipitation data. Such definitions are sensitive to local scale processes (Moron et al. 2009), but attempt to capture onset of conditions characteristic of monsoon precipitation. Detection of onset of ISM at a specific location should not be used as an inference of large scale monsoon system conditions or development.

The onset date of ISM was defined at a grid cell if two criteria were met. Criterion one was that from day *i* a minimum of 10 of the subsequent 21 days must have a positive daily standardised precipitation anomaly (SPA). The SPA was calculated as:

$$SPA = \frac{x_i - \mu}{\sigma}$$

$$i = 1,2,3 \ldots..365 \qquad (8)$$

where x_i is precipitation on day *i* of year *n*, μ is the mean daily precipitation for year *n* and σ is the standard deviation of daily precipitation in year *n* within the given grid cell. The use of the SPA calculated individually for each grid cell means that the threshold for detecting the increased precipitation intensity associated with monsoon conditions is location-specific and sensitive to spatial variation in precipitation. This criterion also prevents ISM onset from being defined by short duration local synoptic precipitation events avoiding a false or bogus onset (Fasullo and Webster 2003; Goswami 2005). If the first criterion was passed then criterion two should be met for day *i* to be defined an onset date of the ISM. Criterion two specified that the sum of daily precipitation on day *i* and the subsequent six days should be greater than 18 times the mean daily precipitation for year *n* for the grid cell. The second criterion detected the characteristic increase in precipitation associated with onset of ISM conditions (Wang et al. 2009). If onset of ISM in a grid cell was not realised for 90% of years between 1951-2007 (51 out of 57 years) that grid cell was discounted from further analysis.

The median and inter-quartile range of ISM onset date in each grid cell was computed. Significant ($p<0.05$) increasing (later) or decreasing (earlier) trends in ISM onset date

were detected using the Mann-Kendall test. To test for trends of increasing or decreasing inter-annual variation in ISM onset date a time series of coefficient of variation of onset date over three, five, seven and nine year moving windows was constructed. The Mann-Kendall test was used to test for significant (p<0.05) trends in inter-annual variation of ISM onset date. During trend analysis if onset date was not realised in a grid cell for a particular year it was replaced with the median onset date of the neighbouring eight cells. This was to ensure the time series contained no missing values.

3.2.5 Field Significance Methodology

To test for field significance of trends in annual ISM precipitation, severe drought years and onset date of ISM bootstrap resampling of the input data at each grid cell was used; similar to the methodology outlined in (Krishnamurthy et al. 2009). Bootstrap resampling samples with replacement from the original input data and, being non-parametric, does not require prior knowledge of the distribution of the input data (Wilks 1997). A bootstrap sample of the time series at each grid cell was generated and the Mann-Kendall test was applied to this bootstrap sample. The number of grid cells with positive and negative significant trends (α_{local}) from the bootstrap samples were summed across the field (i.e. the spatial extent of India). This process was repeated 1000 times to generate histograms of the number of grid cells reporting significant trends when the global null hypothesis of no local significance was true. The 95^{th} percentile value of this histogram was taken as the threshold for field significance. Generating confidence intervals based on bootstrapped percentile intervals did not require the histogram of number of significant grid cells under bootstrap sampling to be normally distributed (Efron and Tibshirani 1993). If the number of grid cells reporting significant trends from the observed data was greater than the 95^{th} percentile value then the field was deemed significant at α_{global}. In this research α_{local} and α_{global} were set equal to p<0.05.

3.3 Results

3.3.1 Annual ISM precipitation

The South West Coast and North East of India received the greatest amounts of annual ISM precipitation between 1951-2007 (Fig. 3-1a). These regions also experienced the greatest inter-annual variation in annual ISM precipitation (Fig. 3-1b). There was a fragmented spatial pattern across India for areas which experienced significant trends (p<0.05) of increasing or decreasing annual ISM precipitation (Fig. 3-1c). The area on the South West Coast of India which experienced significant trends (p<0.05) of decreasing annual ISM precipitation corresponds to the same location as reported by Guhathakurta and Rajeevan (2008). More grid cells reported significant trends (p<0.05) of increasing inter-annual variation in ISM precipitation than decreasing variation (Table 3-1; Fig. 3-1d). The magnitude of increasing or decreasing trends in annual ISM precipitation and inter-annual variation in ISM precipitation are depicted in Fig. 3-2a. The pattern and the spatial distribution of grid cells which reported significant trends in inter-annual variation was consistent regardless of the size of the moving window within which the coefficient of variation was calculated (Table 3-1). This indicates that observed trends were real rather than artefacts of the size of moving window. However, increasing the size of the moving window did increase slightly the number of grid cells where significant trends in inter-annual variation were realised. This may be expected as a larger moving window may capture more high-frequency variation relative to the low frequency trend. Figures are presented using a five year moving window as a balance between a three year moving window which may not be sensitive enough to capture trends in inter-annual variability whereas a nine year moving window may over-emphasise trends in inter-annual variability given a time series spanning 1951-2007. The observed significant increasing and decreasing trends (p<0.05) passed the test for field significance enabling rejection of the global null hypothesis (Table 3-2).

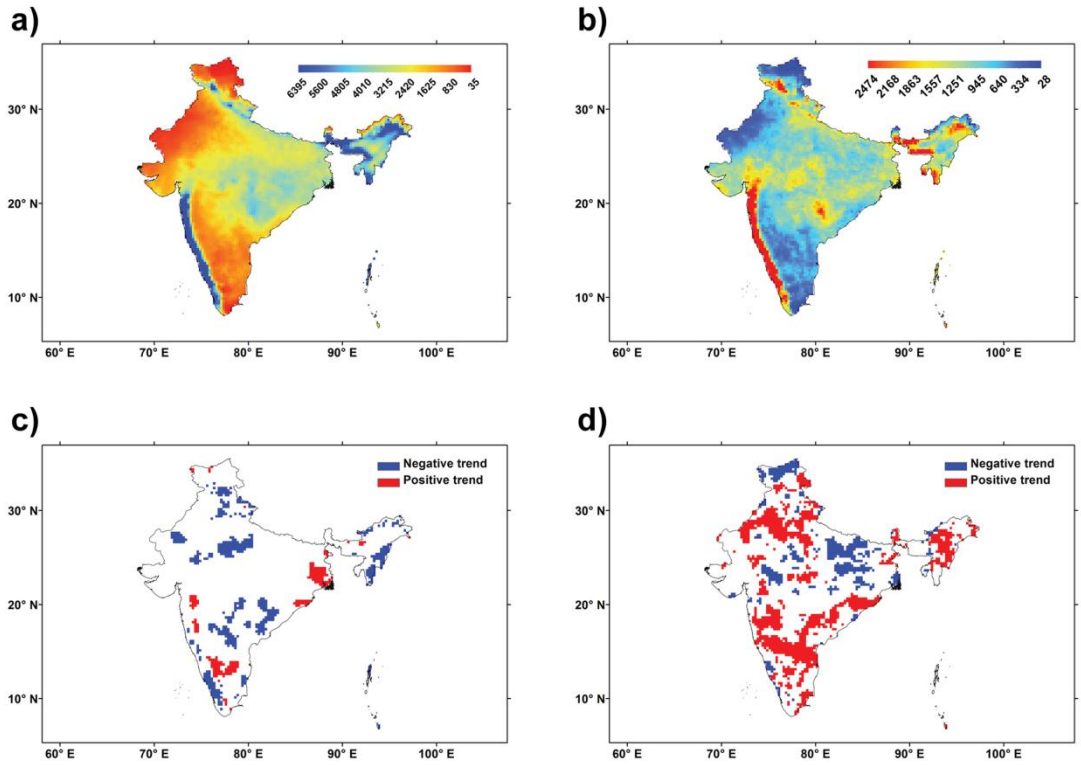

Figure 3-1 a) Median annual ISM precipitation (mm) between 1951-2007 ,b) Inter-quartile range of annual ISM precipitation (mm) between 1951-2007, c) significant trends (*p*<0.05) of increasing or decreasing annual ISM precipitation determined using the Mann-Kendall test and, d) significant trends (*p*<0.05) of increasing or decreasing inter-annual variation in ISM precipitation between 1951-2007 (results show in coefficient of variation calculated over a five year moving window).

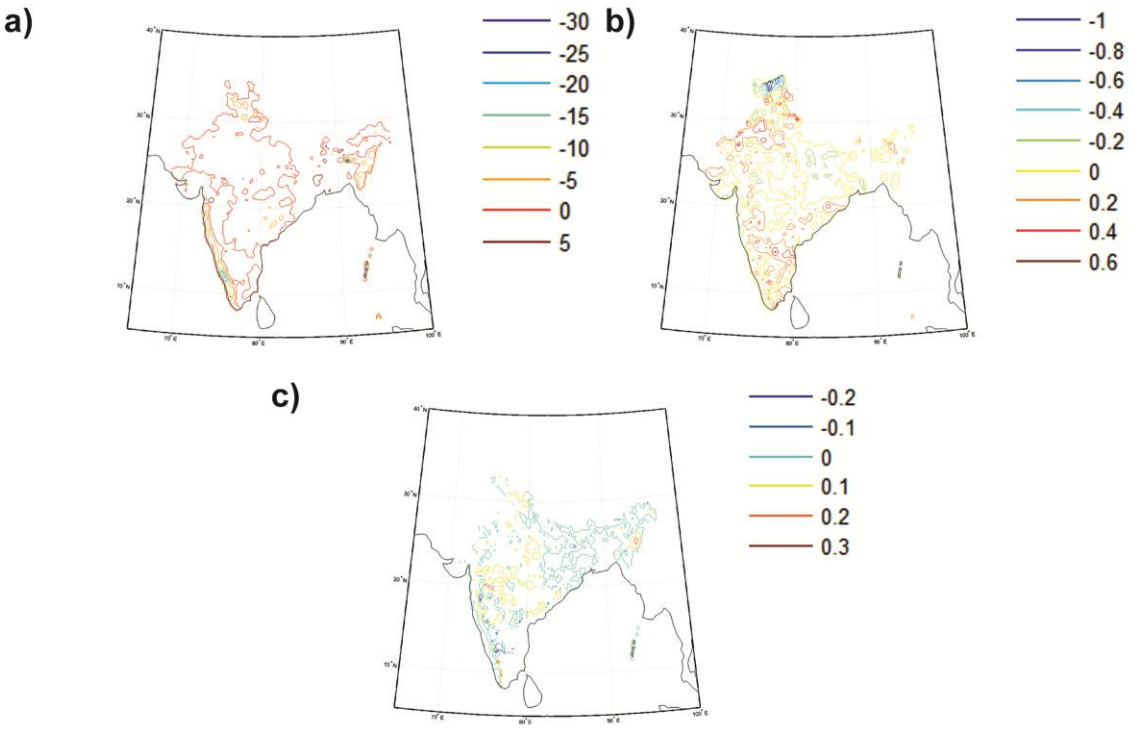

Figure 3-2 Trend calculated as the median slope determined by the Theil-Sen method for: a) trends in annual ISM rainfall between 1951-2007, b) trends of increasing or decreasing inter-annual variation in ISM precipitation between 1951-2007 (results show trends in coefficient of variation calculated over a five year moving window) and, c) trends of increasing or decreasing inter-annual variation in onset date of ISM between 1951-2007 (results show trends in coefficient of variation calculated over a five year moving window).

Table 3-1 Number of grid cells (out of 4475) reporting significant trends (p<0.05) in increasing or decreasing variation in annual ISM precipitation and onset date of ISM with coefficient of variation calculated within three, five, seven and nine year moving windows. The number of grid cells (out of 4475) reporting significant trends (*p*<0.05) in increasing or decreasing recurrence of severe drought years when the time-series was contrstructed using three, five, seven and nine year moving windows. The number in brackets refers to the number of grid-cells reporting significant trends (*p*<0.05) as a percentage of the total number of cells.

Size of moving window	Annual ISM precipitation		Severe Drought Years		Onset date of ISM	
	sig. positive trends	sig. negative trends	sig. positive trends	sig. negative trends	sig. positive trends	sig. negative trends
3	494 (11.04)	288 (6.44)	668 (14.93)	191 (4.27)	825 (18.44)	105 (2.35)
5	1118 (24.98)	471 (10.53)	900 (20.11)	355 (7.93)	1308 (29.23)	201 (4.49)
7	1406 (31.42)	610 (13.63)	956 (21.36)	430 (9.61)	1525 (34.08)	282 (6.30)
9	1548 (34.59)	781 (17.45)	994 (22.21)	474 (10.59)	1607 (35.91)	356 (7.96)

Table 3-2 Field significance test results for significant trends (p<0.05) in annual ISM precipitation, frequency of severe drought years and onset date of ISM.

		95th percentile of number of grid cells reporting significant trends from 1000 bootstrap samples generated under the null hypothesis of no trend	Number of observed grid cells reporting significant trends from real data
Annual ISM precipitation	Sig. positive trends	127	197
	Sig. negative trends	128	514
Severe drought Years	Sig. positive trends	74	900
	Sig. negative trends	73	355
Onset date of ISM	Sig. positive trends	101	62 (not field significant)
	Sig. negative trends	102.5	117

3.3.2 Severe Drought Years

North West India experienced the greatest frequency of severe drought years between 1951-2007 (Fig. 3-3a). The majority of Central, North East and coastal South West India experienced between zero to two severe drought years within the study period (Fig. 3-3a). Most of North Central and North East India experienced no significant trends (p<0.05) of increasing or decreasing frequency of severe drought years between 1951-2007 (Fig. 3-3b). Much of the Southern Peninsula of India showed a fragmented spatial pattern of areas experiencing significant trends (p<0.05) of increasing or decreasing recurrence of severe drought years (Fig. 3-2b). In contrast, large portions of North West India experienced significant trends (p<0.05) of increasing frequency of severe drought years (Fig. 3-3b). The number of grid cells which reported significant trends (p<0.05) of increasing frequency of severe drought years was twice that of grid cells which reported a decreasing frequency (Table 3-1; Fig. 3-3b). The spatial pattern of locations of significant trends and the greater number of grid cells which experienced significant trends (p<0.05) of increasing frequency were consistent regardless of the

size of moving window used in constructing the time series for temporal trend analysis (Table 3-1). The observed significant trends (p<0.05) of increasing or decreasing frequency of severe drought years were field significant (Table 3-2) indicating observed trends were real rather than chance artefacts of performing multiple hypothesis tests simultaneously.

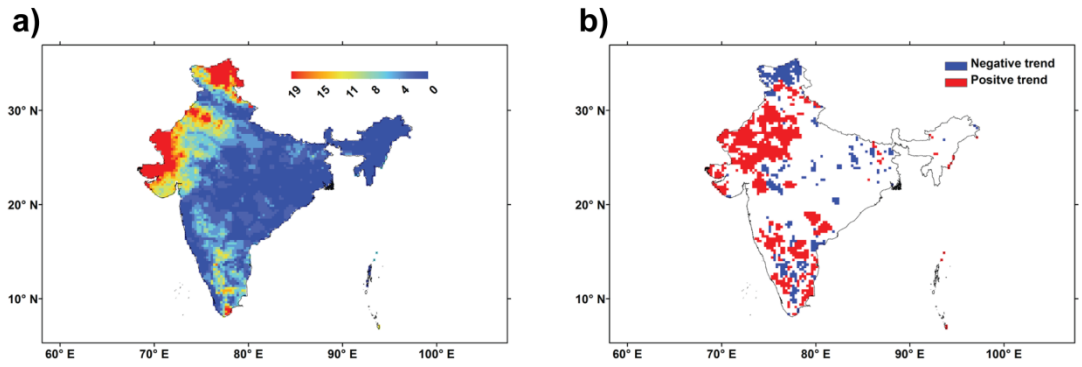

Figure 3-3 a) Number of severe drought years as defined by the IMD over the period 1951-2007 and, b) significant trends (p<0.05) of increasing or decreasing recurrence of severe drought years determined using the Mann-Kendall test (results from time series constructed with mean drought years calculated over a five year moving window).

3.3.3 Onset date of ISM

Onset date of ISM defined using the above method in grid cells containing stations which the IMD used to define onset has a strong positive correlation (r_s= 0.67; p< 0.001 (Spearman's rank correlation), RMSE: 14) with the IMD defined onset dates over Kerala. This significant (p<0.001) correlation indicates the objective method of detecting onset defined here captures the inter-annual variation in onset date. Increasing the threshold in criterion one to a SPA of one inevitably increases the number of grid cells where onset is not detected in regions which receive lower amounts of and more scattered precipitation. The onset date detected was largely insensitive to increasing the threshold in criterion two. Onset detected using a threshold of total precipitation over a seven day period being greater than 18 times mean daily precipitation for year n yielded a slightly stronger correlation and lower RMSE to IMD declared onset dates over Kerala than 22 times mean daily precipitation (r_s= 0.59; p< 0.001, RMSE: 28). As this study focuses on inter-annual variability in onset

date rather climatological mean onset date the subjective choice of threshold will not influence the results (Fasullo and Webster 2003; Moron et al. 2009).

Fig. 3-4 shows grid cells where ISM onset dates from 1951-2007, determined using the method presented here were significantly correlated (p<0.05) with ISM onset date in grid cells containing stations from which the IMD declared onset date over Kerala. Significant correlations (p<0.05) were realised in only 4.65% of grid cells across India highlighting that the onset date of the ISM in Kerala is not representative of the onset date at other locations. Significant correlations were calculated using Spearman's rank correlation. This method of detecting ISM onset performs well in detecting onset in specific years and long-term normal onset at various locations across India and is not limited to detecting onset over Kerala (Table 3-3). As can be seen in Table 3-3 this method of detecting onset is able to detect the northward advance of the ISM across India; later ISM onset dates were realised in the northern cities of Delhi and Lucknow (Table 3-3).

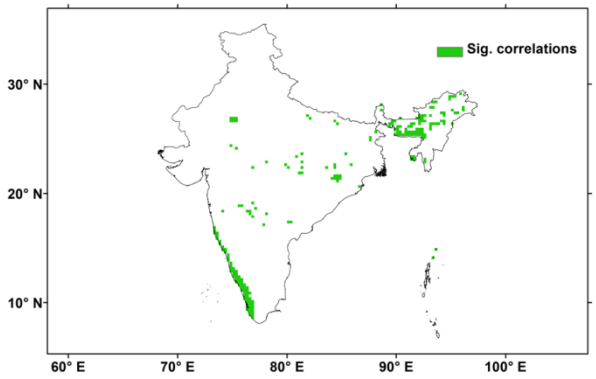

Figure 3-4 Significant correlations (p<0.05) between the time series of onset date of ISM defined using the methodology outlined 3.2.4 in the grid cells covering the location of the individual stations the IMD use to define onset date of ISM and all other grid cells across India. Correlation was calculated using Spearman's rank correlation where a coefficient of 1 indicates perfect positive correlation and -1 indicates perfect negative correlation.

Table 3-3 IMD declared ISM onset date and local onset date detected by method presented in section 2.4.3 for various cities/states across India in 2005, 2006, 2007 and Long-term normal onset dates. The IMD declared long-term normal onset dates and onset dates for 2005, 2006 and 2007 were obtained from (http://www.imd.gov.in/section/nhac/dynamic/Monsoon_framce.htm). The long-term normal determined by local onset is the mean onset date between 1951-2007 in the grid cell containing the city in question. *Onset in Kerala determined by the local onset method is calculated for the grid cells containing the stations the IMD use to declare onset of ISM over Kerala.

		2005	2006	2007	Long-term normal
Lucknow	IMD		175-180	177-181	169
	Local Onset	174	176	188	187
Delhi	IMD		181-190	177-181	180
	Local Onset	175	187	194	181
Mumbai	IMD		148-151	166-169	161
	Local Onset	168	173	168	167
Kerala*	IMD	152	146	148	152
	Local Onset	148	141	153	152

This method compares favourably to the Wang and Lin (2002) method of detecting local onset of ISM (hereafter BWLH) when applied to APHRODITE data. Onset of ISM over Kerala, defined by the BWLH method, does not have a statistically significant correlation with IMD defined onset dates over Kerala (r_s= -0.012 (Spearman's rank correlation)). The BWLH method was developed to detect onset of monsoon from the 2.5°x2.5° Climate Prediction Centre Merged Analysis of Precipitation (CMAP) Climatological Pentad Mean (CPM) precipitation dataset. It defines onset as the first pentad when precipitation rate (RR_i: equation 9) is noticeably larger than dry season precipitation rate (precipitation rate in January), is greater than 5 mm day^{-1} and occurs between May and September (Wang and LinHo, 2002).

$$RR_i = R_i - R_{Jan}$$

$$i = 1,2 \dots \dots 73 \qquad (9)$$

RR_i is relative pentad mean precipitation rate, R_i is pentad mean precipitation rate and R_{Jan} is mean precipitation rate in January (peak dry season) for a given year.

Onset of ISM typically first occurred over the South-Western tip of India and North East India with a median onset date of day of year 145-150 (25^{th}-30^{th} May) (Fig. 3-5a). Onset date of ISM occurred later over North West India (Fig. 3-5a). Inter-annual variation in onset date of ISM from 1951-2007 across Northern, Central and the West Coast of India was characterised by inter-quartile ranges of onset date between 10-20 days (Fig. 3-5b). Greatest inter-annual variation in onset date of ISM occurred in Central-South East India (Fig 3-5b). The observed significant trends (p<0.05) of later occurring onset date were not field significant indicating that the number of observed significant trends was not statistically significantly different (p<0.05) to what would have occurred by chance under the global null hypothesis (Table 3-2, Fig. 3-5c). The low number (117 grid cells out of a possible 4475) of realised significant trends (p<0.05) in earlier occurring onset date, although field significant, has a very limited spatial coverage indicating trends of earlier or later occurring onset date of ISM were not evident over India between 1951-2007 (Table 3-2, Fig. 3-5c). However, large portions of India experienced significant trends (p<0.05) of increasing inter-annual variation in ISM onset date between 1951-2007 (Table 3-1; Fig. 3-5d). The magnitude of increasing or decreasing trends in inter-annual variation in onset date of ISM are depicted in Fig. 3-2c. Again, the size of moving window within which the coefficient of variation of onset date of ISM was calculated did not influence the spatial distribution of or ratio between significant positive and negative trends (p<0.05) (Table 3-1).

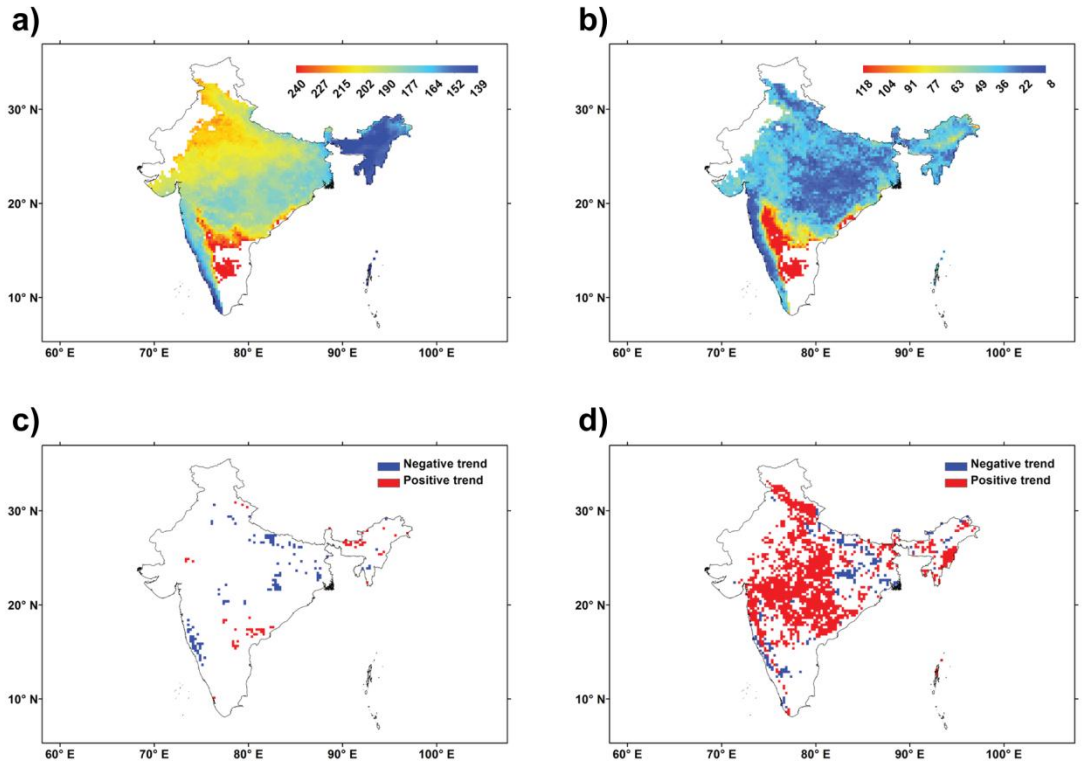

Figure 3-5 a) Median onset date of ISM between 1951-2007, b) inter-quartile range of onset date of ISM between 1951-2007, c) Significant trends (p<0.05) of increasing (later) or decreasing (earlier) onset date of ISM using the Mann-Kendall test and, d) significant trends (p<0.05) of increasing or decreasing inter-annual variation in onset date of ISM between 1951-2007 (results show trends in coefficient of variation calculated over a five year moving window). Day 152 = 1st June.

Grid cells discounted from trend analysis were located in North West and South East India; regions which received low amounts of ISM precipitation (Fig. 3-1a), explaining why thresholds defining onset date were not met. The low amount of ISM precipitation in South East India is due to the rain-shadow effect of the Western Ghats and regional pressure fields which result in an annual precipitation maximum between October and December (Gunnel 1997).

3.4 Discussion

The area in North West India where a high frequency, and increasing trends in frequency of severe drought years were observed corresponds to the arid regions of the Thar Desert and land cover classes of thorn scrub and desert, sparse vegetation (hot) and salt pans as defined by the South Asia Global Land Cover 2000 (GLC 2000) product (Agrawal et al. 2003). Frequent severe drought years would be expected in

such arid conditions. These trends are worrying as frequently recurring drought years on marginal and arid lands can result in top soil erosion and declining soil fertility, thus, reinforcing or spreading the extent of desertification (Shewale and Kumar 2005). The areas which reported frequent occurrence of severe drought years in the far north of India (Fig. 3-3a) predominantly receive precipitation in the form of snow or rain events associated with western disturbances during winter months (Shewale and Kumar 2005; Guhathakurta and Rajeevan 2008). This Himalayan region is mountainous and dominated by land cover classes of snow and alpine meadows, with poor coverage of rain stations to report precipitation events and not dominated by ISM precipitation (Agrawal et al. 2003; Rajeevan et al. 2006). This could explain why frequent drought years were noted in the area when drought was defined by precipitation deficiency. The negative impacts of drought conditions will be exacerbated by increased temperatures, high wind and low humidity (Attri and Tyagi 2010; Pai et al. 2011). A more comprehensive study, with a focus on the impact of droughts, should incorporate all the above mentioned climatic factors and not just precipitation deficiency.

Not only was India characterised by inter-annual variation (Figs. 3-1b, 3-3a and 3-5b), but large portions of India experienced significant increasing trends in inter-annual variation (Figs. 3-1d, 3-3b and 3-5d), in facets of ISM precipitation. The magnitude of this inter-annual variation and the location of trends of increasing variation exhibited a spatially heterogeneous distribution, thus, suggesting the need for local adaptive measures to cope with such variability. This inter-annual variation and observed trends of increasing variation are problematic for agriculture in India given the vulnerability of agriculture to a variable climate (Faures et al. 2010). The inter-annual variation in the ISM inhibits the use of long-term climatic normal conditions in agricultural planning. Indian agriculture is vulnerable to ISM variability with 59% of all agriculture being rainfed (DES 2009) and, thus, dependent on the ISM and lacking the protective buffer provided by irrigation.

Management of water resources at a watershed or river basin level requires knowledge generated from trend analysis of precipitation at a fine spatial resolution (Ghosh et al. 2009). Goal 2 of the National Water Mission specifies the need for basin

level integrated management of water resources; this is a multi-scale approach to water resource management from small (local) spatial units within a basin to the inter-basin level (National Water Mission 2009; Moors et al. 2011). As India exhibits fine-scale spatial variation in ISM precipitation (Satyanarayana and Srinivas 2008; Ghosh et al. 2009; Ghosh et al. 2011) (Fig. 3-1a); aggregating precipitation data over large regions of India may lead to aggregate trends which have false meaning locally, and which are of limited use to water resource planning at the local scale (Ghosh et al. 2009). The loss of local detail when performing trend analysis on precipitation data aggregated over a region is evident when a comparison is made between Fig. 3-1c (0.25°x0.25° grid cell resolution) and Figs. 3 in Guhathakurta and Rajeevan (2008) where a map of subdivisions which experienced significant trends in annual ISM precipitation is presented. While there are some similarities between the two maps, the analysis performed in Fig. 3-1c highlights that observed trends in annual ISM precipitation are not homogeneous across subdivisions or even larger areas. Similar locations experiencing significant (p<0.05) increasing or decreasing trends in annual ISM precipitation were realised when the Mann-Kendall test was applied to IMD 1°x1° gridded precipitation dataset for 1951-2004 (results not shown). This indicates the trends realised in the APHRODITE dataset are real and not artefacts of the method of product generation. The fragmented spatial pattern in the location of significant trends and spatial variation in average values illustrates the importance of undertaking this analysis at a fine spatial resolution. This analysis has produced local detail regarding recent (1951-2007) trends in facets of ISM precipitation complementing an established literature observing trends in extreme events at fine spatial resolution over a similar time frame (Ghosh et al. 2009; Krishnamurthy et al. 2009; Ghosh et al. 2011). This contributes to widening the understanding of recent behaviour in facets ISM precipitation which impact livelihoods and agriculture.

3.5 Conclusion

Daily gridded precipitation data at a 0.25°x0.25° spatial resolution, across all India from 1951-2007, were used to analyse the average and inter-annual variation in annual ISM precipitation, onset date of ISM and the frequency of severe drought years. A robust

method of estimating local onset date of ISM quantitatively from daily precipitation data (rather than qualitative criteria) was developed. This enabled temporal trend analysis to be performed on onset date of ISM at locations across all India for the period 1951-2007. Non-parametric statistical analysis was performed to find locations which experienced significant temporal trends in facets of ISM precipitation. In summary,

- The North East and South West Coast of India experienced the greatest amount of average annual ISM precipitation (greater than 4000mm), earliest onset date of ISM and greatest amount of inter-annual variation in ISM precipitation (an inter-quartile range of over 2000mm). In contrast, North West India experienced the lowest amounts of annual ISM precipitation (less than 1000mm) and the highest frequency of severe drought years (more than 15 drought years between 1951-2007). Median ISM precipitation was 6395mm in some locations compared to less than 800mm in others.
- Locations which experienced significant increasing or decreasing trends in annual ISM precipitation, onset date of ISM and recurrence of drought years were detected (Figs. 3-1c, 3-3b and 3-5c). Observation of such trends was not the norm across India; yet these trends were shown not to be chance occurrences by field significance testing (except in the case of trends of increasing, i.e. later, onset date of ISM). This highlights the importance of performing trend analysis at a fine spatial resolution to ensure that such trends are not lost as could happen when precipitation data are aggregated over larger regions.
- A greater expanse of the country experienced significant increasing trends of inter-annual variation in annual ISM precipitation and onset date of ISM (Figs. 3-1d and 3-5d). Worryingly, large regions of North West India experienced significant increasing trends in the frequency of severe drought years.

Chapter 4: Spatio-temporal dynamics in the phenology of croplands across the Indo-Gangetic Plains[5]

4.1 Introduction

Agricultural production within the IGP is vital for the region, providing food and economic security for its 365 million inhabitants (2011 census levels) as well as contributing to the national food supply (Saharawat et al. 2009; DES 2011; Perveen et al. 2012). However, the agro-ecosystems of the IGP lie at the interface of environment-human interactions and are vulnerable to climatic fluctuations (Aggarwal et al. 2004). Thus, with a growing population increasing demand for food (DES 2009) and pressure on environmental resources (Aggarwal et al. 2004; RWC 2006; Moors et al. 2011) and projections of uncertain and unfavourable trends in climatic parameters (Moors et al. 2011; Mathison et al. 2013) there is a need for comprehensive monitoring of changes in the IGP croplands. This monitoring should be specifically focused on increasing understanding of agro-ecosystem-climate interactions, highlighting potential vulnerabilities in the agricultural system, developing a sustainable and climate resilient agro-ecosystem and feeding into food security assessments in the region. Spatially explicit measures of land surface phenology (LSP) are ideally suited for this monitoring need.

Monitoring LSP is crucial to capture vegetation feedbacks to the atmosphere-climate system; LSP records can inform on numerous variables (e.g. land-surface albedo, surface roughness length, photosynthetic activity) which influence fluxes of energy, water and carbon (Richardson et al., 2013). Over the IGP, vegetation is almost exclusively dominated by a mixture of rainfed and irrigated croplands (Thenkabail et al. 2005). In particular, long-term records of LSP parameters are crucial to identify and understand climatic impacts and controls on agro-ecosystem functioning and, crop and vegetation physiological processes (Brown et al. 2010; Richardson et al. 2013; Xu et al. 2013). This can inform on where agro-ecosystem functioning and service provision are

[5] This chapter is currently in review (Advances in Space Research).

dependent on climatic drivers, or vulnerable to observed or projected shifts and trends in climate. For example, (Lobell et al. 2012) used measures of length of growing season (LGS) and start-of-season (SOS) derived from MODIS data to quantify the vulnerability of, and yield declines in, the wheat crop to extreme heat events in North India. The feedbacks of vegetation activity and agricultural practices across the IGP into the climate system, often with subsequent influences at a wider spatial scale (e.g. irrigation of croplands and crop residue burning have been shown to influence warming trends and Indian Summer Monsoon circulation (Zickfeld et al. 2005; Douglas et al. 2006; Knopf et al. 2008; Ramanathan and Carmichael 2008; Douglas et al. 2009) and, the impacts of climatic variability and projected climate change on crop productivity and yield (Lobell et al. 2012), mean generating a detailed inventory of LSP dynamics over the IGP's agro-ecosystem is of vital importance. This monitoring will enhance understanding of the interaction between cropland dynamics and the climate system, informing management of the agro-ecosystem to increase resilience to climatic variability and mitigate the system's negative climatic footprint. Such information is pertinent for agricultural landscapes (e.g. the IGP) where a changing climate may disrupt crop productivity coinciding with concerns regarding unsustainable cropping practices and population growth increasing food demand (Tilman et al. 2002; Aggarwal et al. 2004; Foley et al. 2011).

Monitoring LSP is now a key component of food security assessment; for example, the Famine Early Warning System Network (FEWSNET) uses NDVI measures of vegetation activity as part of an integrated early warning system for food security (Ross et al. 2009). Crop development and productivity, is one of a range of controlling factors for food security within the food system (Ericksen 2008a; Vrieling et al. 2011) and, in rural smallholder environments is a key determinant of livelihoods. Monitoring LSP over croplands allows discrimination between crop types (Xiao et al. 2005; Xiao et al. 2006; Thenkabail et al. 2007; Gumma et al. 2011b), provides observations which can be assimilated into process-based crop models increasing model prediction accuracy (Doraiswamy et al. 2004; Fang et al. 2011), to assess the impact of, and provide early warning for drought impacts on crop yields (Rojas et al. 2011) and, be used to forecast crop yield (Bolton and Friedl 2013). Long-term records of LSP parameters can be used

in isolation, or integrated with climate datasets, to inform agricultural planning and national and international responses to food shortages (Ross et al. 2009). Vrieling et al., (2013) comment that long-term records of normal LGS and variability in LGS can be used to identify locations suitable, or at higher risk, for different crop types.

Utilising LSP parameters to monitor and understand the dynamics of agro-ecosystem productivity across the croplands of IGP is crucial given the importance of crop production in supporting the livelihoods of the region's inhabitants. Ensuring high levels of productivity is important to national food security efforts; the Government of India purchases large quantities of foodgrains from the IGP states (Fig. 2-1) to supplement national buffer stocks and support the Targeted Distribution Service to poor households (Perveen et al. 2012). Determining seasonal influences on local productivity in croplands will become more important as local productivity will be critical in supporting livelihoods due to increasing polarity in purchasing power and the volatility of global food prices and markets (Brown and Funk 2008; Brown et al. 2012). Therefore, records of LSP parameters elucidating agro-ecosystem dynamics and productivity are key to integrated assessments of regional and national food security, especially given uncertainty in future climatic variability and monsoon dynamics (Annamalai et al. 2007; Brown et al. 2010; Moors et al. 2011; Turner and Annamalai 2012; Mathison et al. 2013).

Inter-annual changes in LSP in India are intrinsically linked to agro-ecosystem functioning which supports the food security of national population of 1.26 billion people (DES, 2011) and act as a driver in the regional climate system with feedbacks to monsoon circulation. Thus, changes in LSP over India potentially impact livelihoods and biophysical processes across the wider South Asia region. Despite this, there is a paucity of studies monitoring changes in LSP parameters over India (Dash et al., 2010; Prasad et al., 2007), let alone studies focusing on the spatio-temporal dynamics of vegetation activity and LSP over the key agricultural landscapes of the IGP. Dash et al., (2010) quantified spatial variation in LSP across India for one year using MERIS MTCI data but focused on all vegetation types rather than specifically croplands. However, they discriminated between areas of single cropping, double cropping and triple cropping across the IGP for one year. Lobell et al., (2012) used MODIS EVI data,

spanning the past decade, in North-West India to quantify links between SOS, LGS and *rabi* wheat crop production. Jeyaseelan et al., (2003) used GIMMS NDVI data to infer trends in photosynthetic activity across a range of vegetation types across India. Biradar and Xiao (2011) used MODIS data to map cropping intensity across India for one year identifying areas of single, double or triple cropping. Cropping intensity refers to the number of crops grown per plot of land per agricultural year. Studies have generated long-term datasets of LSP parameters over sub-Saharan African croplands (Vrieling et al. 2013). However, the studies exploring LSP parameters in the IGP did not generate a dataset of long-term trends in LSP parameters across the croplands of IGP. Thus, there still remains a need to (i) provide a comprehensive set of long-term records of LSP parameters and, (ii) utilise a long-term dataset to capture the spatio-temporal trends in phenology and biophysical performance over IGP croplands. We address the above mentioned gap with two over-arching research goals:

1) To create spatially explicit time-series from 1982-2006, at a spatial resolution of 8 km across the IGP of the following LSP parameters: (i) cropping intensity, (ii) LGS and (iii) agro-ecosystem productivity.

2) To quantify normal conditions, inter-annual variation and long-term trends in these LSP parameters across the IGP croplands from 1982-2006.

4.2 Methods and Data

4.2.1 Data

The GIMMS NDVI dataset used in this study is composed of AVHRR data with a spatial resolution of 4 km processed to produce bimonthly composites of global (except Antarctica) NDVI coverage at a spatial resolution of 8 km (http://glcf.umd.edu/data/gimms/: Tucker et al., 2005)[6]. Further details regarding the GIMMS NDVI product generation can be found in Pinzon et al. (2005) and Tucker et al. (2005). In a comprehensive comparison of four AVHRR-derived NDVI products versus

[6] A longer GIMMS NDVI record (GIMMS NDVI 3g) has now been processed, more information is provided at: http://www.mdpi.com/journal/remotesensing/special_issues/monitoring_global. At the time of analysis this dataset was available for general release.

Landsat samples, assumed as 'ground truth', Beck et al., (2011) found: the GIMMS NDVI dataset performed best in temporal change analysis, had statistically significant (p<0.05) median NDVI values compared to other AVHRR-NDVI datasets and, similar median NDVI values observed at the latitude relevant to this study. The GIMMS NDVI dataset has been used in numerous studies exploring phenology dynamics across croplands and agricultural ecosystems both globally (Brown et al. 2012) and in sub-Saharan Africa (Brown et al. 2010; Vrieling et al. 2011). The GIMMS NDVI data spanning the Indian states of Punjab, Haryana, Uttar Pradesh and Bihar from 1982 till 2006 were extracted from the global datasets.

4.2.2 Data Pre-Processing

The GIMMS NDVI data were reordered to match the agricultural calendar of the IGP; in each month there is a composite corresponding to the time period: day one to 15 and then day 16 till the end of the month (Tucker et al., 2005). Each year, therefore, contains 24 NDVI composite images. The *zaid*, *kharif* and *rabi* cropping seasons span across two calendar years (DES, 2009), thus, necessitating reordering the annual GIMMS NDVI composites to correspond to the agricultural calendar of the IGP. Time step 1, therefore, became the GIMMS NDVI composite for January (days 16-end of month) in year *n* and time step 35 was the GIMMS NDVI composite for June (days 16-end of month) in year *n+1*.

The agricultural time-series GIMMS NDVI data were fitted, with a bias towards the upper envelope of the raw data values, using a maximum polynomial iterative fit, an adaptation of the method used in generating the SPOT VGT4Africa phenology products (Bartholomé et al. 2006). Including a fitting bias towards the maximum raw NDVI values accounts for: (i) the negative bias in AVHRR NDVI data due to the sensor's sensitivity to water vapour in the atmosphere as a result of its wide spectral bands (Brown et al. 2008; Atkinson et al. 2012) and (ii) drop-outs due to cloud cover which do not follow the phenological pattern of vegetation (Chen et al. 2004). Local polynomial fitting was used rather than fitting data to functions (e.g. double logistic, asymmetric Gaussian) or using harmonic analysis as there can be inter-annual variation in phenology due to shifting cropping intensity and crop type per pixel; local polynomial

functions are better suited to capturing complex behaviour (Jönsson and Eklundh 2004; Vrieling et al. 2013). Local polynomial fitting has been used in numerous studies for phenology parameter estimation over croplands using the GIMMS NDVI and other AVHRR-derived datasets (Jönsson and Eklundh 2004; Brown et al. 2010; Vrieling et al. 2011; Vrieling et al. 2013).

Prior to fitting the data, composities contaminated by cloud cover or drop-outs were detected following Vrieling et al. (2011) where an increase of 0.3 NDVI units between composites was masked and replaced with the average NDVI value of the preceding and following composites. The maximum polynomial iterative fit breaks the original 35 composite time-series (t_r) into *two* 21 composite time-series with six overlapping composites. Each time-series was fitted with a 5th degree polynomial (t_p). A smoothed time-series (t_s) was generated by combining the separate t_p time-series and taking average values for the overlapping composites. The maximum envelope was then fitted to the raw values following:

$$t_i = max(t_r, t_s) \quad (1)$$

This process was repeated for three iterations, rather than six as in the method applied to the SPOT VGT4Africa data, to avoid overfitting. The final t_i data were then filtered using a Savitzky-Golay filter (2) with an 11 composite moving window and a 4th degree polynomial. Filtering the maximum fitted NDVI dataset removes any remnant short-term noise or fluctuations along the trend of phenological cycles, thus, increasing the reliability of LSP estimates.

$$N_j^* = \frac{\sum_{i=-m}^{m} C_i N_{j+i}}{n} \quad (2)$$

Equation (2) is the Savitzky-Golay filter where N_j is the raw j^{th} NDVI value and N^*_j is the smoothed NDVI value. C_i is the coefficient for the $_i^{th}$ NDVI value of the filter of a size $2m+1$, n is equal to $2m+1$ and is 11 in this study, thus $m=5$.

A mask of urban, water and forested areas was generated using the GLC 2000 product with a spatial resolution of 1 km (Bartholomé and Belward 2005). The GLC 2000 global product was produced by synthesising regional land cover products generated using SPOT VGT data (Bartholomé and Belward 2005; Herold et al. 2008) and was used in numerous studies investigating land cover change and the interaction between land cover and environmental and climatic processes (Ramankutty et al. 2008; Thenkabail et al. 2009; Douglas et al. 2009). The regional land cover products contain more thematic detail than the global land cover product (Bartholomé and Belward 2005); therefore, the South Asia GLC 2000 product (Agrawal et al. 2003) was used in the development of the urban, water and forest mask. The GLC 2000 product was upscaled using a majority filter to match the spatial resolution of the GIMMS dataset. From the upscaled GLC2000 data the IGP states of Punjab, Haryana, Uttar Pradesh and Bihar were extracted and pixels which contained a majority land cover of urban, water and forest were masked out.

4.2.3 LSP Parameter Estimation

Areas with a double cropping cycle, triple cropping cycle, single zaid cropping season, single kharif cropping season and single rabi cropping season in the IGP have a distinct phenology. A kharif cropping season temporal vegetation index (VI) profile is characterised by (i) an increase in VI values from late May/early June representing SOS, (ii) a peak VI occurring between August and September coinciding with the peak above-ground biomass and (iii) decreasing VI values through October when the crop senesces (Fig. 4-1). A similar pattern occurs during the rabi cropping season (Fig. 4-1) except that the green up period occurs between November and January, peak NDVI occurs in February with crop senescence during March and April; the zaid cropping season is less common than kharif cropping or rabi cropping, but occurs from March to June before the arrival of the monsoon (Fig. 4-1). Double and triple cropping cycles incorporate the phenology profiles of a combination of zaid, kharif and rabi cropping.

The timing of the extracted LSP parameters determined which cropping season was detected.

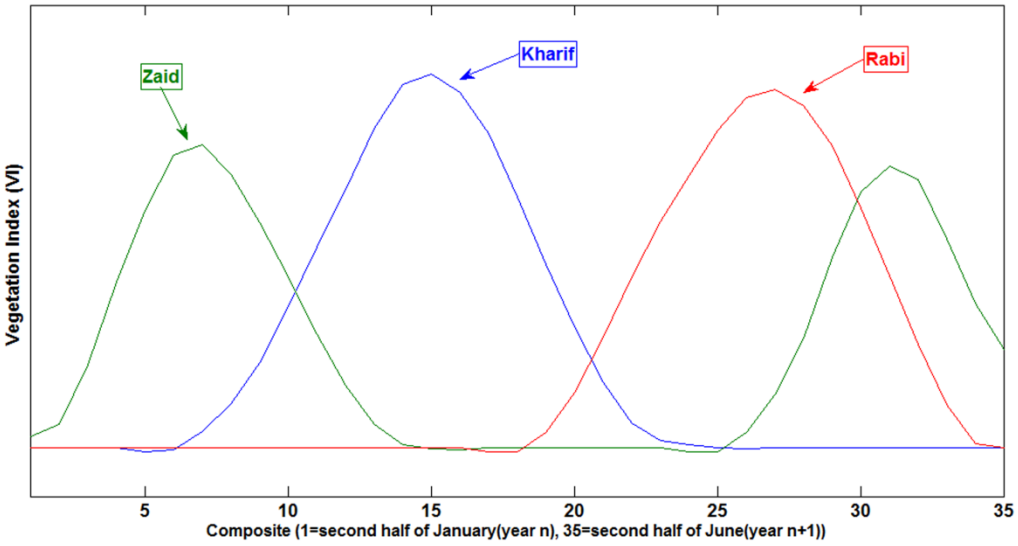

Figure 4-1 Typical phenology profile derived from vegetation indices for the three main cropping seasons of the Indo-Gangetic Plain (*zaid, kharif, rabi*).

A cropping season was detected using an adapted version of Dash et al. (2010); an algorithm was used to search the phenology profile for a peak in the growing season. If a peak was detected the algorithm searched backwards for a SOS. If both a peak and SOS were detected a logical condition detecting rapid green up after SOS was required to be met for a cropping season to be identified. A peak growing season was detected if an NDVI value was preceded by a month (two GIMMS composites) of increasing trend in NDVI values and succeeded by a month of decreasing trend in NDVI values. A month is a sufficient time period to ensure the noted peak is associated with a LSP parameter rather than noise caused by anomalous fluctuations in the NDVI time-series. The logical condition detecting a rapid green up following SOS required the difference between SOS NDVI and peak NDVI to be greater than one fifth of the peak NDVI. This logical condition detects the rapid growth of vegetation following emergence common in many crops (Zhang et al. 2003) including the dominant rice crop in this study area (Xiao et al. 2005; Xiao et al. 2006). Dash et al. (2010) used these conditions to extract LSP parameters over India for a range of vegetation types, including croplands, from Meris terrestrial chlorophyll index (MTCI) data.

Numerous approaches have been used to detect SOS. Common methods include change in rate of curvature of VI values fitted to a logistic function (Zhang et al. 2003), the point when the first derivative changes sign and 'valley points' (Sakamoto et al. 2005; Dash et al. 2010), or a percentage threshold of the amplitude of growing season VI values (White et al. 1997; Jönsson and Eklundh 2004; Lobell et al. 2012; Vrieling et al. 2013). Due to the difficulty of detecting specific vegetation and crop development stages from Earth observation data the choice of method to detect SOS is partly subjective, difficult to validate and, should be tailored towards the vegetation type in question. Here, the point on the rising limb of the phenology profile when NDVI values exceed 30% of the amplitude between minimum and peak NDVI values for a given cropping season was defined as SOS. The minimum NDVI value was defined as the point on the phenology profile, preceeding the peak, when the first derivative changed sign and was preceeded by a decreasing trend in NDVI values for one month and succeeded by an increasing trend in NDVI values for one month. The percentage threshold method is widely used to detect SOS in agricultural lands and has been applied to GIMMS NDVI data for a range of crop types over sub-Saharan Africa (Vrieling et al. 2011) and wheat crops over the IGP (Lobell et al. 2012). The 30% threshold used here gave a sensible retrieval of SOS, end-of-season (EOS) and LGS across the IGP based on prior knowledge of dominant crop types and typical LGS. The EOS was defined using the same method applied to the falling limb of the phenology profile.

Numerous approaches exist to define LGS; often these approaches use climatic data. For example, one common method, often used in crop models, is the use of growing degree days (AGDD) defined as the cumulative sum of hourly or daily temperatures values between crop/vegetation-specific temperature thresholds (Brown et al. 2012). Other approaches, such as the International Institute for Applied Systems Analysis and the FAO define LGS as the number of days per year when rainfed soil moisture availability exceeds half the potential evapotranspiration (Fischer et al. 2002). Such approaches are limited by the need for extensive and reliable coverage of climate data (Vrieling et al. 2013) and in areas of double/triple cropping where dry season crops are grown under irrigation. Therefore, in the IGP, where there is a prevalent double

cropping system, LSP parameters estimated from time-series remote sensing data provide a suitable method to obtain reliable LGS estimates. Here, the LGS was computed by subtracting the SOS from EOS.

A surrogate measure of productivity of the cropping season was computed as the cumulative sum of NDVI (cumNDVI) values from SOS to EOS. The cumulative sum or integrated growing season NDVI is a commonly used measure of biomass and vegetation productivity (Jönsson and Eklundh 2004; Pettorelli et al. 2005; Vrieling et al. 2011).

4.3 Results

4.3.1 Cropping Intensity

State-wise, the area estimated as double cropping from the GIMMS NDVI dataset has a positive correlation (R^2=0.95; Appendix 2) with Government of India land use statistics for state-wise area cropped more than once per agricultural year (DES, 2013). This indicates that the remote sensing derived estimates of cropping intensity here capture the state-wise inter-annual variation in cropping intensity across the IGP[7]. There has been a clear west to east spread in the area under double-cropping from 1982-83 to 2005-06 (Fig. 4-2). In 1982-83 Bihar and Eastern Uttar Pradesh were largely under *kharif* single cropping; however, from 1982-83 to 2005-06 these regions experienced an increase in cropping intensity (Fig. 4-2). Significant trends of increased area under more intensive cropping in Bihar (p<0.01; R^2=0.34) and Uttar Pradesh (p<0.01; R^2=0.33) were detected; this corresponds to an increase in area under double or tripple cropping of 945 $km^2\ yr^{-1}$ and 2680 $km^2\ yr^{-1}$, respectively (Fig. 4-3). The net area cropped in Bihar also increased between 1982-83 and 2005-06 with an increase in the area under *kharif* single cropping (Fig. 4-2). The western portion of the IGP already had a developed intensive double cropping system in 1982-83 which has remained the dominant cropping system; there was no significant increasing trend in area under double cropping in Punjab (Fig. 4-3). However, in Haryana there was a significant

[7] Appendix 2 and section 4.4.1 provide discussion on the limitations of using GIMMS NDVI data for areal estimates of extent under agricultural land cover.

increasing trend in area under double cropping of 136 $km^2\ yr^{-1}$ ($p<0.01$; $R^2 = 0.29$), although the rate of increase was less than that observed in Bihar and Uttar Pradesh and large portions of Haryana were under double cropping in 1982-83 (Fig. 4-2).

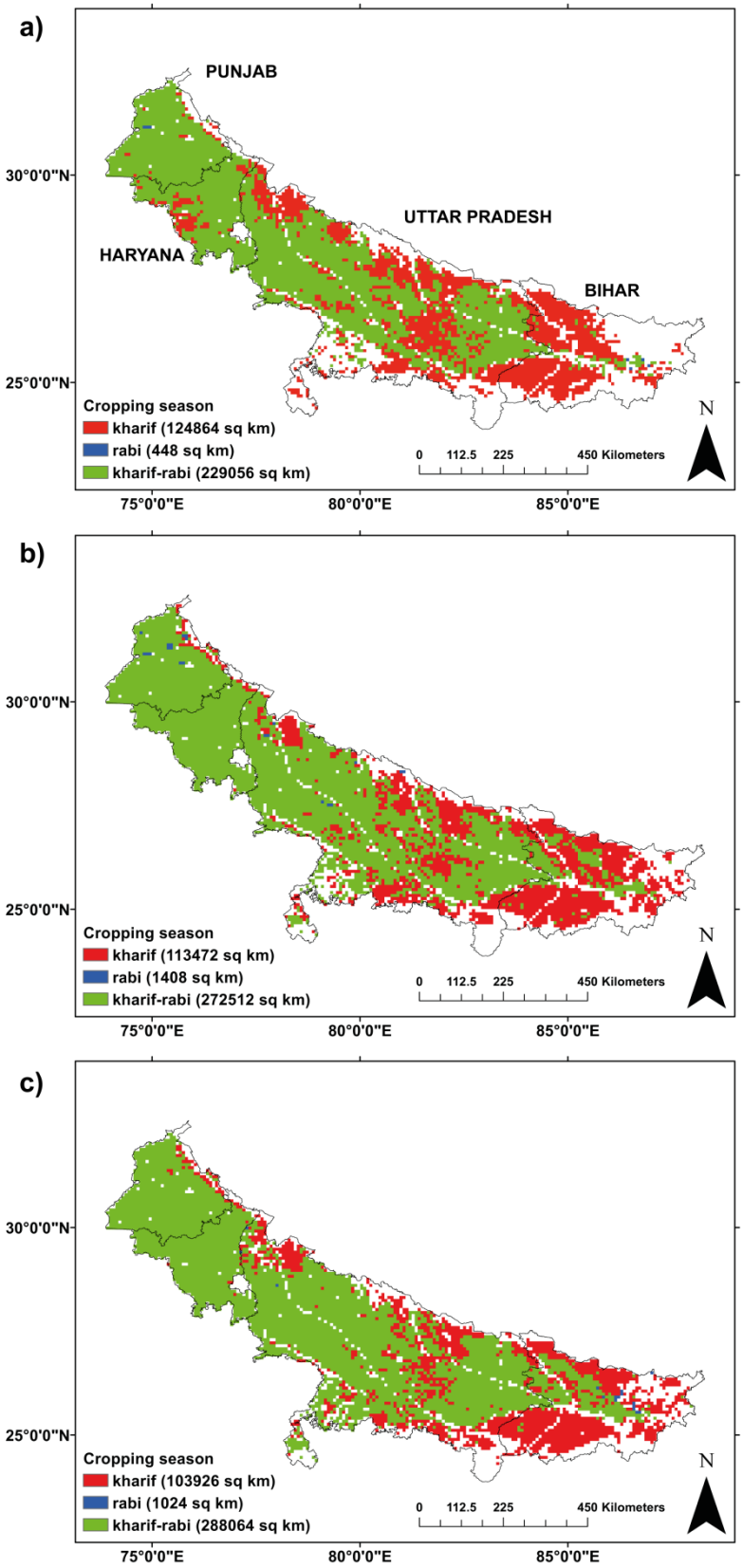

Figure 4-2 Observed cropping intensity across the Indo-Gangetic Plains for three time-periods a) 1982-83 – 1985-86 agricultural years, b) 1992-93 – 1995-96 and, c) 2002-03 – 2005-06 (maps show the majority cropping intensity per agricultural year experienced per pixel over the four year period).

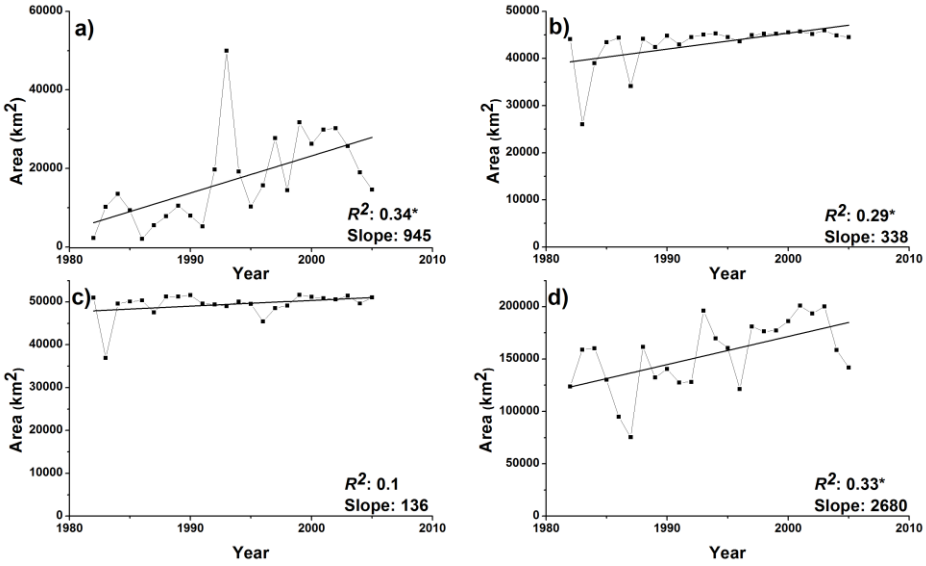

Figure 4-3 State-wise area under double or triple cropping systems per year a) Bihar, b) Haryana, c) Punjab and, d) Uttar Pradesh. *denotes statistical significance at p<0.01. (See Appendix 4 for discussion of the anomaly in 1993 for Bihar).

4.3.2 Length of Growing Season

Most of the IGP had a mean *kharif* LGS between 138 and 150 days (Fig. 4-4a), with Bihar and the southern portion of Punjab having longer mean *kharif* LGS. Parts of southern Haryana and southern Uttar Pradesh had a shorter mean *kharif* LGS between 75-137 days. There was no clear spatial pattern in inter-annual variability in *kharif* LGS across the IGP except in parts of eastern Bihar which experienced greater inter-annual variability (Fig. 4-4b). Inter-annual variability was computed as the coefficient of variation (CV) with years when a cropping season was not detected excluded. The mean *rabi* LGS for most of the central and eastern IGP was between 168 and 185 days with a shorter mean *rabi* LGS generally observed in the western portions of the IGP (Fig. 4-5a). Again there was no dominant spatial pattern in the inter-annual variability in *rabi* LGS. However, in Bihar there was a more fragmented spatial pattern in CV (Fig. 4-5b). This is largely due to the fact that fewer *rabi* cropping seasons were detected here. Fig. 4-4c and 4-5c are bivariate risk maps. Bivariate risk maps are useful to inform agricultural planning as they give a measure of the normal LGS or productivity for a location versus the variability in the given measure. This is important as the normal conditions inform on the suitability of the location for a given crop type or

agronomic practice and the variability informs upon the risk of implementing a certain crop or agronomic practice (Vrieling et al. 2013). The southern portion of Uttar Pradesh experienced shorter mean *kharif* LGS and greater levels of inter-annual variability in *kharif* LGS (Fig. 4-4c). Large portions of Bihar also experienced greater levels of inter-annual variability in LGS with varying lengths of mean *kharif* LGS (Fig. 4-4c). The southern portion of Uttar Pradesh and Haryana have a shorter *rabi* LGS coinciding with greater inter-annual variability in *rabi* LGS (Fig. 4-5c). Much of Punjab and Haryana have longer *rabi* LGS coinciding with lower levels of inter-annual variability in *rabi* LGS (Fig. 4-5c).

Bihar, Uttar Pradesh and Haryana all experienced significant (p<0.01) increasing trends (R^2 = 0.37, 0.31, 0.28, respectively) in the number of growing days per agricultural year (2.52, 1.96, 0.88 days yr^{-1}, respectively) (Fig.4-6). In Bihar, this equated to approximately 60 more growing days per agricultural year in 2005-06 than in 1982-83. There was no significant increasing trend in the number of growing days per year in Punjab.

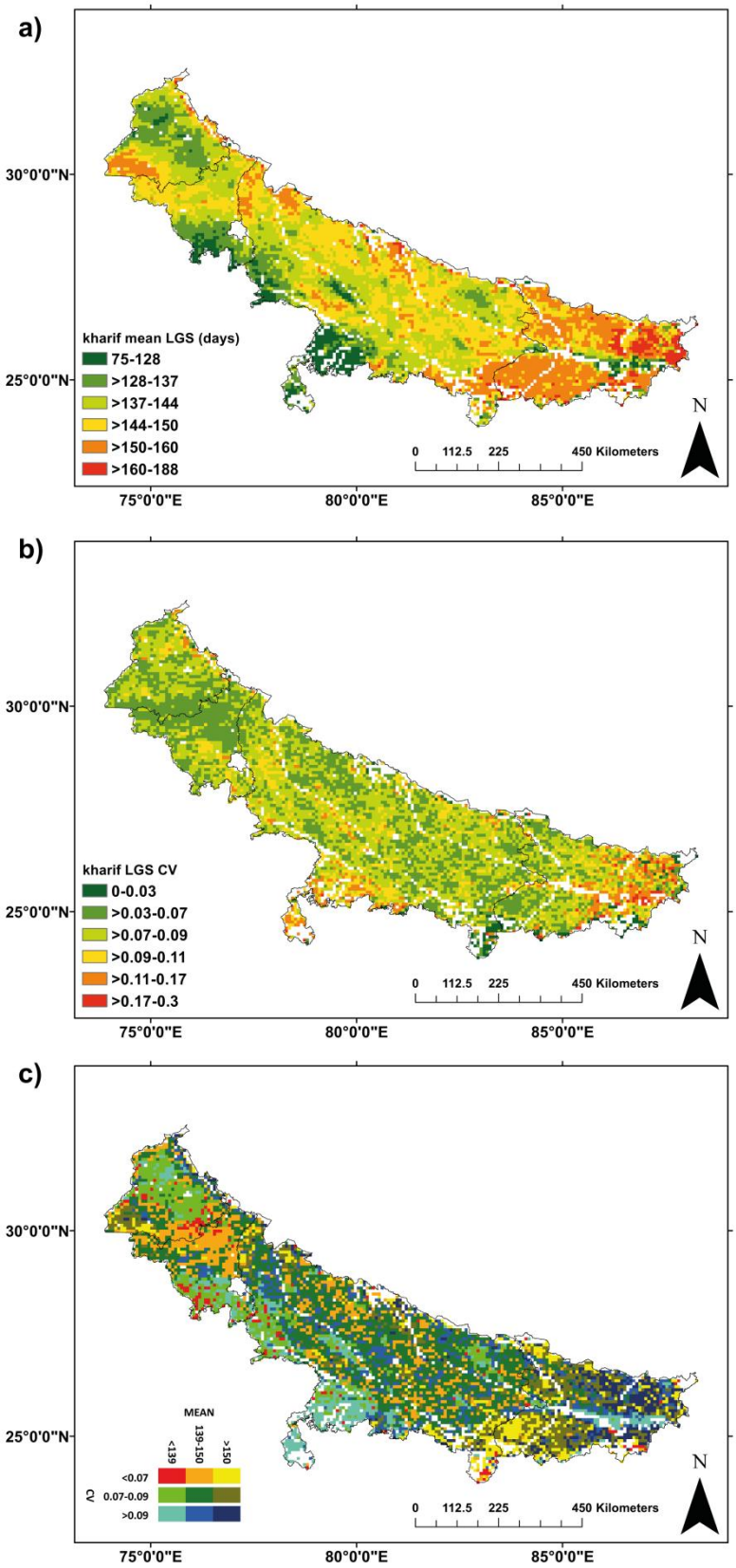

Figure 4-4 a) mean *kharif* LGS, b) coefficient of variation in *kharif* LGS and c) bivariate map of mean *kharif* LGS and coefficient of variation in *kharif* LGS.

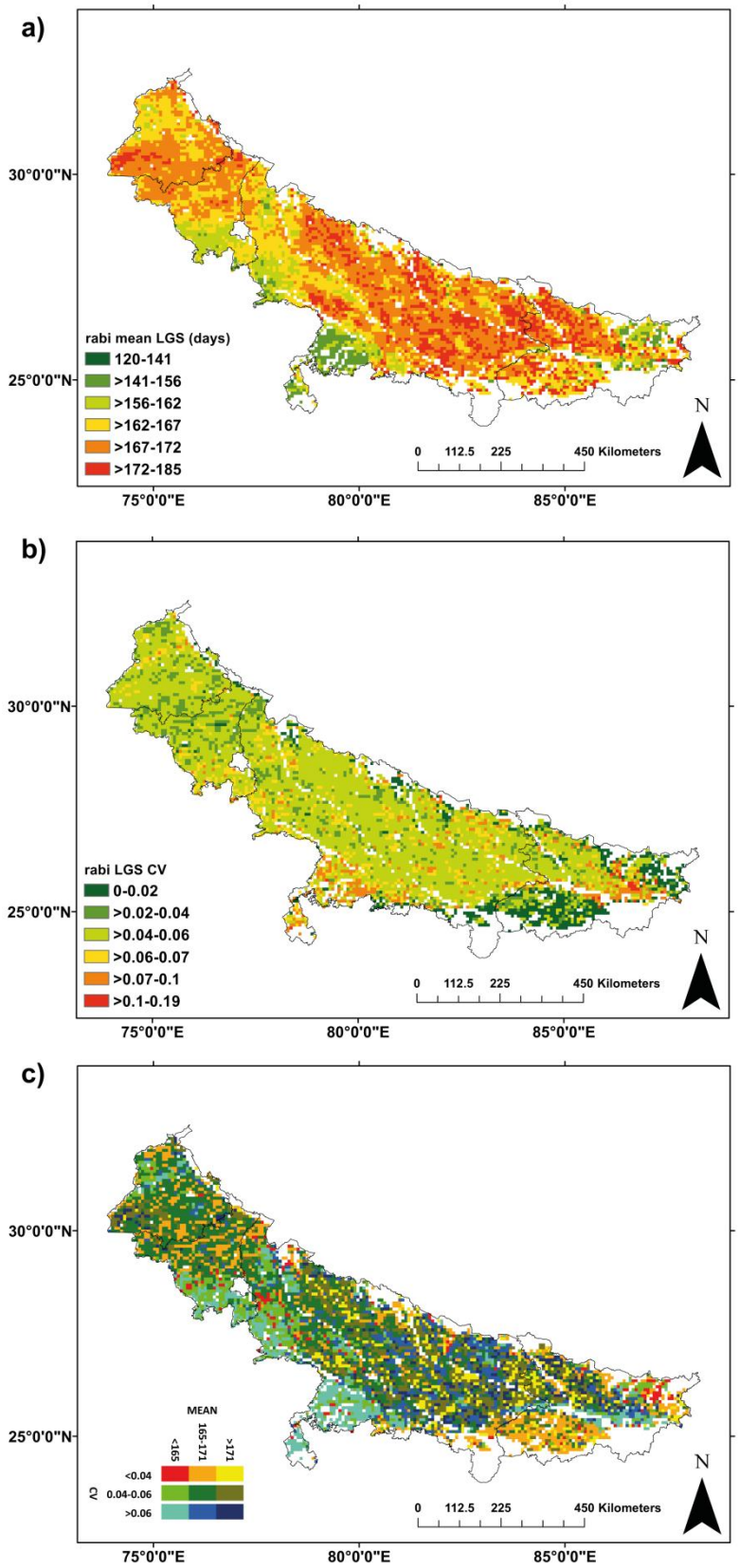

Figure 4-5 a) mean *rabi* LGS, b) coefficient of variation in *rabi* LGS and c) bivariate map of mean *rabi* LGS and coefficient of variation in *rabi* LGS.

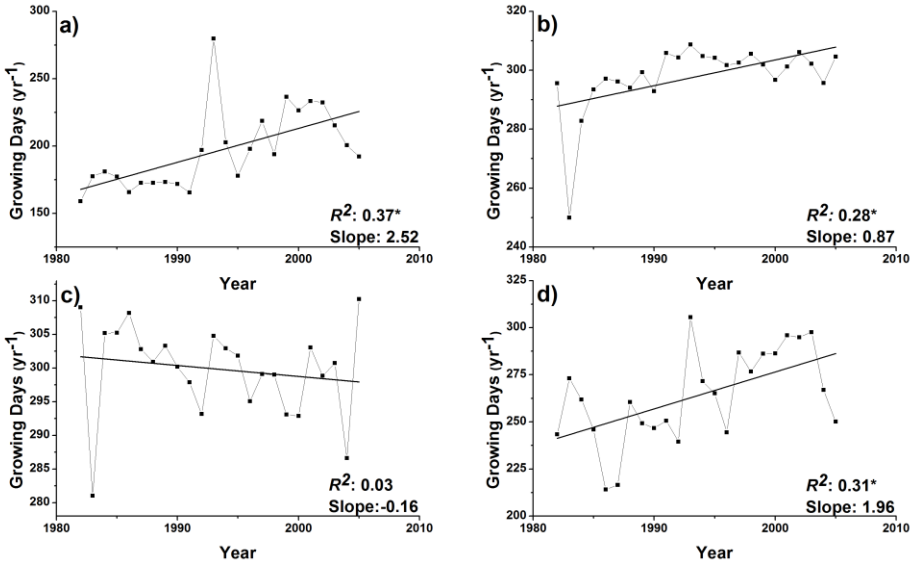

Figure 4-6 State-wise number of growing days (total of all cropping seasons experienced per pixel per agricultural year) a) Bihar, b) Haryana, c) Punjab and, d) Uttar Pradesh. *denotes statistical significance at p<0.01.

4.3.3 Productivity

The state-wise surrogate measures of agricultural productivity derived from remote sensing observations (cumNDVI) were well correlated with state-wise totals of *kharif* foodgrains (R^2=0.76) and *rabi* foodgrains (R^2=*0.88*) (DES, 2011) (Appendix 3). This pseudo-validation indicates that cumNDVI computed from the GIMMS NDVI dataset captures inter-annual and spatial variation in agricultural productivity. The greatest levels of mean *kharif* productivity were found in the far north of Uttar Pradesh and the far east of Bihar (Fig. 4-7a). Punjab, central and northern Haryana, central and northern Uttar Pradesh and Bihar had similar levels of mean *kharif* productivity (cumNDVI: 4.07-5.66) (Fig.4-7a). Lower levels of mean *kharif* productivity were observed in southern Uttar Pradesh and Haryana (Fig. 4-7a). Central and northern Punjab, Haryana and Uttar Pradesh had the lowest levels of inter-annual variation in *kharif* productivity (Fig. 4-7b). Bihar experienced a fragmented spatial pattern in inter-annual variation in *kharif* productivity, whilst high levels of inter-annual variation in *kharif* productivity were observed in southern Haryana (Fig. 4-7b). Much of central and northern Punjab, Haryana and Uttar Pradesh experienced high mean *kharif* productivity coinciding with lower levels of inter-annual variation (Fig. 4-7c). In

contrast the southern portions of Haryana and Uttar Pradesh experienced lower levels of mean *kharif* productivity and greater levels of inter-annual variation (Fig. 4-7c). Both Bihar and Uttar Pradesh experienced significant (p<0.01) increasing trends in *kharif* cropping season productivity from 1982-83 to 2005-06 (R^2=0.35 and 0.31, respectively) (Fig. 4-8). The western IGP states of Punjab and Haryana did not experience any significant increasing trend in *kharif* cropping season productivity.

Central and northern Punjab and Haryana experienced the greatest mean *rabi* productivity (cumNDVI: 6.28-7.17) (Fig. 4-9a). Mean *rabi* productivity was consistent across much of Uttar Pradesh and western Bihar (cumNDVI: 4.92-5.75) with pockets of lower mean *rabi* productivity found in southern Haryana, Uttar Pradesh and eastern Bihar (Fig. 4-9a). There was no clear spatial pattern in inter-annual variation in *rabi* productivity: the lower levels of inter-annual variation observed in southern Bihar are likely due to fewer *rabi* cropping seasons being detected (Fig. 4-9b). Parts of southern Haryana and eastern Bihar experienced lower mean *rabi* productivity coinciding with greater levels of inter-annual variability (Fig. 10c). Central and nothern Punjab had higher mean *rabi* productivity coinciding with lower levels of inter-annual variation (Fig. 4-9c). Bihar and Haryana experienced significant (p<0.01) increasing trends in *rabi* cropping season productivity (R^2=0.28 and 0.6, respectively) (Fig. 4-10). Punjab and Uttar Pradesh also experienced increasing trends in *rabi* cropping season productivity with a p-value of p<0.05 (R^2=0.24 and 0.22) (Fig. 4-10).

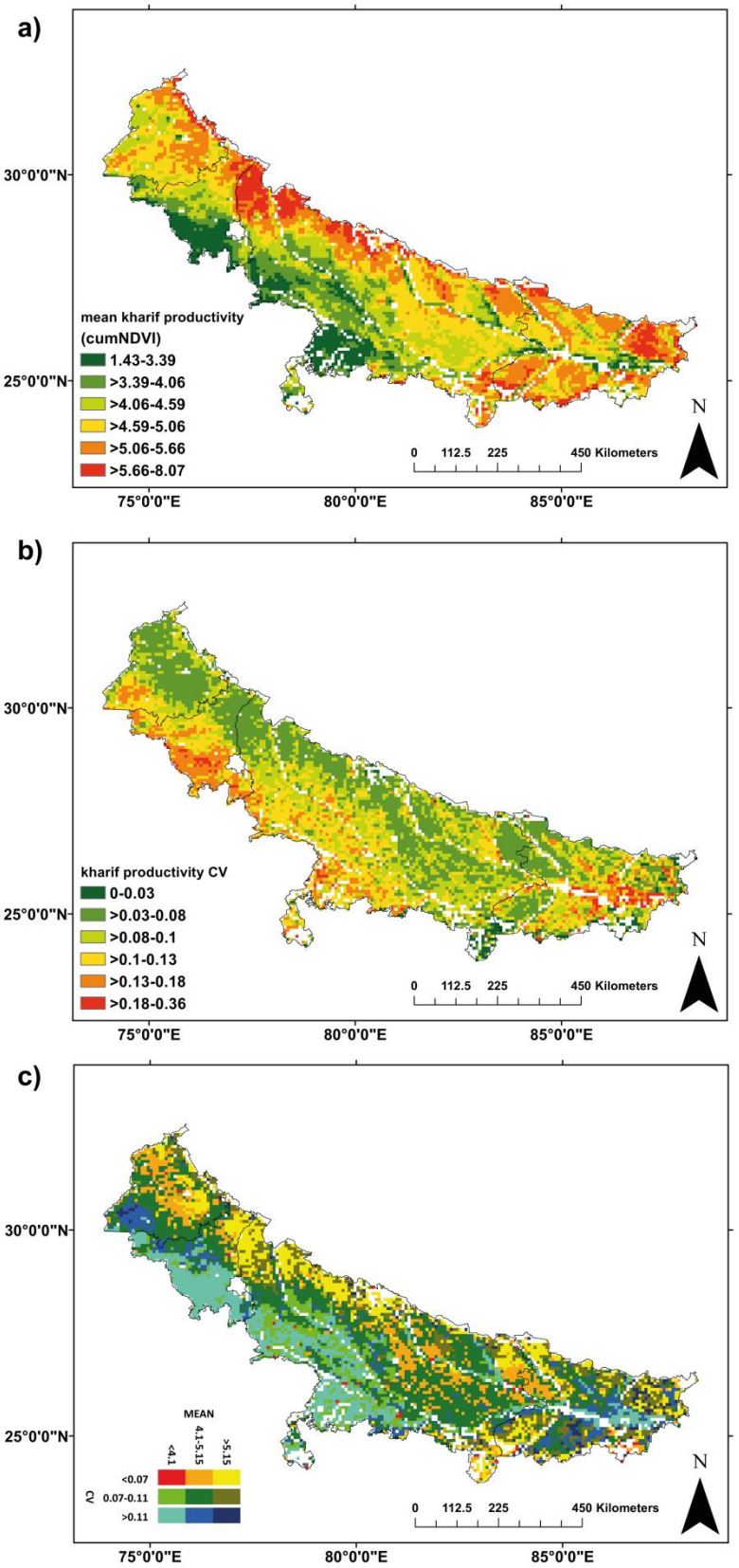

Figure 4-7 a) mean *kharif* growing season productivity, b) coefficient of variation in *kharif* growing season productivity and c) bivariate map of mean *kharif* growing season productivity and coefficient of variation in mean *kharif* growing season productivity.

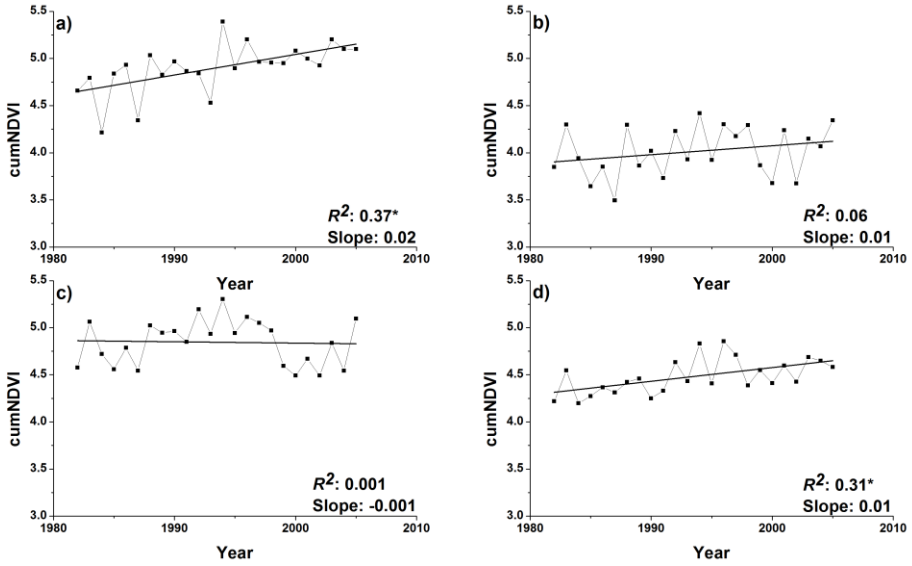

Figure 4-8 State-wise mean *kharif* growing season productivity a) Bihar, b) Haryana, c) Punjab and d) Uttar Pradesh. *denotes statistical significance at p<0.01.

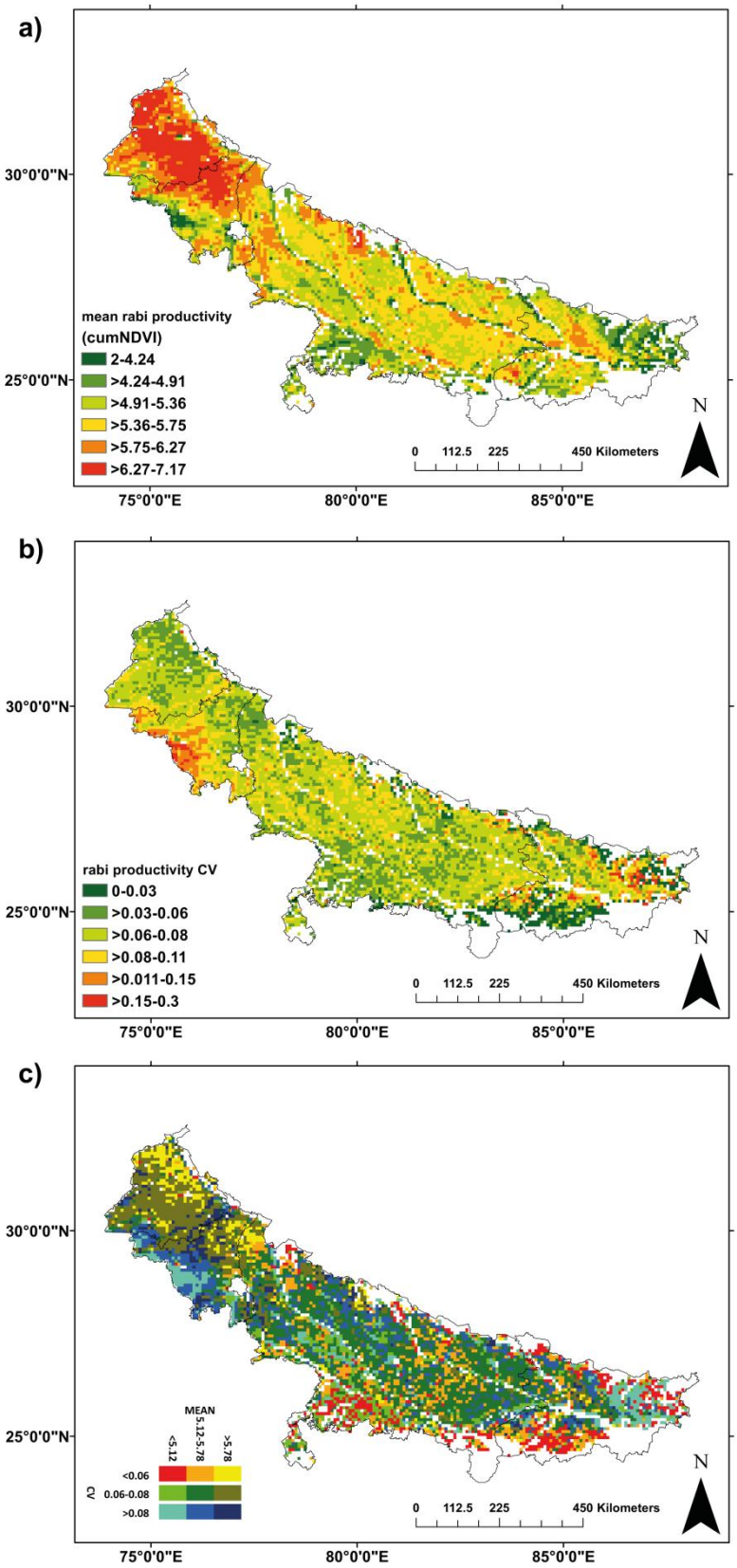

Figure 4-9 a) mean *rabi* growing season productivity, b) coefficient of variation in *rabi* growing season productivity and c) bivariate map of mean *rabi* growing season productivity and coefficient of variation in mean *rabi* growing season productivity.

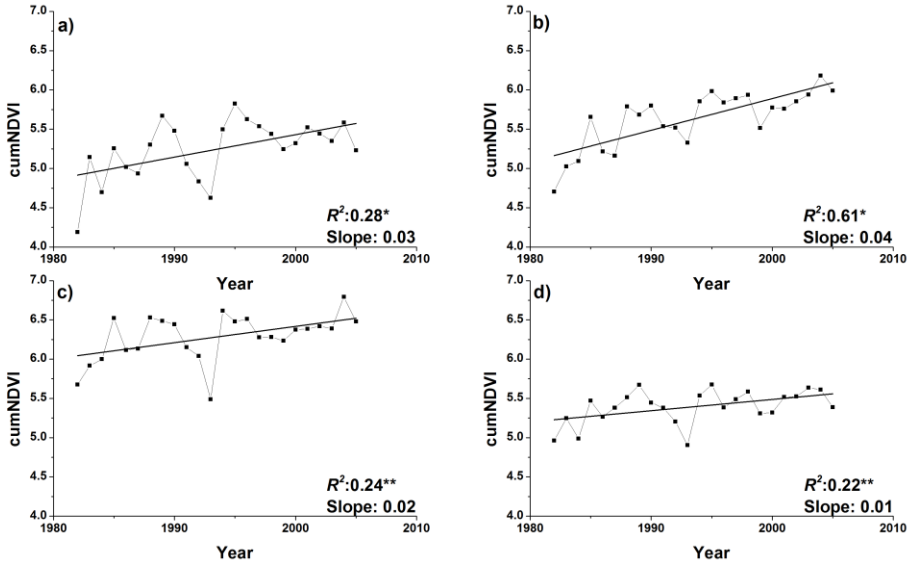

Figure 4-10 State-wise mean *rabi* growing season productivity a) Bihar, b) Haryana, c) Punjab and d) Uttar Pradesh. *denotes statistical significance at p<0.01. **denotes statistical significance at p<0.05.

4.4 Discussion

Kharif single cropping is indicative of rain-fed rice crops grown during the monsoon season and is generally not associated with a developed agricultural infrastructure. The areas under *kharif* single cropping are centred in the less developed regions of the eastern IGP, namely Bihar (Fig. 4-2). In 1982-83 agriculture in Bihar was almost solely *kharif* single cropping (Fig. 4-2). The later uptake of double cropping in Bihar is due to the intensification of agriculture associated with the Green Revolution largely bypassing the eastern IGP (Singh et al. 2009). The greater amounts of ISM precipitation (relative to the western IGP) create more suitable conditions for growth of the *kharif* paddy rice crop which is predominant in the eastern IGP (Narang and Virmani 2001; Duncan et al. 2013). Bihar's population has a lower socio-economic status relative to the other IGP states, with a greater proportion below the poverty line (RWC 2006; Erenstein et al. 2007). There are lower levels of agricultural inputs, irrigation capacity and farm mechanisation in Bihar due to poor economic conditions precluding development, and, frequent flood events associated with heavier monsoon rainfall (Erenstein et al. 2007; Singh et al. 2009). This explains the greater proportion of *kharif* single cropping, lower proportion of double cropped area, fewer number of growing

days per year and lower levels of *rabi* productivity in Bihar compared to the rest of the IGP where intensive double cropping systems are more prominent (Figs. 4-2, 4-3, 4-6, 4-9, 4-10).

The western IGP, Punjab, Haryana and western Uttar Pradesh, had an intensive cropping system already implemented by 1982-83 (Figs. 4-2 and 4-3). This was reflected by the long-standing double cropping system, greater number of growing days per year and high levels of *kharif* and *rabi* productivity (Figs. 4-2 - 4-10). Double cropping systems reflect an advanced agricultural infrastructure with high levels of fertilizer inputs, use of high yielding varieties (HYVs) and irrigation developed under the Green Revolution (Aggarwal et al. 2004; Ladha et al. 2009).

Figs. 4-7c and 4-9c show that northern and central Punjab and Haryana have higher levels of mean productivity and lower levels of inter-annual variability. This can partly be explained by these areas having the most developed agricultural infrastructure including high levels of irrigation and farm mechanisation relative to the other IGP states (Erenstein et al. 2007) affording them some resilience to climatic variability (Perveen et al. 2012). The southern portions of Punjab and Haryana experienced greater inter-annual variation in *kharif* productivity, often coinciding with lower mean productivity (Fig. 4-7c). These regions have a less extensive irrigation infrastructure, with lower densities of tubewell coverage relative to the northern and central portions of Punjab and Haryana (Ambast et al. 2006), with of increasing trends in recurrence of drought years and inter-annual variation in monsoon precipitation and lower (relative to the rest of the IGP) normal monsoon precipitation (Duncan et al. 2013). The cropping systems in these regions are not rice-wheat dominated, but more fragmented with cotton and pearl-millet crops grown (Ambast et al. 2006; Panigrahy et al. 2010). These factors (e.g. unfavourable climate, fragmented cropping system, less access to irrigation) contribute to explaining observed variability in productivity (similar patterns were observed in the *rabi* cropping season; Fig. 4-9c). These bivariate maps are of particular importance to agricultural planning in the IGP where there is a pressing need to increase production in a sustainable and climate resilient manner given projected population growth increasing food demand (Aggarwal et al. 2004; Wassmann et al. 2009).

Whilst Green Revolution practices and intensive cropping increased agricultural production in the western IGP (Ambast et al. 2006; DES 2011), specifically the rice and wheat crops, there have been recently observed trends of stagnating or declining crop yields and environmental degradation (Ladha et al. 2003; Aggarwal et al. 2004; RWC 2006). There were no observed increasing trends in *kharif* productivity in either Punjab or Haryana between 1982-83 and 2005-06 (Fig. 4-8). This is further evidence highlighting concerns about the sustainability of maintaining or increasing rice crop yields in the north-west IGP. Attributed to the intensive cropping in the western IGP have been noted declines in groundwater levels, decreasing groundwater quality, soil salinity, decreasing nutrient levels and a reliance on water-intensive rice cropping in regions which receive relatively low amounts of ISM precipitation (Abrol 1999; Ladha et al. 2003; Aggarwal et al. 2004; RWC 2006; Ambast et al. 2006; Tiwari et al. 2009; Central Ground Water Board 2012; Perveen et al. 2012). Thus, questions may be raised over the current sustainability of intensive cropping and associated agricultural practices in the western IGP. Further intensification of cropping systems in Bihar and eastern Uttar Pradesh could relieve stresses placed on the western IGP's agro-ecosystems to meet the food demand of a growing population (RWC 2006). Such intensification needs to be sustainable in the long-term and avoid the stagnating or declining yields associated with lands intensified under the Green Revolution (Aggarwal et al. 2004; RWC 2006). The delayed (relative to Punjab and Haryana) increasing trend in cropping intensity and LGS in the eastern IGP suggest that this intensification is already occurring (Figs. 4-2, 4-3, 4-6).

Obtaining LSP parameters to monitor the agro-ecosystems of the eastern IGP as they intensify (Figs. 4-2, 4-3, 4-6) is a key facet to informing sustainable agricultural development in the region. Monitoring of the western IGP can inform management of the agro-ecosystems to avoid further environmental degradation and yield declines. It is important to note that current states of ecosystem functioning are determined by current conditions and past trajectories of ecosystem dynamics (Dearing et al. 2012). Thus, long-term records of LSP parameters over IGP can be used to provide a more comprehensive understanding of ecosystem functioning across a range of spatial scales. Such data is especially useful when integrated with other time-series of agro-

ecosystem drivers (e.g. climatic and socio-economic variables). This provides a more comprehensive understanding of how trajectories of cropping intensity and dynamics interact with a range of other actors across the agricultural system which determines agricultural production, food security and environmental sustainability. In the IGP, agricultural planners could analyse spatially explicit metrics of normals and trends in SOS and LGS (e.g. Figs. 4-4, 4-5, 4-6) in conjunction with datasets of observed trends (e.g. Duncan et al. 2013) or projected changes (e.g. Mathison et al. 2013) in climatic parameters relevant to crop growth and yield, information regarding uptake of various agronomic practices (e.g. Erenstein and Laxmi 2008) and, levels of social, financial and physical capital (e.g. Erenstein et al. 2007). This would enable identification of location-specific vulnerabilities in crop productivity, existing levels of adaptive capacity within the agricultural system and potential adaptive measures. For example, in the IGP spatially explicit measures of SOS and LGS for the *rabi* wheat are vital to target adaptive conservation agriculture-zero-tillage practices (Erenstein and Laxmi 2008; Lobell et al. 2013). Zero-tillage should be targeted in areas with a later-sown *rabi* crop as later sown crop yields are impacted by exposure to extreme heat later in the crop growing season (Lobell et al. 2012); this is especially pertinent given projected future increases in the occurrence of extreme heat days during the *rabi* cropping season over North India (Mathison et al. 2013).

4.4.1 Limitations of the GIMMS NDVI dataset

One of the limitations of monitoring cropping intensity using GIMMS NDVI data is that the phenology measured within each 8km pixel incorporates signal from a range of land covers, a mixed pixel problem. In the IGP the average farm size in Punjab is 337m^2 and in Bihar it is 39m^2; therefore, each GIMMS pixel will report the spectral signature from a range of different farms (Agricultural Census 2012). When estimating cropped area using coarser resolution remote sensing data some studies have multiplied full pixel areas by fractional proportions of cropland coverage to glean sub-pixel areal estimates (Thenkabail et al. 2007). Other approaches to addressing circumstances where a pixel is mixed include soft or fuzzy classification techniques such as artificial neural networks or linear mixture modelling (LMM) (Atkinson et al. 1997; Foody 2002).

LMMs assume a linear relationship between a pixel's spectral reflectance and the fraction of vegetative cover. The linearity of the relationship between pixel NDVI and proportion of agriculture was explored within the state of Bihar in an attempt to train a LMM to obtain more accurate estimates of cropping intensity. The proportion of agricultural area within a GIMMS pixel in 2005-06 was determined using the Globcover 2005 V2.2 global land cover product with a spatial resolution of 300 m (Bicheron et al. 2008). This was calculated as the proportion of a GIMMS pixel composed of Globcover classes 11 and 14, which correspond to *post-flooding and irrigated croplands* and *rainfed croplands*, respectively (Bicheron et al. 2008). There existed a non-linear relationship between proportion of agriculture within a GIMMS pixel and mean peak *kharif* growing season NDVI in 2005-06 (Fig. 4-11). Mean peak *kharif* growing season NDVI was used in this case as by this time crops have developed, covering fields, and reducing the spectral interaction of soil backgrounds with green vegetation (Jiang et al. 2006). This corresponds to the findings of Jiang et al. (2006) who observed a non-linear relationship between the NDVI of a pixel with a coarse spatial resolution and within-pixel vegetative fraction.

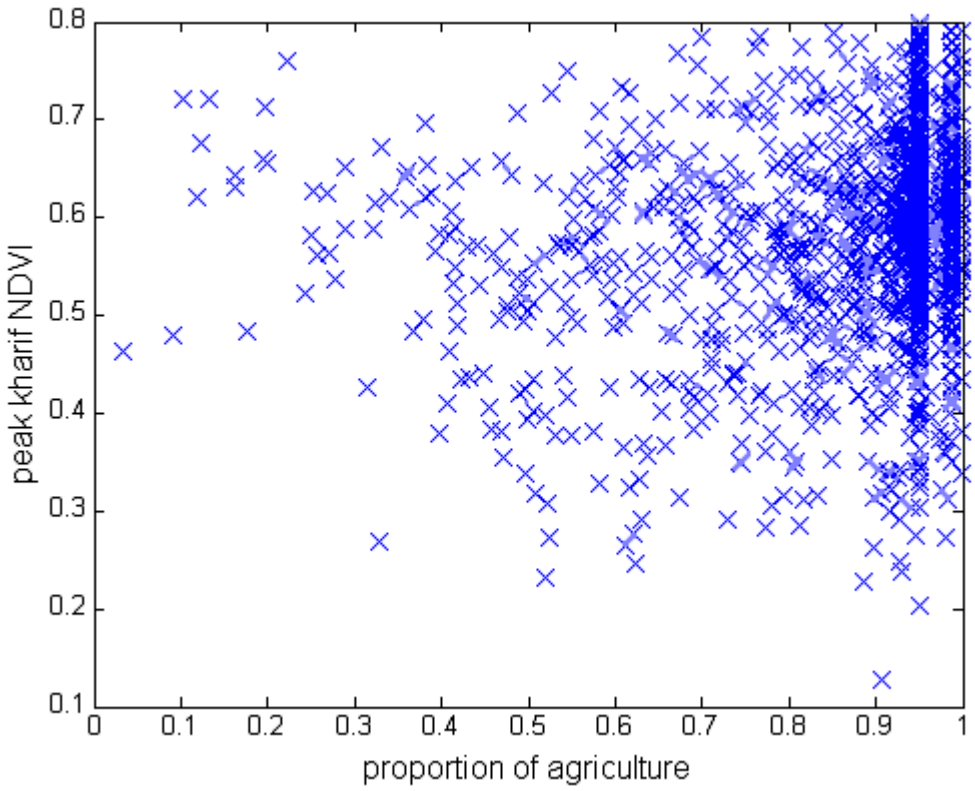

Figure 4-11 Relationship between peak kharif GIMMS NDVI and proportion of agriculture within a GIMMS pixel calculated using the Globcover V2.2 global land cover product for Bihar in 2005-06.

As NDVI does not vary linearly with fraction of vegetative cover, other vegetation indices which preserve linearity needed to be estimated to derive accurate sub-pixel fractions (Lobell and Asner 2004; Jiang et al. 2006). This requires data in individual spectral bands, and preferably at a finer spatial resolution than the GIMMS NDVI data, so a large number of pure agricultural pixels could be used to train the LMM. Jiang et al. (2006) found that the Scaled Difference Vegetation Index (SDVI), calculated using the red and NIR wavelengths, produced a linear relationship with fraction of vegetative cover and was insensitive to variation in soil background brightness. If the study area has a limited spatial and temporal extent, and atmospherically corrected reflectance values for red and NIR spectral bands are available then LMM may yield more accurate estimates of area under different cropping intensities. However, endmember reflectance values are not transferable across time or space due to inter-annual climatic variation, differing environmental conditions and agricultural management inputs. This limits the applicability of using LMM to map cropping intensity across large spatial extents and multiple years.

There is inevitably a trade-off between level of spatial detail and loss of accuracy in measures of productivity, LGS and cropping intensity from phenology derived from mixed pixels and the need to generate long-term time series covering large spatial extents efficiently. Cropping intensity can be monitored at more detailed spatial resolutions using different sensors with sufficient temporal resolution (e.g. MODIS, Landsat). For example, Biradar and Xiao 2011 monitored 'double' and 'triple' cropping across India using phenology derived from one year of MODIS data and Jain et al. 2013 integrated MODIS phenology measures with 'fine' spatial resolution Landsat data to map cropping intensity of smallholder farms in India. Whilst these approaches deliver greater levels of spatial detail they are limited by a lack of long-term coverage. This inhibits their use to inform on the long-term implications of increased cropping intensity on crop productivity and environmental resources.

Whilst the GIMMS NDVI data set has a coarse spatial resolution, it is possible to detect the dominant cropping intensity and inter-annual shifts in LGS and productivity occurring within a 8km pixel in the IGP. The IGP had a dominant agricultural land cover for at least one cropping season, this reduced negative mixed-pixel impacts and enable discrimination of the dominant phenology of the croplands at a regional scale. Even areas of smallholder, subsistence farming have a dominant agricultural landscape with rice cropping mimicking the cropping calendar of the rest of the region. Except in small isolated pockets there is not a mixed, heterogeneous landscape occurring at fine spatial scales (e.g. agro-forestry). However, in mixed landscapes which include smallholder farming (e.g. mountainous and hilly regions of Nepal, deltaic paddy regions) we would expect the GIMMS product to yield less phenological information. Patches of forested, water and urban areas were also masked out using a pre-processed Land Cover Product (GLC 2000) to remove pixels dominated by non-agricultural land covers throughout the time period in question. This is reflected by the fact the GIMMS NDVI dataset represents the state-wise inter-annual variation in cropping intensity and agricultural productivity reported in Government of India agricultural statistics (see Appendix 2 and 3). Appendix 4 provides a more detailed discussion of the limitations of using GIMMS NDVI data over the smallholder dominated portions of the eastern IGP.

Accounting for sub-pixel proportions of agricultural extent can improve estimates of area under cropping (Thenkabail et al. 2007) or weight pixel VI values when estimating crop productivity (Bolton and Friedl 2013) but it is difficult to un-mix the timing and location of phenological parameters within a pixel. In other words, it is hard to reveal sub-pixel variation in the timing of SOS, peak growing season and EOS within a pixel. This limits the use of GIMMS NDVI data for applied monitoring of specific crop types (e.g. wheat) due to its coarse spatial and bimonthly temporal resolution. In the IGP, delays in SOS and LGS by a matter of days can have noticeable impacts on wheat crop yields (Ortiz-Monastrerio et al. 1994). Both field studies and integrated Earth observation and crop model studies have shown yield declines for the wheat crop after an optimal sowing date in mid-November (Ortiz-Monastrerio et al. 1994; Lobell et al. 2012; Chapters 5 and 6). Monitoring SOS and LGS from sensors with increased temporal resolution (e.g. MODIS) can provide more accurate representation of SOS and LGS variability across the IGP. The crop-specific, applied usefulness of LSP parameter retrieval will further increase, relative to information gleaned from GIMMS NDVI datasets, as long-term records from sensors with increased spatial and temporal resolutions are accumulated.

4.5 Conclusion

The ability to estimate accurate LSP parameters is vital to fully characterise vegetation-climate interactions and inform sustainable agro-ecosystem management approaches. Whilst remote sensing datasets have been used to report spatio-temporal trends in LSP across sub-Saharan African croplands there has been limited focus on the IGP croplands. Here, we present long-term records monitoring spatio-temporal trends and dynamics of LSP parameters for the croplands of the IGP. There has been a clear west-to-east spread in the area under double cropping from 1982-83 to 2005-06. In 1982-83 2304 km^2 was detected as being under double cropping in Bihar, in 2003-04 25728 km^2 was detected as double cropping from the GIMMS NDVI dataset. This reflected a state-wise increase in area under double cropping of 945 km^2 $year^{-1}$ between 1982-83 and 2005-06. In Uttar Pradesh an increasing trend of area under double cropping of 2680 km^2 $year^{-1}$ was detected over the same time period. This was reflected by an increase

in: (i) the number of growing days per year in Bihar, Uttar Pradesh and Haryana and (ii) the productivity of *kharif* and *rabi* cropping across the IGP. For example, in Bihar and Uttar Pradesh in 1982-83 there was a state-wise average of 159 and 243 growing days per agricultural calendar year respectively yet in 2003-2004 the state-wise average number of growing days per year were 215 and 297 respectively.

These data contribute to increasing our understanding of local and regional vegetation dynamics and their interactions with climatic and anthropogenic drivers. They are also crucial components in facilitating a holistic understanding of local and regional agricultural and food systems and are, therefore, a useful resource for agricultural management aiming to deliver sustainable crop production and immediate food security. This is pertinent in the IGP considering the pressure placed on the region's agro-ecosystems to maintain food production in a sustainable and climate-resilient manner to meet the food demand from a growing population. In addition to providing information on the long-term dynamics of LSP across the IGP's agro-ecosystem, this dataset can be used as a reference for LSP parameters estimated from sensors with increased spatial and temporal resolutions.

Chapter 5: Climate-smartening India's breadbasket. Locating vulnerability 'hotspots' to target with adaptive practices.[8]

5.1 Introduction

Increasing productivity and production levels from cereal croplands is critical to meeting a growing demand for food from a global population expected to reach 9 billion by 2050 (Godfray et al. 2010; Foley et al. 2011; Misselhorn et al. 2012). The FAO project a required increase in global cereal production of 800 million tonnes by 2030 (FAO 2006). At the same time cereal croplands will have to contend with unfavourable climatic changes, limited room for expansion, increased competition for land and water resources from sectors such as biofuels and grazing, declining quality in the natural resource base limiting levels of production and suitable lands whilst also reducing agriculture's negative environmental and climatic footprint (Tilman et al. 2002; Tyagi et al. 2005; The Royal Society 2009; Power 2010; Hanjra and Qureshi 2010; Foresight: Final Project Report 2011; Tilman et al. 2011; Bogdanski 2012). Plausible management interventions and adaptations are available, which, if implemented should increase production and resilience in cropping systems simultaneously in a sustainable manner. Such adaptations fall under the umbrella term of climate-smart agriculture (FAO 2011b) and often include conservation agriculture practices (Lumpkin and Sayre 2009). Climate-smart agricultural practices and ecosystem management approaches achieve food security whilst: i) increasing productivity and income and, thus, enhancing livelihoods, ii) increasing ecosystem resilience to climate change and variability and, iii) mitigating agriculture's contribution to climate change (Pye-Smith 2011; FAO 2011b). Climate-smart approaches are being promoted by several global institutions (e.g. FAO, World Bank, Consultative Group on International Agricultural Research (CGIAR)). An ecosystems based approach to managing croplands, ensuring agricultural practices have minimal harmful impacts on ecosystem services and

[8] This chapter is currently submitted to Remote Sensing of Environment.

ecological processes, is a key component of climate-smart agriculture (FAO 2011b; Scherr et al. 2012) Conservation agriculture practices increase crop productivity in an environmentally sustainable manner, often with subsequent cost savings and profit gains (Hobbs et al. 2008; Erenstein 2009a; Lumpkin and Sayre 2009), thus, contributing to meeting climate-smart goals (Pye-Smith 2011; FAO 2011b). It is important to note that a wider range of adaptations to agricultural practices can deliver climate-smart gains than those that just meet the definitions of conservation agriculture (Hobbs et al. 2008).

To maximise the climate-smart benefits from targeted adaptations to cropping practices requires holistic approaches that are: i) sensitive to the temporally dynamic and systemic nature of cereal systems and, ii) able to capture spatial dynamics and heterogeneity across the landscape. A systemic or holistic focus is important as it retains awareness that the outcomes of climate-smart developments will be determined by a range of interacting exogenous and endogenous drivers within cereal croplands (FAO 2011a; Scherr et al. 2012). Remote sensing data is attractive for use in holistic assessments of cereal croplands as it can provide multiple metrics of relevance to the cropping system (e.g. crop type and acreage (Thenkabail et al. 2005; Wardlow et al. 2007; Gumma et al. 2011a; Atzberger 2013), crop yield and productivity (Funk and Budde 2009; Becker-Reshef et al. 2010; Rembold et al. 2013), cropping intensity and growing season dynamics (Dash et al. 2010; Biradar and Xiao 2011; Vrieling et al. 2013; Jain et al. 2013), crop health and vigour (Pinter et al. 2003), crop residue burning (Badarinath et al. 2006) and drought impacts (Rojas et al. 2011)). Remote sensing data can also be integrated with a range of ancillary datasets (e.g. socio-economic data (Imran et al. 2014) or climate data (Brown et al. 2010; Lobell et al. 2012)) enhancing the level of systemic detail captured in assessments of cereal croplands. The repeatable coverage of remote sensing data captures temporal detail important to fully understand cropland dynamics; for example, intra-annual monitoring of crop phenology can be used to discriminate crop types (Thenkabail et al. 2005; Thenkabail et al. 2007; Wardlow et al. 2007), highlight vulnerabilities due to late sowing (Lobell et al. 2012; Lobell et al. 2013) and, identify different crop development stages (Sakamoto et al. 2005). Inter-annual monitoring of cereal croplands captures variability in length

of growing seasons which can pin-point 'high risk' locations for particular crop types (Vrieling et al. 2013). There is clear potential to utilise remote sensing datasets to provide agricultural managers with information sensitive to the inherent complexity and spatial fluxes contained within cereal cropping systems which will influence the long-term state of cropland vulnerability and the climate resilience afforded by different adaptation/mitigation options.

To fully achieve climate-smart goals in cereal croplands requires a landscape approach which considers spatial interactions and variation between various facets within cropping systems (FAO 2012; Scherr et al. 2012). A more detailed discussion of the benefits which can be gained from synthesising the multiple goals of climate-smart approaches (resilience to climate change, adaptation and mitigation) into a landscape approach is presented in Chapter 1. However, a brief summary is provided here; landscape approaches inherently recognise that both societal and environmental outcomes are important and acknowledge the spatial and dynamic interactions between multiple processes across croplands. Given that the optimum agricultural practice to deliver climate-smart benefits will vary spatially due to underlying environmental and socio-economic conditions, monitoring at a landscape scale will capture the complex systemic nature of croplands and highlight best practice for a given locale (DeFries and Rosenzweig 2010; FAO 2011a; Scherr et al. 2012). Remote sensing data's synoptic and repeatable coverage and, spatial and thematic detail mean it is ideally suited to landscape scale monitoring of cereal croplands. Here we demonstrate an approach utilising such spatial and thematic detail in a holistic assessment of the rice-wheat production landscape to reveal 'hotspot' or 'high-priority' locations where the sustainability or productivity of cropping is vulnerable and to generate information to facilitate spatial targeting to optimise the benefits of conservation and adaptive agriculture practices across the landscape. Using remote sensing to provide quantified spatial information can minimise spatial trade-offs and maximise synergies in agricultural adaptations between production and sustainability goals and adaptation and mitigation measures.

The dominant crops in Punjab and Haryana are *kharif* rice typically grown from June to October and *rabi* wheat grown from November to April. As discussed in more detail in

Chapters 1 and 2 the rice-wheat croplands of Punjab and Haryana are crucial in supporting the livelihoods of several hundred million people and national food security schemes yet are also being impacted by multiple, interacting stresses. Numerous conservation agriculture practices are applicable to the rice-wheat croplands of Punjab and Haryana which can deliver climate-smart benefits. These include zero-tillage, system of rice intensification, alterations in irrigation practices, laser bed levelling, water harvesting and groundwater recharge, and crop diversification (Ambast et al. 2006; Gupta and Seth 2007; Saharawat et al. 2010; Pathak et al. 2012; Saharawat et al. 2012). For example, zero-tillage wheat in the IGP has been shown to reduce water input requirements, improve water productivity, reduce GHG emissions (via reduced tractor usage) and improve economic returns (Hobbs et al. 2008; Erenstein and Laxmi 2008; Saharawat et al. 2010). Each of these practices is associated with different costs of implementation and variation in the extent, and type, of benefit delivered; these benefits and costs also vary in space requiring location-specific targeting (Saharawat et al. 2010; Pathak et al. 2012). There is spatial heterogeneity in crop yields across small distances in the north-west IGP (Lobell et al. 2010) indicating location-specific, targeted responses are required to reduce yield gaps sustainably. Yield gaps refer to differences between average yield or yield observed in a field and potential yield which would be obtained without water and nutrient limitations and stress from weeds, pests, disease or pollution (Lobell et al. 2009; van Ittersum et al. 2013). Closing yield gaps can help meet increasing demands for food whilst addressing increased competition for land and water resources and reducing the negative outcomes associated with expansion of agricultural lands (e.g. biodiversity loss, increased GHG emissions) (Foley et al. 2005; Brussaard et al. 2010; Foley et al. 2011). Thus, closing yield gaps can contribute to meeting climate-smart goals. Given the complex, spatio-temporal dynamic nature of cereal croplands the size and cause of yield gaps vary across a landscape (Lobell 2013). The spatially explicit nature of remote sensing data can capture this spatial variation and, thus, be used to inform location-specific adaptations to close yield gaps (Lobell 2013).

A major inhibitor to the uptake of conservation agriculture and other practices delivering climate-smart goals in the IGP is the cost of implementation and the

cost:benefit ratio to prospective farmers (Pathak et al. 2012). The uptake of zero-tillage, the most prominent climate-smart-conservation agriculture practice across the IGP, was driven by the immediately realised economic gains to farmers (Erenstein 2009a). Identifying locations where farmers would receive the greatest returns from adopting climate-smart-conservation agriculture practices will increase the cost efficiency of implementation and increase the likelihood of uptake. Thus, it is important to target areas in need of adaptation enabling the agricultural landscapes of the IGP to move onto a climate-smart trajectory characterised by environmental sustainability, climate resilience and socio-economic benefits.

To optimise uptake of agriculture practices delivering climate-smart goals requires integration of multiple, location-specific datasets to provide holistic monitoring of the agricultural landscapes informing optimum adaptive practices. The range of agricultural statistics currently provided at the district level (e.g. http://lus.dacnet.nic.in/) aggregate sub-district spatial heterogeneity in cropping systems and mask local detail. Here, we demonstrate an approach centred on using remote sensing data with greater local detail compared to district level statistics and greater temporal resolutions to characterise various states (e.g. yield, cropping intensity, planting dates) of the agricultural landscape synthesised with the thematic resolution contained within Government of India's agricultural statistical datasets and gridded climate datasets. This enabled identification of locations likely to gain the greatest climate-smart benefits from targeted agriculture adaptation. This chapter highlights the following:

1) where prevailing agricultural practices (e.g. burning crop residue, late-sown wheat) contribute to failure in achieving climate-smart goals such as mitigation of GHG emissions, environmental sustainability or enhanced crop yields,

2) an estimate of the GHG emissions from crop residue burning in 2009-2010,

3) vulnerability 'hotspots' where unfavourable trends in ISM precipitation such as increasing recurrence of drought years coincide in space with water-intensive agricultural practices,

4) the locations and magnitudes of yield gaps,

5) the cropping diversity of a locale in relation to groundwater levels and the expanse of the rice-wheat cropping system,

6) areas where there is potential to address multiple stresses to crop production with targeted adaptations.

5.2 Methods

Holistic, spatially explicit monitoring of the rice-wheat production system initially requires accurate identification of the extent of the rice-wheat croplands and quantified yield estimates from remote sensing data. This information is then integrated with other spatial databases (e.g. climatic data, burned area products, agricultural statistics) to provide a comprehensive characterisation of the current state of the agricultural system across its landscape. This generates several metrics (e.g. GHG emissions from crop residue burning, areas vulnerable to unfavourable trends in precipitation, yield gaps) which are used to identify locations where agricultural productivity is vulnerable, where agricultural practices are sub-optimal or un-sustainable and, to target appropriate conservation agriculture and other adaptive practices based on the needs of a specific locale. Fig. 5-1 displays a generalised workflow for this process.

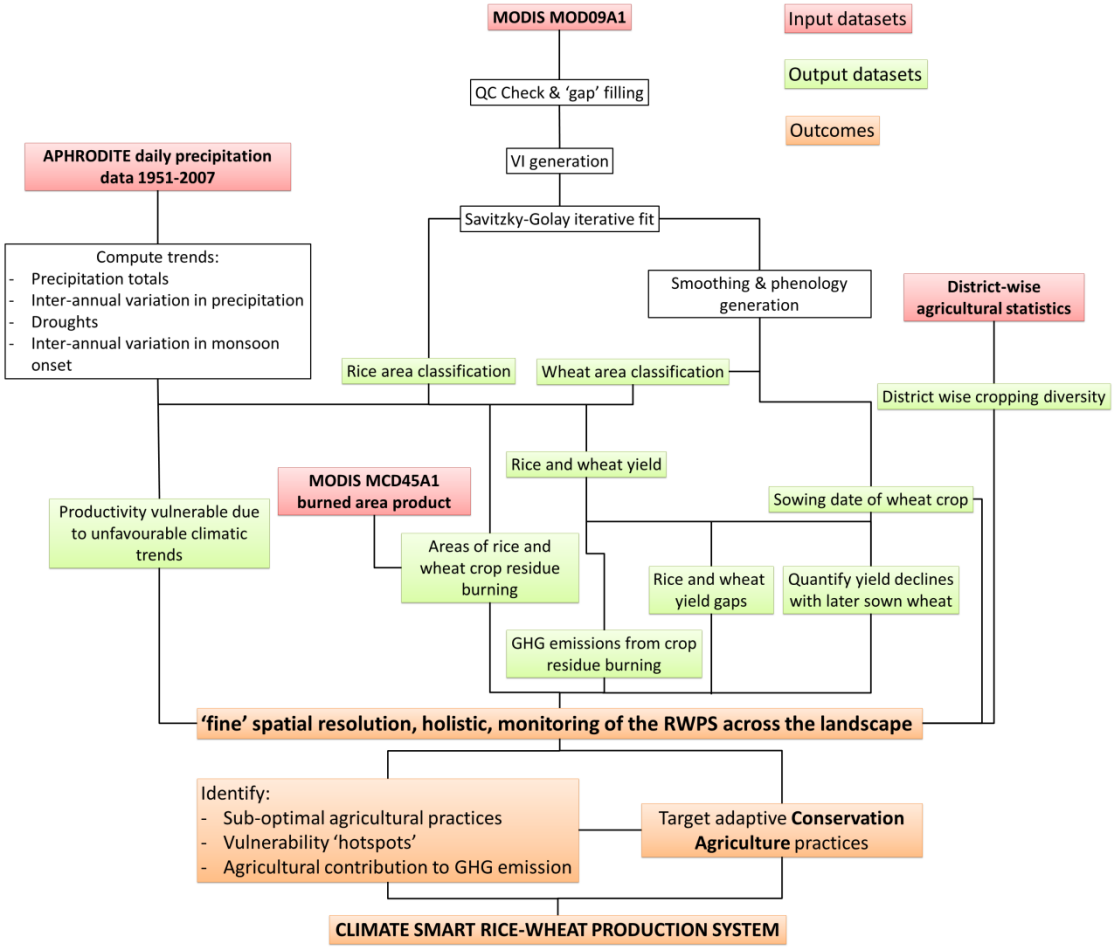

Figure 5-1 Workflow outlining processes undertaken to integrate remote sensing data, climatic data and agricultural statistics to provide holistic monitoring of the rice-wheat production system at a landscape scale.

5.2.1 Rice-wheat cropping area classification

5.2.1.1 Data pre-processing

Remote sensing data is commonly used to map the extent of croplands at varying thematic and spatial resolutions using a variety of classification methods (e.g. Doraiswamy et al. 2004; Thenkabail et al. 2005; Bartholomé and Belward 2005; Thenkabail et al. 2009; Gumma et al. 2011b). A comprehensive review of remote sensing techniques used to distinguish agricultural lands is beyond the scope of this study. However, it is important to note that MODIS data products, with a 500 m^2 spatial resolution, have been used to map croplands and specific crop types in this study area (Thenkabail et al. 2005; Xiao et al. 2006) and, such approaches provide measures of agricultural land cover with greater spatial detail compared to agricultural

land cover statistics aggregated within administrative boundaries (district level in India (http://lus.dacnet.nic.in/)). Areas under a *kharif* rice crop and *rabi* wheat crop were classified using a range of techniques applied to the 8-day composite of MODIS surface reflectance products (MOD09A1) (https://lpdaac.usgs.gov/products/modis_products_table/mod09a1). The MOD09A1 maximum value composite products were used instead of the MODIS daily climate model grid (CMG) 0.05° product. Whilst the MODIS CMG product has been corrected for BRDF and provides greater temporal detail this is traded-off against a loss of spatial detail due to its 'coarser' 0.05° resolution which would impede the ability to capture landscape scale detail. The aim here was not to develop new, universally applicable and validated land cover classification approaches or algorithms but to identify the extent of rice and wheat croplands for an applied purpose. Therefore, existing classification techniques which have been used, and validated, in this region were selected for rice and wheat crop extent classification.

Four VIs were computed from the MOD09A1 data. The NDVI and Normalised Difference Snow Index (NDSI) were computed to develop snow, water and forest masks following Xiao et al. (2005; 2006). The EVI was computed by adjusting red band reflectance using the blue band to account for residual atmospheric contamination and soil background (Huete et al. 1997; Huete et al. 2002). The NDVI is a commonly used measure of vegetation productivity; the EVI utilises advances in the MODIS sensor to reduce limitations with NDVI data providing enhanced responsiveness to canopy structure and not saturating as easily over areas with high levels of 'green' biomass (Pettorelli et al. 2005). The Land Surface Water Index (LSWI) utilises the shortwave infrared band (SWIR 1628-1652 nm) sensitive to soil and vegetation moisture (Xiao et al. 2005; 2006). Both the LSWI and the EVI were utilised to classify rice and wheat croplands. Prior to classification the data was subjected to rigorous pre-processing, removing 'bad pixels', selecting only 'high-quality' pixels using quality assurance (QA) data included with the MODIS products; and identifying cloud contamination not detected in the MODIS QA via the condition $cloud=\rho_{blue}>0.2$ where ρ_{blue} is reflectance in the blue band (459-479nm) (Xiao et al. 2005) before estimating the VI.

'Bad pixels', defined using MOIDS QA flags, were replaced using the gap filling algorithm of Peng et al. (2011):

$$B_T = Min[Max(B_{t-1}, \dots B_{t-4}), Max(B_{t+1}, \dots B_{t+4})] \quad (1)$$

Where B_T is the value assigned to replace the bad pixel B_t located at time-step t. The VI were then iteratively fitted to their maximum envelope using an adapted version of Chen et al. (2004) which incorporates smoothing VI temporal profiles using a Savitzky-Golay filter and a fitting bias towards maximum values. This removes noise and fluctuation in temporal VI profiles due to cloud cover and atmospheric contamination and accounts for the negative bias in reflectance received at the sensor (Chen et al. 2004).

Snow, water and forest masks were generated to avoid non-agricultural land covers influencing the classification procedure using an adapted version of (Xiao et al. 2005; 2006). If a pixel was designated as being snow covered at any time-step, defined as NDSI>0.4, then it was deemed not suitable for rice cropping and removed from the classification process. Pixels covered by permanent water bodies, defined by NDVI<0.1 and NDVI<LSWI for at least 10 composites during the year were masked. Forest areas were detected if 20 successive 8-day MODIS composites had a NDVI>0.5 and masked.

5.2.1.2 Rice crop area classification

Rice cropped areas were classified by adapting Xiao et al. (2005; 2006) and Peng et al. (2011), assuming that rice crops display the following characteristics: i) puddling of fields at the beginning of the growing season and ii) a rapid green up post puddling. Puddling was detected by the condition $LSWI_t+T \geq EVI_t$ where *t* is the time-step corresponding to the 8-day MODIS composite. A temporary inversion of LSWI relative to EVI indicates puddling in fields (Xiao et al. 2005; Xiao et al. 2006; Peng et al. 2011); this assumption is relaxed for improved classification accuracy in specific locations through the threshold *T* (Xiao et al. 2005; Peng et al. 2011). The incorporation of *T* accounts for reflectance containing signatures from a mixture of puddled water, vegetation and soil backgrounds and sub-pixel compositions of land-cover (Xiao et al.

2005; Sun et al. 2009). It is important to note that this classification scheme seeks to detect the presence of rice cropping within a 500m pixel but does not estimate proportion of rice cropping within pixels. To ensure puddling is associated with rice crops, a rapid green up following puddling must be observed (Xiao et al. 2005). This was defined by one of five 8-day MODIS composites after puddling being greater than half the maximum growing season EVI (Xiao et al. 2005; Xiao et al. 2006). A universal approach to rice crop classifications (e.g. Xiao et al. 2006) is limited due to the range of agronomic and climatic conditions under rice cultivation (Peng et al. 2011; Gumma et al. 2011b). Incorporating knowledge of the local crop calendar and agronomic practices into classification procedures will improve accuracy (Sun et al. 2009; Peng et al. 2011; Gumma et al. 2011b). The classification algorithm was focussed at the beginning of the *kharif* growing season avoiding spurious misclassifications of other wetland areas (Sun et al. 2009).

5.2.1.3 Rice cropped area validation

A range of threshold values were tested using district-wise land use statistics for rice cropped area as validation data (http://lus.dacnet.nic.in/) with T=0.16 being most accurate for Punjab and Haryana (Table 5-1; Fig. 5-2a). This increased classification accuracy, R^2=0.96 when validated against district-wise land use statistics (http://lus.dacnet.nic.in/), compared to R^2=0.78 when following the threshold value applied to all of south Asia used by Xiao et al. (2006) (Table 5-1; Fig. 5-2a). Table 5-1 shows the R^2 values for between district-wise rice cropped area detected from MODIS data and district-wise rice cropped area from Government of India land use statistics (http://lus.dacnet.nic.in/).

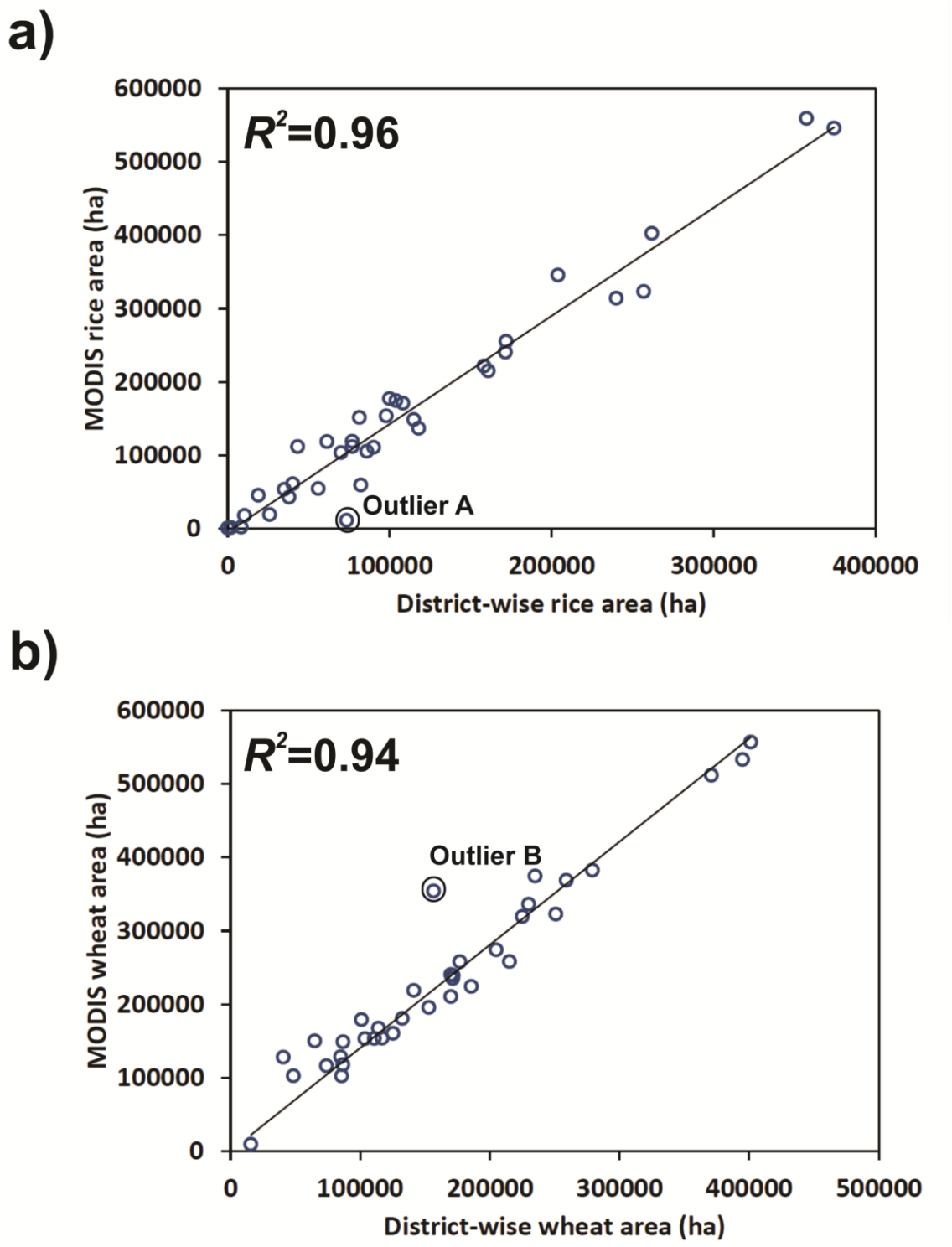

Figure 5-2 District-wise Government of India cropped area statistics plotted against MODIS derived cropped area statistics (full-pixel area) for a) rice (T=0.16) and, b) wheat (SSV=0.55). The black line is the regression fitted to a 1:1 line. Outlier A is district Yamuna Nagar and Outlier B is district Bhiwani.

Table 5-1 R^2 values for the relationship between rice cropped area estimated from the MODIS MOD09A1 product and Government of India's district-wise land use statistics (http://lus.dacnet.nic.in/) for the 2009-2010 agricultural season.

	Threshold (*T*)							
	Xiao et al. (2005) (0.05)	0.1	0.12	0.14	0.15	0.16	0.18	0.2
R^2	0.78	0.89	0.93	0.95	0.95	0.96	0.94	0.84

5.2.1.4 Wheat crop area classification

Additional filtering of the maximum fitted EVI dataset using a Savitzky-Golay filter with a 2nd degree polynomial and a seven time-step moving window generated a smooth phenology profile suitable for LSP parameter extraction. Smoothing prevents residual noise causing misclassifications and generates a phenology profile representative of crop growth. Areas under *rabi* cropping were extracted using LSP parameter extraction methods outlined in Dash et al. (2010) and Lobell et al. (2012); this increased wheat classification accuracy reducing misclassification errors of non-croplands. *Rabi* crops were defined by three LSP parameters:

i) Peak growing season detected by an increasing trend in EVI values for the preceding four 8-day composites and a decreasing trend in the succeeding four 8-day composites (Dash et al. 2010).

ii) SOS was defined as 10% of the amplitude between minimum and peak EVI on the rising limb of the phenology profile. The 10% amplitude method applied to MODIS EVI data has been previously validated using observed sowing dates in Punjab and detects sowing data (adjusted for a three week lag) to within two days (Lobell et al. 2013).

iii) Distinct green up following SOS detected by the magnitude of difference between SOS EVI and peak growing season EVI. The difference between EVI values at SOS and peak growing season should be greater than one fifth of growing season maximum EVI (Dash et al. 2010).

The match between *rabi* crop phenology and 'ideal' wheat phenology was calculated using spectral matching techniques, specifically the spectral similarity value (*SSV*) (equation 2) (Thenkabail et al. 2007; Thenkabail et al. 2009). This approach has been used widely to classify croplands in South Asia (Thenkabail et al. 2007; Thenkabail et al. 2009; Biradar et al. 2009; Gumma et al. 2011b; Gumma et al. 2011a). The phenology profile for 'ideal' wheat pixels was generated by randomly extracting the phenology profiles for 254 pixels identified as containing at least 80% wheat crop coverage from a global map of wheat croplands (Monfreda et al. 2008). This map has been used widely to delineate wheat growing areas in north-west India (Lobell et al. 2012; Lobell et al. 2013). However, it provides a proportion of cropped area within a 5-minute pixel and, thus, is not an optimal discrimination of wheat cropped areas hence the use of a conservative 80% threshold here as opposed to the 40% threshold used in Lobell et al. (2012). The *SSV* compares the shape and magnitude of two phenology profiles (Thenkabail et al. 2007; Thenkabail et al. 2009). The similarity in shape is calculated as the Pearson's Correlation Coefficient, *p*, between pixel phenology profile and 'ideal' wheat phenology profile. The *SSV* also incorporates a measure of magnitude between the two phenology profiles, the Euclidian distance between corresponding points.

$$SSV = \sqrt{E_d^2 + (1-p)^2} \tag{2}$$

Where E_d^2 is the Euclidean distance where Euclidean distance (equation 3) between two points calculated as

$$D_{Euclidean} = \sqrt{\sum_{i=1}^{n} (A_i - x^i)^2} \tag{3}$$

Where x_i is the EVI value of a pixel with *rabi* cropping and A_i is 'ideal' wheat EVI value at time-step *i*. A smaller *SSV* value indicates greater similarity between the pixel in question and 'ideal' wheat phenology. Classification of wheat from other croplands

and land cover types was determined by a threshold *SSV* value. It is important to note that this classification scheme considers full-pixel areas of wheat cropping and does not provide any further information on sub-pixel proportion of wheat cropped area.

5.2.1.5 Wheat cropped area validation

A range of thresholds were tested for accuracy using the district-wise land use statistics (http://lus.dacnet.nic.in/) for wheat cropped area as validation data. The threshold of $SSV \leq 0.55$ yielded most accurate results when compared with district-wise land use statistics (http://lus.dacnet.nic.in/), R^2=0.94 (Table 5-2; Fig. 5-2b). Table 5-2 presents the R^2 values describing the fit between wheat area estimated from MODIS data and district-wise land use statistics for wheat cropped area for a range of *SSV* values. That the accuracy of using *SSV* values higher than the optimum, does not decrease 'rapidly' is likely due to non-cropland land cover being masked pre-classification and the dominance of wheat as a *rabi* land cover in Punjab and Haryana. Once the optimum wheat classification has been reached there is not likely to be large quantities of 'available' pixels to be misclassified via a more lenient *SSV* threshold. As an additional check that classified wheat crop corresponds to vegetative growth the following condition must be met: peak EVI>0.2.

Table 5-2 R^2 values for the relationship between wheat cropped area estimated from the MODIS MOD09A1 product and Government of India's district-wise land use statistics (http://lus.dacnet.nic.in/) for the 2009-2010 agricultural season.

	SSV value													
	0.2	0.25	0.3	0.35	0.4	0.45	0.5	0.55	0.6	0.65	0.7	0.75	0.8	0.85
R^2	0.5	0.65	0.76	0.84	0.89	0.92	0.935	0.937	0.932	0.92	0.92	0.91	0.9	0.89

5.2.2 Estimating rice and wheat crop yield

Crop yield was estimated from EVI phenology profiles generated from the MODIS MOD09A1 product. Several LSP parameters obtained from remote sensing data can be used to estimate biomass, of which crop yield is the economically utilisable portion (Pettorelli et al. 2005; Funk and Budde 2009; Bolton and Friedl 2013).

Cereal crop yield is often estimated using regression models trained with maximum VI or an average or integration of VI values over portions of the growing season corresponding to peak growth and initial senescence (reproductive phase and grain filling (TSP)) and agricultural crop yield measures obtained from fields and agricultural statistics (Rojas 2007; Funk and Budde 2009; Becker-Reshef et al. 2010; Rojas et al. 2011). Such models take advantage of the correlation between spectral reflectance in wavelengths used to compute VI and photosynthetic activity which leads to crop yield formation (Tucker 1979; Pinter et al. 1981; Becker-Reshef et al. 2010). Funk & Budde (2009) comment that often late to end of growing season VI values give a more accurate estimation of crop yield as they correspond to the crop development stages which determine utilisable yield (e.g. grain filling and reproductive stages). Three metrics related to crop yield were tested: cumulative sum of EVI values over a 30 day window post peak EVI (CUM-$EVI_{(TSP)}$), cumulative sum of EVI from SOS to end EOS and, cumulative sum of EVI from peak growing season to EOS. The 30 day window used in the computation of CUM-$EVI_{(TSP)}$ captures the thermo-sensitive period (TSP) of cereal crop development, namely the reproductive phase, and the beginning of the subsequent grain filling stages (Pinter et al. 1981; Sakamoto et al. 2005; Teixeira et al. 2013). It is well established that crop yield is vulnerable to climatic extremes impacting crop physiological processes during this period, and that VI values fluctuate according to green biomass levels, crop stress and photosynthetic activity (Tucker 1979; Jagadish et al. 2007; Becker-Reshef et al. 2010; Teixeira et al. 2013). Therefore, it is likely that a sum of VI values over this period will indicate levels of final crop yield.

SOS for rice was defined as date of puddling and wheat SOS as discussed previously. Peak growing season was defined as maximum growing season EVI and EOS was defined in a similar manner to detecting wheat onset but the 10% threshold was applied to the falling limb of the phenology profile. The accuracy of the crop yield estimates were improved by masking non-rice/wheat land cover using crop maps and discounting pre-growing season noise (Kastens et al. 2005; Funk and Budde 2009). This is an important aspect of improving the ability to accurately estimate crop yield from remotely sensed data as discussed in Atzberger (2013) and Funk and Budde (2009). Bolton and Friedl (2013) compared the impact of using a ‘fine’ spatial resolution

cropland mask to capture sub-pixel extents of cropland and subsequently weight MODIS 500m pixel EVI values and a 500m spatial resolution MODIS Land Cover Product with a generic agricultural land cover class using full-pixel EVI values in crop production estimation. They observed comparable estimates of crop production using both land cover products and note that using a 500m land cover product to isolate cropland spectral signals for estimating crop production is a 'viable alternative when higher resolution products are not available' (Bolton and Friedl (2013), p. 78). Bolton and Friedl (2013) also used a generic agricultural land cover class as a cropland mask; here, rice and wheat crop extents are delineated rather than just using a generic cropland class further minimising a noisy signal from other crop and land cover types.

Other studies have also used 'coarse' or 'medium' resolution (relative to the field scale) land cover maps to mask non-cropland land covers when estimating crop production from MODIS derived EVI. For example, Funk and Budde (2009) used a 1:250,000 SADC land cover dataset for Zimbabwe and obtained R^2 values greater than 0.85 when estimating maize crop production from cumulative sums of EVI around peak growing season and the beginning of crop senescence. In Punjab and Haryana Lobell et al. (2012) created a wheat cropland mask based on the condition that a 5-minute spatial resolution pixel contained at least 40% wheat crop coverage; the initial input dataset for their wheat cropland mask was the global cropland map produced by Monfreda et al. (2008). Using this wheat cropland mask, and 1km spatial resolution MODIS EVI data, Lobell et al. (2012) detected climate impacts on wheat phenology. If the focus here was on estimating crop production at a district or state level based on peak growing season, or early senescence EVI values, district-wise or state-wise area weighted EVI values could be constructed (Bolton and Friedl 2013). However, such an approach would aggregate local variation in crop phenology and preclude capturing landscape scale detail.

It is important to note the usefulness of a 500m level cropland mask may decline in areas of the world with a more fragmented agricultural landscape (Bolton and Friedl 2013); however, Punjab and Haryana have a dominant agricultural land cover and limited cropping diversity (http://apy.dacnet.nic.in/). The 500m spatial resolution can provide useful landscape scale information over Punjab and Haryana as the region is

dominated by a rotating rice-wheat land cover, with predominantly large and medium sized operational holdings and larger average farm holding size relative to the national average (Panigrahy et al. 2010; DES 2011; Agricultural Census 2012). Whilst the footprint of a MODIS pixel is 500m^2 compared to average operational holding size of 225m^2 in Haryana and 377m^2 in Punjab, less information will be lost and landscape complexity masked, due to mixed pixel effects than would occur over smallholder dominated landscapes with small farm sizes (e.g. in Bihar with average holding size of 39m^2) (Agricultural Census 2012). The launch of the Sentinel-2 constellation of two satellites will provide multispectral imaging of the earth's surface at a 10m spatial resolution every 5 days (ESA 2010). This will enhance the level of detail (i.e. intra-farm or individual field) which can be gleaned from remote sensing data and enable monitoring of crop phenology with reduced mixed pixel effects. This will result in more accurate monitoring of conditions in specific fields and reduce error in propagating into crop production regression models. This will increase the applied value of using remote sensing data to monitor crop production accurately in fragmented farming landscapes.

5.2.2.1 Crop production validation

The three metrics were validated using district-wise crop production statistics (http://apy.dacnet.nic.in/: Table 5-3). All three metrics had a strong positive correlation with district-wise crop production statistics (Table 5-3). CUM-EVI$_{(TSP)}$ was used from this point on as the metric to determine crop yield using linear regression models trained using district-wise crop production totals. The use of CUM-EVI$_{(TSP)}$ was justified given the metric performed comparably well relative to the other metrics for both crop types in 2009-2010, the sound theoretical basis underlying the metric and, it avoids signals introduced from early and late growing season activity not related to crop yield formation as discussed in Rojas et al. (2011) and Funk and Budde (2009). Using regression model developed using 2009-2010 CUM-EVI$_{(TSP)}$ district-wise crop production was estimated for the 2002-2003 to the 2005-2006 growing season. For the rice crop this model provided R^2 values ranging from 0.85 to 0.95 and for the wheat crop R^2 values ranging from 0.80 to 0.94 (Appendix 5). This further indicates CUM-

$EVI_{(TSP)}$ is a time-invariant indicator of crop production across rice and wheat in Punjab and Haryana. Rice yield (Tonnes ha^{-1}) per pixel was estimated as:

$$Y = 20.041x/s \quad (4)$$

Where *x* is CUM-$EVI_{(TSP)}$ and *s* is the scaling factor between the area of a MODIS pixel and hectares. Wheat yield was estimated as:

$$Y = 24.74x/s \quad (5)$$

A regression through the origin approach was used to estimate crop yield based on the premise that cultivated areas were extracted prior to yield estimation (Eisenhauer 2003). Therefore the assumption that no crop yield reported in a district would correspond to no cropped area and, thus, not register a VI signal associated with crop yield was applied, thus, the assumption was also made that all cropped areas generate some yield; under these assumptions a 1:1 regression is justified. A regression through the origin was used by in a similar methodological framework to estimate wheat yield from MODIS NDVI data with wheat crop masks applied in the USA and Ukraine (Becker-Reshef et al. 2010).

Table 5-3 Correlation coefficient values for the relationship between yield estimates from EVI phenological parameters and Government of India's district-wise Area, Production and Yield statistics (http://apy.dacnet.nic.in/).

	Rice	Wheat
CUM-$EVI_{(TSP)}$	0.93	0.95
Cumulative sum of EVI from onset to end of growing season	0.93	0.94
Cumulative sum of EVI from peak growing season to end of growing season	0.94	0.92

5.2.3 Burning of rice and wheat crop residue and quantifying GHG emissions

The operational MODIS monthly burned area product (MCD45A1), which provides an estimate of burning date, extent of burning and associated QA

(https://lpdaac.usgs.gov/products/modis_products_table/mcd45a1), was used to delineate burned areas corresponding to the end of the *kharif* and *rabi* growing seasons. A full description of the methods for generation of the burned area product is beyond the scope of this paper. However, Roy et al. (2008) and Roy and Boschetti (2009) provide further details. The areal extent of *kharif* rice and *rabi* wheat crop residue burned were extracted using maps of crop extent previously generated. The GHG emissions from rice and wheat crop residue burning for the 2009-2010 agricultural season were estimated using the methodology recommended by the IPCC (2006a). Inputs include maps of burned croplands generated from the MCD45A1 product, accurate maps of crop extent, remote sensing measures of crop biomass, country and crop specific parameters from the literature and default parameters for Tier 1 estimation from IPCC (2006a). The IPCC advocates estimation of GHG emissions from residue burning via:

$$L_{fire} = A \cdot M_B \cdot C_f \cdot G_{ef} \cdot 10^{-3} \quad (6)$$

Where L_{fire} is emissions (Tonnes), A is area burned (ha), M_b is mass of fuel available to be burned (Tonnes ha^{-1}), C_f is the combustion factor (dimensionless) and G_{ef} is the emission factor (g/kg^{-1} of dry matter burned). Crop specific default values of C_f and GHG specific values of G_{ef} were obtained from the IPCC (IPCC 2006b) (Table 5-4). C_f values were 0.9 for wheat and 0.8 for rice, C_f refers to the proportion of fuel (crop residue) consumed by the fire (IPCC 2006b). A for rice and wheat crops were estimated utilising burned area (MCD45A1) and crop extent maps already generated. M_b was estimated as:

$$M_b = Y \cdot D \cdot S \quad (7)$$

Where Y is crop yield in (Tonnes ha^{-1}), D is dry matter content, S is the ratio of residue mass to crop yield. S was determined using crop specific values from Webb et al. (2009), the residue:yield ratio for wheat and rice were 1.3 and 1.4 respectively. D was obtained from (IPCC 2006a) and had a value of 0.89 for both rice and wheat. We have

not included a factor to account for fraction of residue removed as specified in Webb et al. (2009) and Garg et al. (2011) as we have already detected burned sites and incorporated them into estimates of *A*.

As a point of comparison emissions are computed using default Tier 1 estimates provided by the IPCC (2006b) for M_b and C_f. The FAO use this methodology to estimate global and regional emissions of CH_4 and N_2O from residue burning on croplands (FAOSTAT 2013). The FAO adjust estimates of residue available to be burnt on fields, assuming 10% of crop residue is burnt (IPCC 2000; FAOSTAT 2013). These results are presented in Table 5-5.

Table 5-4 Emission factor (G_{ef}) for range of GHG from burning of agricultural residue (IPCC 2006b).

	CO_2	CO	CH_4	N_2O	NO_x
Agricultural Residue	1515	92	2.7	0.07	2.5

5.2.3.1 Uncertainties and error in GHG estimating emissions from crop residue burning

There are uncertainties involved with the use of satellite-derived burned area products over croplands which were used as inputs into *A*. This is exemplified by the differences between MODIS burned area product (MCD45A1) and the MODIS active fire product (MOD14A1 (Terra) and MYD14A1 (Aqua)) (Roy et al. 2008); and, by differences between burned area products derived from different sensors (L3JRC: SPOT-VEGETATION; GlobCarbon: SPOT-VEGETATION and ERS2-ASTR2/ENVISAT AATSR) (Roy and Boschetti 2009). However, validation against Landsat observations of burned area suggested the MODIS burned area product was most accurate across Southern Africa (Roy and Boschetti 2009). Both MODIS burned area and active fire products suffer from cloud cover obscuring detection of active burning or burned area scars on the terrestrial land surface; the burned area product includes omission errors over croplands if the burned area scar is small relative to the $500m^2$ pixel whereas the active fire product is sensitive to omission errors due to short lived fires missing sensor overpass or if the fire temperature is not high, or spatially distributed enough (Roy et al. 2008). The burned area product detects burning using an algorithm modelling

temporal changes in land surface reflectance; this algorithm can be confounded over croplands where anthropogenic agricultural management causes swift changes in land cover after burning (Roy et al. 2008). However, integrating crop specific maps and burnt area maps means that locations where specific crops were burnt can be delineated. This enables use of crop specific parameters in equation 6 for estimating emissions reducing uncertainty.

There will be error in estimates of M_b due to variations in biomass left on fields due to different harvesting techniques (e.g. manual harvesting or combine harvesting) which will vary within and between pixels (McCarty, 2011). The distribution within a field, the orientation of biomass and the compaction of biomass will affect resultant emissions (Webb et al. 2009). The, distribution and compaction of residue in a field, moisture content of the residue and nature of the fire and climatic conditions at time of burning will also create uncertainty in the combustion factor (ratio of fuel available to be burnt which actually combusts) (IPCC 2006b; McCarty 2011). There will also be error in M_b as a result of differences between harvest date and burning date with differential rates of, and time periods for, decay of crop residues in fields (Webb et al. 2009; McCarty, 2011). However, we have used location specific estimates of rice and wheat crop production in M_b as opposed to applying a spatially universal value for wheat and rice yield following Tier 1 parameters provided by the IPCC (2006b). The approach here using location and crop specific estimates of production is a conceptual advance on previous efforts quantifying GHG emissions from biomass burning over rice-wheat croplands in Punjab using remote sensing; Badarinath et al. (2006) used satellite-derived burned area maps but spatially universal values for wheat and rice biomass obtained from the literature.

Here it is assumed that pixels where crop residue burning was detected in the MODIS MCD45A1 product correspond to locations where farmers burnt residue in fields. This assumption was made on the basis we have not used a generic croplands mask in *A* but a burnt area cropland mask; and if proportion of residues from fields is not known then all residues should be assumed burnt (Webb et al. 2009). However, this assumption is limited as there is likely sub-pixel variation in farmer management practices and proportions of intra-pixel burnt areas. At a regional scale errors of

omission (missing fractions of burnt croplands due to a $500m^2$ pixel not being detected as burnt) and commission (assuming all of a $500m^2$ pixel is burnt when in reality portions may not be) may cancel out but mask local level uncertainty.

Here we have used G_{ef} (emissions factors) for agricultural residues consistent with the IPCC methodology (Table 5-4). These estimates G_{ef} are in close agreement with crop specific emission factors reported by McCarty (2011) for CO_2 and CH_4; however, McCarty (2011) note there is a considerable range of uncertainty in estimates of crop specific values for G_{ef}. There is likely to be considerable within landscape variation GHG emissions per amount of residue burnt due to variations in the moisture content of the residue at the time of burning, the prevailing climatic conditions at the time of burning the carbon and the carbon content of the residue (Yevich and Logan 2003; IPCC 2006b; McCarty 2011). Here, we have used the same values as provided by the IPCC as they are equivalent to crop specific emission factors for rice and wheat and enable comparison with the FAO methodology (Table 5-5).

5.2.4 Determining the relationship between onset of wheat growing season and crop yield

SOS was defined as 10% of the amplitude between minimum pre-growing season EVI and peak growing season EVI and wheat crop yield was estimated using the regression models previously mentioned. Average yield (Tonnes ha^{-1}) per SOS date, in units of 8-day MODIS composites, was calculated to determine the effect of later sowing of the wheat crop on yield.

5.2.5 Identifying vulnerability 'hotspots' to climatic trends and variability

Identifying 'hotspots' where rice-wheat production systems are vulnerable to climatic trends and variability was achieved via an overlay of two datasets: i) spatio-temporal trend analysis identifying locations experiencing unfavourable trends in facets of ISM precipitation and, ii) rice-wheat cropping area classifications for the 2009-10 agricultural season.

5.2.5.1 Locations of unfavourable trends in facets of ISM precipitation:

Facets of ISM precipitation with unfavourable trends experienced at locations in Punjab and Haryana were: i) decreasing ISM precipitation, ii) increasing variability in ISM precipitation, iii) increasing frequency of drought years, and iv) increasing variability in onset date of ISM and, were detected utilising the datasets generated in Duncan et al. (2013). Increasing date of onset of ISM would also undermine agricultural productivity in the region (Moors and Siderius 2012), but such trends were not prevalent (Duncan et al. 2013). These trends were identified per 0.25˚ grid cell using non-parametric trend analysis, and robust bootstrap resampling, testing for field significance and spatial autocorrelation, applied to APHRODITE daily gridded precipitation products from 1951-2007; a more detailed description of the methods and data is outlined in Duncan et al. (2013).

5.2.6 Yield Gaps

To monitor yield gaps requires estimating or defining potential yield (Y_p), methods to estimate Y_P include use of simulation models, 'ideal' experiments on farms or taking maximum yields from real world farms; a full review and critique of these approaches can be found in Lobell et al. (2009). Remote sensing approaches to quantifying yield gaps correspond to the latter method where maximum yield estimated from remote sensing data is used as a proxy of Y_p within a given spatial unit (Lobell 2013). For example, Bastiaanssen and Ali (2003) used the 95th percentile value of yield estimated from AVHRR data in the Indus Basin in Pakistan as an estimate of Y_p. Lobell et al. (2010) also the used 95th percentile of yield values estimated from Landsat data, per-district, in Punjab as a measure of Y_p. Here, yield gaps were estimated as the difference between yield in a pixel reporting rice or wheat cropping and maximum yield, Y_p, within a 5km moving window. The same approach was repeated using a 20km moving window to explore whether the size and spatial distribution of observed yield gaps were artefacts of the size of moving window.

5.2.7 Cropping Diversity

Cropping diversity per district in Punjab and Haryana was computed, from a range of 64 possible food and non-food crops, using the Shannon-Weaver diversity index for the 2009-2010 agricultural season (Brush et al. 2003; Abebe et al. 2009). The district-wise statistics for cropped areas were obtained from the Government of India's land use database (http://lus.dacnet.nic.in/). The Shannon-Weaver diversity index was computed as:

$$H = -\sum_{i=i}^{n} P_i ln P_i \quad (8)$$

Where *H* is the Shannon-Weaver diversity index, *P* is area under i^{th} crop cultivated in the district and *n* is the total number of crops cultivated in the district. The Shannon-Weaver diversity index incorporates a measure of evenness and also the number of different crops cultivated, the greater the value the greater the cropping diversity.

5.3 Results

5.3.1 Water availability 'hotspots'

Water usage, availability and governance is a key factor determining the sustainability and productivity of the rice-wheat croplands (Abrol 1999; Ambast et al. 2006; CCAFS 2010; Moors et al. 2011; Perveen et al. 2012). Rice-wheat production systems (see Fig. 5-7b) are water intensive, requiring 1800 mm water annually (Ambast et al. 2006), less than the median ISM precipitation over Punjab and Haryana which ranges from 156 to 1091mm with large amounts of inter-annual variability (Duncan et al. 2013). Facets of ISM precipitation displaying unfavourable trends include: decreasing ISM precipitation, increasing recurrence of drought years and, increasing inter-annual variation in ISM precipitation and ISM onset date (Duncan et al. 2013). Trends from observational data were deemed more useful and more informative due to uncertainty in ISM projections from climate models (Annamalai et al. 2007; Moors et al. 2011; Turner and Annamalai 2012; Mathison et al. 2013), and adaptive climate-smart

responses need to be implemented immediately where the time-frame of observational data is still relevant. 2.52 million ha of the rice-wheat cropping system experienced unfavourable trends in at least one facet of ISM precipitation, 2.53 million ha experienced such trends in two facets of ISM precipitation and 0.24 million ha experienced three such trends simultaneously (Fig. 5-3a). Trends of increasing recurrence of drought years and inter-annual variation in ISM precipitation have the greatest spatial coverage (Fig. 5-3b and c). 'Hotspots' were identified (Fig. 5-3a) where observed unfavourable trends in facets of ISM precipitation limit available water resources, thus, increasing vulnerability to reduced productivity and pressure on already exploited groundwater reserves (Fig. 5-4).

These 'hotspots' (Fig. 5-3a) should be prioritised for targeting with climate-smart and conservation agriculture approaches which reduce water requirements without compromising livelihoods. This will increase the resilience in the most vulnerable areas of rice-wheat cropping landscapes to increasing, unfavourable, variability in the ISM. The majority of 'hotspots' were located in southern Punjab and Haryana (Fig. 5-3a, b and c), receiving lower normal and more inter-annual variability in ISM precipitation (Duncan et al. 2013), thus, compounding water availability issues. These regions should be prioritised for targeting with drought resistant cultivars (Wassmann et al. 2009; National Mission for Sustainable Agriculture 2010; Moors et al. 2011) or conservation agriculture practices with increased water use efficiency. Such practices include laser bed levelling, zero-tillage and residue retention (Erenstein and Laxmi 2008; Jat et al. 2009a; Saharawat et al. 2010; Chauhan et al. 2012). These 'hotspot' locations across southern Punjab and Haryana also match up to locations identified as being climate sensitive by O'Brien et al. (2004). However, as opposed to the district level spatial resolution of the O'Brien et al. (2004) study which masks fuzzy transitions in vulnerability the use of remote sensing derived 500m spatial resolution crop maps here delivers greater landscape scale spatial detail.

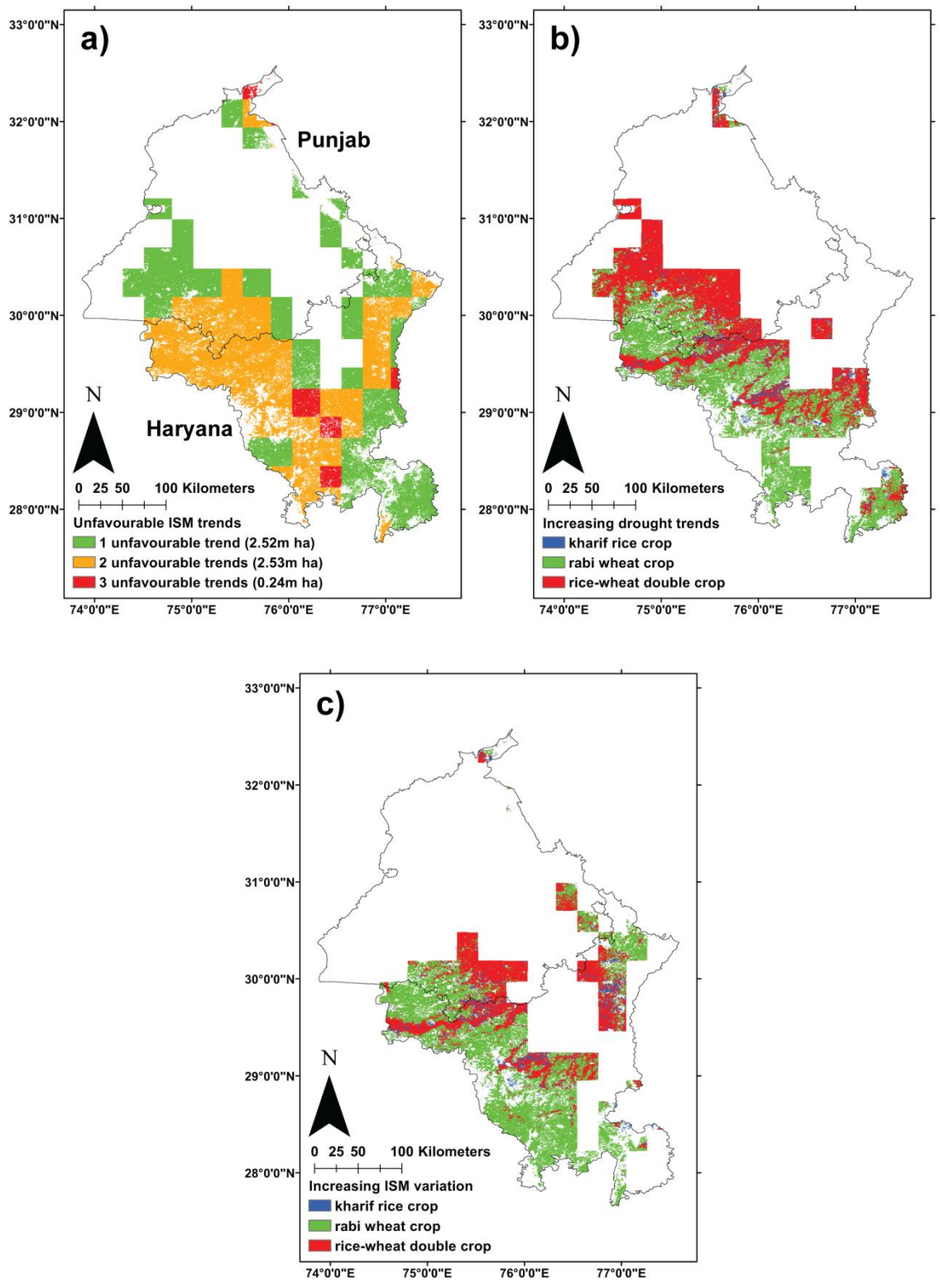

Figure 5-3 'hotspots' where *kharif* rice, *rabi* wheat or rice-wheat double cropping systems coincide in space with a) unfavourable trends in facets of ISM precipitation. These trends are one or more of decreasing ISM precipitation, increasing recurrence of drought years, increasing inter-annual ISM variation and increasing inter-annual variation in onset date of ISM, b) increasing trends of recurrence in drought years alone and, c) increasing inter-annual variation in ISM precipitation alone.

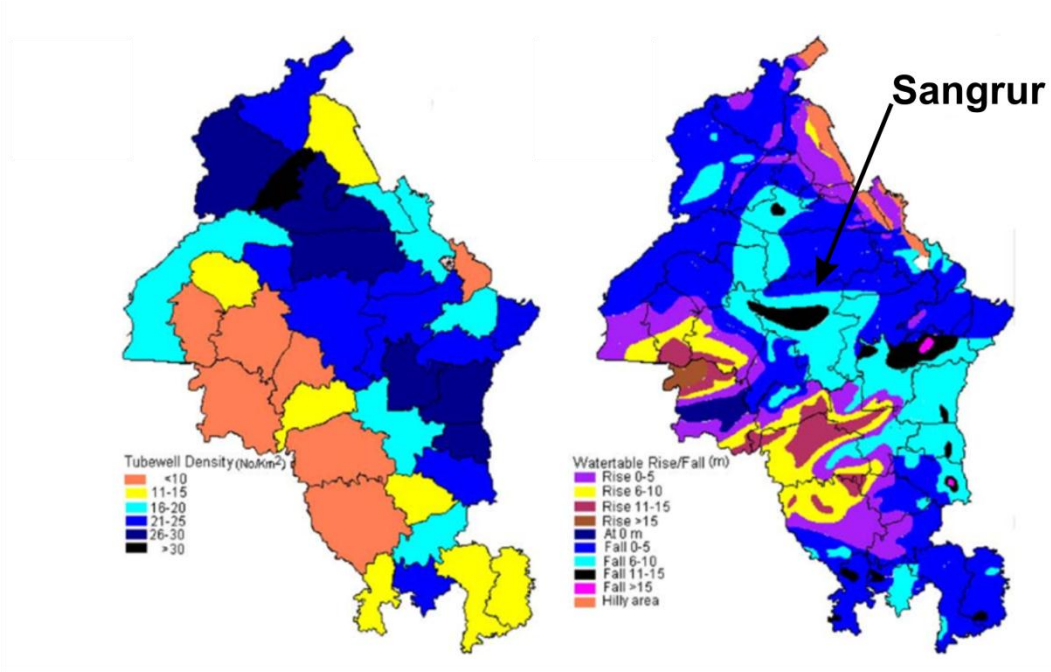

Figure 5-4 District-wise tubewell Density (left) and watertable rise/fall (right) reproduced from Ambast et al. (2006).

5.3.2 Late-sown wheat crop and yield declines

Later sown wheat, exposes the wheat crop to higher temperatures later in the growing season which has an adverse effect on several crop development processes which determine final crop yield (Wassmann et al. 2009; Lobell et al. 2012). Both coarse grid GCM and finer grid RCM are consistent in forecasting warming trends over north India with greater numbers of extreme heat days (>28°C and >35°C) (Moors et al. 2011; Mathison et al. 2013); seasonally the greatest magnitude of projected warming occurs in the wheat growing season (Mathison et al. 2013). This implies that later sown wheat crops are increasingly vulnerable to warming trends and extreme heat events (Lobell et al. 2012). The spatial pattern of wheat SOS in Fig. 5-5a captures accurately the later wheat SOS in south Punjab associated with the later harvesting dates of the *kharif* cotton crop (Ambast et al. 2006; Lobell et al. 2010). Field experiments from Punjab suggest a yield decline of ~1% day^{-1} after the optimal sow date in mid-November (Ortiz-Monastrerio et al. 1994). Similar trends are noted in (Fig. 5-5b and 5-5c) with the advantage of demonstrating that trends reported in field studies are spatially explicit. There is a consistent decline in wheat yield with later wheat crop SOS (Fig. 5-5c). It should be noted that the date of sowing will be earlier than SOS detected from remote

sensing data which places the remote sensing observations (Fig. 5-5b and 5-5c) in line with existing field studies (Ortiz-Monastrerio et al. 1994; Lobell et al. 2013). This is due to LSP parameters detecting onset of greenness, which occurs after seeds have emerged, with a time lag from sowing date. Simulations of wheat in Punjab using the CERES-wheat model suggest a 3 week lag between sowing and 10% amplitude of LAI (correlated with EVI) being reached (Lobell et al. 2013). The areas of late sown wheat should be targeted with zero-tillage practices encouraging earlier sowing of the wheat crop (Ortiz-Monastrerio et al. 1994; Erenstein and Laxmi 2008; Lobell et al. 2013) whilst also delivering other socio-economic and environmental benefits (Gupta and Seth 2007; Erenstein and Laxmi 2008; Erenstein 2009a). It should be noted here that the high wheat yields obtained on some farms in Punjab and Haryana (Aggarwal et al. 2004) are not estimated from MODIS data in Fig. 5.5b. This may be due to sub-pixel compositions of land cover and crop productivity masking high yielding plots.

5.3.3 Crop Residue Burning

Burning crop residue is a contributor to CO_2, CH_4 and N_2O emissions and is a positive feedback to climate change (Aggarwal et al. 2004; Pathak et al. 2006; Bhatia et al. 2012). Residue burning lowers soil nutrient content lowering yields, unless mitigated by fertiliser application (Pathak et al. 2006), and undermines sustainability gains by decreasing efficiency of water use via lower infiltration rates and increased evaporation (Lumpkin and Sayre 2009). Further negatives from residue burning include the impacts of pollutants and aerosols on human health (Erenstein and Laxmi 2008) and ISM circulation (Knopf et al. 2008; Ramanathan and Carmichael 2008). Detected from remote sensing data rice and wheat residue burning occurred over 1.17 million ha and 2.4 million ha, respectively (Fig. 5-5d). This equated to hundreds of thousands of Tonnes of GHG emissions (e.g. over 566987 Tonnes of CO_2 from wheat residue burning) which impacts both regional (e.g. ISM) and global climate systems (Table 5-5). Targeting burnt areas with adaptive residue management, (e.g. zero-tillage drills which can seed through residue (Erenstein 2009a)), would deliver environmental benefits, increase resource use efficiency and mitigate climate change and deteriorating air quality. Estimates of GHG emissions from crop residue burning generated using

location specific estimates of crop residue burnt using MODIS data were lower than GHG emissions estimated using default Tier 1 parameters provided by the IPCC (2006b) and used by the FAO (FAOSTAT 2013). The default Tier 1 parameters specify a spatially universal value of M_b (crop residue mass burnt in fields) which does not account for inter-growing season and spatial variation in levels of crop production and biomass generation. It is possible that emissions are underestimated using as the signal from high yielding farms maybe masked by a mixture of land covers and crop productivity levels within 500m^2 MODIS pixels.

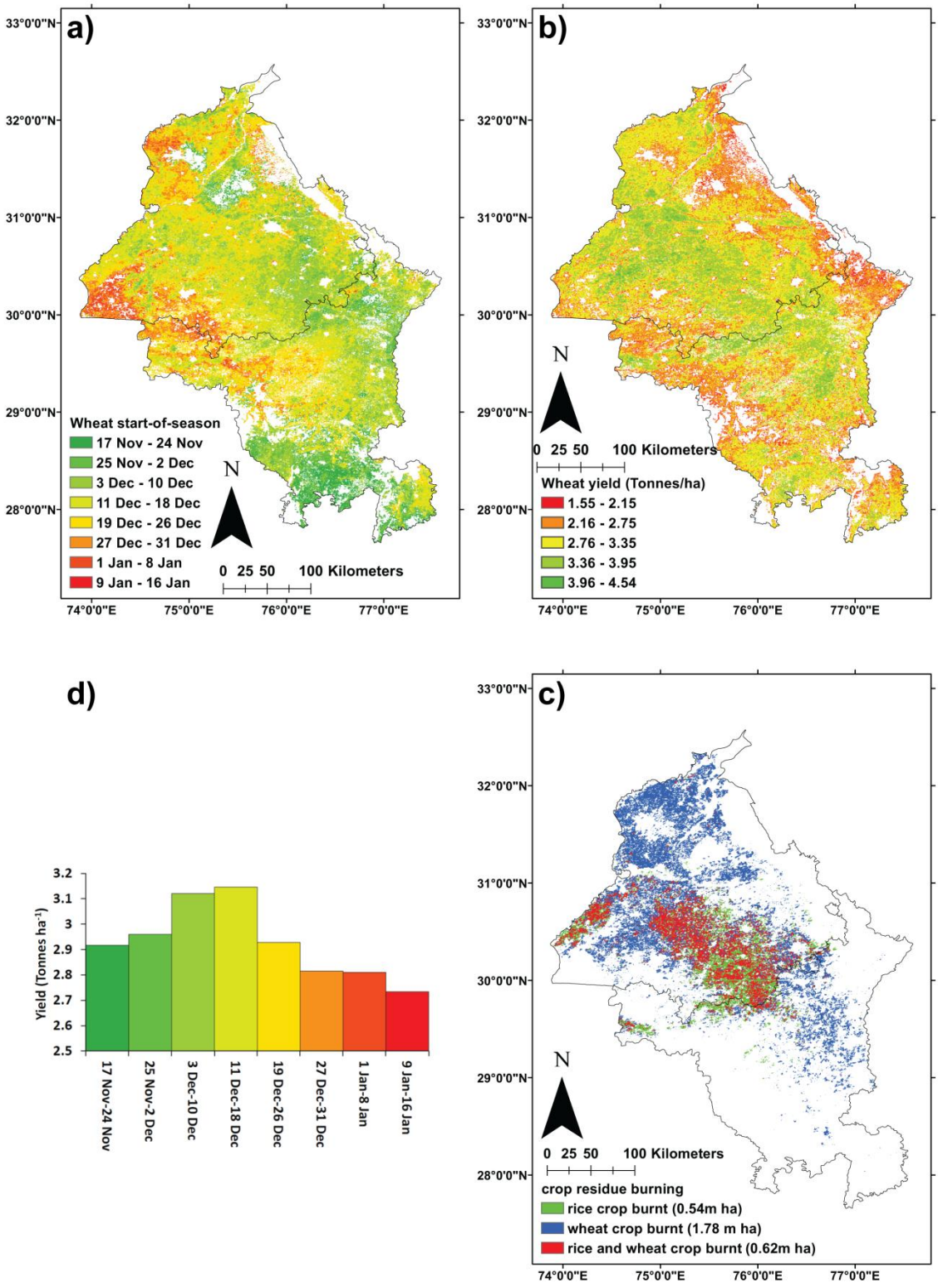

Figure 5-5 a) SOS date for the 2009-2010 wheat rabi crop. SOS dates detected prior to the 17th of November and after the 9th January were masked out due to few pixels reporting onset during these periods; pixels reporting SOS on the 17th November corresponds to sowing around the 1st November assuming a three week lag between sowing date and SOS detected by the satellite sensor. Nearly all wheat is sown after the 1st November (Lobell et al. 2012), b) wheat yield (Tonnes ha-1), c) average

yield (Tonnes ha^{-1}) plotted against SOS of wheat growing season, d) areas where crop residue was burnt for rice crop and wheat crops.

Table 5-5 Emissions of GHG from residue burning of rice and wheat crops over pixels identified as burnt from the MODIS MCD45A1 product. Emissions were estimated using the standard IPCC methodology (IPCC 2006b) and with location-specific model inputs provided from estimates of cropped area and productivity from the MOD09A1 product. The final column presents emissions estimated using globally applicable default Tier 1 estimates provided by the IPCC (2006b).

Greenhouse Gas	Emissions (Tonnes)	Emissions (Tonnes ha^{-1})	Emissions estimated following IPCC and FAO methodology (Tonnes ha^{-1})
CO_2 wheat burning	566987	0.23673	0.606
CO_2 rice burning	236243.770	0.20187	0.83325
CH_4 wheat burning	1010.479	0.00018	0.00108
CH_4 rice burning	421.027	0.00036	0.001485
CO wheat burning	34431.121	0.01438	0.0368
CO rice burning	14346.136	0.01226	0.0506
N_2O wheat burning	26.198	0.00001	0.000028
N_2O rice burning	10.916	0.00001	0.0000385
NO_x wheat burning	935.627	0.00039	0.001
NO_x rice burning	389.842	0.00033	0.001375

5.3.4 Yield Gaps

Fig. 5-6a and b shows the spatial locations of yield gaps greater than 0.5 Tonnes ha^{-1}, 1 Tonnes ha^{-1} and 2 Tonnes ha^{-1} for the rice and wheat crops. In 2009-10 it was estimated that 965,363 ha of wheat croplands had yield gaps greater than 1 Tonnes ha^{-1} and 4336 ha had yield gaps greater than 2 Tonnes ha^{-1}. For rice croplands, 321,580 ha had yield gaps greater than 1 Tonnes ha^{-1} and 3349 ha had yield gaps greater than 2 Tonnes ha^{-1}. These are priority locations within croplands which should be targeted with sustainable adaptations to raise yield levels up to their local maximum and, thus, reduce the need to expand cropped areas. There was not a clear spatial pattern of locations which experienced yield gaps greater than 2 Tonnes ha^{-1}. This suggests that that yield gaps of the largest magnitude are not explained by regional scale factors but likely have a location specific cause. Also, it may be that the 500m pixels with largest

magnitude yield gaps have a lower proportion of wheat cropping within the pixel reducing the EVI values. Figs. 5-6c and d indicates that the spatial pattern and magnitude of yield gaps was robust to the size of moving window Y_p was computed within. Yield gaps estimated within a 5km moving window are a more conservative estimate than yield gaps computed within a larger moving window (e.g. 20km) (Figs. 5-6c and d). A 5km moving window will likely sample a large enough region of farms to capture yields performing close to Y_p whilst also better representing the underlying spatial gradients in variables (e.g. soil type, access to irrigation) which determine Y_p at a given location.

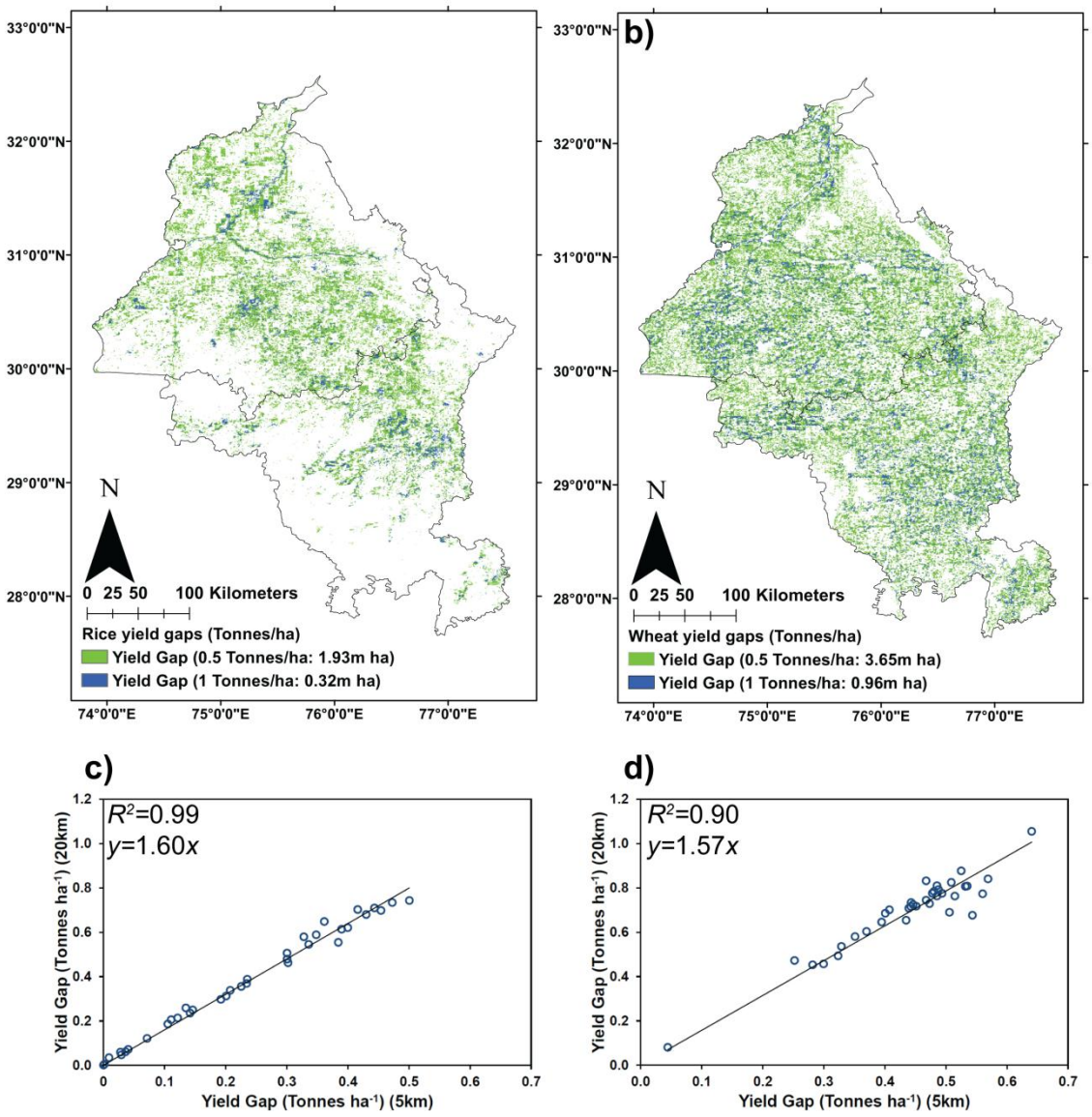

Figure 5-6 locations where yield gaps greater than 0.5 and 1 Tonnes ha-1 were detected for a) rice crops and, b) wheat crops. The relationship between average district-wise yield gaps computed with 5km and a 20km moving window for c) rice and, d) wheat.

Remote sensing derived estimates of Y_p are lower than the true genetic potential of yield or Y_p estimated from crop simulation models or 'ideal' experimental farms (Lobell et al. 2007; Lobell et al. 2009). However, it is likely some farmers in Punjab and Haryana approach true Y_p given access to high levels of inputs (HYVs, irrigation and fertiliser). Also, Y_p estimated from remote sensing data may be a more realistic measure of what can be achieved in real world croplands given prevailing economic and technological limitations (Lobell and Ortiz-Monasterio 2006); for example, crop simulation models may overestimate Y_p as they do not adequately simulate the impact of yield limiting extreme heat events on pollination processes (Lobell et al. 2009). Computing yield gaps using remote sensing data captures spatial patterns in yield gaps and yield variability and, thus, pin-points locations of underperformance; quantifying both the location and size of yield gaps means areas where the size of yield gap is greatest can be prioritised for targeting. By generating spatial patterns of yield gaps enables integration with a range of other spatial datasets to identify adaptation options to close yield gaps. For example, Lobell et al. (2002) used remote sensing data to link yield gaps with soil and climate and Lobell et al. (2010) linked yield variability to sowing date and proximity to roads and canals.

5.3.5 Integrating spatial datasets: Holistic assessments of cereal croplands

Discussed thus far are examples of how information contained within remote sensing observations can reveal locations where agricultural productivity or sustainability are undermined by prevailing stresses (e.g. climate) or sub-optimal agricultural practices (e.g. residue burning). Remote sensing can provide spatially explicit information to target appropriate conservation agriculture and other adaptive practices. However, integrating multiple remote sensing datasets and ancillary datasets can better capture the complex, systemic nature of cereal cropping systems and, thus, reveal more options for adaptation. Cereal croplands represent a type of complex socio-environmental system where outcomes span socio-economic (e.g. income, food security, crop yield) and environmental (e.g. soil degradation) spheres. Such outcomes are determined by interactions between socio-economic (e.g. policy, markets) and environmental (e.g. climate) drivers. Approaches to identify and target optimum

climate-smart practices in cereal croplands are therefore limited if they do not account for the prevailing policy environment. The following discussion explores examples of integrating multiple spatial datasets to inform climate-smart adaptations whilst remaining sensitive to, and addressing the limitations of, current policy.

5.3.5.1 Water resources for cereal croplands

Integration of crop extent maps and locations experiencing unfavourable trends in ISM precipitation highlight 'hotspot' locations where water intensive cereal cropping is exposed to unreliable, or decreasing quantities of, precipitation (Fig. 5-3). These spatial datasets can be viewed in conjunction with maps of groundwater extraction capacity and trends in groundwater levels (Fig. 5-4) to enable more complex responses in how to manage water resources across the landscape. The precipitation availability 'hotspots' were predominately located across south Punjab and Haryana which correspond to areas with a low density of tubewells and trends of rising watertable levels (Ambast et al. 2006) (Fig. 5-4). This suggests that managed extraction of groundwater, supplemented through artificial recharge via recharge tubewells and rainwater harvesting (Ambast et al. 2006) and consistent monitoring, could be utilised as a buffer to climatic variability. This would require a policy-shift, and to be incorporated within an Integrated Water Resource Management (IWRM) approach recognising that the water balance is part of a dynamic hydrological regime within the river basin linked to other watersheds by surface and sub-surface flows of water (Moors et al. 2011). Targeting holistic approaches, in the identified vulnerable locations (Fig. 5-3a), would contribute to meeting the goals outlined in the Government of India's National Action Plan on Climate Change: National Water Mission to promote IWRM at the basin level to cope with precipitation variability, ensure equitable distribution of water and prioritise vulnerable watersheds (National Water Mission 2009).

5.3.5.2 Policy traps, cropping diversity and excessive groundwater extraction

Spatially explicit measures of cropping diversity (Fig. 5-7a), the extent of the rice-wheat cropping system (Fig. 5-7b), groundwater extraction capacity (Fig. 5-4) and trends in groundwater levels (Fig. 5-4) highlight a spatial coincidence in low levels of cropping

diversity, declining groundwater levels and an intensive double cropping system. This situation is an artefact of low governance diversity (e.g. subsidised electricity for groundwater, procurement of rice and wheat) promoting a lack of diversity in farmer's practices and a dominant rice-wheat monoculture and a more homogenous cropping landscape (Fig. 5-7b; Aggarwal et al. 2004; Perveen et al. 2012). Government policy has generated a positive feedback creating 'brittleness' (Biggs et al. 2012) or a 'rigidity trap' (Holling 2001) lowering the resilience of the rice-wheat cropping system to future disturbances.

Fig. 5-8 is a schematic representation of the socio-ecological and climate interactions of the rice cropping system in Punjab and Haryana. It illustrates how government policy, which initially created an enabling environment for intensive rice cropping, has instigated numerous positive feedbacks which accentuate environmental degradation and harmful climate change. Fig. 5-8 illustrates a system 'locked-in' to a trajectory of environmental degradation, increasing exposure to unfavourable climate change and potentially resulting in a state when it can no longer deliver required yield levels. A shift in government policy and the underlying political economy of the agricultural sector is required to move the rice-wheat cropping system onto a climate-smart trajectory, incentivising uptake of sustainable crop types and practices to break the cycle of increasing environmental degradation and harmful climate change. However, as a result of government policy a large proportion of the electorate's livelihoods are dependent upon rice cropping, unsustainable subsides for irrigation and profits guaranteed from assured markets and minimum support prices for rice (Murgai et al. 2001; Perveen et al. 2012; Ojha et al. 2013). Therefore, there is little political willpower to develop policies, provide incentives for, and explore more sustainable and adaptive management of the croplands (Murgai et al. 2001; Ojha et al. 2013). This is problematic due to the excessive water demand of the rice crop (10 times more than other *kharif* crops) meaning the only way to reduce excessive groundwater extraction and environmental degradation is to restrict the land coverage of puddled rice cropping (Ojha et al. 2013). There is a need to overcome the institutional and political barriers which are rigidly holding the system on an environmentally unsustainable trajectory which contributes to its increasing exposure to harmful climate change.

Diverse cropping maintains ecological resilience, and diversity in governance delivers management flexibility (Ojha et al. 2013), vital to increase the adaptive capacity and resilience of the rice-wheat cropping system to uncertain futures (e.g. ISM precipitation) (Annamalai et al. 2007; Moors et al. 2011).

The rice-wheat double cropping system requires more water input than is received via precipitation and rechargeable groundwater (Ambast et al. 2006; Central Ground Water Board 2012). Altering the pricing of irrigation water would encourage appropriate water use and diversification of cropping (Aggarwal et al. 2004). Provision of weather-based crop insurance or subsidies are policy options which should be applied in rice-wheat croplands to overcome farmer concerns with diversifying cropping (Aggarwal et al. 2004). Diversification options, such as replacing conventional puddled *kharif* rice with maize, delivers environmental and economic benefits with irrigation water savings of 50-60%, a 90-100% reduction in methane emissions and a 20-25% reduction in labour and energy costs (Pathak et al. 2012). Diversifying cropping away from the rice-wheat cropping system to cash crops can deliver win-win situations of increased incomes and reduced environmental degradation (e.g. less pressure on groundwater, reduced GHG emissions) (Aggarwal et al. 2004; Perveen et al. 2012). Government incentives encouraging farmers to diversify will alleviate biotic and abiotic problems associated with rice-wheat cropping (Chauhan et al. 2012). For example, incorporation of legume crops in rice-wheat cropping systems increases nitrogen use efficiency and reduces nitrate contamination of groundwater (Chauhan et al. 2012). This indicates there is potential for a few or a single spatially targeted adaptive measure to deliver multiple benefits simultaneously. However, currently farmers are not keen to pursue legume cropping despite its environmental benefits as there is no assured market and it is not as profitable as rice (Ojha et al. 2013).

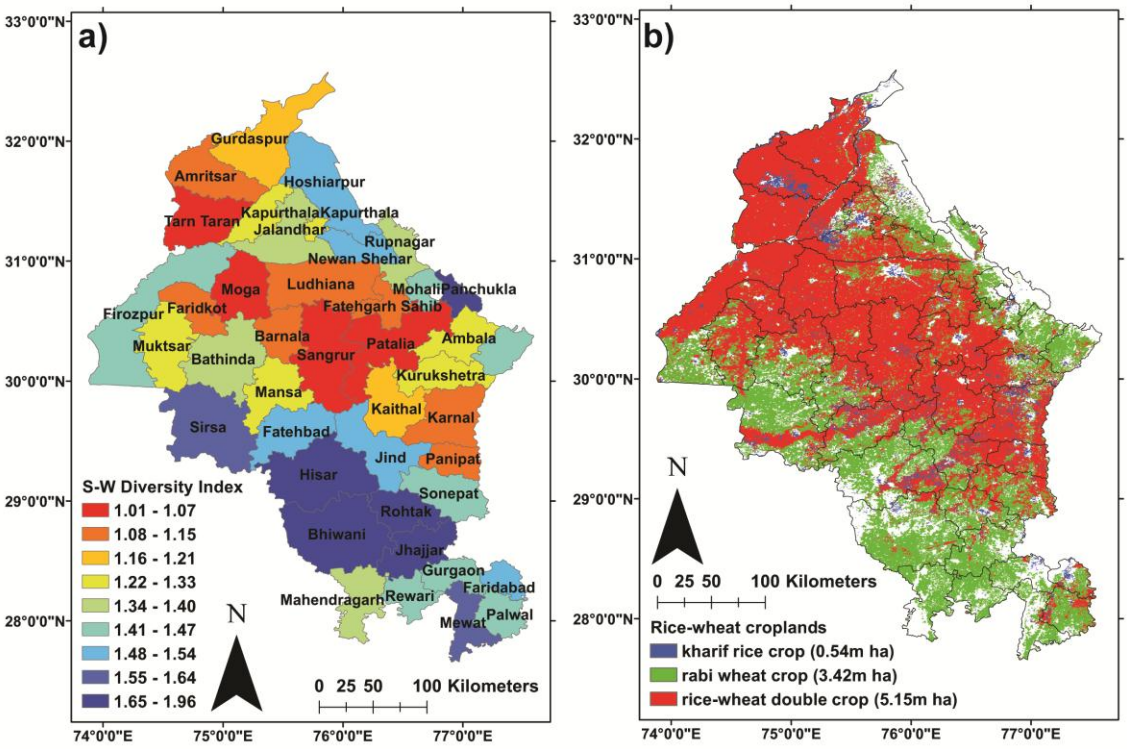

Figure 5-7 a) district-wise cropping diversity (Shannon-Weaver Diversity Index) computed from the Government of India district-wise land use datasets (http://lus.dacnet.nic.in/), lower values correspond to lower cropping diversity and, b) areas under *kharif* rice (0.5 million ha), *rabi* wheat (3.4 million ha) and rice-wheat double cropping (5.1 million ha) cultivation during the 2009-2010 agricultural season detected from MODIS MOD09A1 data.

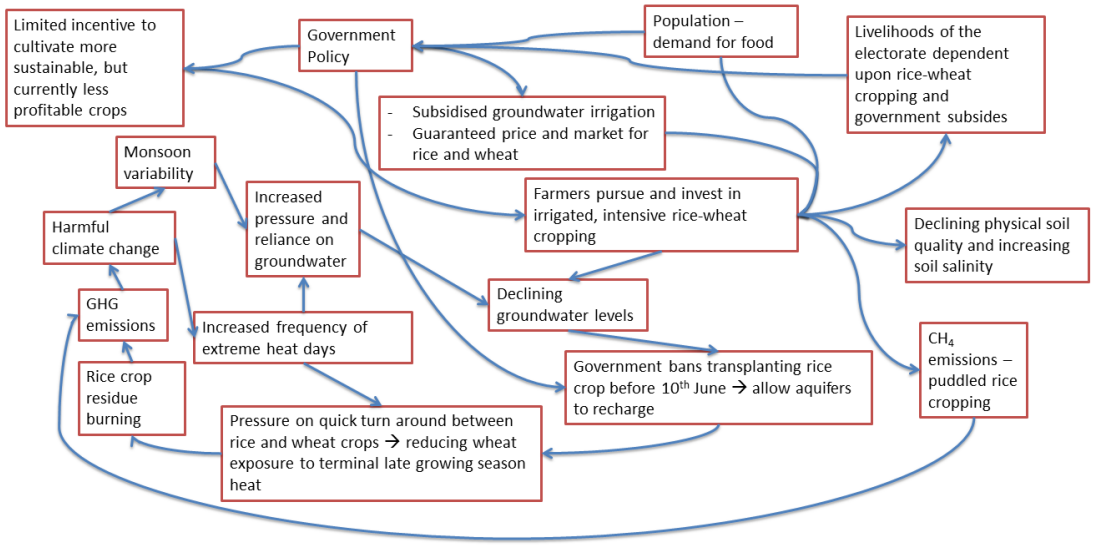

Figure 5-8 Schematic representation of the socio-ecological-climate processes, interactions and feedbacks of the rice-wheat cropping system in Punjab and Haryana.

5.3.6 Capturing synergies and navigating trade-offs via targeted implementation of agricultural adaptations

Instead of viewing a particular stress in isolation (e.g. exposure to unfavourable trends in ISM precipitation) more holistic approaches recognise interactions between different stresses and underlying agricultural practices within the cropping system. Therefore holistic approaches integrating thematic detail across a landscape can inform on capturing synergies and minimising trade-offs, inherent in implementing agricultural adaptations, which occur spatially to maximise environmental and social benefits and optimise use of resources for adaptation.

5.3.6.1 Capturing spatial synergies

When Figs. 5-5a, b, and c and Fig. 5-3 are viewed in conjunction it is clear that the southern portions of Punjab and Haryana exposed to unfavourable trends in ISM precipitation also have a wheat crop sown after the optimal window for maximum yield returns (mid-November). Identifying such locations from integrating spatial datasets to target with zero-tillage practices will deliver multiple benefits. Zero-tillage wheat crops have been shown to reduce water requirements and improve water productivity whilst also enabling timely sowing of the wheat crop with associated yield increases (Erenstein and Laxmi 2008; Jat et al. 2009a; Saharawat et al. 2010). It is important to note that a large proportion of the wheat crop in southern Punjab and Haryana is grown as part of a cotton-wheat cycle (Lobell et al. 2010). Cotton matures later that other *kharif* crops (e.g. rice) so economic losses from shifting to earlier wheat SOS need to be considered alongside other climate-smart gains. This further exemplifies the complexity of cereal croplands which can only be addressed through holistic spatial assessments.

Groundwater levels across the district of Sangrur, Punjab, are declining at a greater or equivalent rate to the rest of Punjab and Haryana (Fig. 5-4). This is attributed to excessive irrigation to support a rice-wheat cropping system (Ambast et al. 2006; Rodell et al. 2009). Conservation agriculture practices which preserve soil cover (e.g. mulch or not burning or removing crop residues from the previous crop) reduce water losses from the soil (reduced evaporation and increased infiltration) (Hobbs et al.

2008). Soil cover also lowers soil and canopy temperature which will reduce the water demand from crops (Hobbs et al. 2008; Jat et al. 2009c). Therefore, ensuring soils are covered with residue or mulch will reduce the water requirements for crop growth and, thus, reduce pressure on irrigation. This point is pertinent over Sangrur where there is near complete coverage of rice and wheat crop residue burning (Fig. 5-9a) coinciding with declining groundwater levels. Therefore incorporating residue retention or soil cover into agronomic practices will deliver multiple benefits simultaneously (or capture synergies) including: reduced GHG emissions from crop burning, better water use efficiency and, thus, reduced pressure on groundwater resources, reduced soil erosion and enhanced soil physical and biological quality and lower canopy temperatures reducing crop exposure to extreme heat events (Hobbs et al. 2008; Jat et al. 2009b; Lobell et al. 2012).

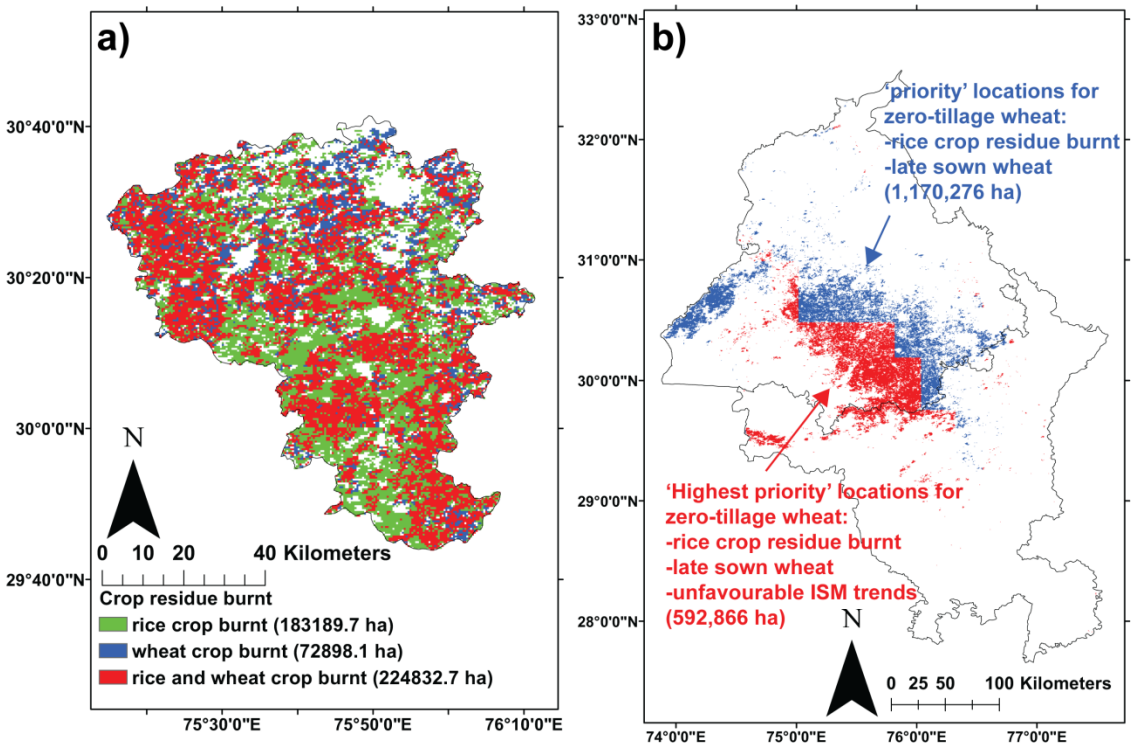

Figure 5-9 a) locations where rice and wheat crop residue burning was detected in the district of Sangrur, Punjab, which is experiencing declines in groundwater levels. The location of Sangrur relative to the rest of Punjab and Haryana is displayed in Fig. 5-5 (It should be noted the 2006 district outline for Sangrur is displayed here), b) spatial trade-offs to discriminate high-priority locations for targeting with 'zero-tillage' technologies for the *rabi* wheat crop. Late-sown wheat is any pixel with a SOS after the 11th December 2009 as detected from MODIS derived phenology profiles (there is an approximate three week lag between SOS date and sowing).

5.3.6.2 Trade-offs: prioritising locations for adaptation and mitigation

It is important to recognise trade-offs and costs in implementing climate-smart and conservation agriculture practices. For example, there is a trade-off between the environmental benefits of improved residue retention in conjunction with zero-tillage and the costs required to develop zero-tillage drills which can seed through crop residue ('happy seeder' drills) (Erenstein and Laxmi 2008; Erenstein 2009a). Through integration of multiple spatial datasets it is possible to rank locations in order of priority for adaptation to agricultural practices. For example, 'highest' priority locations for targeting with resources to implement uptake of 'happy seeder' zero-tillage drills would be those where crop residue is burnt, the wheat crop is sown late and unfavourable trends in ISM precipitation were observed (Fig. 5-9b). Through an integration of remote sensing derived and climatic spatial datasets 592,866 ha of the rice-wheat cropping system were designated 'highest-priority' to receive support in implementing technologies to facilitate zero-tillage wheat with residue retention (Fig. 5-9b). The variable 'unfavourable trends in ISM precipitation' was then dropped (based on the premise that the *rabi* wheat crop is irrigated) to illustrate how other locations could be prioritised, but with lesser urgency or importance attached (Fig. 5-9b). A further 1.17 million ha were identified which would benefit from zero-tillage with residue retention but, ideally, should not be targeted above the 'high priority' locations.

It is recognised that greater complexity could be incorporated into this approach for spatially resolving trade-offs on where and how to allocate resources and technological capacity for adaptation. Advances could range from including more detail into the existing variables (e.g. how late the wheat crop is sown, the nature of unfavourable climatic trends), including more variables to capture a greater level of systemic detail (e.g. groundwater levels, financial resources to fund adaptations), assigning weights of importance to variables (e.g. via stakeholder consultation and implement multi-criteria analysis in a GIS framework) or utilising approaches to measure the degree of spatial vulnerability (e.g. the vulnerability surface (Luers 2005)). However, the more simplistic approach presented here demonstrates the advantages of integrating remote sensing and ancillary datasets to resolve trade-offs spatially, prioritising locations for targeting

with conservation and other agriculture practices to deliver maximum climate-smart gains whilst optimising use of available resources over a landscape (e.g. money, machinery or environmental services).

5.4 Conclusions

Here, an approach integrating the greater local detail in remote sensing measures of an agricultural landscape with climatic data and agricultural statistics allowing holistic, spatially explicit, monitoring of the rice-wheat production system is demonstrated. This can inform on 'vulnerable' locations and facilitate targeting of spatially optimum conservation agriculture and adaptive practices to maximise climate-smart benefits across the landscape. There is potential to upscale and adapt this approach to other agricultural landscapes within South Asia, and also globally. Monitoring of food provisioning ecosystem services often does not incorporate sufficient thematic detail (e.g. crop type) (Crossman et al. 2013). Here, rice and wheat crop extent, and yield, were mapped accurately[9] (R^2=0.96 (rice) and 0.94 (wheat) for full-pixel area extents computed from MODIS data compared to district-wise land use statistics) (Figs. 5-2 and 5-7b). These techniques for detecting crop extents can be 'rolled out' to other 'focal' regions of agricultural productivity with minimal adjustment (e.g. Terai in Nepal). Such detail will improve results of secondary studies requiring land use inputs, especially studies utilising a landscape scale approach which are often limited by paucity of data between the farm and district/regional level (e.g. quantification of GHG emissions from agriculture; Table 5-5) (Milne et al. 2012). The local (i.e. sub-district) and integrated thematic detail presented here demonstrates an approach which facilitates navigation of trade-offs, and captures synergies, inherent in climate-smartening agricultural landscapes globally (FAO 2012). This is achieved by identifying locations which will deliver greatest returns from uptake of climate-smart practices enabling efficient allocation of resources (either machinery or money). For example, here we identify 592,866 ha of croplands across southern Punjab and Haryana which

[9] It should be noted that as full-pixel areas were accounted for here accuracy may be inflated due to sub-pixel errors of cropland occurring within a pixel not being detected as cropped (omission) and areas of non-cropland within a pixel detected as cropped (commission) cancelling out.

experienced unfavourable trends in ISM precipitation, crop residue burning and later sowing dates for the wheat crop highlighting where adoption of optimum conservation agriculture practices can deliver multiple benefits (e.g. zero-tillage encouraging water savings and earlier sowing dates).

In the 2009-2010 agricultural season rice and wheat crop residue burning occurred on 1.17 million ha and 2.4 million ha respectively with a range of subsequent environmental dis-benefits including hundreds of thousands of tonnes of GHG emissions; for example wheat crop residue burning generate 566987 Tonnes of CO_2. The SOS of the wheat cropping season, and subsequent yield declines with later sowing dates were quantified from remote sensing data. Across Punjab and Haryana 5.3 million ha of rice and wheat croplands coincided with locations experiencing at least one, and up to three simultaneously, unfavourable trends in facets of ISM precipitation such as increasing recurrence of drought years. The locations of unfavourable trends in facets of ISM precipitation were computed from daily precipitation data from 1951-2007. Also, 965,363 ha of wheat croplands returned yields of 1 Tonne ha^{-1} lower than potential yields and 321,580 ha of rice croplands had yield gaps of at least 1 Tonne ha^{-1}. The spatial distribution of these yield gaps was captured using remote sensing data. Often the areas of rice-wheat double cropping coincided with areas where groundwater levels were falling and the lowest cropping diversity suggesting lower levels of ecological resilience and existent adaptive capacity to uncertain and variable futures in ISM precipitation. These, locations were mainly in the central districts of Punjab and Haryana, such as the district of Sangrur as highlighted in Fig. 5-9a.

Chapter 6: Satellite observations reveal the impact of climatic extremes and variability on cereal croplands

6.1 Introduction

Similar to other cereal crops levels of production and productivity for rice and wheat crops are vulnerable to a changing climate. Increases in mean growing season temperature, an increase in the frequency of extreme heat stress events at key phenological stages (e.g. the thermo-sensitive reproductive and grain filling periods (TSP)), uncertain precipitation futures and increased risk of droughts and subsequent moisture shortages all have a potentially negative impact on crop yield (Ortiz et al. 2008; Asseng et al. 2012; Lobell and Gourdji 2012; Lobell et al. 2012; Teixeira et al. 2013; Gourdji et al. 2013b; Koehler et al. 2013).

Increases in average growing season temperatures hastens phenological development, reducing time available for biomass accumulation and photosynthetic activity thus, reducing final yield (Sadras and Monzon 2006; Oh-e et al. 2007; Welch et al. 2010; Hatfield et al. 2011; Lobell et al. 2011a; Lobell et al. 2012). Different crops have also shown different sensitivities to daily maximum or minimum temperatures; for example, maize yield is negatively correlated with maximum temperature whereas dry season rice yield is negatively correlated with minimum temperature (Peng et al. 2004; Welch et al. 2010; Lobell et al. 2011a). Adequate moisture levels are also vital for crop growth. Both rice and wheat yields in India are significantly correlated with all-India monsoon precipitation (Krishna Kumar et al. 2004) and, negatively impacted by drought conditions during the ISM (Auffhammer et al. 2012). Both levels of soil moisture and atmospheric moisture (relative humidity) have the potential to exert control on crop growth and development; soil moisture deficit is a limiting factor negatively impacting vegetative and reproductive growth processes (Wassmann et al. 2009).

Increasing evidence is mounting highlighting that rice and wheat cereal crop production and yield formation is sensitive to, and negatively impacted by, warming

during the TSP (Asseng et al. 2010; Wassmann et al. 2009; Teixeira et al., 2013). The TSP spans crop reproductive period and subsequent grain-filling stages which largely determine final crop yield (Teixeira et al. 2013). Remote sensing observations of croplands have shown that spectral relectance measures during these periods of crop development explain the largest amounts of variation in crop production (Funk and Budde 2009; Bolton and Friedl 2013). Cereal crops are particularly sensitive to warming during anthesis where increasing temperatures impede pollination and fertilisation processes resulting in increased spikelet sterility and reduced final yield (Jagadish et al. 2007; Wassmann et al. 2009). Increasing temperature during grain filling accelerates crop senescence reducing growth rates for grains which determine final yield and production; cereal crops are also more sensitive to warming events closer to anthesis than maturity and harvest (Asseng et al. 2010). Several studies have highlighted that crops display a threshold temperature response to warming during the TSP; in controlled experimental settings Jagadish et al. (2007) noted that air temperatures greater than 35˚C were terminal for rice reproductive processes. Asseng et al. (2010) observed yield decreases with increased wheat crop exposure to heat stress events (daily maximum temperatures greater than 34˚C) during the TSP.

The presence of adequate soil moisture and lower relative humidity or higher vapour pressure deficit facilitate transpiration cooling which helps crops escape heat stress during the TSP (Shah et al. 2011; Lobell and Gourdji 2012; Gourdji et al. 2013a; Teixeira et al. 2013). Under moisture stress, rice crops have shorter peduncle length and reduced percentage of panicle exsertion (Rang et al. 2011b). The timing of dry-spells, or drought conditions, determine the degree of crop failure; drought or moisture shortages coinciding with the TSP have a marked negative impact on yield (Wassmann et al. 2009; Lobell et al. 2011a; Lobell and Gourdji 2012).

Across the world's major wheat croplands including north-west India, the thermo-sensitive periods (TSP) of crop development for wheat crops coincide with the timing of highest average maximum temperatures annually (Asseng et al., 2010), and growing season temperature and extreme heat events during the TSP are projected to increase in the next century (Gourdji et al. 2013b; Mathison et al. 2013; Teixeira et al. 2013). Punjab and Haryana will likely experience warming trends, with increased frequency of

extreme heat days damaging to crop growth due to climate change (Rupa Kumar et al. 2006; Mathison et al. 2013). This will coincide with observed trends of increasing inter-annual variation in monsoon precipitation and recurrence of drought years affecting large portions of both states. In addition, difficulty in predicting, accurately, future monsoon conditions provides further uncertainty (Annamalai et al. 2007; Moors et al. 2011; Turner and Annamalai 2012). Climate change impacts are already limiting wheat crop yields globally: models indicate that warming trends since 1980 led to a 5.5% reduction in wheat production (Lobell et al. 2011b). Model projections of increased exposure to heat stress up to 2100 suggest that suitable adaptations need to be implemented urgently to secure climate resilient crop production. The underlying agricultural system (e.g. access to irrigation, cultivar type, soil type and ecosystem services), which varies within and between cropping landscapes, can increase the sensitivity of crops to harmful climate impacts (Asseng et al. 2010; Gourdji et al. 2013a; Luers 2005; Luers et al. 2003; Teixeira et al. 2013). For example, access to sufficient irrigation can enable transpiration which cools canopy temperatures relative to atmospheric temperatures, reducing the potential negative impact of warming on the crop during key physiological processes during the TSP but will lower levels of water productivity (Asseng et al. 2010; Gourdji et al., 2013b; Teixeira et al. 2013; Wassmann et al. 2009).

While cereal crops across the globe display similar responses to climatic variables, the vulnerability of crops and the ability to adapt to climatic variation are determined by location-specific factors inherent to each agricultural system (Teixeira et al. 2013). Therefore, to understand the impacts of climatic variation on crop yields occurring in real world cropping landscapes one requires the ability to observe and test a variety of climatic variables through time whilst capturing the spatial variation in the underlying agricultural system. Studies exploring the impacts of climatic variables on wheat crop yield are more informative to climate resilient adaptation when there is a local or regional focus because potential adaptations often include shifting dates of cropping systems, implementing zero-tillage to avoid periods of heat stress coinciding with the TSP, and the need to be sensitive to location-specific double/triple cropping rotations

which can only be captured at the local scale (Lobell et al. 2012, 2013; Teixeira et al. 2013).

Crop yield-climate interactions are usually explored using either (i) crop simulation models which aim to replicate crop physiological responses to climatic variation (Asseng et al. 2010; Challinor et al. 2005; Koehler et al. 2013) or (ii) regression models trained with crop yield and climate data aggregated within administrative boundaries (Lobell and Burke 2010; Rowhani et al. 2011; Schlenker and Lobell 2010; Urban et al. 2012). Crop simulation models are often complex and require large amounts of input data to represent the underlying complexity of the agricultural system (Welch et al. 2010; White et al. 2011); they are, therefore, limited in their application to large spatial extents. Moreover, often crop simulation models do not capture the differential impacts of heating events during key phenological stages, such as the TSP, well. In a review of 221 peer-reviewed climate-crop simulation model studies only 14 partially or fully addressed the issue of heat stress (White et al. 2011). Crop model uncertainty was deemed a larger or equivalent source of uncertainty than that introduced through climate models when simulating wheat yield under future climates using the Global Large Area Model (GLAM) (Koehler et al. 2013). Uncertainty in representing thermal time accumulation was the largest source of uncertainty in final yields (Koehler et al. 2013). In Lobell et al. (2012) it was shown that CERES and APSIM crop simulation models underestimated the shortening of the wheat growing season when exposed to increased warming. This suggests that climate-crop simulation models will underestimate the true negative impacts of climate change on crop yield; this is pertinent given projected future warming and increases in extreme heat days (Gourdji et al. 2013b; Mathison et al. 2013). Key interactions between climatic variables and crop growth processes within many crop models are too simplified to adequately provide confidence in regional projections of responses to climate change (Tubiello et al. 2007). However, remote sensing provides the opportunity for widespread monitoring of the response of cereal croplands to climatic variability and, thus, validate the use of crop simulation models for capturing regional scale impacts of climate change.

In contrast, crop yield-climate models trained at the administrative boundary level aggregate the complexity of the underlying agricultural system which can be problematic in heterogeneous agricultural landscapes. Also, crop yield-climate models trained at the administrative boundary level cannot capture the differential impact of climatic variables at varying phenological stages, thus, missing information to inform optimum climate resilient adaptations.

In this chapter, we demonstrate how remote sensing data can be used to quantify the impacts of climatic variables, particularly the influence of warming during the TSP, on crop production in real world cropping landscapes, thus, overcoming the limitations of the two, previously discussed approaches. Remote sensing data enables a more appropriate representation of spatially heterogeneous agricultural systems compared to district-wise land use and agricultural statistics. Remote sensing estimates of crop production incorporate measures of underlying system factors within a pixel (e.g. farmer decisions, access to irrigation, sowing date). The repeat coverage of remote sensing enables monitoring of crop phenology across a large spatial extent. This, therefore, enables the discrimination of climatic variables which occur at different phenological stages such as the TSP and an assessment of their impacts on final crop yield.

The overarching goal for this chapter is to explore the impact of temperature during the TSP on crop production, at the landscape scale in Punjab and Haryana. This is done by utilising the wide coverage and spatial and phenological detail in remote sensing data to develop statistical models between climatic variables during the TSP and crop production. This will reveal whether warming during the TSP has had a limiting impact on rice and wheat crop yield in Punjab and Haryana. Specific questions addressed in this chapter are:

1) what are the relative impacts of daily minimum temperature, daily maximum temperature and extreme heat events above incrementing temperature thresholds during the TSP on rice and wheat crop yield?

2) what is the impact of temperature variables during the TSP on crop yield in relation to growing season average temperature, growing season precipitation and

precipitation during the TSP by including all climatic variables in a multivariate fixed-effects model. Precipitation predictor terms were included in the model to account for potential transpiration cooling benefits reducing crop sensitivity to warming during the TSP. Growing season average temperature was included as a predictor term to account for potential crop sensitivity to temperature impacts not occurring during the TSP.

6.2 Methods

The extent, and yield, of rice and wheat croplands across Punjab and Haryana were estimated using remote sensing data. These datasets were integrated with climatic variables to create panel-datasets used to train linear fixed-effects crop yield-climate models. Panel-datasets are mutli-dimensional in time and space and, thus, can capture year-to-year variability in precipitation and also a wider range of temperatures which exhibit greater spatial variation relative to temporal variation at one location (Lobell and Burke 2010). Panel-regression models have shown improved performance (in terms of both strength of association and reduced scatter) for capturing temperature-crop yield relationships relative to time-series models (Lobell and Burke 2010).

The temporal extent of the panel-data was restricted to five years to negate the impact of shifting agricultural practices or technological advances on crop yield. Several studies have incorporated linear, quadratic or cubic regression spline time terms into crop yield-climate regression models to account for such technological development (Schlenker and Lobell 2010; Rowhani et al. 2011; Hawkins et al. 2013). However, this requires the assumption that the impact of developmental change on crop yield is universal across the spatial extent of the panel. Given the spatial variability in cropping-systems (Panigrahy et al. 2010) and levels of natural, physical, social and financial capital, which influence uptake of agricultural practices (Erenstein et al. 2007), across the panel, utilising a time term to capture development and assuming its spatial universality was not justified. Crop yield-climate regression models trained using panel-data are less sensitive to the temporal extent over which observations were taken (Lobell and Burke 2010). For example, Welch et al. (2010) detected the signal of minimum and maximum temperature impacts on rice yield using panel data with observations taken over five years.

6.2.1 Remote sensing data pre-processing

To map the extent of *kharif* rice and *rabi* wheat croplands, and estimate associated crop yields, for each year from 2002-2003 to 2006-2007 several VI were computed from 8-day composites of MODIS surface reflectance products (MOD09A1) (https://lpdaac.usgs.gov/products/modis_products_table/mod09a1). Only 'high-quality' pixels, determined using quality QA incorporated within the MODIS product were retained. 'Bad-pixels' and potential cloud pixels (determined via the condition ρ_{blue}>0.2 where ρ_{blue} is blue band reflectance (459-479nm) (Xiao et al. 2005)) were replaced using the gap filling algorithm of Peng et al. (2011). The following VI were computed NDVI, NDSI, EVI and the LSWI. The VIs were fitted iteratively towards their maximum envelope using an adapted version of the method of Chen et al. (2004) which smoothed the data using a Savitzky-Golay filter and includes a fitting bias towards maximum values. This removes noise and fluctuation in temporal VI profiles due to cloud cover and atmospheric contamination and accounts for the negative bias in reflectance at the sensor (Chen et al. 2004). Snow and water masks were generated using the NDSI, NDVI and LSWI products following Xiao et al. (2005, 2006) and forest masks were generated following the condition that a pixel had 20 successive 8-day MODIS composites with an NDVI>0.5.

6.2.2 Wheat and rice crop area classifications

The extents of the *kharif* rice crop and *rabi* wheat crop were mapped using a range of classification techniques applied to crop phenology profiles derived from the EVI and LSWI. Different classification techniques were used for each crop to generate the most accurate maps of crop extent per year. The rice crop was classified using an adapted version of the rice crop classification algorithm of Xiao et al. (2005, 2006) which detects the presence of puddling in paddy fields and subsequent rapid green up associated with crop vegetative development via LSWI-EVI inversion followed by a rapid increase in EVI. Thus, the puddling preceding a rice crop is defined by the logical condition:

$$LSWI_i + T \geq EVI_i$$

(1)

Where *i* corresponds to pixel location and *T* is a threshold which is adjusted inter-annually and is optimised using district-wise agricultural land use data (http://lus.dacnet.nic.in/). Xiao et al. (2005, 2006) used a global threshold value of *T*=0.05 for all of South-Asia, however, the accuracy of this classification method can be increased by adjusting *T* to account for locally varying agronomic and climatic factors and incorporating knowledge of local cropping calendars (Sun et al. 2009; Peng et al. 2011; Gumma et al. 2011b). The impact of the threshold *T* is illustrated in Fig. 6-1 where the unadjusted LSWI profile does not invert with EVI during puddling but LSWI+*T* does.

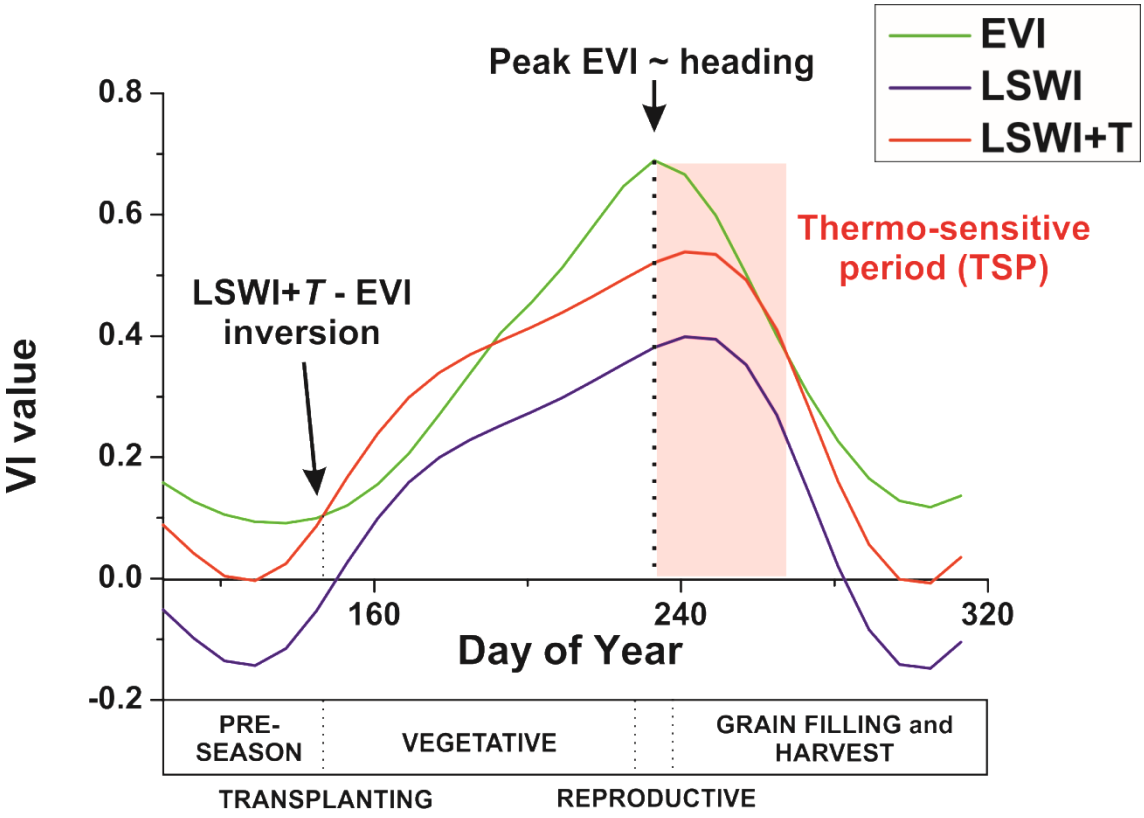

Figure 6-1 Schematic diagram illustrating the LSWI+T-EVI inversion at the time of puddling, and the benefit of incorporating T to make the classification more sensitive to puddling of fields at the beginning of the *kharif* rice season. This diagram also illustrates the thermo-sensitive period (TSP) over which EVI values are summed to approximate final yield and includes a temporal approximation of key rice crop development stages as stated in Wassmann et al. (2009) and Teixeira et al. (2013).

The LSWI-EVI inversion method is not suitable to map the extent of the wheat crop as fields are not puddled at SOS. Spectral matching techniques were used to statistically match the EVI-derived phenology profile per-pixel to an ideal wheat phenology profile.

This approach has been used widely to classify croplands in the region, and globally, from a range of sensors (Thenkabail et al. 2005; Thenkabail et al. 2007; Thenkabail et al. 2009; Biradar et al. 2009; Gumma et al. 2011b). A spectral similarity value (*SSV*) was computed comparing the per-pixel EVI phenology profile to an 'ideal' wheat phenology profile; further details regarding classification of wheat croplands using spectral matching techniques can be found in *section 5.2.1*. Phenology parameters were computed to extract the portions of the phenology profile corresponding to *rabi* cropping. SOS and EOS were defined as 10% of the amplitude between minimum and peak EVI on the rising and falling limbs of the phenology profile. This is a common approach to extracting phenology parameters from time-series VI and has been previously applied to the wheat crop in North India using MODIS data (Jönsson and Eklundh 2004; Lobell et al. 2012; Lobell et al. 2013). Focusing on only the growing period of the *rabi* season ensured pre- and post-season noise did not influence the computation of the *SSV* value. The *SSV* value is a similarity measure of the shape and curvature (Pearson's correlation coefficient) and, amplitude (Euclidean distance) of two phenology profiles (Thenkabail et al. 2007). Similar to rice, a threshold *SSV* to determine a match between pixel phenology profile and ideal wheat phenology profile was optimised, per year, using district-wise land use statistics (http://lus.dacnet.nic.in/).

Optimising the threshold values of *T* (for rice) and *SSV* (for wheat) inter-annually ensured the most accurate (full-pixel area) crop extent maps were generated per year. These crop extent maps were used as a binary mask to minimise the effect of non-agricultural land covers from propagating up to the crop yield-climate models, ensuring the models accurately captured the interaction between climatic variables and crop yields and not a noisy signal. A discussion of the merits and limitations of using cropland masks in crop production estimation from remote sensing data is provided in the previous chapter (see section 5.2.1 and 5.2.2). It is worth mentioning that an attempt was not made to generate an optimum time-independent, universal crop area classification technique but to generate maps where presence of rice or wheat cropping within a pixel was detected for each year to improve the wider modelling methodology. To generate optimum areal estimates of the area under rice

and wheat cropping using 500m spatial resolution MODIS data would require addressing sub-pixel areal coverage of croplands (Thenkabail et al. 2007) or use of 'fine' spatial resolution land cover maps capturing field extents (Bolton and Fried 2013).

6.2.3 Wheat and rice yield estimation

For each pixel classified as *kharif* rice or *rabi* wheat, crop yield was estimated using a cumulative sum of EVI values over an approximation of the TSP (CUM-$EVI_{(TSP)}$). It is difficult to define specific crop development stages accurately from remotely sensed data. However the period of maximum EVI has been shown to correspond to heading date in cereal crops (Sakamoto et al. 2005). Teixeira et al. (2013) found that a 30 day period around the reproductive crop development phase represented the TSP and captured extreme heat impacts on crop yield. Here, a 30 day period post maximum EVI was taken to represent the TSP for the rice and wheat crops (Fig. 6-1). A cumulative sum, or integration of VI values, and maximum VI values are commonly used as surrogate measures of vegetation productivity and crop yield (Pettorelli et al. 2005; Funk and Budde 2009; Vrieling et al. 2011; Rembold et al. 2013). VI values on the falling limb of the phenology profile of crops often provide more accurate estimates of crop yield as they correspond to the reproductive and grain filling development stages of cereal crops (Funk and Budde 2009; Rojas et al. 2011). Utilising the crop extent maps previously generated and phenology parameters for SOS and EOS per-pixel, ensured noise was not introduced into the yield estimation from either non-rice or wheat land covers or time-periods not-associated with the crop growing season (Funk and Budde 2009). The same method was used to define EOS for the rice crop as was used for the wheat crop but the LSWI-EVI inversion was used as a measure for rice SOS.

6.2.4 Climate data

The APHRODITE (V1003R1) precipitation dataset was obtained for the 2002-2003 to 2006-2007 growing seasons. Further details regarding the product generation and validation can be found in (Xie et al. 2007; Yatagai et al. 2009; Yatagai et al. 2012), and

examples of its use in studies over south Asia in (Andermann et al. 2011; Duncan and Biggs 2012; Duncan et al. 2013; Mathison et al. 2013).

The APHRODITE daily temperature product (V1204R1) provides daily mean temperature only, which inhibits exploring the impact of minimum and maximum temperature, and extreme temperatures, on crop yield. Therefore, Global Summary of the Day (GSOD) stations in Punjab and Haryana with a near complete record of daily minimum and maximum temperatures were extracted from: http://www.ncdc.noaa.gov/. Fewer weather stations were included (five), but selected on the basis of spatial coverage over Punjab and Haryana and completeness in temporal coverage with minimal missing data. Conservatively selecting stations with reliable and comprehensive temperature records was appropriate over Punjab and Haryana as there is minimal orographic variability, especially over cultivated lands, which would cause dramatic shifts in temperatures over short distances.

The data from these stations were used to generate gridded fields, at the same spatial resolution as the MODIS data, using an inverse-distance weighting algorithm. GSOD weather stations have been used as inputs in the generation of gridded climate products (e.g. Yasutomi et al., 2011) and to assess climate impacts on crops in North India (Lobell et al. 2012). We also applied a thin-plate spline interpolation method following (Lobell et al. 2012); however, this method generated spurious curvatures in the temperature surface due to the fewer number of weather stations used as inputs. Therefore, a simple inverse-distance weighting interpolation provided a more reliable spatial estimate of temperature.

6.2.5 Crop yield-climate regression models

All climatic variables (see Table 6-1) were regressed against the natural logarithm of CUM-$EVI_{(TSP)}$(log$CUM\text{-}EVI_{(TSP)}$), implying a percentage or relative change in crop yield with a given change in climatic, predictor, variables irrespective of a baseline yield level and accounting for skewed distribution in crop yields (Lobell and Burke 2010; Lobell et al. 2011a; Urban et al. 2012). This is a common approach in numerous statistical crop yield-climate models (Schlenker and Roberts 2009; Schlenker and Lobell 2010; Lobell and Burke 2010; Lobell et al. 2011a; Urban et al. 2012). The results from all regression

models were similar whether using logCUM-$EVI_{(TSP)}$ or CUM-$EVI_{(TSP)}$ without a log transformation, suggesting the climate-crop yield signal was robust to the transformation. Panel-datasets were created and regression models were fitted for varying SOS dates. This highlighted how SOS influenced crop exposure to extreme heat events and climatic variables and, accounts for the fact that varying day length over a season can influence crop development rates (Lobell et al. 2012). This is important as shifting sowing dates and cropping calendars are a potential adaptation to reduce exposure to extreme heat events (Teixeira et al. 2013). Regression models were fitted for rice crops SOS on day-of-year 153, 161, 169, 177 and, 185 and wheat crops SOS on 329, 337, 345, 353 and, 361. These dates cover the majority of SOS dates for both the rice and wheat crops across Punjab and Haryana.

Table 6-1 Description of climatic variables included in the crop yield-climate regression models.

Climatic Variable	Description
$EDD_{(T)}$	Extreme degree days during the TSP. Computed as the number of days during the TSP above a threshold temperature (*T*) per-pixel.
$T_{(TSP)}$ (minimum)	Average daily minimum temperature during the TSP, computed individually per-pixel using pixel specific heading date (peak-EVI) derived from EVI phenology profiles.
$T_{(TSP)}$ (maximum)	Average daily maximum temperature during the TSP computed individually per-pixel using pixel specific heading date (peak-EVI) derived from EVI phenology profiles.
T	Average growing season temperature, computed individually per-pixel using pixel specific SOS and EOS dates derived from EVI phenology profiles.
P	Total growing season precipitation, computed individually per-pixel using pixel specific SOS and EOS dates derived from EVI phenology profiles.
$P_{(TSP)}$	Total precipitation during the TSP, computed individually per-pixel using pixel specific heading date (peak-EVI) derived from EVI phenology profiles.

6.2.6 Extreme heat events during the TSP

Simple linear regression models with fixed-effects terms (equation 2) were fitted to explore whether the impact of temperature and extreme heat events during the TSP on crop yield could be detected using remote sensing data. logCUM-EVI$_{(TSP)}$ was regressed against average minimum, maximum and mean temperature and, extreme degree days (EDD) during the TSP. Average daily minimum and maximum temperature were computed separately as they have been shown to have differing impacts on crop yield (Peng et al. 2004; Welch et al. 2010).

$$logCUMEVI_{(TSP)it} = \beta x_{it} + c_i + \varepsilon_{it} \quad (2)$$

Where *i* refers to pixel *i* and *t* refers to time of observation *t*=2002….2007. x_{it} is the predictor temperature variable in pixel *i* at observation *t*, c_i is the fixed effects term for pixel *i* and ε_{it} is an error term. EDD was defined as:

$$EDD_{(T)} = \sum_{i-1}^{N} DD \qquad DD \begin{cases} 0 \ \ if \ t_i < T \\ 1 \ \ if \ t_i \geq T \end{cases} \quad (3)$$

Where *T* is the threshold temperature for which EDD is computed individually for each temperature from 32-42˚C at 1˚C increments, t_i is the maximum temperature on day *i* and *N* is the number of days in the TSP (*N*=30). Computing EDD above a threshold maximum temperature, increasing with 1˚C intervals enabled assessment of: i) whether declines in yield due to exceedance of critical temperatures during the TSP can be detected from remote sensing data and ii) if such critical temperatures exist in the reality of farmers' fields. Including a fixed-effects term accounts for time-invariant effects unique to each location (these effects are not specified but could include omitted variables such as soil condition and fertiliser application). The term enables

each pixel to have a unique constant for all observations from that pixel. On the basis of performing a Hausman test fixed-effects terms were preferred over random-effects term. This analysis was repeated with squared predictor terms to investigate possible non-linear relationships. Non-linear terms did not alter the signal of the regressions, and often yielded similar or reduced model fit (in terms of R^2) suggesting linear terms were adequate. The same sign in the relationship between climatic variable and crop yield was obtained when using random-effects terms indicating results were not artefacts of including fixed-effects terms.

6.2.7 Multivariate crop yield-climate models

Multivariate linear fixed-effects models were used to assess the impact of climatic variables on rice and wheat crop yield.

$$logCUMEVI_{(TSP)it} = \beta T_{it} + \beta T_{(TSP)it} + \beta P_{it} + \beta P_{(TSP)it} + c_i + \varepsilon_{it} \quad (4)$$

where T is average growing season temperature, $T_{(TSP)}$ is either average maximum or minimum temperature during the TSP, P is growing season total precipitation, $P_{(TSP)}$ is total precipitation during the TSP, c_i is a fixed-effects term for pixel i, ε_{it} is an error term, i refers to pixel location and t refers to the year of observation (t=2002, 2003…..2007). Including precipitation terms is important to capture moisture stress accentuated by extreme heat events, or the presence of moisture mitigating against heat impacts (via transpiration cooling) (Wassmann et al. 2009; Lobell et al. 2011a). Both the rice and wheat crops in Punjab and Haryana are heavily irrigated (DES 2011); the fixed-effects term accounting for time-invariant omitted factors per pixel will capture spatial variation in inputs and, thus, account for access to irrigation that may mitigate the magnitude of extreme heat event impacts. Average maximum and minimum temperature during the TSP were not included in the same model to avoid multicolinearity among predictor variables. For all SOS dates, for both crops, average maximum and minimum TSP temperature had the largest variance inflation factors (VIF) out of all predictor variables; for the wheat crop the VIF was always greater than 6 and in some cases exceeded 11, an indicator of high levels of multicolinearity. Again,

a Hausman test indicated using fixed-effects terms rather than random-effects terms in a multivariate model although including random-effects terms did not alter the sign from the regression model outputs. Squared predictor terms were tested to explore for non-linear relationships between climatic predictor variables and crop yield but these generally returned lower R^2 values indicating reduced model fit. Thus, simple linear terms with fixed-effects were deemed adequate.

6.3 Results

6.3.1 Crop area classifications and yield estimates

Utilising a per-year optimised value of *T kharif* rice crop extent was classified with R^2 values ranging from 0.96 to 0.99 between 2002-2003 and 2006-2007 when compared with district-wise land use statistics (http://lus.dacnet.nic.in/). R^2 values for the relationship between remote sensing derived wheat crop extent and district-wise land use statistics (http://lus.dacnet.nic.in/) ranged between 0.86 and 0.92 between 2002-2003 and 2006-2007.

CUM-$EVI_{(TSP)}$ was significantly (p<0.01) correlated with district wise *kharif* rice and *rabi* wheat yields between 2002-2003 and 2006-2007 (R^2=0.91 and 0.84 respectively) (Fig. 6-2; http://apy.dacnet.nic.in/). This suggests CUM-$EVI_{(TSP)}$ provided an accurate estimation of yield for both crops. Other methods of estimating crop yield were tested including cumulative sum of EVI values from maximum EVI to EOS and just maximum EVI values alone. The CUM-$EVI_{(TSP)}$ provided a more accurate measure of crop yield than cumulative sum of EVI values from maximum EVI to EOS and equivalent accuracy to maximum EVI. The cumulative sum of EVI values from maximum EVI to EOS still maintained a large correlation with district-wise crop yield, but the association was likely weakened due to incorporating EVI values corresponding to crop growth not associated with yield development (Rojas et al. 2011). CUM-$EVI_{(TSP)}$ was used as a proxy for of crop yield as it included more information than just maximum EVI (up to four EVI values rather than one) without any penalty in accuracy.

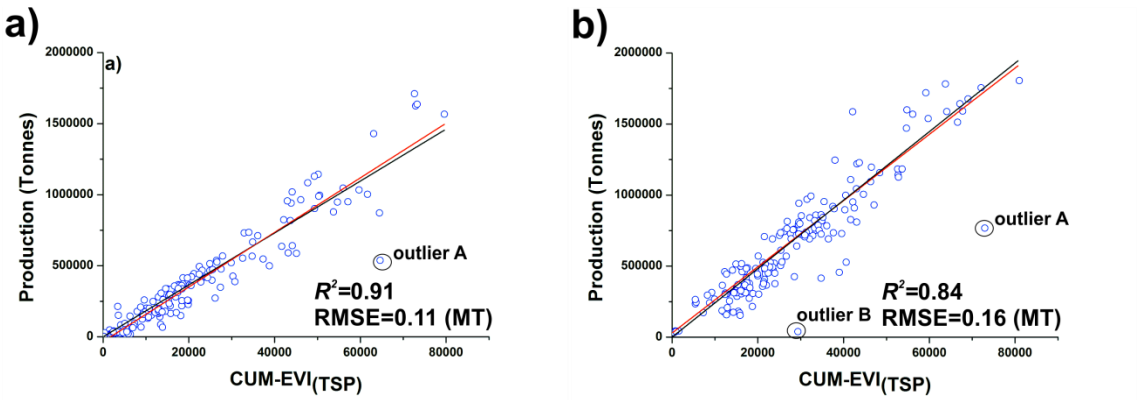

Figure 6-2 Relationship between remote sensing estimates of district-wise crop production (CUM-$EVI_{(TSP)}$) and district-wise crop production as reported by government agricultural statistics (http://apy.dacnet.nic.in/) for the 2002-2003 to the 2006-2007 growing seasons for a) the *kharif* rice crop and, b) the *rabi* wheat crop. The black line is the 1:1 regression line.(Outlier A corresponds to Amritsar district, in 2006-07 Amritsar district was split into a smaller district still named Amritsar and a new district named Tarn Taran. The estimates of crop production from the remote sensing data include the extent of 'old' district Amritsar due to the global administrative database layer not being updated whereas the crop production statistics from http://apy.dacnet.nic.in/ do not. This explains the over estimation of crop production from the remote sensing data. Outlier B likely reflects erroneous reporting in the Government of India's crop production statistics for the district of Bhiwani in 2005-06. Production of wheat in Bhiwani was 425000, 456000, 415000 and 527000 Tonnes in 2002-03, 2003-04, 2004-05 and 2006-07; Government statistics reporting an 39000 Tonnes for 2005-06 are therefore likely due to an error in reporting, especially as there was not an associated drop in area under wheat cropping (http://apy.dacnet.nic.in/)).

6.3.2 Wheat: temperature during the TSP and crop yield relationship

Average minimum and maximum TSP temperatures generally have a greater explanatory power compared to EDD above incrementing temperature thresholds or growing season average temperatures for the wheat crop (Figs. 6-3 and 6-4). Rate of change in average minimum and maximum TSP temperatures and average growing season temperatures have a greater, negative influence on wheat crop yield compared to EDD above incrementing temperature thresholds; however it should be noted that mean growing season temperatures explains a very small amount of variation in wheat crop yield (Figs. 6-3, 6-5 and 6-6). With a later SOS date average minimum TSP temperature has a greater fit (Fig. 6-3) and causes a greater rate of change wheat yield (Fig. 6-5) compared to average maximum TSP temperature. Generally, an increase in temperature threshold above which EDD is computed registers a greater negative influence on wheat crop yield (slope coefficient) (Fig. 6-6). However, a temperature threshold of 35°C had a noticeable larger R^2 compared to all other temperature thresholds (Fig. 6-4), there was also an increase in the size of the slope coefficient at

35°C compared to lower temperature thresholds (Fig. 6-6). The negative impact of temperature during the TSP, determined by both the value of the slope coefficient and the fit of the model, increased with later SOS dates (Figs. 6-3 - 6-6). The negative impact of exposure to heating events greater than 35°C during the TSP also increased with later SOS dates (Fig. 6-4 and 6.6).

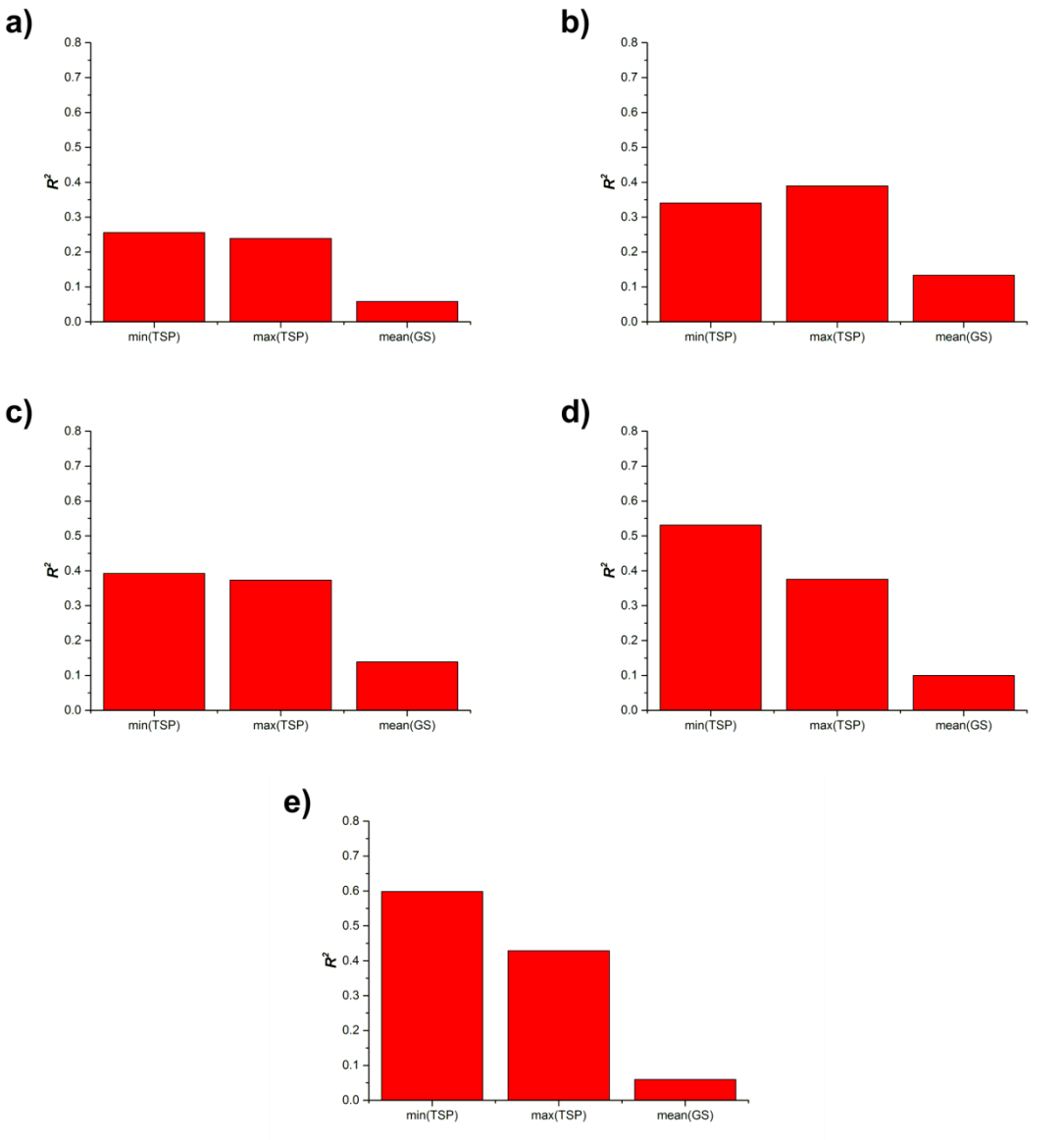

Figure 6-3 The R^2 values for average minimum and maximum TSP temperature and, average growing season temperature when regressed against wheat crop yield (logCUM-EVI$_{(TSP)}$) for SOS dates: a) 329, b) 337, c) 345, d) 353 and, e) 361. Only statistically significant (p<0.001) relationships are presented.

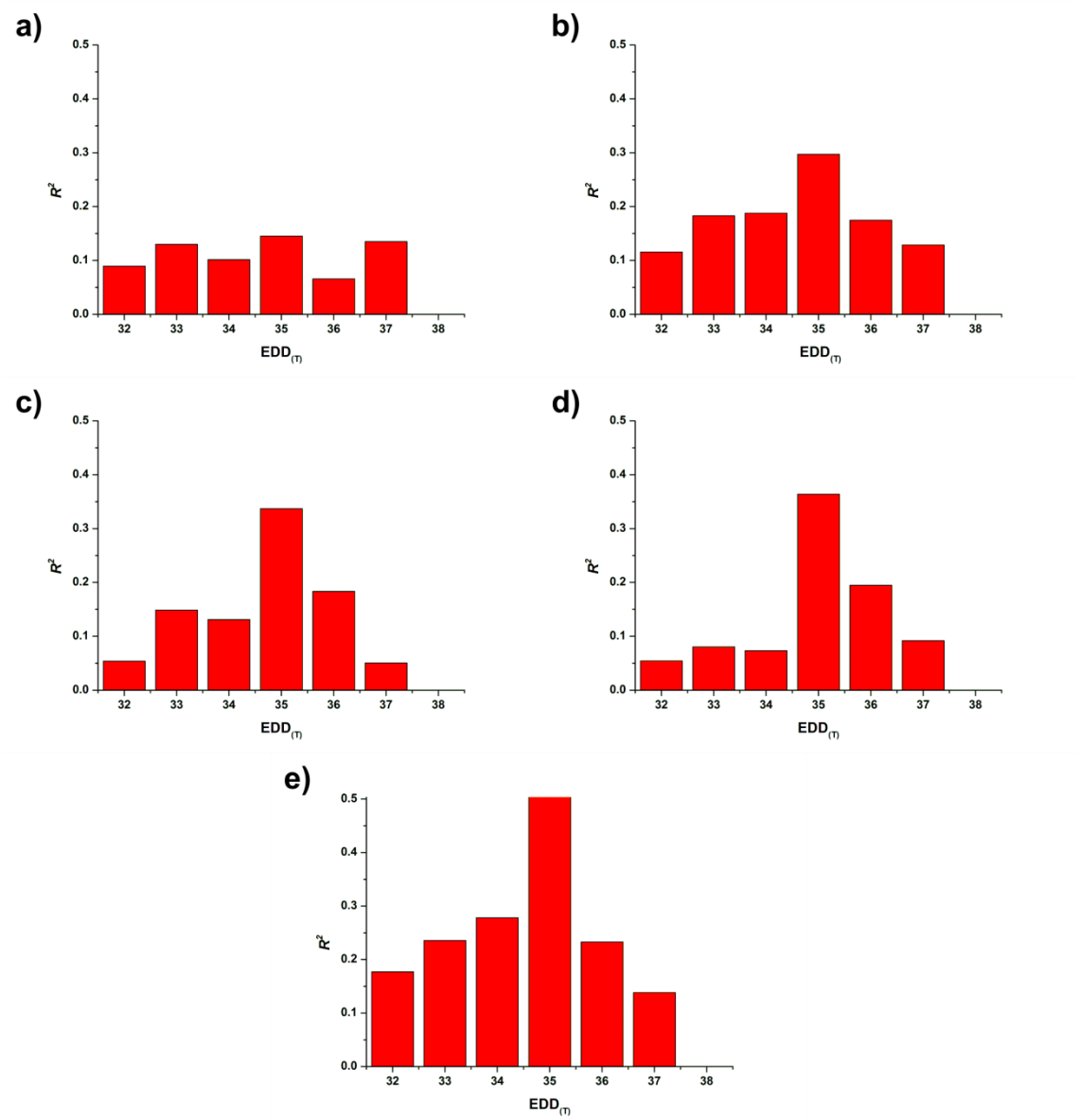

Figure 6-4 The R^2 values for EDD when regressed against wheat crop yield (logCUM-$EVI_{(TSP)}$) for SOS dates: a) 329, b) 337, c) 345, d) 353 and, e) 361. Only statistically significant ($p<0.001$) relationships are presented.

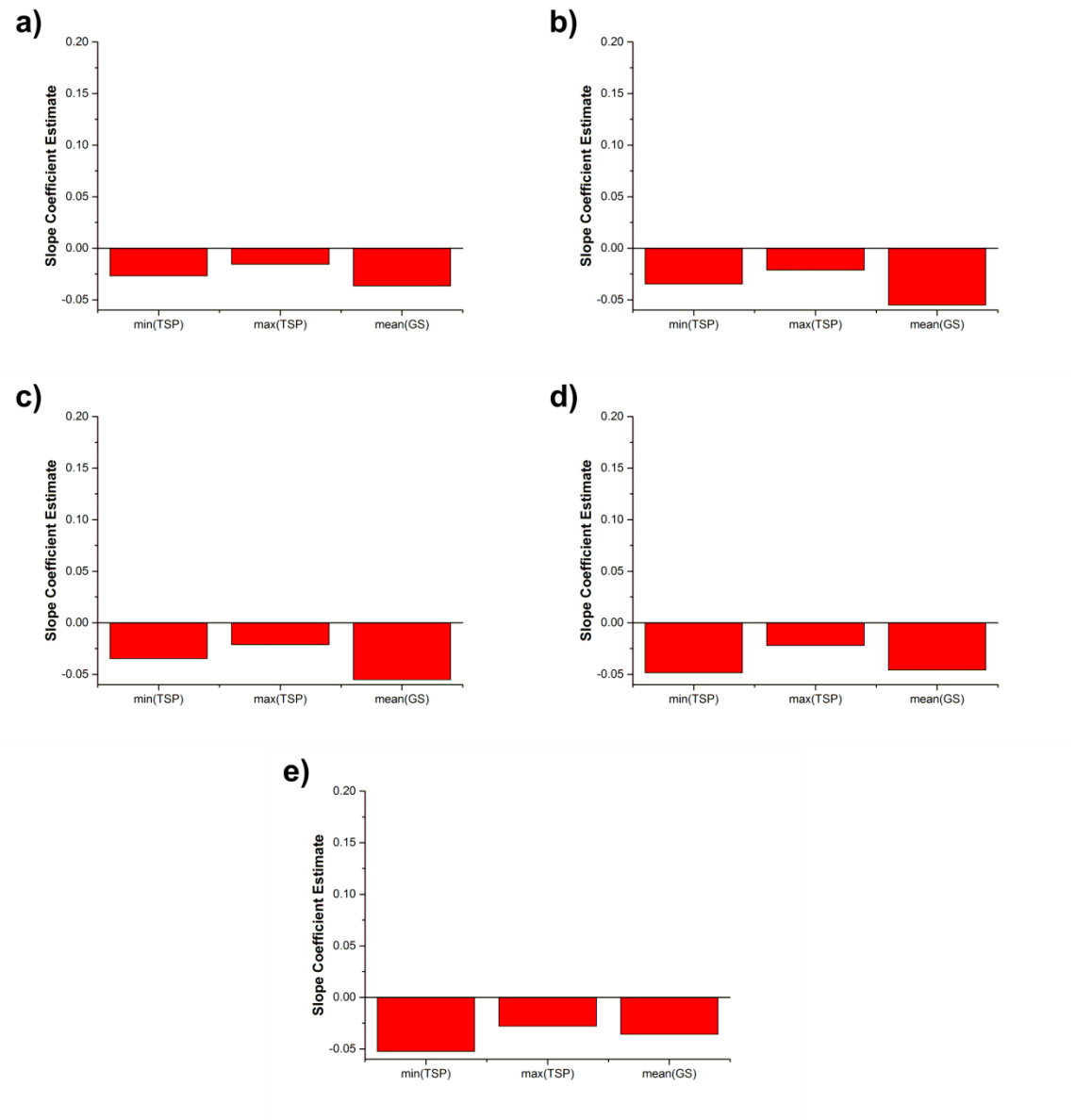

Figure 6-5 The slope coefficients for average minimum and maximum TSP temperature and, average growing season temperature determining rate of change in wheat crop yield (logCUM-EVI$_{(TSP)}$) for SOS dates: a) 329, b) 337, c) 345, d) 353 and, e) 361. Only statistically significant (p<0.001) slope coefficients are presented.

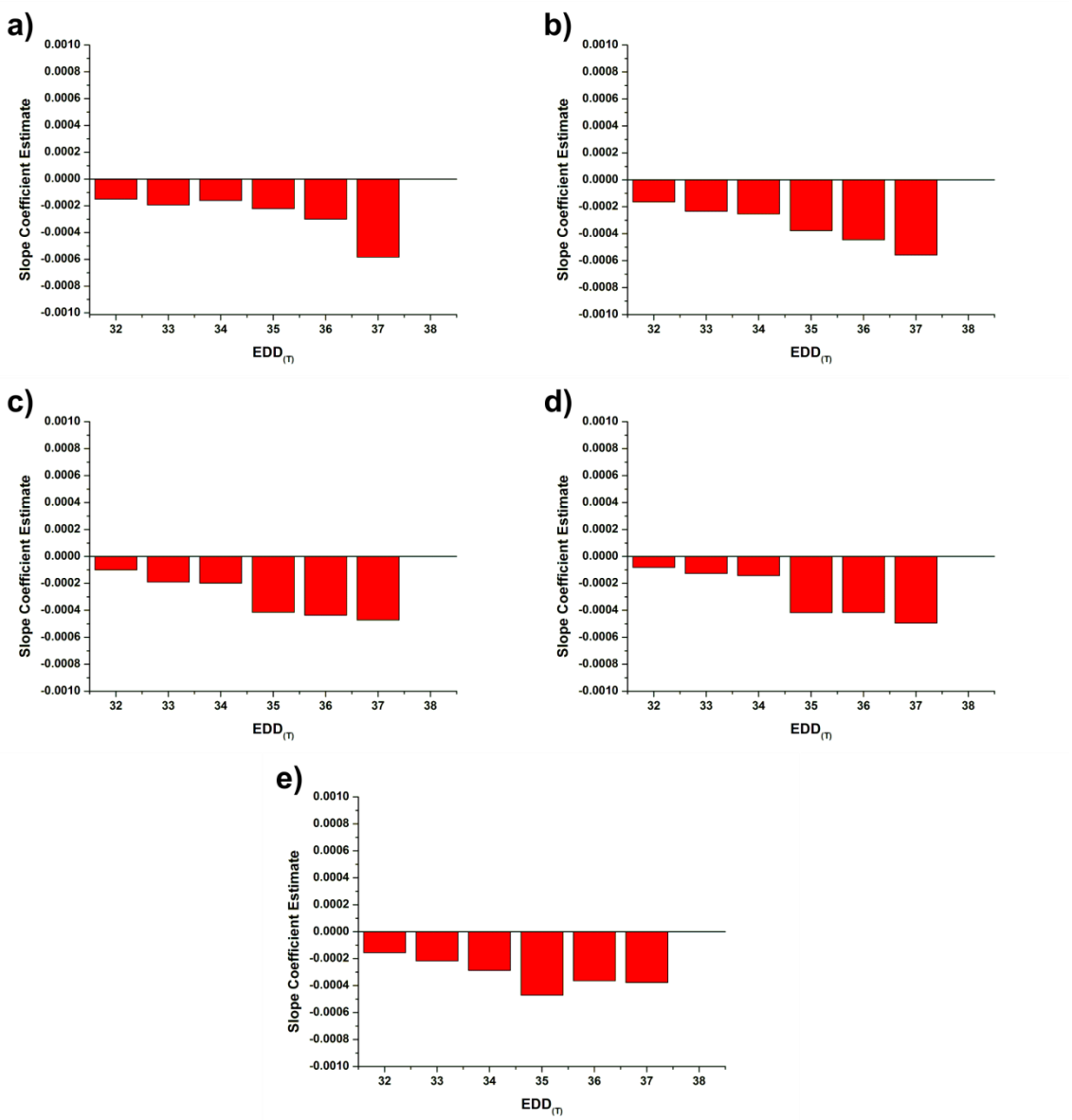

Figure 6-6 The slope coefficients for EDD determining rate of change in wheat crop yield (logCUM-EVI$_{(TSP)}$) for SOS dates: a) 329, b) 337, c) 345, d) 353 and, e) 361. Only statistically significant (p<0.001) slope coefficients are presented.

6.3.3 Rice: temperature during the TSP and crop yield relationship

Similar to the wheat crop, average minimum and maximum TSP temperatures explain a greater amount of variation in rice crop yield compared to EDD computed above incrementing temperature thresholds (Figs. 6-7 and 6-8). However, the sign of this relationship is positive rather than negative as in the wheat crop. Growing season average temperature was negatively correlated with rice crop yield (Figs. 6-7 and 6-9). EDD, regardless of the temperature threshold except for 38°C, showed a positive, but small, association with rice crop yield (Figs. 6-8 and 6-10).

Table 6-2 Slope coefficients and R2 values for multivariate fixed-effects crop yield (logCUM-EVI(TSP))-climate models for the wheat crop. All terms significant at (p<0.001) except * denoting significance at (p<0.01).

SOS date	T	$T_{(TSP)}$ (minimum)	P	$P_{(TSP)}$	R^2
329	-0.03617	-0.02287		-0.00223	0.40958
337	-0.04562	-0.02936	0.00044	-0.00248	0.46383
345	-0.05229	-0.03723	0.00080	-0.00234	0.49770
353	-0.03906	-0.04509	0.00051	-0.00146	0.55196
361	-0.02854	-0.04794	-0.00022	-0.00012*	0.55724
		$T_{(TSP)}$ (maximum)			
329	0.00207	-0.01710	-0.00039	-0.00198	0.42496
337	-0.00111	-0.02121	-0.00001	-0.00221	0.46005
345		-0.02420	0.00013	-0.00214	0.45283
353	0.01432	-0.02641	-0.00014	-0.00148	0.45974
361	0.02828	-0.02911	-0.00147	0.00059	0.47467

6.3.4 Multivariate crop yield-climate model

In the multivariate models average minimum and maximum TSP temperatures often had the greatest influence on crop yield, though the sign of this influence was negative for wheat and positive for rice (Table 6-2 and 6-3). The slope coefficient values for average minimum TSP temperature were greater than average maximum TSP temperature for the wheat crop and increased with later SOS, similar to when the variables were regressed as a sole climatic predictor (Table 6-2; Fig. 6-5). This suggests that this signal is robust and not a statistical artefact. Change in totals of growing season precipitation and TSP precipitation caused minimal changes in crop yield with small slope coefficient values (Table 6-2 and 6-3). The multivariate models for wheat, either with average minimum or maximum TSP temperature included as predictor terms had R^2 values between 0.41 and 0.58 indicating that climatic variables explain a large proportion of the variation in crop yield (Table 6-2). The multivariate models for rice also explain a large proportion of variation in crop yield (R^2: 0.27 – 0.54). The rice crop multivariate models with average minimum TSP temperatures have a greater

explanatory power than models including average maximum TSP temperature (Table 6-3).

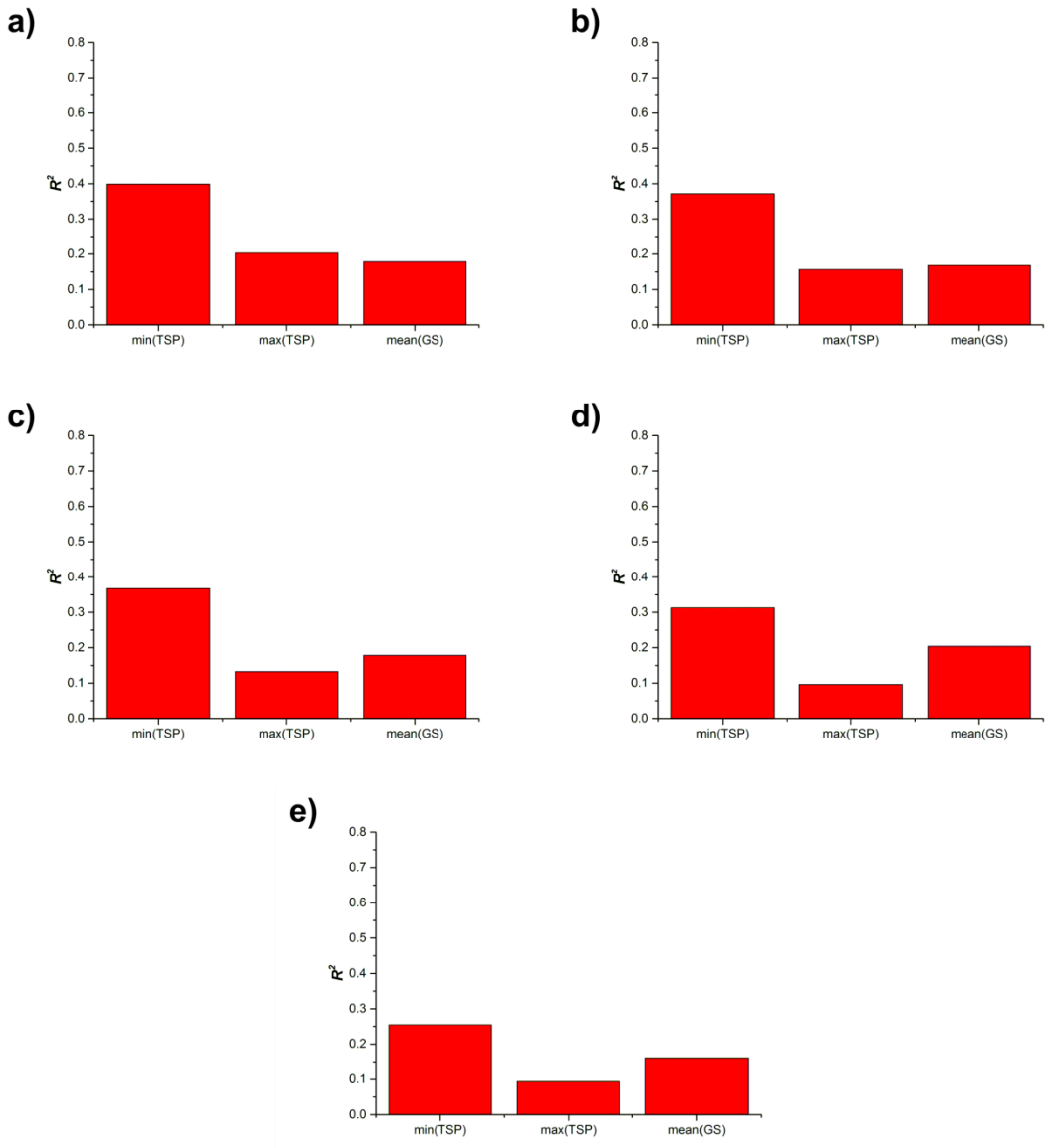

Figure 6-7 The R^2 values for average minimum and maximum TSP temperature and, average growing season temperature when regressed against rice crop yield (logCUM-EVI$_{(TSP)}$) for SOS dates: a) 153, b) 161, c) 169, d) 177 and, e) 185. Only statistically significant (p<0.001) relationships are presented.

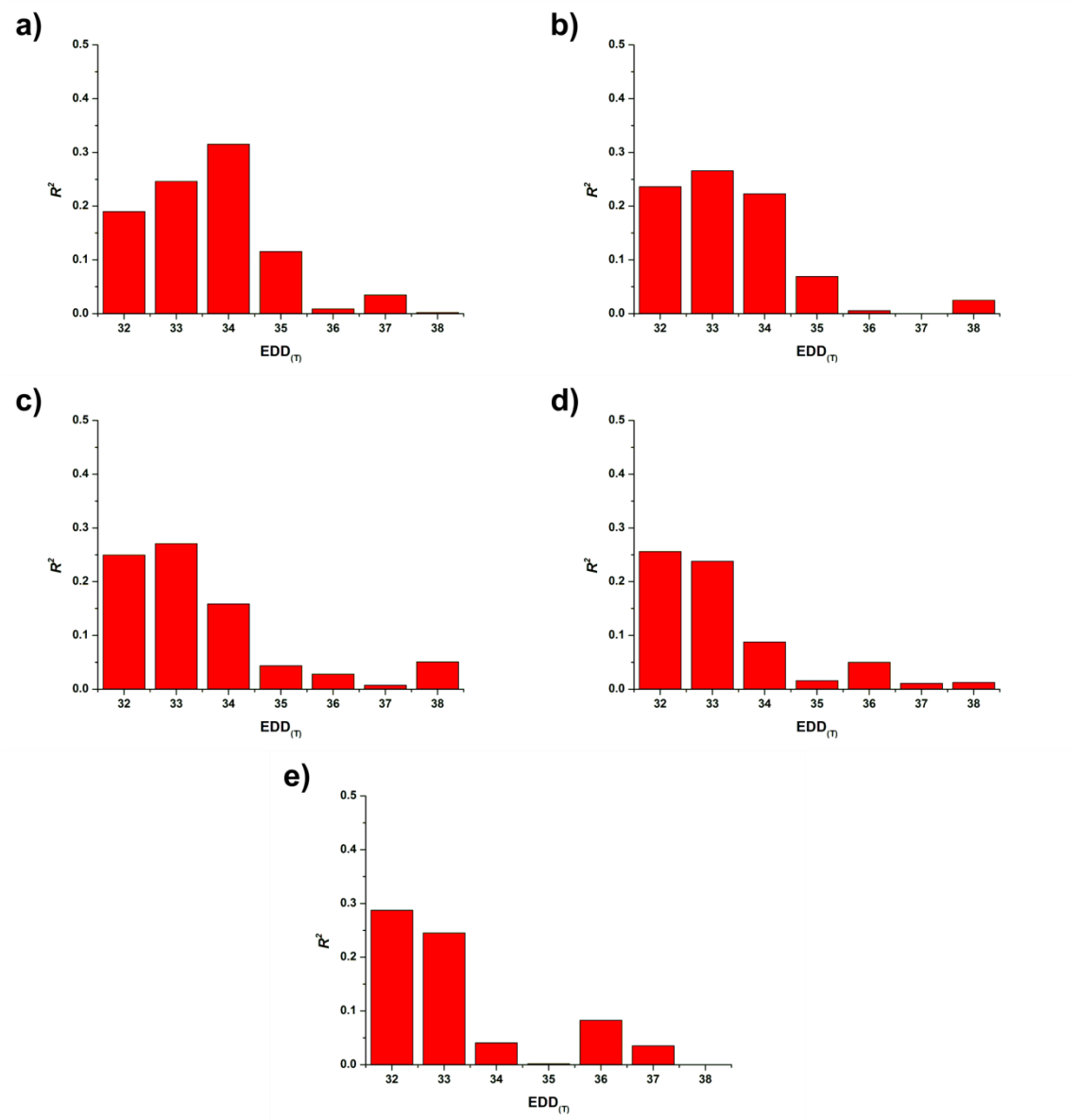

Figure 6-8 The R^2 values for EDD when regressed against rice crop yield (logCUM-$EVI_{(TSP)}$) for SOS dates: a) 153, b) 161, c) 169, d) 177 and, e) 185. Only statistically significant (p<0.001) relationships are presented.

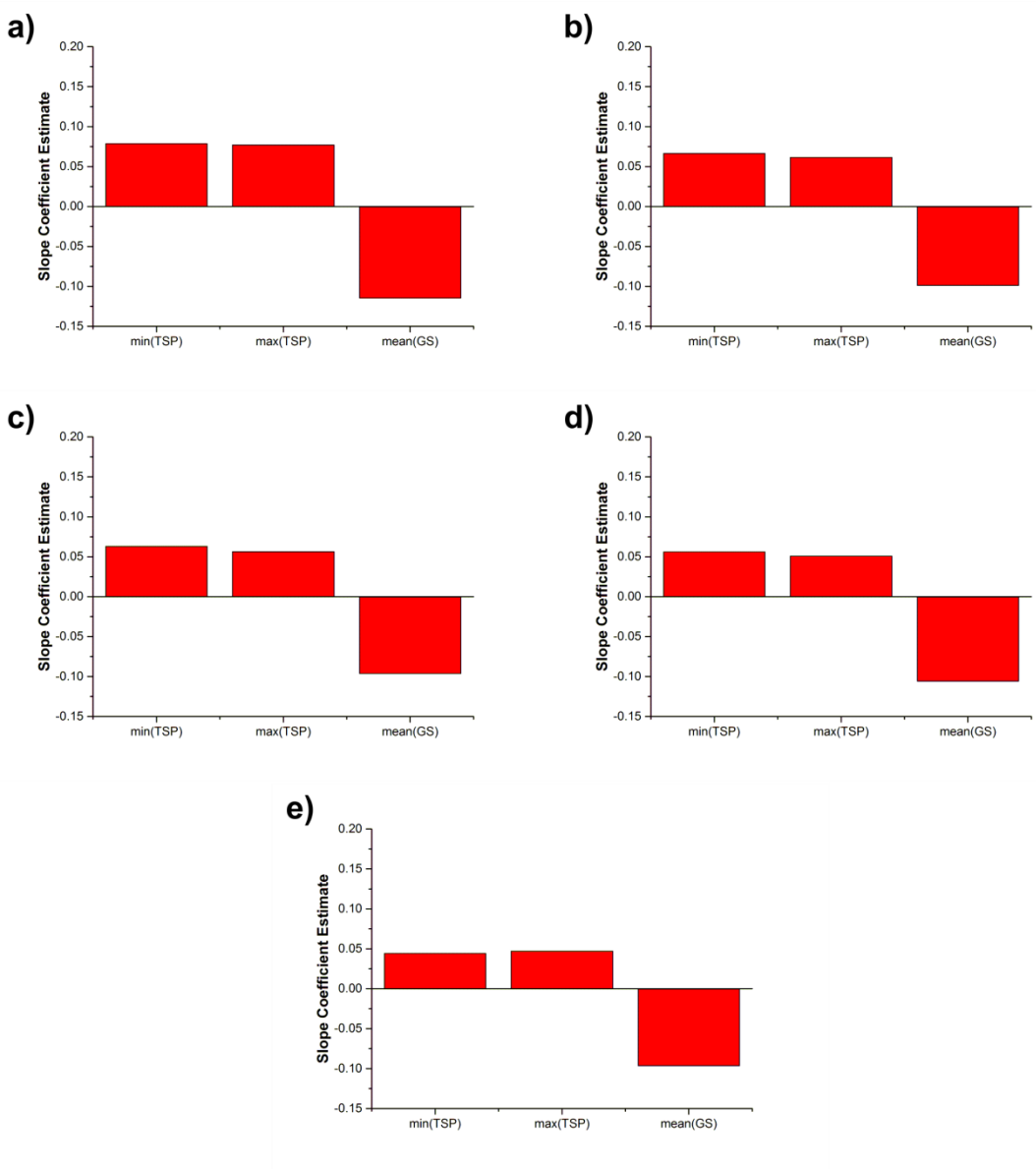

Figure 6-9 The slope coefficients for average minimum and maximum TSP temperature and, average growing season temperature determining rate of change in rice crop yield (logCUM-EVI$_{(TSP)}$) for SOS dates: a) 153, b) 161, c) 169, d) 177 and, e) 185. Only statistically significant (p<0.001) slope coefficients are presented.

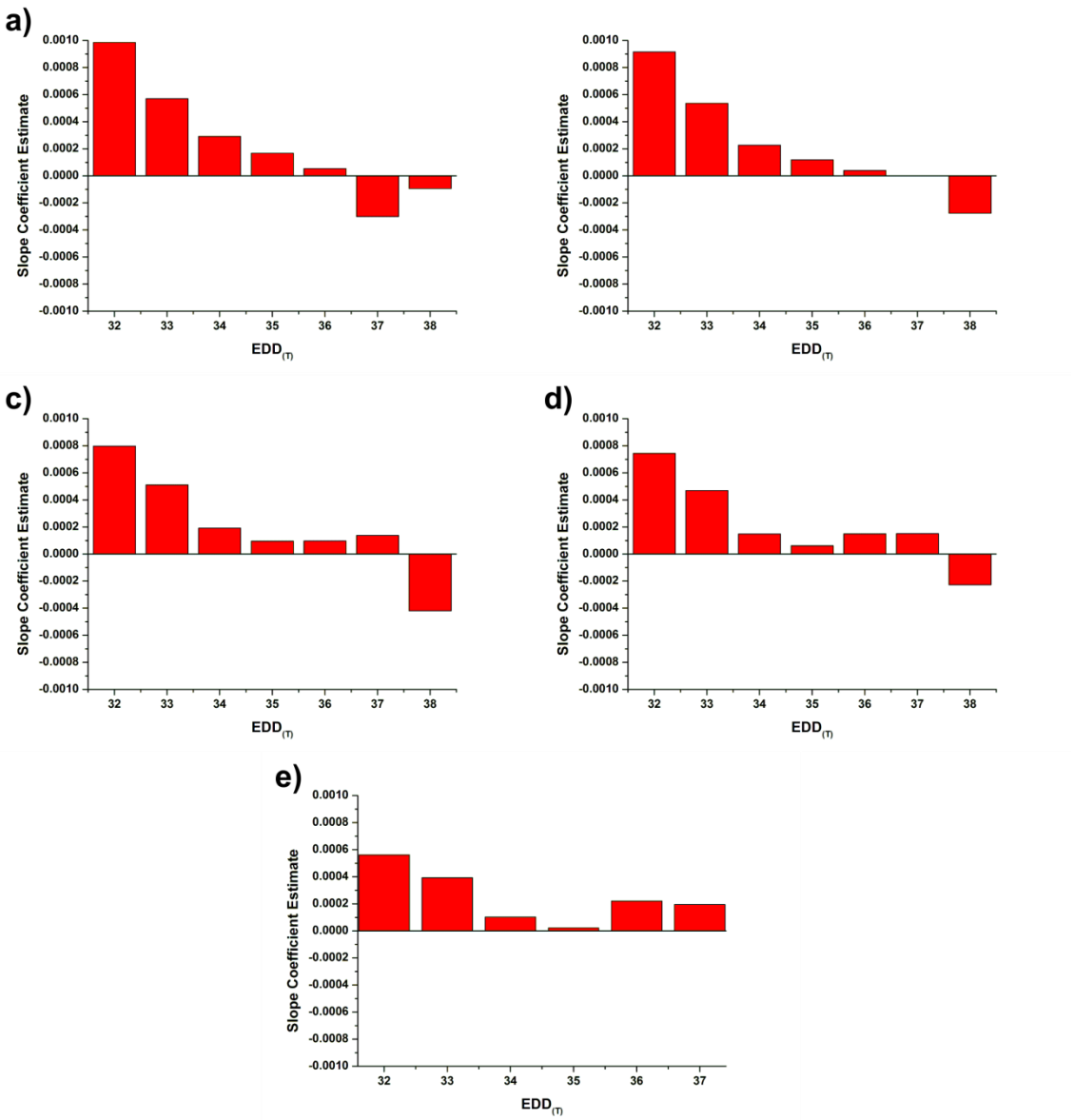

Figure 6-10 The slope coefficients for EDD determining rate of change in rice crop yield (logCUM-$EVI_{(TSP)}$) for SOS dates: a) 153, b) 161, c) 169, d) 177 and, e) 185. Only statistically significant (p<0.001) slope coefficients are presented.

Table 6-3 Slope coefficients and R2 values for multivariate fixed-effects crop yield (logCUM-EVI(TSP))-climate models for the rice crop.

SOS date	T	$T_{(TSP)}$ (minimum)	P	$P_{(TSP)}$	R^2
153	-0.0632	0.0794	0.0009	-0.0023	0.54
161	-0.0600	0.0708	0.0010	-0.0018	0.51
169	-0.0744	0.0632	0.0008	-0.0014	0.49
177	-0.0722	0.0549	0.0016	-0.0014	0.49
185	-0.0920	0.0453		-0.0005	0.43
		$T_{(TSP)}$ (maximum)			
153	-0.0704	0.0783	0.0014	-0.0009	0.38
161	-0.0651	0.0653	0.0013	-0.0004	0.32
169	-0.0804	0.0481	0.0008	-0.0001	0.27
177	-0.0767	0.0526	0.0018	-0.0009	0.31
185	-0.0968	0.0553	0.0005	-0.0006	0.29

6.4 Discussion

Average minimum and maximum TSP temperature have the greatest influence on wheat crop yield explaining a greater amount of yield variation compared to mean growing season temperature (Figs. 6-3; Table 6-2). The TSP approximates the reproductive and the beginning of the grain filling development stages; that warming during the TSP impacted wheat yield is consistent with analysis in Asseng et al. (2010) showing that heat events closer to maturity have less impact on final wheat yield. While several studies focus on the impacts of daily maximum temperature or daytime temperatures above a critical threshold (Asseng et al. 2010; Lobell et al. 2012; Teixeira et al. 2013; Gourdji et al. 2013b; Koehler et al. 2013), it is shown here that minimum temperature during the TSP has an equivalent if not greater negative impact on wheat

yields (Figs. 6-3 and 6-5; Table 6-2). It is important for further research to contribute to a better understanding of the differential impacts of daily minimum and maximum temperature, and associated physiological processes, given an observed (1970-2005) trend of increasing 'hot nights' in northwest India during the pre-monsoon season (Kothawale et al. 2010) and an observed (1970-2003) increasing trend in winter minimum temperatures (Kothawale and Rupa Kumar 2005). These results also suggest that the negative influence of average growing season temperature may be due to it capturing heating events during the TSP and, that adaptive efforts to increase wheat crop resilience to warming, should focus on the TSP.

Regressing EDD above incrementing temperature thresholds showed the expected negative impact of increasing temperature during the TSP on wheat crop yield (Figs. 6-4 and 6-6). These results suggest wheat yields in Punjab and Haryana are more sensitive to daily maximum temperatures greater than 35 ˚C than the crop-specific critical temperature, often reported as 34 ˚C for wheat (Hatfield et al. 2011; Lobell et al. 2012; Gourdji et al. 2013b). The impact of cumulative exceedance of 35 ˚C during the TSP on wheat yield also varied with SOS date (Figs. 6-4 and 6.6); this is consistent with a range of other observational and crop simulation studies which did not reveal a uniform yield response to heating events greater than 34 ˚C (Fig. 4b and Fig.8 in Asseng et al. (2010)). It is worth noting that average minimum and maximum TSP temperature cause a greater, negative, rate of change in wheat yields than exceedance of the 35 ˚C threshold. This indicates the presence of a critical temperature threshold is less pronounced in real world cereal cropping systems compared to more controlled, experimental environments or modelling frameworks where the critical temperature signal can be isolated (Jagadish et al. 2007; Asseng et al. 2010; Teixeira et al. 2013). There is likely spatial variation in genotype, irrigation and vapour pressure deficit during the TSP across Punjab and Haryana which will alter wheat crop response to extreme heat events masking a critical temperature threshold (Asseng et al. 2010; Gourdji et al. 2013a; Teixeira et al. 2013). It is worth noting that observations were taken over five years and there may be too few extreme heat events, coinciding with the TSP, in the distribution of daily maximum temperatures to detect a critical temperature accurately.

The negative influence of average TSP temperature on final wheat yield increased with later SOS dates. This trend is consistent with observations by Lobell et al. (2012) who observed declines in wheat growing season length associated with later SOS dates in North India; this was attributed to increased exposure to extreme heat days (>34 ˚C) later in the *rabi* growing season. These results (Figs. 6-3 – 6-6, Table 6-2) suggest that climatic events, namely warming during the TSP, are limiting potential wheat yields in Punjab and Haryana. For wheat crops with a later SOS earlier sowing may be an escape route reducing exposure to damaging heat events and, thus, closing existing yield gaps. Widespread adoption of zero-tillage represents a suitable adaptive, climate-resilient, management strategy with earlier SOS reducing TSP exposure to extreme heat events with subsequent environmental and socio-economic benefits and, no yield penalty (Erenstein and Laxmi 2008; Jat et al. 2009a). However, even wheat crops with a SOS of day-of-year 329, were still negatively impacted by warming during the TSP (Figs. 6-3 – 6-6). This indicates that alongside reducing later sown wheat crops exposure to higher temperatures (avoidance strategies) adaptations need to be explored which increase wheat crop tolerance to warming during the TSP to reduce temperature induced yield gaps (e.g. develop wheat varieties tolerant to extreme temperatures (Gourdji et al. 2013a)). Implementing such adaptations are important given i) current temperatures are limiting wheat yield and, ii) projected future trends of *rabi* growing season warming and increased frequency of extreme heat days which would further limit wheat yields (Mathison et al. 2013; Gourdji et al. 2013b). Such adaptations could have important, future, food security implications given coincidental pressures of increased demand for food being placed on these croplands due to population growth (Aggarwal et al. 2004), alongside unfavourable warming (Mathison et al. 2013; Gourdji et al. 2013b).

The negative influence of mean growing season temperature on crop yield was observed when regressed as a single predictor variable against crop yield for all SOS dates for both crops and, when included as a variable in multivariate models (except when including average maximum TSP temperature for the wheat crop as a predictor variable) (Table 6-2 and 6-3, Figs. 6-3, 6-5, 6-7 and, 6-9). This is an expected response consistent with observations from statistical models for a variety of cereal crops

(Schlenker and Lobell 2010; Lobell and Burke 2010; Lobell et al. 2011a; Rowhani et al. 2011; Lobell et al. 2012; Gourdji et al. 2013a).

For all SOS dates average growing season temperature has limited explanatory power (R^2) for wheat crop yield (e.g. R^2=0.13 for SOS on day-of-year 345 and R^2=0.06 for SOS on day-of-year 361) (Fig. 6-3). For later SOS dates (day-of-year 353 and 361) average minimum temperature during the TSP has a large slope coefficient value in both univariate and multivariate regression models (Fig. 6-5; Table 6-2). In the multivariate regression models average maximum temperature during the TSP has a larger slope coefficient value than average growing season temperature, and in the univariate regression models average maximum temperature during the TSP explains a much greater proportion of variation in wheat yield than average growing season temperature (Fig. 6-3). This may indicate that the lack of negative influence of average growing season temperature on wheat crop yield when average maximum TSP temperature was included as a predictor term is an artefact of the multivariate statistical model and the fact that average growing season temperature explains a very low proportion of the variation in wheat yield (Table 6-2). The precipitation terms have little influence on crop yield relative to the temperature terms for both crops (Table 6-2 and 6-3). This is probably due to the region being extensively irrigated allowing mitigation against shortfalls in precipitation (DES 2011; Teixeira et al. 2013).

Table 6-3 and Figs. 6-7, 6-8, 6-9 and 6-10 show that increased temperature, either average minimum or maximum temperature or EDD during the TSP, did not cause a decrease in rice crop yield. This contrasts with experimental field and laboratory studies which have shown that exposure to high temperatures negatively impacts physiological processes during the reproductive phase of rice crops (Jagadish et al. 2007; Rang et al. 2011b). However, an observational study of rice farms across Asia showed that changes in neither minimum nor maximum temperature during the reproductive phase of rice crop development impacted final yield (Welch et al. 2010). However, the same study showed that warming minimum temperatures during the vegetative and ripening development stages negatively impacted final yield (the opposite signal was observed for maximum temperatures) (Welch et al. 2010). The lack of negative signal from temperature impacts on rice yield during the TSP observed

from remote sensing monitoring can be explained by several factors. The critical temperature negatively affecting the rice reproductive phase varies in the literature, and with genotype; it is often reported as an air temperature of 35˚C (Jagadish et al. 2007; Hatfield et al. 2011; Teixeira et al. 2013). Rice crops are sensitive to exposure to extreme heat events (>33.7 ˚C canopy temperature, ~35˚C air temperature) for less than an hour during anthesis (Jagadish et al. 2007). Therefore, using an approximation of the TSP from MODIS data with a coarser temporal resolution (8 days) may not be sufficient to capture heat impacts on the reproductive phase.

Rice crops in hot, dry environments with sufficient moisture, lower relative humidity and, higher vapour pressure deficit can take advantage of transpiration cooling, lowering canopy temperature, as an escape from extreme heat events (Wassmann et al. 2009). Semi-dwarf HYV of the rice crop enhance transpiration cooling mechanisms through improved canopy architecture with panicles surrounded by leaves (Wassmann et al. 2009). Relative to other rice growing regions across South and South-East Asia, Punjab and Haryana have a hot, drier climate (Rupa Kumar et al. 2006; Duncan et al. 2013), with widespread irrigation (DES 2011) and access to HYVs (Aggarwal et al. 2004; Rang et al. 2011a) suggesting that transpiration cooling may mitigate the negative heat impacts on the reproductive phase of the rice crop. Transpiration cooling can result in canopy temperatures several degrees lower than air temperature (measured in this study) thus, reducing the impact of harmful warming events (Asseng et al. 2010). It is shown here that exposure to temperature greater than 38 ˚C had a negative impact on rice yield (Fig. 6-10). This suggests that it takes warming of this magnitude, which has a low frequency of occurrence, to overcome the benefits of transpiration cooling in well irrigated rice croplands. If irrigation, enabling transpiration cooling, is the mechanism protecting rice crops from heating during the TSP then the climate resilience of rice yields in Punjab and Haryana must be questioned given concerns regarding the sustainability of current irrigation water management practices (Ambast et al. 2006; Perveen et al. 2012).

Remote sensing observations (Lobell et al. 2012) and (Figs. 6-3-6-10) and field experiments (Jagadish et al. 2007) both reveal intra-growing season variability in crop sensitivity to climatic conditions. Increased temporal resolution in remote sensing data

facilitates enhanced detail in detecting occurrence of phenological development stages providing increased observations during such stages and, thus, capturing intra-growing season variability in sensitivity to climate. This is in direct contrast to crop yield-climate models trained with yield data aggregated to administrative boundary units which masks all phenological detail and preclude detailed assessment of intra-growing season variation in sensitivity to climatic drivers. However, it is important that the spatial resolution of remote sensing data is data is of sufficient spatial resolution to prevent informational gains from an increased temporal resolution being lost through aggregation into larger spatial units. For example, a single $8km^2$ GIMMS pixel would provide a single date of heading (peak VI; beginning of TSP) masking significant sub-pixel variation in crop phenology; this is illustrated in the inset in Fig. 6-11. As exemplified over the district of Bathinda, Punjab, aggregation, of spectral detail within coarse spatial resolution pixels or political boundaries, can lead to masking both phenological and spatial detail and is therefore not suitable to approximate the timing of climate sensitive crop development stages (Fig. 6-11). Remote sensing data with sufficient spatio-temporal resolution can capture intra-growing season response to climate drivers and, thus, be used to monitor the response of real cropping systems to climatic events.

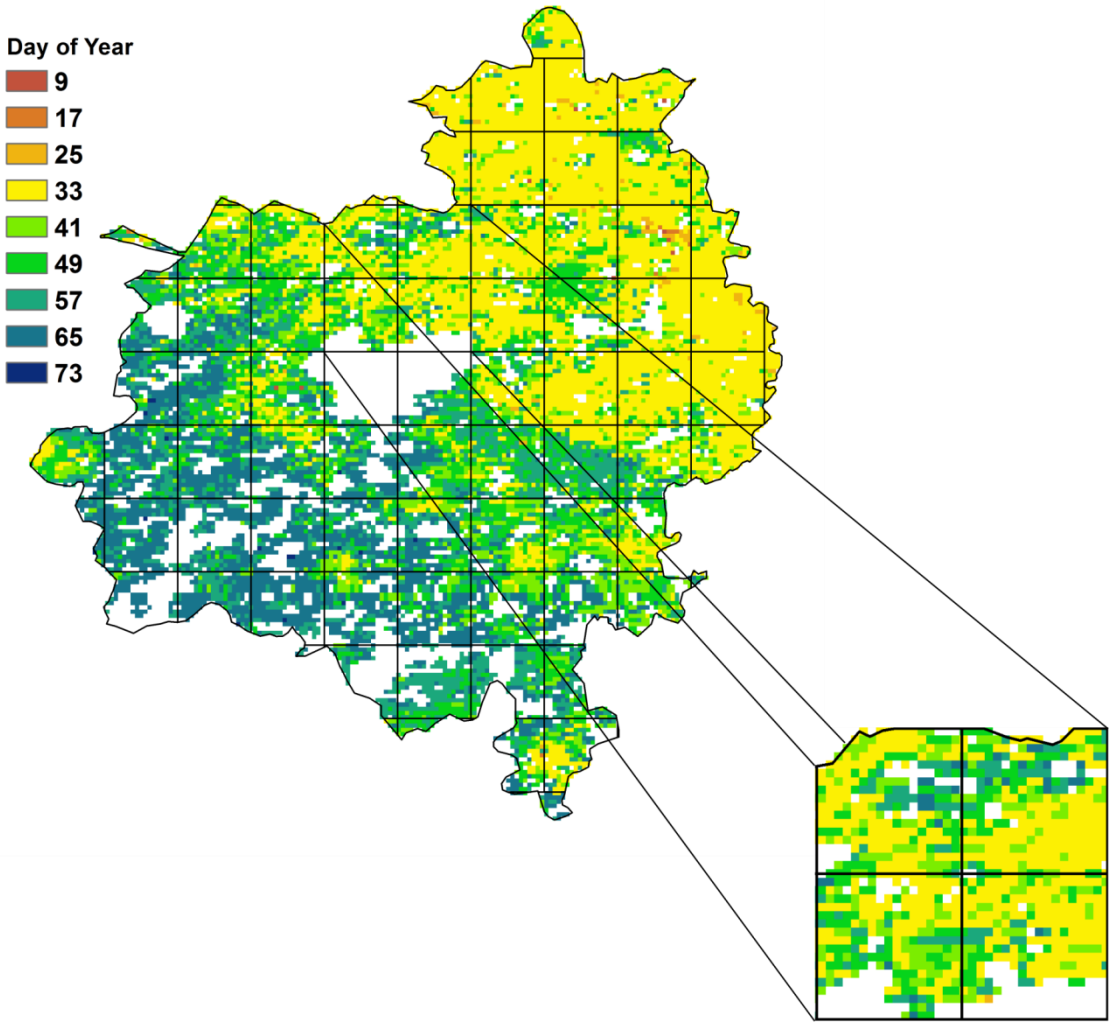

Figure 6-11Heading date across Bahtinda district, Punjab, for the *rabi* wheat crop as detected from MODIS MOD09A1 products, the black gridlines correspond to the pixel footprint of the 8km GIMMS NDVI product. The inset exemplifies the pattern displayed across the image where local spatial variation in the timing of key phenological events mean it is inappropriate to aggregate such measures up to coarse spatial units.

6.5 Conclusion

Multivariate fixed-effects models trained using panel-data derived from remote sensing observations and gridded climate datasets capture a large proportion of variation in rice and wheat crop yields. The panel-datasets used here capture the impacts of climate variables on crop yields as they occur in real world cropping systems, accounting for spatial variation in system specific factors (e.g. access to irrigation, farmer decisions) and can also account for intra-growing season variation in the impacts of climate on crop yields. It is important to note that no loss of explanatory power was observed using panel-datasets of remote sensing data to train crop yield-

climate models compared to models in the literature which used district-wise yield statistics. The key findings are highlighted below:

- Previous studies have used remote sensing data to demonstrate the impact of increased warm days above 34 ˚C during the entire growing season on shortening growing season lengths for wheat crops in north-west India (Lobell et al. 2012). Here, we have utilised the phenological detail in remote sensing data to isolate the impact of temperature during the TSP (the reproductive and grain-filling stages when final yield is set) on final crop yields for both rice and wheat crops in north-west India.
- Warming average minimum temperatures during the TSP have a greater negative impact on wheat crop yield than warming maximum temperatures during the TSP (e.g. R^2=0.53($Min_{(TSP)}$) and 0.38($Max_{(TSP)}$) and slope coefficient values in units of logCUM-$EVI_{(TSP)}$ of -0.049($Min_{(TSP)}$) and -0.022($Max_{(TSP)}$) for wheat crops sown on day-of-year 353). This suggests that studies which focus on the negative warming impacts of extreme heat events and maximum temperatures on anthesis, crop reproductive process and grain-filling should not neglect the impact of warming minimum temperatures during the TSP. This is pertinent given observed trends of warming night-time and minimum temperatures in northern India.
- Warming temperatures during the TSP are currently limiting wheat crop production in Punjab and Haryana. The negative impact of warming temperature during the TSP increases with later SOS dates. This suggests that earlier sowing for late sown wheat may mitigate some temperature induced shortfalls in production. However, given that earlier sown wheat is still negatively impacted by warming during the TSP (slope coefficient values in units of logCUM-$EVI_{(TSP)}$ of -0.027($Min_{(TSP)}$)) it suggests there is a need for heat tolerant varieties to prevent temperature induced yield gaps.
- For both rice and wheat crops average growing season temperature had a negative impact on crop production. This suggests that crop production in the region is vulnerable to observed and projected warming trends.

- Warming during the TSP did not have a negative impact on rice crop yield, this could be explained by an extensive irrigation infrastructure enabling transpiration cooling mechanisms to mitigate heat stress at key phenological stages. However, given projected warming trends which will increase evaporative demand coinciding with increasing pressure to use water resources more sustainably there may be a future reduction in transpiration cooling capacity. This would have a negative temperature impact on rice crop yields or reduce levels of water productivity to maintain current levels of production.
- Experimental and simulation studies often report 34˚C as a critical temperature threshold for wheat crop growth. However, remote sensing observations accounting for the complexity of a real world cereal cropping landscape do not show a uniform yield response after threshold exceedance but do reveal a more pronounced negative impact on wheat yield with increased warming events above 35˚C.
- Temperature only had a negative impact on rice yield after crops were exposed to temperatures greater than 38 ˚C during the TSP; given the irrigation capacity in Punjab and Haryana transpiration cooling may be mitigating the negative yield impacts of warming events on rice crops.
- Growing season precipitation, and precipitation during the TSP had little impact on either rice or wheat crop yield.

Chapter 7: Discussion: The vulnerability of the rice-wheat production system to climatic drivers.

This discussion will synthesise the conclusions from the separate research papers (Chapters 3 – 6) around the central theme of the thesis: an assessment of the vulnerability of the rice-wheat production systems in the north-west IGP to climatic drivers. It does so by addressing the three research questions posed at the end of Chapter 2.

7.1 What is the exposure the of rice-wheat crop production system to harmful climate drivers?

Abundance of water resources is considered a limiting factor for crop yield (van Ittersum et al. 2013), in India the main climate driven water resource for agriculture is the ISM (Krishna Kumar et al. 2004; Mall et al. 2006). Levels of ISM precipitation exert a statistically significant level of control on rice and wheat yields in India, and are correlated with foodgrain yields in Punjab and Haryana (Krishna Kumar et al. 2004). Exposure to lower relative normal levels of ISM precipitation, higher relative levels of variability in ISM precipitation, and increasing trends in, or frequency of recurrence in unfavourable facets of ISM precipitation will have a negative impact on agricultural production systems either limiting yield or increasing pressure on the system to buffer against precipitation shortfalls (e.g. increase groundwater irrigation). Analysis in Chapters 3 and 5 reveal the extent of exposure of rice-wheat croplands in Punjab and Haryana to unfavourable and harmful ISM conditions.

It was shown in Chapter 3 that normal levels of ISM precipitation over the period from 1951 to 2007 were lower relative to the rest of India, and also to the water requirements of a rice-wheat cropping system placing pressure and reliance upon groundwater irrigation (Ambast et al. 2006). Fig. 3-1a shows the spatial patterns of normal ISM precipitation totals across all of India and Fig. 1-6a presents a zoomed-in version of this for Punjab and Haryana. Fig. 3-3a shows that parts of Punjab and Haryana have a higher frequency of occurrence of drought years relative to large

portions of India, and also a later onset date of ISM placing pressure on the length of growing season supported by a renewable water resource (Fig. 3-5a).

The above mentioned precipitation datasets were integrated with maps of rice and wheat crop extent, generated at a 500 m spatial resolution using remote sensing data, in Chapter 5 to reveal that 2.52 million ha of rice or wheat croplands in Punjab and Haryana were exposed to unfavourable trends in at least one facet of ISM precipitation, a further 2.53 million ha experienced unfavourable trends in two facets of ISM precipitation and, 0.24 million ha experienced unfavourable trends in three facets of ISM precipitation (Fig. 5-3a). Trends of increasing recurrence of drought years and increasing variability in ISM precipitation intersecting in space with rice-wheat croplands had the largest spatial coverage in Punjab and Haryana (Fig. 5-3b and c). The spatial coverage of increasing trends in recurrence of drought years intersecting with rice-wheat croplands was focussed across southern and central Punjab and Haryana (Fig. 5-3b); the corresponding spatial coverage of increasing trends in variation in ISM precipitation over rice-wheat croplands occurred in south-west Punjab, southern and central Haryana and patches of northern Haryana (Fig. 5-3c).

In Chapter 6 it was shown that exposure to increased temperatures during the TSP of crop development had a negative impact on wheat yields. The TSP of crop development corresponds to the reproductive and grain filling phenological stages. Exposure to increasing daily minimum (night time) temperatures had a greater negative impact on wheat yields than exposure to increasing daily maximum (day time) temperatures. Exposure to daily maximum temperatures greater than 35˚C for wheat and 38˚C for rice during the TSP registered a marked decrease in crop yield. GCM and RCMs predict an increase in warming over Punjab and Haryana with an increase in extreme heat days (Rupa Kumar et al. 2006; Moors et al. 2011; Mathison et al. 2013) suggesting future increases in exposure to harmful warming. Exposure to warming growing season temperatures has a negative impact on both rice and wheat crops.

Exposure can be considered as a function of external processes to the system (e.g. climatic processes) and also the relationship and feedbacks between internal system factors and the external processes controlling the perturbation or stress (Gallopín

2006). This is of relevance to the agricultural production systems of Punjab and Haryana, where crop residue burning has a direct influence on climate processes with short-term impacts on agriculture (e.g. monsoon circulation interrupted by atmospheric particulates and brown clouds (Zickfeld et al. 2005; Auffhammer et al. 2006; Knopf et al. 2008; Ramanathan and Carmichael 2008)), but also increasing GHG concentrations influencing the slower process of atmospheric warming. Thus, when viewed through a systems perspective crop residue burning is a positive feedback increasing the exposure of the agricultural production system to harmful climate changes which if sensitivity and adaptive capacity are kept constant would increase vulnerability. The extent of crop residue burning for the rice and wheat crops were estimated using remote sensing data in Chapter 5 (Fig. 5-5d) and the associated GHG emissions were computed (Table 5-5).

7.2 What is the sensitivity of rice-wheat crop production to variations in climate drivers?

Viewing the outputs of Chapters 5 and 6 in conjunction highlights the importance of not assessing the exposure and sensitivity of a system in isolation. Chapter 5 highlighted that large portions of the rice-wheat production landscape were exposed to unfavourable trends in ISM precipitation (e.g. increasing recurrence of drought years, increasing variation in ISM precipitation; Fig. 5-3). However, fixed-effects multivariate crop yield-climate models in Chapter 6 showed that neither rice nor wheat crop yields were sensitive to reduced ISM precipitation. This indicates that other factors within the system are reducing crop production sensitivity to variation in precipitation; this is likely a factor of the widespread irrigation (both groundwater and surface canal) subsidised by the state government (Murgai et al. 2001; Aggarwal et al. 2004; Tyagi et al. 2005; Ambast et al. 2006; DES 2011; Perveen et al. 2012).

Internal system factors can create space-time differences in the sensitivity of the system or variable to similar climatic stresses or perturbations (Luers 2005). In Chapter 6 it was demonstrated that the sensitivity of wheat crop yields to warming (both minimum and maximum temperatures) during the TSP was not uniform for SOS dates, but increased with later SOS dates (Fig. 6-3, 6-4, 6-5 and 6.6; Table 6-2). The modelling

framework employed in Chapter 6 accounted for endogenous system processes (e.g. farmer decisions, access to irrigation, soil type) and other omitted variables using fixed-effects terms to isolate the crop yield-climate signal. This approach recognised that remote sensing observations are not only a direct measure of crop response to climate drivers but of all other system processes influencing crop growth and yield. The difference in SOS dates for the wheat crop could be explained by numerous factors exogenous to the system; for example, the temperature distribution of the preceding *kharif* rice growing season which determines time till crop maturity and the temporal distribution of extreme heat events during the *rabi* wheat growing season (Lobell et al. 2012).

However a range of endogenous factors to the system determine the SOS date for the wheat crop and, thus, cause differential sensitivity and vulnerability of wheat crop yield to temperature such as: the rice variety grown during preceding *kharif* season (some varieties are shorter duration where as others such as basmati are longer duration (Rang et al. 2011a)), the crop type grown during the preceding *kharif* season (*kharif* cotton is longer duration than rice (Lobell et al. 2013)), the perception of farmers of the need for conventional tillage practices with repeated ploughing of fields after harvest of the rice crop, awareness of conservation tillage practices and access to, and ability to use and procure, zero-tillage drills (Erenstein and Laxmi 2008; Erenstein 2009a; Ojha et al. 2013). This illustrates the importance retaining an awareness of the underlying system when assessing the vulnerability of crop yields to climate drivers. It is likely other endogenous system factors will cause differential vulnerability in crop yields such as management practices or soil type (Luers 2005).

Contrary to expected theory, and laboratory and controlled field experiments, there was no decrease in rice yield associated with increased warming during the TSP (Jagadish et al. 2007; Wassmann et al. 2009). It was only when temperatures exceeded 38˚C during the TSP that there was a negative influence on rice yield. This is likely a system specific (lack of) sensitivity to warming during the TSP associated with the extensive irrigation infrastructure enabling transpiration cooling to lower canopy temperatures when exposed to increasing air temperatures (Wassmann et al. 2009; DES 2011; Teixeira et al. 2013). Currently rice crop yields do not appear to be sensitive

to exposure to warming temperatures during the TSP. However, much of the rice croplands are reliant upon groundwater irrigation (Ambast et al. 2006), associated with rapidly declining groundwater levels (Ambast et al. 2006; Rodell et al. 2009; Tiwari et al. 2009), with extraction levels far exceeding renewable limits (Central Ground Water Board 2012; Gleeson et al. 2012) and, with large areas exposed to unfavourable trends in ISM precipitation and a high frequency of drought years (Fig. 5-4; Pai et al. 2011; Duncan et al. 2013). This is coupled with a growing awareness of a need to use irrigation water resources more sustainably and concerns that water resources cannot indefinitely meet the demands of the rice cropping system (Perveen et al. 2012; Ojha et al. 2013), that normal levels of precipitation are well below water requirements for rice cropping (Fig. 2-2) and, uncertainty in projections of future levels of ISM precipitation due to long term climate changes (Annamalai et al. 2007; Moors et al. 2011; Turner and Annamalai 2012; Mathison et al. 2013) and atmospheric particulates and brown clouds with a shorter residency time in the atmosphere (Ramanathan and Carmichael 2008). Decreasing soil quality and increasing soil salinity require excess irrigation water to return the soil to a quality acceptable for crop growth (Tyagi et al. 2005).

This is illustrative of the need to understand system processes for a comprehensive assessment of the vulnerability of crop yields to climate change. Whilst rice crop yields are not currently displaying outcomes of vulnerability to warming temperatures during the TSP the trajectories in underlying system processes and ecosystem services indicate the system may not be able to continue mitigating against warming events in the TSP. This is pertinent as it highlights that the rice cropping system is vulnerable to climate even if it does not appear to be so, and the likelihood of outcomes of vulnerability (a decrease in yield) being realised will increase due to the confluence of warming trends (Kothawale and Rupa Kumar 2005; Rupa Kumar et al. 2006; Moors et al. 2011; Mathison et al. 2013) and indicators that the system will not be able to continue supplying such high levels of irrigation water.

As mentioned, Luers (2005) measured the vulnerability of agricultural production by its location in vector space defined by variables on the *x* axis (sensitivity and exposure: coefficient of variation in crop yield) and the *y* axis (the state of the system: crop yield,

normalised by a threshold of well-being). This is similar to the bivariate maps produced in chapter 4 where the value assigned to each location is a function of coefficient of variation and normal (mean) conditions for the variable of interest. The variables assessed in this manner in chapter 4 were *kharif* and *rabi* LGS and *kharif* and *rabi* productivity (Figs. 4-4, 4-5, 4-7 and 4-9). These bivariate maps can be used to assess the relative risk of cropping in a location, normal conditions (either average LGS or productivity) inform on the suitability of a location for a given cropping practice whereas the coefficient of variation is an indicator of the risk of implementing such a cropping practice (Vrieling et al. 2013). Applying the framework of Luers (2005) to the bivariate maps, low normal conditions and a high coefficient of variation would imply high vulnerability. In Chapter 4 GIMMS NDVI data were used to assess long-term (1982-2006) normal, coefficient of variation and trends in *kharif* and *rabi* productivity and produce bivariate plots. Taking vulnerability as defined by Luers (2005) the most vulnerable regions in Punjab and Haryana were the southern and south-central portions (Fig. 4-7 and Fig. 4-9). There is a clear spatial overlap between these regions of high vulnerability and low normal ISM precipitation (Fig. 2-2), high frequency of drought years (Fig. 3-3a), increasing recurrence of drought years (Fig. 3-3b and Fig. 5-3b), increasing variation in ISM precipitation (Fig. 5-3c) and later onset date of ISM (Fig. 3-5). It is in these southern portions of Punjab and Haryana that the wheat crop has the latest SOS (Fig. 5-3b), which increases sensitivity to harmful increases in temperature (Chapter 6) and the lowest density of tubewells (proxy for irrigation capacity) (Fig. 5-4; Ambast et al. 2006). This suggests that agricultural productivity, long-term, in the absence of infrastructural capacity is sensitive to prevailing climatic conditions.

7.3 Where are locations which can be targeted with adaptations, accounting for location-specific stresses and thereby enhance the resilience of crop production to climate changes and variation whilst minimising environmental impacts?

As discussed in Chapter 1 it is now accepted that any assessments of vulnerability of croplands to climate change and potential adaptations to reduce vulnerability are

limited if they are not nested within a holistic understanding of the underlying system and also contribute to reducing agriculture's environmental and climatic footprint (Tilman et al. 2002; The Royal Society 2009; Foresight: Final Project Report 2011; Foley et al. 2011). There are therefore inherent trade-offs in agricultural production systems between competing goals of maximising production, reducing vulnerability to climate change, reducing negative impacts on environmental resources and supporting a range of ecosystem services (FAO 2011a; FAO 2011b; FAO 2012; Dobermann and Nelson 2013). Often these trade-offs occur spatially, where a landscape must support multiple social and economic systems and agricultural production and land use practices must be traded-off with environmental sustainability goals (Scherr et al. 2012; Dobermann and Nelson 2013). Therefore, there is a research need to identify adaptations, and locations where these adaptations can be targeted in a landscape, to minimise trade-offs and capture synergies between the various climate-smart goals. Outcomes generated through these four papers contribute to identifying locations where these synergies exist and where trade-offs can be minimised. This delivers an advance in knowledge to system managers and the policy environment on where and what adaptations to implement to reduce the vulnerability of agricultural production to climate change whilst also delivering other climate-smart development goals (FAO 2011b).

The locations of 592,866 ha of cropland across Punjab and Haryana exposed to unfavourable trends in monsoon precipitation, where the wheat crop was sown late and so sensitive to increased warming during the TSP and where crop residue was burnt were highlighted. In this situation, such locations could be targeted with zero-tillage drills which can seed through residue delivering multiple benefits of earlier sown wheat with increased yields and reduced sensitivity to warming but also improved water use productivity and reduced GHG emissions (Erenstein and Laxmi 2008; Jat et al. 2009a). It is important to note zero-tillage has been shown to deliver other environmental benefits contributing to climate-smart goals including improved soil quality (Hobbs et al. 2008; Erenstein and Laxmi 2008).

In 2009-2010 the locations where rice and wheat yield gaps occurred were detected and using longer-term measures from the GIMMS datasets locations where production

had greater levels of inter-annual variation were identified. Closing these yield gaps or creating more stable levels of production will reduce pressure to expand croplands with subsequent environmental benefits.

Across all India, and in Punjab and Haryana, there was a fragmented spatial pattern in the occurrence of trends in facets of ISM precipitation which could impact agricultural production, or necessitate extra irrigation withdrawals. By applying trend analysis to daily precipitation data for a long time-period (1951-2007) it was possible to detect locations experiencing unfavourable trends and avoid masking local detail by aggregating data up to larger spatial units. This analysis was important in highlighting the need for locally sensitive water resources management and also in targeting locations in need of adaptation for water management practices. In the context of croplands, it can highlight cropland locations which would benefit from adapting to more water efficient practices such as residue retention, laser bed levelling or shifting crop type (e.g. from rice to wheat or maize) (Hobbs et al. 2008; Jat et al. 2009a Saharawat et al. 2010).

The ability to quantify landscape scale GHG emissions from residue burning, and track year on year variability in burning within and across a landscape, moves farmers closer to receiving financial benefits from carbon markets (Milne et al. 2012). Access to these financial benefits would have obvious economic benefits to farmers enhancing their adaptive capacity. Using remote sensing data as inputs GHG emissions from crop residue burning were quantified using the standard IPCC methodology (IPCC 2006b). Using phenology to distinguish between crop types meant that crop specific combustion factors could be used to more accurately estimate emissions from different crop types. Satellite-derived estimates of GHG emissions from residue burning, complements the need for landscape scale quantification of GHG emissions, targeting 'hotspot' sources of GHGs and improving the efficiency of resources available for mitigation (Milne et al. 2012). There are uncertainties which need to be quantified before this approach can be used to inform payment for carbon credits and, thus, deliver any enhancement to farmer's adaptive capacity (see *section* 5.2.3.1). The use of optical remote sensing datasets and burned area products here only monitors GHG emissions from crop residue burning and does not address the whole range of

emissions from cereal cropping (e.g. N_2O emissions from fertiliser application or CH_4 emissions from anaerobic decomposition in rice cropping systems (Power 2010; DeFries and Rosenzweig 2010)).

Chapter 8: Conclusions and future work

To conclude a list of key findings drawn from the four research papers are presented. These findings are all key to understanding the vulnerability of the rice-wheat production system of the north-west Indo-Gangetic Plains to climate drivers.

- Locations experiencing unfavourable trends for agricultural production in facets in ISM precipitation (decreasing ISM precipitation, increasing variation in ISM precipitation, increasing recurrence of drought years, later onset date and increasing variation in onset date) were generated by performing trend analysis at a 0.25˚ spatial resolution. This analysis highlighted that at a national, and sub-national, level there was a fragmented spatial pattern in locations experiencing negative or positive trends in facets of ISM precipitation. This suggests there is a need, nationally, to manage water resources at the local level.
- A new method of identifying location-specific onset date of ISM was developed and validated; characterising spatial patterns and trends in onset date of the ISM is important to identify locations where the timing or length of the ISM season can impact the length of growing season. This has important implications for regions with a high cropping intensity and limited amounts of renewable water resources, as occurs across most of Punjab and Haryana.
- Agricultural systems in southern Punjab and Haryana have the greatest inter-annual variability in productivity and length-of-growing season suggesting these regions are particularly vulnerable to climatic drivers.
- 5.3 million ha of rice-wheat croplands experienced at least one, and up to three, unfavourable trends (between 1951 and 2007) in facets of ISM precipitation. In Punjab and Haryana it was predominantly cropland exposure to increasing frequency of occurrence of drought years and increasing variation in ISM precipitation.
- Using a combination of location-specific remote sensing metrics, rice and wheat crop residue burning over 1.17 million and 2.4 million ha respectively during the 2009-2010 growing season was detected. The associated GHG emissions from the crop residue burning were estimated using the standard IPCC methodology.
- In 2009-2010, 965,363 ha of wheat croplands had yield gaps greater than 1 Tonne ha^{1} and 4336 ha had yield gaps greater than 2 Tonnes ha^{-1}; 321,580 ha of rice croplands had yield gaps greater than 1 Tonne ha^{-1} and 3349 ha had yield gaps greater than 2 Tonnes ha^{-1}. This suggests potential to increase production without expanding cropland areas.

- 592,866 ha of rice-wheat croplands were detected as priority locations for targeting with zero-tillage and residue retention. These were locations exposed to unfavourable trends in ISM precipitation, where the wheat crop was sown late increasing sensitivity to warming during the TSP and crop residue was burnt emitting GHGs and reducing soil water holding capacity.
- It was shown here that the phenological detail in remote sensing datasets can reveal the impact of temperature events during the TSP periods of crop development on final yield. Warming minimum and maximum temperatures during the TSP had a negative impact on wheat crop production. This negative impact increased with later planting dates for the wheat crop.
- Warming during the TSP did not have a negative impact on rice crop production, though warmer average growing season temperatures did. The lack of negative impact of warming during the TSP period may be due to irrigation enabling transpiration cooling.
- There was not a clear crop critical threshold above which warming events during the TSP had a terminal impact on crop production. However, increased frequency of warming events during the TSP above 35˚C and 38˚C, for wheat and rice respectively, resulted in a noticeable decrease in yield. These values differ from those reported in experimental studies suggesting cropland system factors create crop differential sensitivity to warming.

8.1 Concluding Remarks

The rice-wheat production systems of Punjab and Haryana are key to supporting the livelihoods and food security of several hundred million people, are vulnerable to climatic change and variability, and current agricultural practices are unsustainable degrading the ecosystem services upon which agricultural production relies. In response to this situation there is a need to adapt the rice-wheat cropping systems so that they are less vulnerable to climatic drivers whilst also attempting to meet other climate-smart development goals. Alongside their unique conclusions and contributions, the four research papers which constitute this thesis provide a body of work assessing the vulnerability of the rice-wheat production system to climatic drivers and provide information to target adaptations spatially to deliver climate-smart goals and enhanced climate resilience. It was shown through this research that remote sensing can be used to monitor how individual crops, within their unique geographical location and underlying agricultural system, respond to climatic variables and can

identify optimum adaptations to capture synergies between multiple development goals. This enables adaptive responses to be location- and system-sensitive.

List of References

Abebe T, Wiersum KF, Bongers F (2009) Spatial and temporal variation in crop diversity in agroforestry homegardens of southern Ethiopia. *Agroforestry Systems* 78:309–322.

Abrol I (1999) Sustaining rice–wheat system productivity in the Indo-Gangetic plains: water management-related issues. *Agricultural Water Management* 40:31–35.

Abson DJ, Fraser ED, Benton TG (2013) Landscape diversity and the resilience of agricultural returns: a portfolio analysis of land-use patterns and economic returns from lowland agriculture. *Agriculture and Food Security* 2:2.

Adger WN (2006) Vulnerability. *Global Environmental Change* 16:268–281.

Adger WN, Agrawala S, Mirza MMQ, et al. (2007) Assessment of adaptation practices, options, constraints and capacity. In: Parry ML, Canziani OF, Palutikof JP, et al. (eds) Climate Change 2007 Impacts, Adaptation and Vulnerability. Contribution to Working Group II to the Fourth Assessment Report Intergovermental Panel on Climate Change. Cambridge University Press, Cambridge, UK., pp 717–743

Aggarwal PK, Baethegan WE, Cooper P, et al. (2010) Managing Climatic Risks to Combat Land Degradation and Enhance Food security: Key Information Needs. *Procedia Environmental Science* 1:305–312.

Aggarwal PK, Joshi PK, Ingram JSI, Gupta RK (2004) Adapting food systems of the Indo-Gangetic plains to global environmental change: key information needs to improve policy formulation. *Environmental Science and Policy* 7:487–498.

Agrawal S, Joshi PK, Shukla Y, Roy PS (2003) Spot-Vegetation Multi Temporal Data for Classifying Vegetation in South Central Asia. Indian Institute of Remote Sensing, vol. 4. Kalidas Road, Dehradun-248001, Uttaranchal

Agricultural Census (2012) Agricultural Census 2010-11.

Ambast SK, Tyagi NK, Raul SK (2006) Management of declining groundwater in the Trans Indo-Gangetic Plain (India): Some options. Agricultural Water Management 82:279–296.

Andermann C, Bonnet S, Gloaguen R (2011) Evaluation of precipitation data sets along the Himalayan front. *Geochemistry Geophysics Geosystems.* 12:7.

Annamalai H, Hamilton K, Sperber KR (2007) The South Asian Summer Monsoon and Its Relationship with ENSO in the IPCC AR4 Simulations. *Journal of Climate* 20:1071–1092.

Asseng S, Foster I, Turner NC (2010) The impact of temperature variability on wheat yields. *Global Change Biology* 17:997–1012.

Atkinson PM, Cutler MEJ, Lewis H (1997) Mapping sub-pixel proportional land cover with AVHRR. *International Journal of Remote Sensing.* 18:917-935.

Atkinson PM, Jeganathan C, Dash J, Atzberger C (2012) Inter-comparison of four models for smoothing satellite sensor time-series data to estimate vegetation phenology. *Remote Sensing of Environment* 123:400–417.

Attri SD, Tyagi A (2010) Climate Profile of India. Environment Monitoring and Research Centre, Indian Meteorological Department, New Delhi

Atzberger C (2013) Advances in Remote Sensing of Agriculture: Context Description, Existing Operational Monitoring Systems and Major Information Needs. *Remote Sensing* 5:949–981. doi: 10.3390/rs5020949

Auffhammer M, Ramanathan V, Vincent JR (2012) Climate change, the monsoon, and rice yield in India. *Climatic Change* 111:411–424.

Auffhammer M, Ramanathan V, Vincent JR (2006) Integrated model shows that atmospheric brown clouds and greenhouse gases have reduced rice harvests in India. *Proceedings of the National Academy of Sciences of the USA* 103:19668-19672

Badarinath KVS, Kiran Chand TR, Krishna Prasad V (2006) Agriculture crop residue burning in the Indo-Gangetic Plains – A study using IRS-P6 AWiFS satellite data. *Current Science* 91:1085–1089.

Bae D, Jung I, Chang H (2008) Long-term trend of precipitation and runoff in Korean river. *Hydrological Processes* 2656:2644–2656.

Bansod SD, Singh SV, Kripalani RH (1991) The Relationship of Monsoon Onset with Subsequent Rainfall over India. *International Journal of Climatology* 11:809–817.

Bartholomé E, Baret F, Bicheron P, et al. (2006) VGT4Africa user manual. European Commission Joint Research Centre, Medias, Vito, Ispra, Italy

Bartholomé E, Belward AS (2005) GLC2000: a new approach to global land cover mapping from Earth observation data. *International Journal of Remote Sensing* 26:1959–1977.

Bastiaanssen WGM, Ali S (2003) A new crop yield forecasting model based on satellite measurements applied across the Indus Basin, Pakistan. *Agriculture, Ecosystems and Environment* 94:321–340.

Beck HE, McVicar TR, van Dijk AIJM, et al. (2011) Global evaluation of four AVHRR–NDVI data sets: Intercomparison and assessment against Landsat imagery. *Remote Sensing of Environment* 115:2547–2563.

Becker-Reshef I, Vermote E, Lindeman M, Justice C (2010) A generalized regression-based model for forecasting winter wheat yields in Kansas and Ukraine using MODIS data. *Remote Sensing of Environment* 114:1312–1323.

Beddington J (2009) Presentation given to the Sustainable Development UK Annual Conference, London, 19 March 2009. http://webarchive.nationalarchives.gov.uk/+/http://www.dius.gov.uk/news_and_speeches/speeches/john_beddington/perfect-storm.

Beddington JR, Asaduzzaman M, Clark ME, et al. (2012a) What Next for Agriculture After Durban ? *Science* 335:289–290.

Beddington JR, Asaduzzaman M, Clark ME, et al. (2012b) The role for scientists in tackling food insecurity and climate change. *Agriculture and Food Security* 1:10.

Bhatia A, Jain N, Pathak H (2012) Greenhouse Gas Emissions from Indian Agriculture. In: Pathak H, Aggarwal PK (eds) Low Carbon Technologies for Agric. A Study on Rice an Wheat Systems in the Indo-Gangetic Plains. Indian Agricultural Research Institute, New Delhi, India, pp 12–40

Bicheron P, Huc M, Henry C et al. (2008) Globcover products description manual. ESA. http://postel.obs-mip.fr/IMG/pdf/GLOBCOVER_PDM_I2.2.pdf.

Biggs EM, Atkinson PM (2011) A characterisation of climate variability and trends in hydrological extremes in the Severn Uplands. *International Journal of Climatology* 31:1634-1652.

Biggs R, Schluter M, Biggs D, et al. (2012) Towards Principles for Enhancing the Resilience of Ecosystem Services. *Annual Review of Environmental Resources* 37:421–448.

Biradar CM, Thenkabail PS, Noojipady P, et al. (2009) A global map of rainfed cropland areas (GMRCA) at the end of last millennium using remote sensing. *International Journal of Applied Earth Observation and Geoinformation* 11:114–129.

Biradar CM, Xiao X (2011) Quantifying the area and spatial distribution of double- and triple-cropping croplands in India with multi-temporal MODIS imagery in 2005. *International Journal of Remote Sensing* 32:367–386.

Bogdanski A (2012) Integrated food–energy systems for climate-smart agriculture. *Agriculture and Food Security* 1:9.

Bolton DK, Friedl MA (2013) Forecasting crop yield using remotely sensed vegetation indices and crop phenology metrics. *Agricultural and Forest Meteorology* 173:74–84.

Brown ME, de Beurs K, Vrieling A (2010) The response of African land surface phenology to large scale climate oscillations. *Remote Sensing of Environment* 114:2286–2296.

Brown ME, de Beurs KM, Marshall M (2012) Global phenological response to climate change in crop areas using satellite remote sensing of vegetation, humidity and temperature over 26years. *Remote Sensing of Environment* 126:174–183.

Brown ME, Funk CC (2008) Climate. Food security under climate change. *Science* 319:580–1.

Brown ME, Lary DJ, Vrieling A. et al. (2008) Neural networks as a tool for constructing continuous NDVI time series from AVHRR and MODIS. *International Journal of Remote Sensing* 29:7141–7158.

Brush SB, Tadesse D, Van Dusen E (2003) Crop Diversity in Peasant and Industrialized Agriculture : Mexico and California. *Society and Natural Resources* 16:123:141.

Brussaard L, Caron P, Campbell B, et al. (2010a) Reconciling biodiversity conservation and food security: scientific challenges for a new agriculture. *Current Opinion in Environmental Sustainability* 2:34–42.

Carpenter SR (2005) Eutrophication of aquatic ecosystems: bistability and soil phosphorus. *Proceedings of the National Academy of Sciences of the USA* 102:10002-10005.

Carpenter SR, Caraco NF, Correl DL, et al. (1998) Nonpoint pollution of surface waters with phosphorus and nitrogen. *Ecological Applications* 8:559–568.

CCAFS (2010) Climate Change, Agriculture and Food Security in the Indo-Gangetic Plain - Developing Regional Scenarios. New Delhi, India

Central Ground Water Board (2012) Ground Water Year Book - India. Faridabad

Central Ground Water Board (2009) Ground Water Year Book - India. Faridabad

Challinor A. J, Wheeler TR, Craufurd PQ, Slingo JM (2005) Simulation of the impact of high temperature stress on annual crop yields. *Agricultural and Forest Meteorology* 135:180–189.

Chauhan BS, Mahajan G, Sardana V, et al. (2012) Productivity and Sustainability of the Rice-Wheat Cropping System in the Indo-Gangetic Plains of the Indian Subcontinent: Problems, Opportunities, and Strategies. *Advances in Agronomy* 117:315–369.

Chen J, Jönsson P, Tamura M, et al. (2004) A simple method for reconstructing a high-quality NDVI time-series data set based on the Savitzky–Golay filter. *Remote Sensing of Environment* 91:332–344.

Christensen JH, Hewitson B, Busuioc A, et al. (2007) Regional Climate Projections. Climate Change 2007: The Physical Science Basis. Contribution of Working Group I to the Fourth Assessment Report of the Intergovernmental Panel on Climate Change. Cambridge University Press, Cambridge, UK.

Comprehensive Assessment of Water Management in Agriculture (2007) Water for Food, Water for Life. A Comprehensive Assessment of Water Management in Agriculture. Earthscan and International Water Management Institute, London and Colombo

Cooper PJM, Cappiello S, Vermeulen SJ, Campbell BM, Zougmoré R, Kinyangi J (2013) Large-scale implementation adaptation and mitigation actions in agriculture. CCAFS Working Paper 50. Copenhagen.

Crossman ND, Burkhard B, Nedkov S, et al. (2013) A blueprint for mapping and modelling ecosystem services. *Ecosystem Services* 4:1-4.

Dash J, Jeganathan C, Atkinson PM (2010) The use of MERIS Terrestrial Chlorophyll Index to study spatio-temporal variation in vegetation phenology over India. *Remote Sensing of Environment* 114:1388–1402.

Dash SK, Kulkarni M a., Mohanty UC, Prasad K (2009) Changes in the characteristics of rain events in India. *Journal of Geophysical Research* 114:D10.

Daughtry CST, Doraiswamy PC, Hunt ER, et al. (2006) Remote sensing of crop residue cover and soil tillage intensity. *Soil and Tillage Research* 91:101–108.

Dearing JA, Yang X, Dong X, et al. (2012) Extending the timescale and range of ecosystem services through paleoenvironmental analyses, exemplified in the lower Yangtze basin. *Proceedings of the National Academy of Sciences of the USA* 109:1111-1120.

DeFries R, Rosenzweig C (2010) Toward a whole-landscape approach for sustainable land use in the tropics. *Proceedings of the National Academy of Sciences of the USA* 107:19627–32.

DES (2011) Agricultural Statistics at a glance. New Delhi

DES (2009) Agricultural Statistics at a glance. Directorate of Economics and Statistics, Government of India, New Delhi

Dobermann A, Nelson R (2013) Solutions for Sustainable Agriculture and Food Systems. Technical Report for the Post-2015 Development Agenda. 1–98.

Doraiswamy PC, Hatfield JL, Jackson TJ, et al. (2004) Crop condition and yield simulations using Landsat and MODIS. *Remote Sensing of Environment* 92:548–559.

Douglas EM, Beltrán-Przekurat a., Niyogi D, et al. (2009) The impact of agricultural intensification and irrigation on land–atmosphere interactions and Indian monsoon precipitation — A mesoscale modeling perspective. *Global and Planetary Change* 67:117–128.

Douglas EM, Niyogi D, Frolking S, et al. (2006) Changes in moisture and energy fluxes due to agricultural land use and irrigation in the Indian Monsoon Belt. *Geophysical Research Letters* 33:1–5.

Douglas EM, Vogel RM, Kroll CN (2000) Trends in Foods and low Flows in the United States : impact of spatial correlation. *Journal of Hydrology* 240:90–105.

Duncan JMA, Biggs EM (2012) Assessing the accuracy and applied use of satellite-derived precipitation estimates over Nepal. *Applied Geography* 34:626–638.

Duncan JMA, Dash J, Atkinson PM (2013) Analysing temporal trends in the Indian Summer Monsoon and its variability at a fine spatial resolution. *Climatic Change* 117:119–131.

Eakin H, Luers AL (2006) Assessing the Vulnerability of Social-Environmental Systems. *Annual Review of Environmental Resources* 31:365–394.

Easterling WE, Aggarwal PK, Batima P, et al. (2007) Food, fibre and forest products. In: Parry ML, Canziani OF, Palutikof JP, et al. (eds) Climate Change 2007: The Physical Science Basis. Contribution of Working Group I to the Fourth Assessment Report of the Intergovernmental Panel on Climate Change. Cambridge University Press, Cambridge, UK. pp 273–313

Efron B, Tibshirani RJ (1993) An Introduction to the Bootstrap. Chapman and Hall

Eisenhauer JG (2003) Regression through the Origin. *Teaching Statistics* 25:76–80.

Erenstein O (2009a) Zero Tillage in the Rice-Wheat Systems of the Indo-Gangetic Plains - A Review of Impacts and Sustainability Implications. 1–19.

Erenstein O (2011) Cropping systems and crop residue management in the Trans-Gangetic Plains: Issues and challenges for conservation agriculture from village surveys. *Agricultural Systems* 104:54–62.

Erenstein O (2009b) Comparing water management in rice–wheat production systems in Haryana, India and Punjab, Pakistan. *Agricultural Water Management* 96:1799–1806.

Erenstein O (2010a) Triangulating Technology Diffusion Indicators: Zero Tillage Wheat in South Asia's Irrigated Plains. *Expiremental Agriculture* 46:293–308.

Erenstein O (2010b) A comparative analysis of rice–wheat systems in Indian Haryana and Pakistan Punjab. *Land Use Policy* 27:869–879.

Erenstein O, Hellin J, Chandna P (2007) Livelihoods , poverty and targeting in the Indo-Gangetic Plains: a spatial mapping approach. CIMMYT and the Rice-Wheat Consortium for the Indo-Gangetic Plains (RWC), New Delhi

Erenstein O, Laxmi V (2008) Zero tillage impacts in India's rice–wheat systems: A review. *Soil and Tillage Research* 100:1–14.

Erenstein O, Thorpe W (2011) Livelihoods and agro-ecological gradients: A meso-level analysis in the Indo-Gangetic Plains, India. *Agricultural Systems* 104:42–53.

Ericksen PJ (2008a) Conceptualizing food systems for global environmental change research. *Global Environmental Change* 18:234–245.

Ericksen PJ (2008b) What Is the Vulnerability of a Food System to Global Environmental Change? *Ecology and Society* 13(2).

ESA (2010) GEMS Sentinel-2 Mission Documentation. European Space Agency Sentinel-2 Team.

Fang H, Liang S, Hoogenboom G (2011) Integration of MODIS LAI and vegetation index products with the CSM–CERES–Maize model for corn yield estimation. *International Journal of Remote Sensing* 32:1039–1065.

FAO (2013) FAOSTAT. In: FAOSTAT. http://www.fao.org/home/en/.

FAO (1996) Rome Decleration and World Food Summit Plan of Action. FAO, Rome

FAO (2006) World agriculture : towards 2030 / 2050. Rome

FAO (2011a) "Climate-Smart" Agriculture: Policies, Practices and Financing for Food Security, Adaptation and Mitigation. FAO, Rome, Italy

FAO (2011b) Climate-Smart Agriculture for Development: Managing Ecosystems for Sustainable Livelihoods. FAO

FAO (2012) Mainstreaming climate-smart agriculture into a broader landscape approach. Second Global Conference on Agriculture, Food Security and Climate Change, Hanoi, Vietnam.

FAO (2013) Climate-Smart Agriculture Sourcebook. FAO, Rome, Italy

Fasullo J, Webster PJ (2003) A Hydrological Definition of Indian Monsoon Onset and Withdrawal. *Journal of Climate* 16:3200.

Faures J-M, Bernardi M, Gommes R (2010) There Is No Such Thing as an Average: How Farmers Manage Uncertainty Related to Climate and Other Factors. *Water Resources Development* 26:523–542.

Fischer G, van Velthuizen H, Shah M, Nachtergaele FO (2002) Global Agro-Ecological Assessment for Agriculture in the 21st Century: Methodology and Results. 119.

Foley JA, Monfreda C, Ramankutty N, Zaks D (2007) Our share of the planetary pie. *Proceedings of the National Academy of Sciences of the USA* 104:12585–6.

Foley JA, Defries R, Asner GP, et al. (2005) Global consequences of land use. *Science* 309:570–4.

Foley JA, Ramankutty N, Brauman KA, et al. (2011) Solutions for a cultivated planet. *Nature* 478:337–42.

Foley JA (2011) Can we feed the world and sustain the planet? *Scientific American*. 60-65.

Folke C (2006) Resilience: The emergence of a perspective for social–ecological systems analyses. *Global Environmental Change* 16:253–267.

Folke C, Hahn T, Olsson P, Norberg J (2005) Adaptive Governance of Social-Ecological Systems. *Annual Review of Environmental Resources* 30:441–473.

Foody GM. (2002) Status of land cove classification accuracy assessment. *Remote Sensing of Environment*. 80:185-201.

Foresight: Final Project Report (2011) The Future of Food and Farming: Challenges and choices for global sustainability. London

Funk C, Budde ME (2009) Phenologically-tuned MODIS NDVI-based production anomaly estimates for Zimbabwe. *Remote Sensing of Environment* 113:115–125.

Gajbhiye KS, Mandal C (2000) Agro-Ecological Zones, their Soil Resource and Cropping Systems. National Bureau of Soil Survey and Land Use Planning. 1-32.

Gallopín GC (2006) Linkages between vulnerability, resilience, and adaptive capacity. *Global Environmental Change* 16:293–303.

Garg A, Shukla PR, Upadhyay J (2011) N2O emissions of India: an assessment of temporal, regional and sector trends. *Climatic Change* 110:755–782.

Ghosh S, Das D, Kao S-C, Ganguly AR (2011) Lack of uniform trends but increasing spatial variability in observed Indian rainfall extremes. *Nature Climate Change* 2:86–91.

Ghosh S, Luniya V, Gupta A (2009) Trend analysis of Indian summer monsoon rainfall at different spatial scales. *Atmospheric Science Letters* 10:285–290.

Giller KE, Witter E, Corbeels M et al. (2009) Conservation agriculture and smallholder farming in Africa: The heretics' view. *Field Crops Research.* 114:23-34.

Gleeson T, Wada Y, Bierkens MFP, van Beek LPH (2012) Water balance of global aquifers revealed by groundwater footprint. *Nature* 488:197–200.

Global Water Partnership (2013) Water and food security - Experiences in India and China: Technical Focus Paper. 1–42.

Godfray HCJ and Garnett T (2014) Food security and sustainable intensification. *Philosophical Transactions of the Royal Society B.* 369:20120273

Godfray HCJ, Beddington JR, Crute IR, et al. (2010) Food security: the challenge of feeding 9 billion people. *Science* 327:812–8.

Goswami BN (2005) South Asian monsoon. In: Lau WKM, Waliser DE (eds) Intraseasonal Var. Atmos. Clim. Syst. Springer, Chichester, pp 20–61

Goswami BN, Venugopal V, Sengupta D, et al. (2006) Increasing trend of extreme rain events over India in a warming environment. *Science* 314:1442–5.

Gourdji SM, Mathews KL, Reynolds M, et al. (2013a) An assessment of wheat yield sensitivity and breeding gains in hot environments. Proceedings of the Royal Society B. 280

Gourdji SM, Sibley AM, Lobell DB (2013b) Global crop exposure to critical high temperatures in the reproductive period: historical trends and future projections. *Environmental Research Letters* 8:024041.

Guhathakurta P, Rajeevan M (2008) Trends in the rainfall pattern over India. *International Journal of Climatololgy* 1469:1453–1469.

Gumma MK, Gauchan D, Nelson A, et al. (2011a) Temporal changes in rice-growing area and their impact on livelihood over a decade: A case study of Nepal. *Agriculture, Ecosystems and Environment* 142:382–392.

Gumma MK, Nelson A, Thenkabail PS, Singh AN (2011b) Mapping rice areas of South Asia using MODIS multitemporal data. *Journal of Applied Remote Sensing* 5.

Gunnel Y (1997) Relief and climate in South Asia: the influence of the western ghats on the current climate pattern of peninsular India. *International Journal of Climatology* 17:1169–1182.

Gupta R, Seth A (2007) A review of resource conserving technologies for sustainable management of the rice–wheat cropping systems of the Indo-Gangetic plains (IGP). *Crop Protection* 26:436–447.

Hajkowicz S, Negra C, Barnett P, et al. (2012) Food price volatility and hunger alleviation – can Cannes work? *Agriculture and Food Security* 1:8.

Hanjra MA, Qureshi ME (2010) Global water crisis and future food security in an era of climate change. *Food Policy* 35:365–377.

Harvey M, Pilgrim S (2011) The new competition for land: Food, energy, and climate change. *Food Policy* 36:S40–S51.

Hatfield JL, Boote KJ, Kimball BA, et al. (2011) Climate impacts on Agriculture: Impalications for Crop Production. *Agronomy Journal* 103:351–370.

Hawkins E, Fricker TE, Challinor AJ, et al. (2013) Increasing influence of heat stress on French maize yields from the 1960s to the 2030s. *Global Change Biology* 19:937–47.

Herold M, Mayaux P, Woodcock CE, et al. (2008) Some challenges in global land cover mapping: An assessment of agreement and accuracy in existing 1 km datasets. Remote Sensing of Environment 112:2538–2556.

Hobbs PR, Sayre K, Gupta R (2008) The role of conservation agriculture in sustainable agriculture. *Proceedings of the Royal Society B* 363:543–55.

Holling CS (2001) Understanding the Complexity of Economic, Ecological, and Social Systems. *Ecosystems* 4:390–405.

Huete AR, Didan K, Miura T, et al. (2002) Overview of the radiometric and biophysical performance of the MODIS vegetation indices. *Remote Sensing of Environment* 83:195–213.

Huete AR, Liu HQ, Batchily K, Leeuwen W Van (1997) A Comparison of Vegetation Indices over a Global Set of TM Images for EOS-MODIS. *Remote Sensing of Environment* 59:440–451.

Hughes TP, Carpenter S, Rockström J, et al. (2013a) Multiscale regime shifts and planetary boundaries. *Trends in Ecology and Evolution* 28:389–95.

Hughes TP, Linares C, Dakos V, et al. (2013b) Living dangerously on borrowed time during slow, unrecognized regime shifts. *Trends in Ecology and Evolution* 28:149–55.

Imran M, Stein A, Zurita-Milla R (2014) Investigating rural poverty and marginality in Burkina Faso using remote sensing-based products. *International Journal of Applied Earth Observation and Geoinformation* 26:322–334.

IPCC (2013) Summary for Policymakers. In: Climate Change 2013: The Physical Science Basis. Contribution of Working Group I to the Fifth Assessment Report of the Intergovernmental Panel on Climate Change [Stocker TF, Qin G.-K. Plattner M.et al.(eds.)] Cambridge University Press, Cambridge, United Kingdom and New York, NY, USA.

IPCC (1996) Chapter 4: Agriculture. Revised 1996 IPCC Guidelines for National Greenhouse Gas Inventories.

IPCC (2000) Good Practice Guidance and Uncertainty Management in National Greenhouse Gas Inventories. In Pentmen et al. (eds) IPCC National Greenhouse Gas Inventories Programme, Technical Support Unit, Hayama, Japan.

IPCC (2006a) N2O Emissions from Managed Soils and CO2 Emissions from Lime and Urea Application. Guidelines for National Greenhouse Gas Inventories. Vol. 4 Agric. For. Other L. Use. Global Environmental Strategies (IGES)., Hayama, Japan., pp 11.1–11.54

IPCC (2006b) Generic Methodologies Applicable to Multiple Land-Use Categories. Guidel. Natl. Greenh. Gas Invent. Vol. 4 Agriculture, Forestry and Other Land Use. Global Environmental Strategies (IGES)., Hayama, Japan., pp 2.1–2.59

Van Ittersum MK, Cassman KG, Grassini P, et al. (2013) Yield gap analysis with local to global relevance—A review. *Field Crops Research* 143:4–17.

Jagadish SVK, Craufurd PQ, Wheeler TR (2007) High temperature stress and spikelet fertility in rice (Oryza sativa L.). Journal of Expirmental Botany 58:1627–35.

Jain M, Mondal P, DeFries RS, et al. (2013) Mapping cropping intensity of smallholder farms: A comparison of methods using multiple sensors. *Remote Sensing of Environment* 134:210–223.

Jat ML, Gathala MK, Ladha JK, et al. (2009a) Evaluation of precision land leveling and double zero-till systems in the rice–wheat rotation: Water use, productivity, profitability and soil physical properties. *Soil and Tillage Research* 105:112–121.

Jat ML, Singh RG, Saharawat YS, et al. (2009b) Innovations through Conservation Agriculture: Progress and Prospects of Participatory Approach in the Indo-Gangetic Plains. Lead Papers: 4th World Congress on Conservation Agriculture, Innovations for Improving Efficiency, Equity and Environment. New Delhi, India, pp 60–64

Jeyaseelan AT, Roy PS, Young SS (2003) Persistent changes in NDVI between 1982 and 2003 over India using AVHRR GIMMS (Global Inventory Modeling and Mapping Studies) data. *International Journal of Remote Sensing* 28:21:37–41.

Jiang Z, Huete AR, Chen J et al. (2006) Analysis of NDVI and scaled difference vegetation index retrievals of vegetation fraction. *Remote Sensing of Environment.* 301:366-378.

Jönsson P, Eklundh L (2004) TIMESAT—a program for analyzing time-series of satellite sensor data. *Computers and Geosciences* 30:833–845.

Joseph P V, Sooraj KP, Rajan CK (2006) The Summer Monsoon onset process over South Asia and an objecetive method for the date of onset over Kerala. *International Journal of Climatology* 26:1871–1893.

Kastens J, Kastens T, Kastens D, et al. (2005) Image masking for crop yield forecasting using AVHRR NDVI time series imagery. *Remote Sensing of Environment* 99:341–356.

Kendall MG (1975) Rank Correlation Methods. Griffin, London

Knopf B, Zickfeld K, Flechsig M, Petoukhov V (2008) Sensitivity of the Indian Monsoon to Human Activities. *Advances in Atmospheric Sciences* 25:932–945.

Koehler A-K, Challinor AJ, Hawkins E, Asseng S (2013) Influences of increasing temperature on Indian wheat: quantifying limits to predictability. *Environmental Research Letters* 8:034016.

Kothawale DR, Revadekar J V, Rupa Kumar K (2010) Recent trends in pre-monsoon daily temperature extremes over India. *Journal of Earth System Science* 119:51–65.

Kothawale DR, Rupa Kumar K (2005) On the recent changes in surface temperature trends over India. *Geophysical Research Letters* 32:L18714.

Krishna Kumar K, Rupa Kumar K, Ashrit RG, et al. (2004) Climate impacts on Indian agriculture. *International Journal of Climatology* 24:1375–1393.

Krishnamurthy CKB, Lall U, Kwon H-H (2009) Changing Frequency and Intensity of Rainfall Extremes over India from 1951 to 2003. *Journal of Climate* 22:4737–4746.

Ladha J, Dawe D, Pathak H, et al. (2003) How extensive are yield declines in long-term rice–wheat experiments in Asia? *Field Crops Research* 81:159–180.

Ladha J k., Kumar V, Alam MM, et al. (2009) Integrating crop and resource management technologies for enhanced productivity, profitability and sustainability of the rice-wheat system in South Asia. In: Ladha J k., Yadvinder-Singh., Erenstein O, Hardy B (eds) Integrated Crop Resource Management in the

Rice-Wheat System of South Asia. International Rice Research Institute, Los Banos (Philippines), pp 69–109

Lee J-Y, Wang B (2012) Future change of global monsoon in the CMIP5. *Climate Dynamics*

Livezey RE, Chen WY (1983) Statistical Field Significance and its Determination by Monte Carlo Techniques. *Monthly Weather Reviews* 11:46–59.

Lobell DB (2013) The use of satellite data for crop yield gap analysis. *Field Crops Research* 143:56–64.

Lobell DB, Bänziger M, Magorokosho C, Vivek B (2011a) Nonlinear heat effects on African maize as evidenced by historical yield trials. *Nature Climate Change* 1:42–45.

Lobell DB, Asner GP (2004) Cropland distributions from temporal unmixing of MODIS data. *Remote Sensing of Environment.* 93:412-422.

Lobell DB, Burke MB (2010) On the use of statistical models to predict crop yield responses to climate change. *Agricultural and Forest Meteorology* 150:1443–1452.

Lobell DB, Cassman KG, Field CB (2009) Crop Yield Gaps: Their Importance, Magnitudes, and Causes. *Annual Review of Environmental Resources* 34:179–204.

Lobell DB, Gourdji SM (2012) The influence of Climate Change on Global Crop Productivity. *Plant Physiology* 160:1686–1697.

Lobell DB, Ortiz-Monasterio JI (2006) Regional importance of crop yield constraints: Linking simulation models and geostatistics to interpret spatial patterns. *Ecological Modelling* 196:173–182.

Lobell DB, Ortiz-Monasterio JI, Falcon WP (2007) Yield uncertainty at the field scale evaluated with multi-year satellite data. *Agricultural Systems* 92:76–90.

Lobell DB, Ortiz-Monasterio JI, Lee Addams C, Asner GP (2002) Soil, climate, and management impacts on regional wheat productivity in Mexico from remote sensing. *Agricultural and Forest Meteorology* 114:31–43.

Lobell DB, Ortiz-Monasterio JI, Lee AS (2010) Satellite evidence for yield growth opportunities in Northwest India. *Field Crops Research* 118:13–20. d

Lobell DB, Ortiz-Monasterio JI, Sibley AM, Sohu VS (2013) Satellite detection of earlier wheat sowing in India and implications for yield trends. *Agricultural Systems* 115:137–143.

Lobell DB, Schlenker W, Costa-Roberts J (2011b) Climate Trends and Global Crop Production Since 1980. *Science* 333:616-620.

Lobell DB, Sibley A, Ivan Ortiz-Monasterio J (2012) Extreme heat effects on wheat senescence in India. *Nature Climate Change* 2:1–4.

Luers AL (2005) The surface of vulnerability: An analytical framework for examining environmental change. *Global Environmental Change* 15:214–223.

Luers AL, Lobell DB, Sklar LS, et al. (2003) A method for quantifying vulnerability, applied to the agricultural system of the Yaqui Valley, Mexico. *Global Environmental Change* 13:255–267.

Lumpkin TA, Sayre K (2009) Enhancing Resource Productivity and Efficiency through Conservation Agriculture. Lead Papers: 4th World Congress on Conservation Agriculture, Innovations for Improving Efficiency, Equity and Environment. New Delhi, India, pp 3–9

Mall RK, Singh R, Gupta A, et al. (2006) Impact of Climate Change on Indian Agriculture: A Review. *Climatic Change* 78:445–478.

Mann HB (1945) Non-parametric tests against trend. *Econometrica* 13:245–259.

Mathison C, Wiltshire A, Dimri AP, et al. (2013) Regional projections of North Indian climate for adaptation studies. *Science of the Total Environment*. (in press).

McCarty JL. (2011) Remote Sensing-Based Estimates of Annual and Seasonal Emissions from Crop Residue Burning in the Contiguous United States. *Journal of the Air and Waste Management Association*. 61:22-34.

Millenium Ecosystem Assessment (2005) Ecosystems and Human Well-Being: Synthesis. Island Press, Washington DC

Milne E, Neufeldt H, Smalligan M, et al. (2012) Methods for the quantification of emissions at the landscape level for developing countries in smallholder contexts, CCAFS Report. 1–60.

Misselhorn A, Aggarwal P, Ericksen P, et al. (2012) A vision for attaining food security. *Current Opinion in Environmental Sustainability* 4:7–17.

Modarres R, de Paulo Rodrigues da Silva V (2007) Rainfall trends in arid and semi-arid regions of Iran. *Journal of Arid Environments* 70:344–355.

Monfreda C, Ramankutty N, Foley JA. (2008) Farming the planet: 2. Geographic distribution of crop areas, yields, physiological types, and net primary production in the year 2000. *Global Biogeochemical Cycles* 22:1–19.

Moors EJ, Groot A, Biemans H, et al. (2011) Adaptation to changing water resources in the Ganges basin, northern India. *Environmental Science and Policy* 14:758-769.

Moors EJ, Siderius C (2012) Adaptation to Climate Change in the Ganges Basin, Northern India: A Science and Policy Brief. 1–48.

Moron V, Robertson AW, Boer R (2009) Spatial Coherence and Seasonal Predictability of Monsoon Onset over Indonesia. *Journal of Climate* 22:840–850.

Morton JF (2007) The impact of climate change on smallholder and subsistence agriculture. *Proceedings of the National Academy of Sciences of the USA* 104:19680–5.

Murgai R, Ali M, Byerlee D (2001) Productivity Growth and Sustainability in Post-Green Revolution Agriculture: The Case of the Indian and Pakistan Punjabs. World Bank Reseearch Observer 16:199–218.

Narang RS, Virmani SM (2001) Rice-Wheat Cropping Systems of the Indo-Gangetic Plain of India. Consort. Pap. Ser. 11. Rice-Wheat Consortium for the Indo-Gangetic Plains, New Delhi, India, pp 1–37

National Mission for Sustainable Agriculture (2010) National Action Plan on Climate Change.

National Water Mission (2009) National Action Plan on Climate Change. Ministry of Water Resources, Government of India

Nelson GC (2010) The perfect storm food security and nutrition under climate change. *Significance* 7:13–16.

O'Brien K, Leichenko R, Kelkar U, et al. (2004) Mapping vulnerability to multiple stressors: climate change and globalization in India. *Global Environmental Change* 14:303–313.

Oh-e I, Saitoh K, Kuroda T (2007) Effects of High Temperature on Growth , Yield and Dry-Matter Production of Rice Grown in the Paddy Field. *Plant Production Science* 10:412–422.

Ojha H, Sulaiman R, Sultana P, et al. (2013) Is South Asian Agriculture Adapting to Climate Change? Evidence from the Indo-Gangetic Plains. *Agroecology and Sustainable Food Systems*.

Ortiz R, Sayre KD, Govaerts B, et al. (2008) Climate change: Can wheat beat the heat? *Agriculture, Ecosystems and Environment* 126:46–58.

Ortiz-Monastrerio JIR, Dhillon SS, Fischer RA (1994) Effects of Date of Sowing on the Yield and Yield Components of Spring Wheat and their Relationship with Solar

Radiation and Temperature at Ludhiana, Punjab, India. *Field Crops Research* 37:169–184.

Pai DS, Rajeevan M (2007) Indian Summer Monsoon Onset : Variability and Prediction Indian Summer Monsoon Onset: National Climate Centre, Indian Meteorological Department.

Pai DS, Sridhar L, Guhathakurta P, Hatwar HR (2011) District-wide drought climatology of the southwest monsoon season over India based on standardized precipitation index (SPI). *Natural Hazards* 59:1797–1813.

Panigrahy S, Upadhyay G, Ray SS, Parihar JS (2010) Mapping of Cropping System for the Indo-Gangetic Plain Using Multi-Date SPOT NDVI-VGT Data. *Journal of the Indian Society of Remote Sensing* 38:627–632.

Partal T, Kahya E (2006) Trend analysis in Turkish precipitation data. *Hydrological Processes* 20:2011–2026.

Pathak H (2010) Trend of fertility status of Indian soils. *Current Advances Agricultural Sciences* 2:10–12.

Pathak H, Chakrabarti B, Aggarwal PK (2012) Promotion of low carbon technologies in Indian Agriculture: Opportunities and Constraints. In: Pathak H, Aggarwal PK (eds) Low Carbon Technologies for Agriculture: A Study on Rice and Wheat Systems in the Indo-Gangetic Plains. Indian Agricultural Research Institute, New Delhi, India, pp 66–78

Pathak H, Ladha JK, Aggarwal PK, et al. (2003) Trends of climatic potential and on-farm yields of rice and wheat in the Indo-Gangetic Plains. *Field Crops Research* 80:223–234.

Pathak H, Singh R, Bhatia A, Jain N (2006) Recycling of rice straw to improve wheat yield and soil fertility and reduce atmospheric pollution. *Paddy and Water Environment* 4:111–117.

Peng D, Huete AR, Huang J, et al. (2011) Detection and estimation of mixed paddy rice cropping patterns with MODIS data. *International Journal of Applied Earth Observation and Geoinformation* 13:13–23.

Peng S, Huang J, Sheehy JE, et al. (2004) Rice yields decline with higher night temperature from global warming. *Proceedings of the National Academy of Sciences of the USA* 101:9971–5.

Perfecto I, Vandermeer J (2010) The agroecological matrix as alternative to the land-sparing/agriculture intensification model. *Proceedings of the National Academy of Sciences of the USA* 107:5786–91.

Perveen S, Krishnamurthy CK, Sidhu RS, et al. (2012) Restoring Groundwater in Punjab, India's Breadbasket: Finding Agricultural Solutions for Water Sustainability. 1–28.

Pettorelli N, Vik JO, Mysterud A, et al. (2005) Using the satellite-derived NDVI to assess ecological responses to environmental change. *Trends in Ecology and Evolution* 20:503–10.

Pinter PJ, Hatfield JL, Schepers JS, et al. (2003) Remote Sensing for Crop Management. *Photogrammetric Engineering and Remote Sensing* 69:647–664.

Pinter PJ, Jackson RD, Idso SB, Reginato RJ (1981) Multidate spectral reflectance as predictors of yield in water stressed wheat and barley. *International Journal of Remote Sensing* 2:43–48.

Pinzon JE, Brown ME, Tucker CJ (2005) Satellite time series correction of orbital drift artifacts using empirical mode decomposition. Hilbert-Huang Transform: Introduction and Applications. pp 167–186

Poppy GM, Chiotha S, Eigenbrod F, et al. (2014) Food security in a perfect storm: using the ecosystems framework to increase understanding. *Philosophical Transactions of The Royal Society B*. 369:20120288.

Postel S (1998) Water for food production: Will there be enough in 2025? *Bioscience.* 48:629-637.

Power AG (2010) Ecosystem services and agriculture: tradeoffs and synergies. *Proceedings of the Royal Society B* 365:2959–71.

Prasad PVV, Boote KJ, Allen LH, et al. (2006) Species, ecotype and cultivar differences in spikelet fertility and harvest index of rice in response to high temperature stress. *Field Crops Research* 95:398–411.

Prasad VK, Badarinath KVS, Eaturu A (2007) Spatial patterns of vegetation phenology metrics and related climatic controls of eight contrasting forest types in India – analysis from remote sensing datasets. *Theoretical and Applied Climatology* 89:95–107.

Pye-Smith C (2011) Farming's climate-smart future, placing agriculture at the heart of climate-change policy. Policy Pointers CTA and CCAFS.

Rajeevan M, Bhate J (2008) A High Resolution Daily Gridded Rainfall Data Set (1971-2005) for Mesoscale Meteorological Studies. National Climate Centre, Indian Meteorological Department.

Rajeevan M, Bhate J, Jaswal a. K (2008) Analysis of variability and trends of extreme rainfall events over India using 104 years of gridded daily rainfall data. Geophysical Research Letters 35:1–6.

Rajeevan M, Bhate J, Kale JD, Lal B (2006) High resolution daily gridded rainfall data for the Indian region : Analysis of break and active monsoon spells. *Current Science* 91:296-306

Ramanathan V, Carmichael G (2008) Global and regional climate changes due to black carbon. *Nature Geosciences* 1:221–227.

Ramankutty N, Evan AT, Monfreda C, Foley JA. (2008) Farming the planet: 1. Geographic distribution of global agricultural lands in the year 2000. *Global Biogeochemical Cycles* 22:1–19.

Ramesh Kumar MR, Prabhu Dessai UR (2004) A new criterion for identifying breaks in monsoon conditions over the Indian subcontinent. *Geophysical Research Letters* 31:1–4.

Ramirez-Villegas J, Challinor AJ, Thornton PK, Jarvis A (2013) Implications of regional improvement in global climate models for agricultural impact research. *Environmental Research Letters* 8:024018.

Rang A, Mangat GS, Kaur R (2011a) Status Paper on Rice in Punjab.

Rang ZW, Jagadish SVK, Zhou QM, et al. (2011b) Effect of high temperature and water stress on pollen germination and spikelet fertility in rice. *Environmental and Expiremental Botany* 70:58–65.

Ray DK, Mueller ND, West PC, et al (2013) Yield Trends Are Insufficient to Double Global Crop Production by 2050. *PLOS One* 8:e66428.

Ray and Foley (2013) Increasing global crop harvest frequency: recent trends and future directions. *Environmental Research Letters.* 8:044041.

Rembold F, Atzberger C, Savin I, Rojas O (2013) Using Low Resolution Satellite Imagery for Yield Prediction and Yield Anomaly Detection. *Remote Sensing* 5:1704–1733.

Richardson AD, Keenan TF, Migliavacca M, et al. (2013) Climate change, phenology, and phenological control of vegetation feedbacks to the climate system. *Agricultural and Forest Meteorology* 169:156–173.

Rockstrom J, Steffen W, Noone K, et al. (2009) A safe operating space for humanity. *Nature* 461:472–475.

Rodell M, Velicogna I, Famiglietti JS (2009) Satellite-based estimates of groundwater depletion in India. *Nature* 460:999–1002.

Rojas O (2007) Operational maize yield model development and validation based on remote sensing and agro-meteorological data in Kenya. *International Journal of Remote Sensing* 28:3775–3793.

Rojas O, Vrieling A, Rembold F (2011) Assessing drought probability for agricultural areas in Africa with coarse resolution remote sensing imagery. *Remote Sensing of Environment* 115:343–352.

Ross KW, Brown ME, Verdin JP, Underwood LW (2009) Review of FEWSNET biophysical monitoring requirements. *Environmental Research Letters* 4:1-10.

Rowhani P, Lobell DB, Linderman M, Ramankutty N (2011) Climate variability and crop production in Tanzania. *Agricultural and Forest Meteorology* 151:449–460.

Roy DP, Boschetti L (2009) Southern Africa Validation of the MODIS, L3JRC, and GlobCarbon Burned-Area Products. *IEEE Transactions on Geoscience Remote Sensing* 47:1032–1044.

Roy DP, Boschetti L, Justice CO, Ju J (2008) The collection 5 MODIS burned area product — Global evaluation by comparison with the MODIS active fire product. *Remote Sensing of Environment* 112:3690–3707.

Rupa Kumar K, Sahai AK, Krishna Kumar K, et al. (2006) High-resolution climate change scenarios for India for the 21st century. *Current Science* 90:334-345.

RWC (2006) A research strategy for improved livelihoods and sustainable rice-wheat cropping in the Vision for 2006 – 2010 and beyond. Rice-Wheat Consortium for the Indo-Gangetic Plains 1–8.

Sadras VO, Monzon JP (2006) Modelled wheat phenology captures rising temperature trends: Shortened time to flowering and maturity in Australia and Argentina. *Field Crops Research* 99:136–146.

Saharawat YS, Gathala MK, Ladha J k., et al. (2009) Evaluation and promotion of integrated crop and resource management in the rice-wheat system in northwest India. In: Ladha J k., Yadvinder-Singh., Erenstein O, Hardy B (eds) Integrated Crop and Resource Management in the Rice-Wheat System of South Asia International Rice Research Institute, Los Banos (Philippines), pp 111–132

Saharawat YS, Ladha JK, Pathak H, et al. (2012) Simulation of resource-conserving technologies on productivity , income and greenhouse gas GHG emission in rice-wheat system. *Journal of Soil Science and Environmental Management* 3:9–22.

Saharawat YS, Singh B, Malik RK, et al. (2010) Evaluation of alternative tillage and crop establishment methods in a rice–wheat rotation in North Western IGP. *Field Crops Research* 116:260–267.

Sakamoto T, Yokozawa M, Toritani H, et al. (2005) A crop phenology detection method using time-series MODIS data. *Remote Sensing of Environment* 96:366–374.

Satyanarayana P, Srinivas VV (2008) Regional frequency analysis of precipitation using large-scale atmospheric variables. *Journal of Geophysical Research* 113:1–16.

Scheffer M, Carpenter S, Foley JA, et al. (2001) Catastrophic shifts in ecosystems. *Nature* 413:591–6.

Scheffer M, Carpenter SR, Lenton TM, et al. (2012) Anticipating critical transitions. *Science* 338:344–8.

Scherr SJ, McNeely JA (2008) Biodiversity conservation and agricultural sustainability: towards a new paradigm of "ecoagriculture" landscapes. *Proceedings of the Royal Society B* 363:477–94.

Scherr SJ, Shames S, Friedman R (2012) From climate-smart agriculture to climate-smart landscapes. *Agriculture and Food Security* 1:12.

Schlenker W, Lobell DB (2010) Robust negative impacts of climate change on African agriculture. *Environmental Research Letters* 5:014010.

Schlenker W, Roberts MJ (2009) Nonlinear temperature effects indicate severe damages to U.S. crop yields under climate change. *Proceedings of the National Academy of Sciences of the USA* 106:15594–8.

Schmidhuber J, Tubiello FN (2007) Global food security under climate change. *Proceedings of the National Academy of Sciences of the USA* 104:19703–8.

Shah F, Huang J, Cui K, et al. (2011) Impact of high-temperature stress on rice plant and its traits related to tolerance. *The Journal of Agricultural Science* 149:545–556.

Shewale MP, Kumar S (2005) Climatological Features of Drought Incidences in India. Meteorological Monograph. Natonal Climate Centre, Indian Meteorological Department.

Siebert S, Doll P (2010) Quantifying blue and green virtual water contents in global crop production as well as production losses without irrigation. *Journal of Hydrology*. 384:198-217.

Singh RB (2000) Environmental consequences of agricultural development: a case study from the Green Revolution state of Haryana, India. *Agriculture, Ecosystems and Environment* 82:97–103.

Singh UP, Singh Y, Kumar V, Ladha J k. (2009) Evaluation and promotion of resource-conserving tillage and crop establishment techniques in the rice-wheat system of eastern India. In: Ladha J k., Yadvinder-Singh., Erenstein O, Hardy B (eds) Integrated Crop and Resource Management in the Rice-Wheat System of South Asia. International Rice Research Institute, Los Banos (Philippines), pp 151–176

Smit B, Wandel J (2006) Adaptation, adaptive capacity and vulnerability. *Global Environmental Change* 16:282–292.

Sperber KR, Annamalai H, Kang I-S, et al. (2012) The Asian summer monsoon: an intercomparison of CMIP5 vs. CMIP3 simulations of the late 20th century. *Climate Dynamics*.

Sun H, Huang J, Huete AR, et al. (2009) Mapping paddy rice with multi-date moderate-resolution imaging spectroradiometer (MODIS) data in China. *Journal of Zhejiang University Science A* 10:1509–1522.

Teixeira EI, Fischer G, van Velthuizen H, et al. (2013) Global hot-spots of heat stress on agricultural crops due to climate change. *Agricultural and Forest Meteorology* 170:206–215.

The Royal Society (2009) Reaping the benefits: science and the sustainable intensification of global agriculture. 1–69.

Thenkabail PS, Hanjra MA, Dheeravath V et al. (2010) A holistic view of global croplands and their water use for ensuring global food security in the 21st Century through advanced remote sensing and non-remote sensing approaches. *Remote Sensing.* 3:211-261.

Thenkabail PS, Biradar CM, Noojipady P, et al. (2009) Global Irrigated Area Maps (GIAM) and Statistics Using Remote Sensing. In: Thenkabail PS, Lyon JG, Turral H, Biradar CM (eds) Remote Sensing of Global Croplands for Food Security. Taylor and Francis, pp 41–121

Thenkabail PS, Gangadhararao P, Biggs TW, et al. (2007) Spectral Matching Techniques to Determine Historical Land-use / Land-cover (LULC) and Irrigated Areas Using Time-series 0.1-degree AVHRR Pathfinder Datasets. *Photogrammetric Engineering and Remote Sensing* 73:1029–1040.

Thenkabail PS, Schull M, Turral H (2005) Ganges and Indus river basin land use/land cover (LULC) and irrigated area mapping using continuous streams of MODIS data. *Remote Sensing of Environment* 95:317–341.

Thenkabail PS, Biradar CM, Noojipady P, et al. (2007) Sub-pixel Area Calculation Methods for Estimating Irrigated Areas. *Sensors.* 7:2519-2538.

Tilman D, Balzer C, Hill J, Befort BL (2011) Global food demand and the sustainable intensification of agriculture. *Proceedings of the National Academy of Sciences of the USA* 108:20260–4.

Tilman D, Cassman KG, Matson PA, et al. (2002) Agricultural sustainability and intensive production practices. *Nature* 418:671–7.

Tiwari VM, Wahr J, Swenson S (2009) Dwindling groundwater resources in northern India, from satellite gravity observations. *Geophysical Research Letters* 36:1-5.

Tubiello FN, Soussana J-F, Howden SM (2007) Crop and pasture response to climate change. *Proceedings of the National Academy of Sciences of the USA* 104:19686–90.

Tucker C, Pinzon J, Brown M, et al. (2005) An extended AVHRR 8-km NDVI dataset compatible with MODIS and SPOT vegetation NDVI data. *International Journal of Remote Sensing* 26:4485–4498.

Tucker CJ (1979) Red and Photographic Infrared linear Combinations for Monitoring Vegetation. *Remote Sensing of Environment* 150:127–150.

Turner AG, Annamalai H (2012) Climate change and the South Asian summer monsoon. *Nature Climate Change* 2:587-595.

Turner BL, Kasperson RE, Matson P A, et al. (2003) A framework for vulnerability analysis in sustainability science. *Proceedings of the National Academy of Sciences of the USA* 100:8074–9.

Tyagi NK, Agrawal A., Sakthivadivel R, Ambast SK (2005) Water management decisions on small farms under scarce canal water supply: A case study from NW India. *Agricultural Water Management* 77:180–195.

UN (1948) The Universal Declaration of Human Rights. http://www.un.org/en/documents/udhr/.

Uphoff N (2012) Supporting food security in the 21st century through resource-conserving increases in agricultural production. *Agriculture and Food Security* 1:18.

Urban D, Roberts MJ, Schlenker W, Lobell DB (2012) Projected temperature changes indicate significant increase in interannual variability of U.S. maize yields. *Climatic Change* 112:525–533.

Vermeulen S, Zougmoré R, Wollenberg E, et al. (2012a) Climate change, agriculture and food security: a global partnership to link research and action for low-income agricultural producers and consumers. *Current Opinion in Environmental Sustainability* 4:128–133.

Vermeulen SJ, Aggarwal PK, Ainslie A, et al. (2010) Agriculture , Food Security and Climate Change : Outlook for Knowledge , Tools and Action. CCAFS Rep. 3.

Vermeulen SJ, Campbell BM, Ingram JSI (2012b) Climate Change and Food Systems. *Annual Review of Environmental Resources* 37:195–222.

Vitousek PM, Mooney HA, Lubchenco J, Melillo JM (1997) Human Domination of Earth's Ecosystems. *Science* 277:494–499.

Vrieling A, Beurs KM, Brown ME (2011) Variability of African farming systems from phenological analysis of NDVI time series. *Climatic Change* 455–477.

Vrieling A, de Leeuw J, Said M (2013) Length of Growing Period over Africa: Variability and Trends from 30 Years of NDVI Time Series. *Remote Sensing* 5:982–1000.

Walker B, Holling CS, Carpenter S., Kinzig A (2004) Resilience , Adaptability and Transformability in Social–ecological Systems. *Ecology and Society* 9:2.

Wang B, Ding Q, Joseph P V. (2009) Objective Definition of the Indian Summer Monsoon Onset. *Journal of Climate* 22:3303–3316.

Wang B, Lin H (2002) Rainy Season of the Asian – Pacific Summer Monsoon. *Journal of Climate* 15:386–398.

Wardlow B, Egbert S, Kastens J (2007) Analysis of time-series MODIS 250 m vegetation index data for crop classification in the U.S. Central Great Plains. *Remote Sensing of Environment* 108:290–310.

Wassmann R, Jagadish SVK, Heuer S, et al. (2009) Climate Change Affecting Rice Production : The Physiological and Agronomic Basis for Possible Adaptation Strategies. *Advances in Agronomy* 101:59–122.

Webb J, Hutchings N, Amon B (2009) Field burning of agricultural wastes. EMEP/EEA air Pollut. Emiss. Invent. Guid. European Environment Agency, Luxembourg. Office for Official Publications of the European Communities, p 4.F

Welch JR, Vincent JR, Auffhammer M, et al. (2010) Rice yields in tropical/subtropical Asia exhibit large but opposing sensitivities to minimum and maximum temperatures. *Proceedings of the National Academy of Sciences of the USA* 107:14562–7.

Wheeler T, von Braun J (2013) Climate change impacts on global food security. *Science* 341:508–13.

White JW, Hoogenboom G, Kimball B a., Wall GW (2011) Methodologies for simulating impacts of climate change on crop production. *Field Crops Research* 124:357–368.

White MA, Thornton PE, Running W (1997) A continental phenology model for monitoring vegetation responses to interannual climatic variability. *Global Biogeochemical Cycles* 11:217–234.

Wilks DS (2006) On " Field Significance " and the False Discovery Rate. *Journal of Climate 45:1181–1189.*

Wilks DS (1997) Resampling Hypothesis Tests for Autocorrelated Fields. *Journal of Climate* 10:65–82.

World Bank (2011) Climate-Smart Agriculture: A Call to Action. Washington D.C.

Xiao X, Boles S, Frolking S, et al. (2006) Mapping paddy rice agriculture in South and Southeast Asia using multi-temporal MODIS images. *Remote Sensing of Environment* 100:95–113.

Xiao X, Boles S, Liu J, et al. (2005) Mapping paddy rice agriculture in southern China using multi-temporal MODIS images. *Remote Sensing of Environment* 95:480–492.

Xie P, Chen M, Yang S, et al. (2007) A Gauge-Based Analysis of Daily Precipitation over East Asia. *Journal of Hydrometeorology* 8:607–626.

Xu L, Myneni RB, Chapin III FS, et al. (2013) Temperature and vegetation seasonality diminishment over northern lands. *Nature Climate Change* 3:581–586.

Yasutomi N, Hamada A, Yatagai A (2011) Development of a Long-term Daily Gridded Temperature Dataset and Its Application to Rain / Snow Discrimination of Daily Precipitation. *Global Environmental Research* V15N2:165–172.

Yatagai A, Arakawa O, Kamiguchi K, et al. (2009) A 44-Year Daily Gridded Precipitation Dataset for Asia Based on a Dense Network of Rain Gauges. *SOLA* 5:137–140.

Yatagai A, Kamiguchi K, Arakawa O, et al. (2012) APHRODITE: Constructing a Long-Term Daily Gridded Precipitation Dataset for Asia Based on a Dense Network of Rain Gauges. *Bulletin of the American Meteorological Society* 93:1401–1415.

Yevich R, Logan JA (2003) An assessment of biofuel use and burning of agricultural waste in the developing world. *Global Biogeochemical Cycles*. 17:1095.

Zhang X, Friedl M A, Schaaf CB, et al. (2003) Monitoring vegetation phenology using MODIS. *Remote Sensing of Environment* 84:471–475.

Zickfeld K, Knopf B, Petoukhov V, Schellnhuber HJ (2005) Is the Indian summer monsoon stable against global change? *Geophysical Research Letters* 32:1–5.

Appendix

8.1 Appendix 1

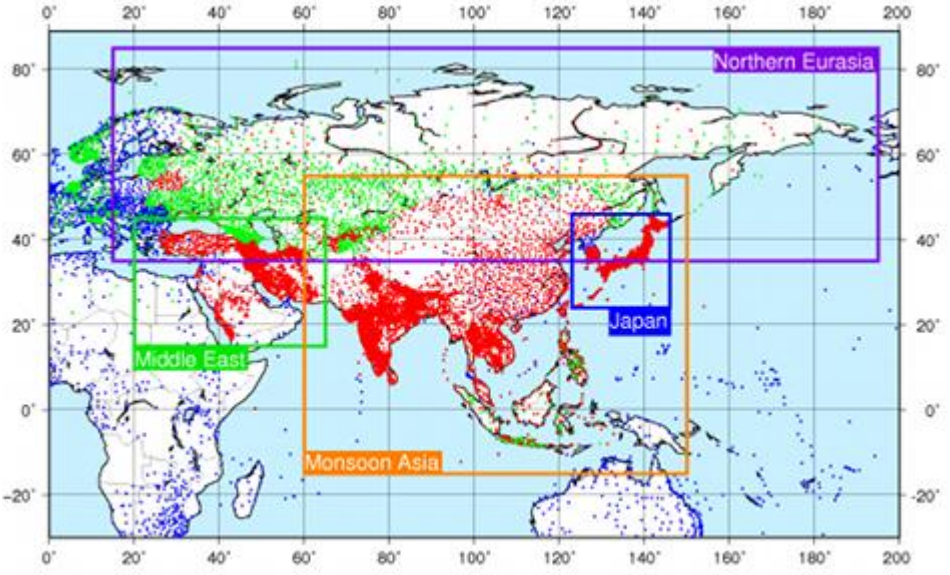

A1. Rain gauges used in the computation of the APRHODITE daily precipitation product (http://www.chikyu.ac.jp/precip/products/index.html). Red gauges correspond to national meteorological organisation collections, blue dots correspond to Global Telecommunications System (GTS) data and other dots correspond to a range of precompiled datasets listed in: file:///C:/Users/jmd1v13/Downloads/5_137_2.pdf and file:///C:/Users/jmd1v13/Downloads/5_137_1.pdf.

8.2 Appendix 2

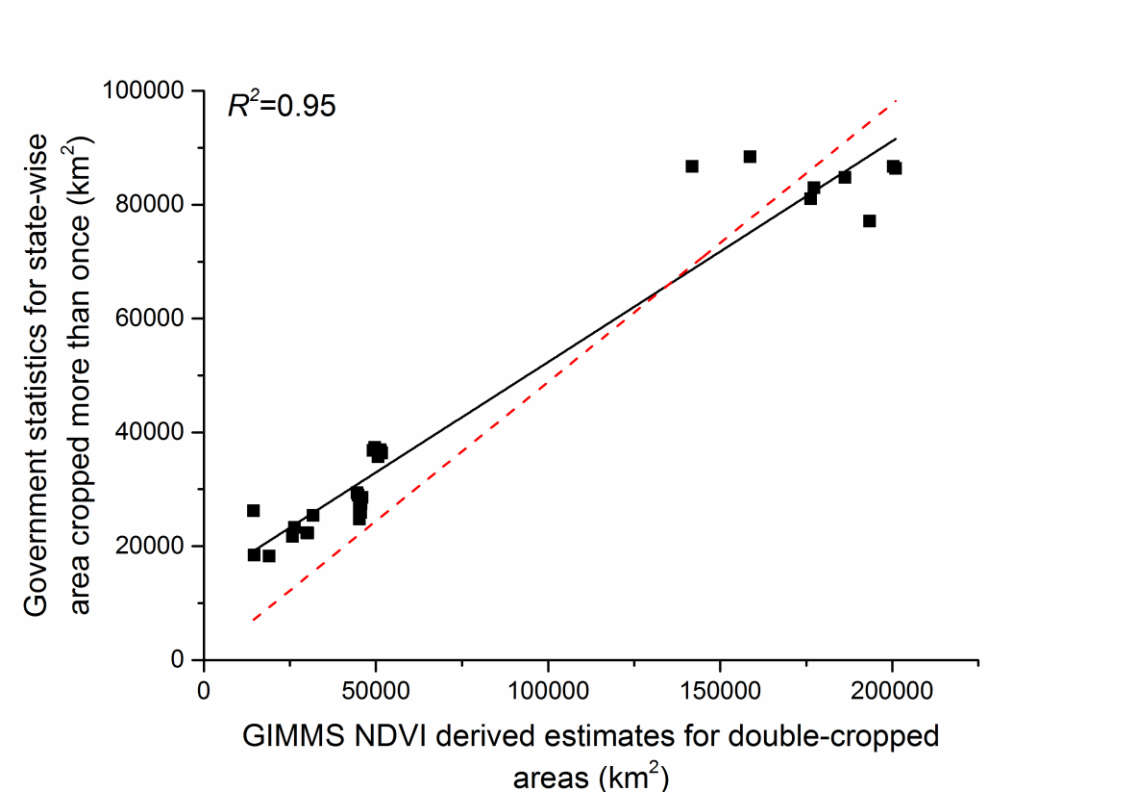

A2. The relationship between state-wise area detected as double cropping from GIMMS NDVI data and Government of India land-use statistics for area cropped more than once for Punjab, Haryana, Bihar and Uttar Pradesh (1998-99 to 2005-06). The R^2 value is likely inflated due to including Uttar Pradesh in the analysis, which corresponds to the collection of points in the upper right of the plot. However discounting Uttar Pradesh from the analysis still yields an R^2 of 0.68. This indicates the GIMMS NDVI data captures the state-wise inter-annual variation in cropping intensity though may be sub-optimal for exact areal estimates. That the GIMMS NDVI data tends to overestimate area cropped more than once relative to the Government of India estimates is likely due to it considering full-pixel areas not accounting for sub-pixel proportions (Thenkabail et al. 2007). However, the purpose of this study is not to provide accurate, census-style, estimates of land-use but to capture spatial and temporal patterns in the change in LSP across an agricultural landscape at a regional scale. Given the dominant agricultural land cover across the IGP the GIMMS dataset is suitable for this purpose (please see section 4.4.1 for a more detailed discussion of the limitations of the GIMMS NDVI dataset). The red dotted line is a 1:1 fit.

8.3 Appendix 3

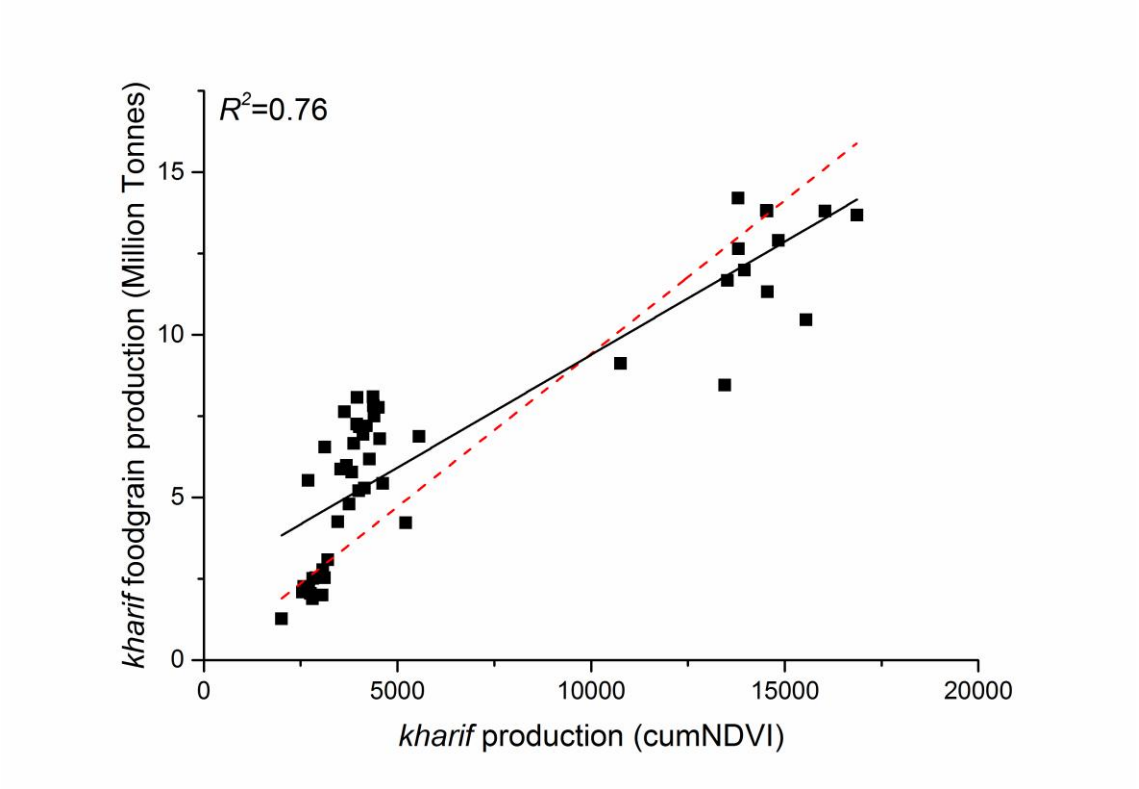

A3.1 State-wise *kharif* cumNDVI plotted against state-wise foodgrain production statistics for Punjab, Haryana, Uttar Pradesh and Bihar (1982-83 to 1994-95). Excluding Uttar Pradesh from the analysis (upper right collection of points on the plot which inflates the R^2 value) yields an R^2 value of 0.56. The red dotted line is a 1:1 fit. It should be noted this is not a perfect validation, no attempt has been made to discriminate between crop types using the GIMMS NDVI dataset, cumNDVI is taken as a proxy for agricultural production over the landscape and is not an exact or validated measure of foodgrain production. We have chosen to validate against foodgrain production as it covers a range of crop types. This provides an indication the cumNDVI captures broad inter-annual and spatial patterns in agricultural production.

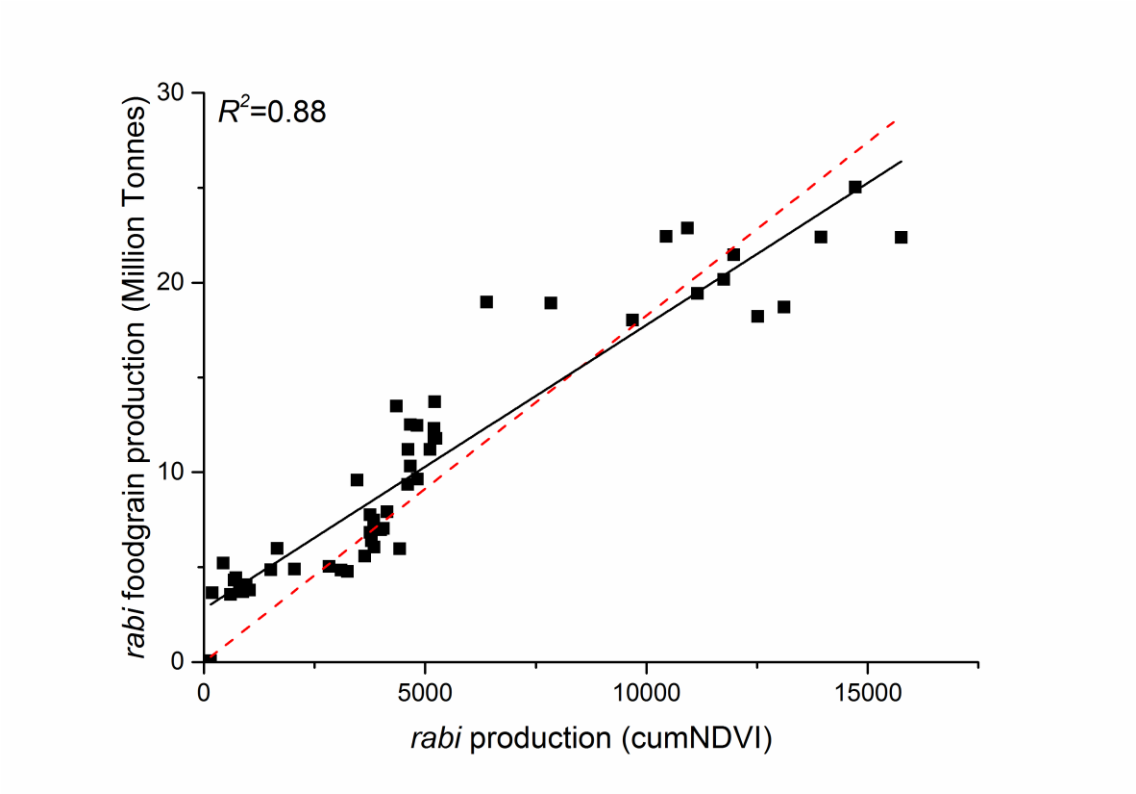

A3.2 State-wise *rabi* cumNDVI plotted against state-wise foodgrain production statistics for Punjab, Haryana, Uttar Pradesh and Bihar (1982-83 to 1994-95). Excluding Uttar Pradesh from the analysis (upper right collection of points on the plot which inflates the R^2 value) yields an R^2 value of 0.72. The red dotted line is a 1:1 fit. It should be noted this is not a perfect validation, no attempt has been made to discriminate between crop types using the GIMMS NDVI dataset, cumNDVI is taken as a proxy for agricultural production over the landscape and is not an exact or validated measure of foodgrain production. We have chosen to validate against foodgrain production as it covers a range of crop types. This provides an indication the cumNDVI captures broad inter-annual and spatial patterns in agricultural production.

8.4 Appendix 4

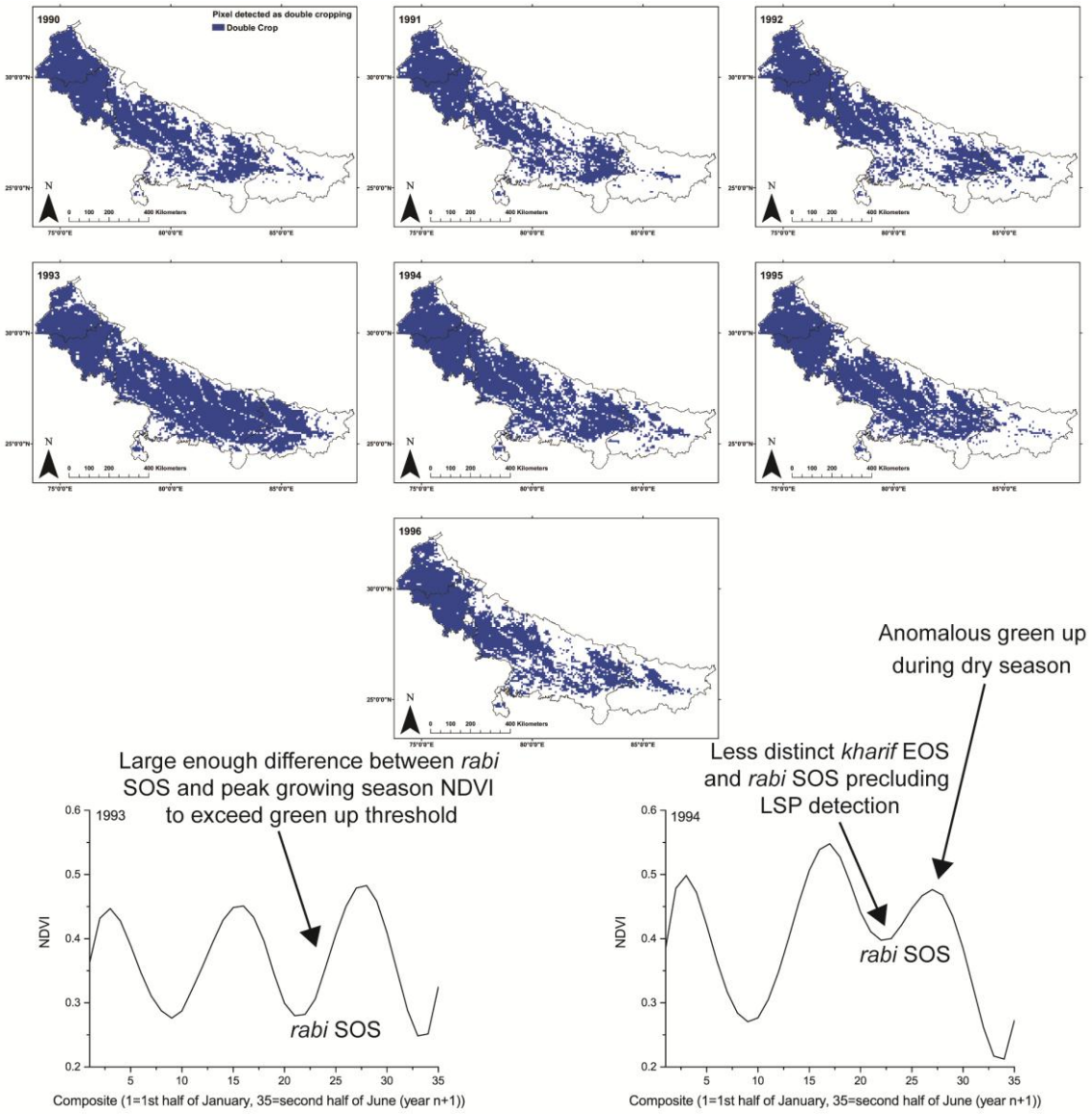

NDVI Phenology profiles for GIMMS NDVI pixel at 29.95 N and 85.67 E (Bihar). In 1993 it met threshold green up requirements for *rabi* cropping but in 1994 it did not.

A4. Areas under double cropping from 1990 through to 1996. It illustrates the larger area under double cropping detected in 1993 compared to other years across the eastern portions of the IGP. This was particularly pronounced in Bihar in 1993 (see Fig. 4-3 and Fig. 4-6). This anomaly is an artefact of using GIMMS NDVI data with an 8 km spatial resolution in areas of the IGP where there are a larger proportion of smallholder farmers (Bihar has an average farm size of 39 m^2 (Agricultural Census 2012)). Fig. 6-11 illustrated that there was a large variation in the timing of phenological events occurring within a GIMMS NDVI pixel in Punjab, this variation will be more pronounced in more fragmented smallholder landscapes in Bihar. This will result in large within pixel variations in timing of SOS dates, EOS dates, peak growing dates and the levels of biomass in fields at different times. This will create a mixed spectral signal averaged out as a GIMMS NDVI value at an 8 km spatial resolution masking phenological detail and making it harder to discriminate between growing seasons. For example, the phenology profile for the pixel displayed above in 1994 suggests some *rabi* cropping is occurring as the second small peak is anomalous to the natural cycle of vegetation in a monsoonal

climate. However, there is not a clear EOS for the *kharif* crop and SOS for the *rabi* crop in the phenology profile of GIMMS NDVI data which precludes meeting the threshold requirements for detecting green up associated with agricultural growth. However, in 1993 the difference between SOS NDVI and peak NDVI was large enough to meet the threshold green up requirements. Whilst the GIMMS NDVI dataset captures the eastward advance of double cropping between 1982-83 and 2005-06 at a regional scale a lot of local detail is missed or masked out at the 8 km spatial resolution, especially in the smallholder agricultural regions of the eastern IGP. As such, these estimates of area should not be considered as accurate areal extents. The release of Sentinel-2 in 2015 with a 10 m spatial resolution and 5 day revisit period will increase the accuracy, and level, of phenological detail over smallholder and fragmented agricultural landscapes (ESA 2010).

8.5 Appendix 5

A5. Table showing the R^2 values estimates of district-wise rice and wheat crop production using CUM-EVI$_{(TSP)}$ for the 2002-2003 to the 2006-2007 growing seasons using regression coefficients derived from the 2009-2010 growing season. That these regression coefficients enable accurate estimates of rice and wheat production across multiple years suggests CUM-EVI$_{(TSP)}$ is a time-invariant indicator of crop production.

Year	Rice	Wheat
2002-2003	0.95	0.94
2003-2004	0.94	0.81
2004-2005	0.95	0.87
2005-2006	0.94	0.89
2006-2007	0.85	0.80